



UNIVERSITY OF
LIVERPOOL

**Understanding Immunoglobulin G
mediated dorsal root ganglion anti-
neuronal autoimmunity in Complex
Regional Pain Syndrome**

Thesis submitted in accordance with the requirements of the University of Liverpool
for the degree of Doctor in Philosophy by

Serena Sensi

June 2022

Abstract

Complex Regional Pain Syndrome (CRPS) is a post-traumatic pain condition characterized by a “burning” pain and motor dysfunction in the injured limb. In case CRPS persists beyond six months, it becomes a chronic condition with patient experiencing extremely poor quality of life. The pathophysiological basis of pain in CRPS is unknown and there is a lack of effective treatments and diagnostic tests. Preliminary works reported that plasma exchange can alleviate pain in long-standing CRPS patients, and that some patients experience good pain relief with intravenous immunoglobulin. Recent works demonstrate that a transfer of CRPS immunoglobulins induces the condition in hind paw injured mice, and that patients IgG bind to cell-surface epitopes. Surface binding of CRPS-serum-IgG to neuronal cells is still unclear.

The aim of this project is to identify neuronal surface binding by CRPS serum IgG. Since traumatic soft tissue injury that releases inflammatory mediators, enables CRPS IgG induced hyperalgesia, Dorsal Root Ganglia (DRG) neurons were incubated with a mixture of inflammatory mediators or cytokines and IgG binding was assessed using flow cytometry, to confirm the role of inflammatory mediators in activating the patient IgG. The majority of cultured neurons had a strong and standardized binding with human IgG; this effect appeared to be increased only by cytokines and not by inflammatory mediators. In order to identify the neuronal population involved in binding, DRG tissue was

harvested from injured mice and then processed for IHC staining or immunofluorescence (IF) staining. Immunohistochemical staining revealed the presence of human IgG on cell surface of some neurons and in particular CRPS IgG staining was stronger than healthy control IgG staining; this staining pattern was confirmed also by Western Blot. Immunofluorescence staining *in vitro* revealed no difference in staining between CRPS and HC IgG. In order to investigate *in vivo* staining we injected animals with IgG before hind-paw injury and then harvested DRGs (L3, L4, L5) and we processed the tissue for IHC. Immunofluorescence staining revealed no difference in staining between CRPS and HC IgG but staining was clearly visible on cell membrane of DRG cells. Together, these findings suggest that CRPS autoantibodies may bind neuronal epitopes present only in a post-traumatic environment and that the binding could be facilitated by mediators (in particular cytokines) that are released after the hind paw injury.

Table of contents

Chapter 1 – INTRODUCTION: CRPS and primary chronic pain.....	1
1.1 Complex Regional Pain Syndrome (CRPS)	1
1.1.1 Historical description of CRPS.....	1
1.1.2 Diagnosis	2
1.1.3 Clinical presentation.....	4
1.1.4 Epidemiology	8
1.1.5 Pathophysiology	9
1.1.6 Treatments.....	13
1.1.7 New Pain Classifications.....	18
1.2 The human sensory system and pain.....	19
1.3 Immune system and pain	27
1.3.1 Inflammation	27
1.3.2 Autoimmunity	32
1.3.3 Inflammation and pain.....	40
1.3.4 Autoimmunity and chronic pain.....	43
1.3.5 Autoimmunity in CRPS	48
1.4 Hypothesis and Aims.....	54
Chapter 2 – MATERIALS AND METHODS	56
2.1. Materials.....	56
2.1.1 Antibodies and solutions.....	56

2.1.2 Animals	60
2.2. Methods.....	66
2.2.1 Serum Isolation and storage	66
2.2.2 IgG purification.....	66
2.2.3 Animal incision protocol for tissue staining	74
2.2.4 IgG injection protocol for tissue staining	75
2.2.5 Tissue harvest and fixation	77
2.2.6 Dissection of Dorsal Root Ganglion	79
2.2.7 Dorsal Root Ganglion dissociation and cell culture	81
2.2.8 Immunocytochemistry staining.....	82
2.2.9 Flow cytometry and data analysis.....	83
2.2.10 Western Blot of DRG homogenates.....	93
2.2.11 Immunohistochemistry	95
2.2.12 Immunofluorescence.....	103
 Chapter 3 – RESULTS: ASSESSMENT OF CRPS IgG BINDING TO DRG	
NEURONAL CELLS.....	110
3.1 Introduction.....	110
3.2 Aim	111
3.3 Results	112
3.3.1 Flow cytometry analysis of DRG neuronal population.....	112
3.3.2 Western Blot with DRG neuronal cell homogenates	125

3.3.3 Immunocytochemistry staining with DRG neuronal cells	127
Chapter 4 – STAINING OF DRGS HARVESTED FROM INJURED MICE	136
4.1 Introduction to CRPS murine trauma model.....	136
4.2 Aim	141
4.3 Results	142
4.3.1 IHC Staining of DRG harvested from injured mice.....	142
4.3.2 IF Staining of DRG harvested from injured mice.....	162
4.4 Discussion	173
Chapter 5 – STAINING OF DRGS HARVESTED FROM INJECTED AND INJURED MICE	178
5.1 Introduction.....	178
5.2 Aim	181
5.3 Results	182
5.3.1 IHC Staining of DRG harvested from injected and injured mice	182
5.3.2 IF Staining of DRG harvested from injured and injected mice ...	185
5.4 Discussion	198
Chapter 6 - DISCUSSION AND CONCLUSION	202
Chapter 7 – APPENDIX	218
Chapter 8 - REFERENCES	223

List of Figures

Figure 1.1 Other names for CRPS.....	2
Figure 1.2 CRPS signs.	6
Figure 1.3 Signs and symptoms of CRPS.....	7
Figure 1.4 Possible mechanisms involved in CRPS	10
Figure 1.5 The four pillars of care for CRPS.	14
Figure 1.6 Plasma exchange therapy (PE) or plasmapheresis.	16
Figure 1.7 Intravenous immunoglobulin treatment (IVIg).	17
Figure 1.8 Pseudo-unipolar neuron.....	22
Figure 1.9 Nociceptive fibers in the peripheral sensory system.	24
Figure 1.10 The immune response to injury and infection.	30
Figure 1.11 Antibody structure.	35
Figure 1.12 IgG isotypes.	36
Figure 1.13 Fab and fc mechanism of action.	38
Figure 1.14 Mechanism of auto antibody induced pathology.	40
Figure 1.15 Antibody mediated model for CRPS	50
Figure 2.1 IgG purification protocol.	67
Figure 2.2. HiTrap® Protein G High Performance.....	68
Figure 2.3 IgG purification steps.	72
Figure 2.4 The Brennan model of rat incisional pain.....	74
Figure 2.5 IgG Injection protocol.	76
Figure 2.6 DRG snap-freezing.	78
Figure 2.7 DRG dissection.....	80
Figure 2.8 Diagram of flow cytometric analysis.....	84

Figure 2.9 Flow cytometry staining.	87
Figure 2.10 Gating on dot plot.....	90
Figure 2.11 Back-gating.....	90
Figure 2.12 fluorescence intensity histogram.....	91
Figure 2.13 Western blot sandwich.....	94
Figure 2.14 Agar embedded DRGs.....	98
Figure 2.15 Antigen retrieval mechanism.....	99
Figure 2.16 IHC staining protocol.....	100
Figure 2.17 HRP polymer.	101
Figure 2.18 DRG snap-freezing.	104
Figure 2.19 Sectioning of tissue.....	105
Figure 2.20 IF staining protocol.....	106
Figure 2.21 DRG neuron-rich area.....	108
Figure 3.1 Chapter aims.	112
Figure 3.2 DRG cell culture.....	113
Figure 3.3 HC IgG staining after 24 hours of neuronal cell culture.....	114
Figure 3.4 CRPS IgG staining after 24 hours of neuronal cell culture.....	115
Figure 3.5 Incubation with inflammatory mediators for 24 hours.....	117
Figure 3.6 Cytokine pool treatment.	118
Figure 3.7 Single cytokine treatment.....	119
Figure 3.8 Fluorescence staining of DRG primary neurons after cytokines treatment.....	120
Figure 3.9 Staining of DRG primary neurons after combined inflammatory mediator and cytokine treatment.....	122
Figure 3.10 P1 CRPS Patient staining pattern.....	123

Figure 3.11 P1-CRPS cell sorting.	124
Figure 3.12 Western Blot of protein homogenates of DRG ganglia incubated with HC P1-CRPS and P2-CRPS.	126
Figure 3.13 PGP9.5 staining (1:500).....	128
Figure 3.14 CRPS/HC IgG staining (1:100)	129
Figure 3.15 P1-CRPS IgG (1:100) staining on the cytoplasm.....	130
Figure 3.16 Fibroblast staining with CRPS and HC IgG (1:100).	131
Figure 4.1 Hind paw plantar incision model.	138
Figure 4.2 L3, L4, L5 spinal nerves in mouse hind-paw skin	139
Figure 4.3 Different sections from the same DRG block.	144
Figure 4.4 Lumbar dorsal root ganglion H&E staining.....	145
Figure 4.5 Example of right side DRG staining with pool HC/CRPS IgG. ...	147
Figure 4.6 Antigen retrieval staining.....	148
Figure 4.7 HRP polymer staining.	148
Figure 4.8 Tissue fixed with Buffered formalin.	149
Figure 4.9 Staining of slides 51-53.....	152
Figure 4.10 Right part individual control's and patient's staining patterns..	155
Figure 4.11 Right paw-injured individual healthy control's and patient's L3-L5 DRG staining patterns.	156
Figure 5.1 Experiment 1, 2, 3 Flow-chart.	180
Figure 5.2. Experiment 1. IHC DRGs staining right and left.....	184
Figure 5.3 Experiment 1.....	190
Figure 5.4 Experiment 2.....	192
Figure 5.5 Experiment 3.....	194
Figure 5.6 Experiment 1,2,3 comparison.	195

Figure 5.7 Experiment 1,2, 3 comparison. 197

List of Tables

Table 1.1 The Budapest criteria for CRPS.....	4
Table 1.2 IASP Pain definitions.....	5
Table 1.3 Primary afferent nerve fibres.....	23
Table 1.4 Nociceptors subpopulations.....	25
Table 1.5 Autoimmune disease classification.....	32
Table 1.6 Mechanism of auto antibody pain.....	47
Table 2.1 Details of materials for IgG purification.....	56
Table 2.2 Details of all materials for Flow Cytometry, IHC and immunofluorescence (IF).....	57
Table 2.3 Details of the media used for cell culture, flow cytometry, IHC and immunofluorescence.....	58
Table 2.4 Details of secondary antibodies used for flow cytometry IHC and immunofluorescence.....	59
Table 2.5 Details of inflammatory mediators used for flow cytometry.....	60
Table 2.6 Plasma CRPS samples.....	62
Table 2.7 Pooled CRPS and HC serum samples used for staining.....	63
Table 2.8 Protein G specifications.....	68
Table 2.9 IgG injection protocols.....	76
Table 2.10 Fixation methods.....	79
Table 2.11 Flow cytometry inflammatory factors pre-incubation experiments.	88
Table 2.12 Tissue processing schedule.....	96
Table 2.13 Blocking solution for IF staining.....	107

Table 4.1 Comparison between mouse and human innervation of L3, L4, L5 neurons.....	140
Table 5.1 IHC experiment 1 experimental design.	183
Table 5.2 IF experiment 1 experimental design. The first experiment had 4 injection days and sacrifice was on day 2.....	187
Table 5.3 IF experiment 2 experimental design. The second experiment had 6 injection days and sacrifice was on day 8.....	187
Table 5.4 IF experiment 1 experimental design. The third experiment had 6 injection days and sacrifice was on day 13.....	188

Chapter 1 – INTRODUCTION: CRPS and primary chronic pain

1.1 Complex Regional Pain Syndrome (CRPS)

1.1.1 Historical description of CRPS

The first comprehensive clinical descriptions of Complex Regional Pain Syndrome (CRPS) were recorded by military surgeons in mid-1800s, in particular many soldiers with gunshot wounds suffered from a persistent burning pain even after the bullets and missiles were removed from their limbs. That “burning pain” was later recognized as a hallmark of CRPS.

Alexander Denmark was the first surgeon to write a case report of a wounded soldier with CRPS, he described a violent pain with a “burning nature” (THOMAS and FRS (1813))

But it was only during the America Civil war that an US army physician called Silas Weir Mitchell published the first medical report with an exhaustive description of signs and symptoms of CRPS. In particular he noted the presence of "...a painful swelling of the joints....it is distinct from the early swelling due to the inflammation about the wound itself..." then he identified an initial phase and a second phase "... Once fully established, it keeps the joint stiff and sore for weeks or months. When the acute stage has departed, the tissues become hard and partial ankylosis results." (Mitchell et al. (2007)). Mitchel was so impressed by the burning nature of this pain, that he began to call the condition Causalgia (Greek for burning pain).

Since mid-1800s CRPS has been described by other clinicians such as Paul Sudeck, Rene Leriche and James A. Evans by other names including Sudeck's Atrophy, Reflex Sympathetic Dystrophy (RSD), Algodystrophy, Algoneurodystrophy, Shoulder-hand syndrome and Reflex Neurovascular Dystrophy (Steinbrocker et al. (1954); Sudeck (1901); (Stanton-Hicks et al. (1995); Aradillas et al. (2015); Merskey and Bogduk (1994))

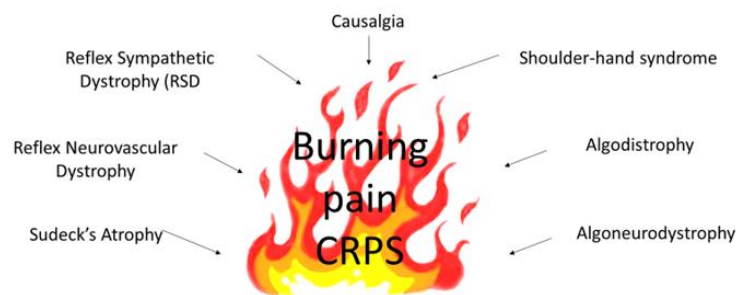


Figure 1.1 Other names for CRPS.

Only in 1994 during the International Association for the Study of Pain conference (IASP) held in Orlando (Florida), previous names used to describe this "burning pain" condition were replaced by the updated Complex Regional Pain Syndrome (CRPS) (Harden et al. (2007)).

1.1.2 Diagnosis

CRPS is a form of chronic pain that commonly affects the distal part of a limb. Symptoms can vary but often present are an incapacitating, burning or allodynic pain in the extremities, with patients also experiencing joint stiffness,

muscle atrophy, changes in skin temperature and swelling (Skaribas et al. (2019)).

CRPS is divided into two main clinical sub-types: Type I, which is very common and Type II (Harden et al. (2010)). The main symptoms of type I are led by tissue injury without injury to a major nerve; an eliciting trauma is typically to the distal part of the affected extremity, and with pain often localized in deep somatic tissues. Whereas type II symptoms are led by a known major peripheral nerve injury that causes biochemical, morphological and physiological changes of the injured and adjacent primary afferent neurons, although the CRPS symptoms always extend beyond the territory of the injured nerve; Type II is also called Mitchell's Causalgia (Wilson and Serpell (2007)). Considering that CRPS is a heterogeneous disease, there is another CRPS sub-type, 'Not Otherwise Specified or NOS' for patients who do not fully meet the criteria for group I or II. (Sebastin (2011)). Finally, a recently introduced sub-type 'CRPS with remission of some features' captures those patients whose condition initially fulfilled the full criteria for CRPS (Budapest Criteria), but who have since lost some signs and symptoms (Valencia Consensus), (Goebel et al. (2021a)).

Currently no specific test can support and help the clinical diagnosis of CRPS; for this reason, the syndrome is diagnosed using revised clinical criteria termed the "Budapest Criteria" which was developed by the International Association for the Study of Pain (IASP) in 2012 (Table 1.1) (Harden et al. (2007)).

Table 1.1 The Budapest criteria for CRPS.

The Budapest criteria for CRPS was developed by the International Association for the Study of Pain (IASP) in 2012 (Harden et al. (2007)).

The Budapest Criteria for CRPS	
A) Continuing pain, which is disproportionate to any inciting event	
B) Must report at least one symptom in three of the following four categories *	
C) Must display at least one sign at time of evaluation in two or more of the following categories*	
D) There is no other diagnosis that better explains the signs and symptoms	

* Categories for B and C	
Sensory	Evidence of hyperalgesia and/or allodynia
Vasomotor	Evidence of temperature asymmetry and/or skin colour changes and/or colour asymmetry
Sudomotor/oedema	Evidence of oedema and/or sweating changes and/or sweating asymmetry
Motor/trophic	Evidence of decreased range of motion and/or motor dysfunction (weakness, tremor, dystonia) and/or trophic changes (hair, nails, skin).

Other terms are commonly used to help clinical diagnosis of CRPS, hot/warm, intermediate and cold/blue CRPS, are based on skin temperature difference between affected and unaffected limb (). Hot/Warm-CRPS is also referred as "acute" phase and it is related to an increased skin temperature in the affected limb, caused by an initial tissue inflammation after injury. While Cold/Blue-CRPS is sometimes referred to as the chronic stage with an apparent resolution of inflammation. Of note, though the original assumption that CRPS occurs in stereotypic 'stages' has been disproven by more recent research results. A label of 'intermediate CRPS' is sometimes given in absence of warm and cold- CRPS (Dirckx et al. (2015)).

1.1.3 Clinical presentation

CRPS is a painful, usually post-traumatic, condition characterised by sympathetic, sensory and motor dysfunction in the affected limb, and its

cardinal symptom is an incapacitating severe pain. Although spontaneous resolution often occurs, the persistence of CRPS beyond 6-18 months typically leads to the development of a chronic condition with profound adverse impact on quality of life (Veldman et al. (1993)). CRPS is usually diagnosed after tissue injury with a varied clinical presentation with the most frequent sign being disproportionate pain in the affected limb (de Mos et al. (2007)). Patients with CRPS have most of the symptoms related with spontaneous and burning pain, such as: Allodynia, Hyperaesthesia, Hyperalgesia, Hyperpathia (Table 1.2).

Table 1.2 IASP Pain definitions.

Symptom	Definition
Pain	An unpleasant sensory and emotional experience that we primarily associate with tissue damage or describe in terms of tissue damage or both.
Allodynia	Pain due to a stimulus that does not normally provoke pain.
Hyperaesthesia	Increased sensitivity to stimulation, excluding special senses.
Hyperalgesia	An increased response to a stimulus that is normally painful.

Hyperpathia	Pain characterised by an increased reaction to a stimulus, especially a repetitive one, as well as an increased threshold.
--------------------	--

A common clinical presentation for CRPS is an initial small bone fracture, or some form of moderate injury, followed by an acute inflammation phase called “warm CRPS” that commonly develops into “cold CRPS” with cyanotic appearance (see also note about ‘stages’ in the previous section). CRPS patients present autonomic signs on their affected limb like oedema, vasodilation, vasoconstriction and swelling, in addition to motor signs like limb weakness and tremor. Sometimes clinicians can also observe abnormalities in hair and nail growth in addition to changes in skin colour. A reduction in bone density is often observed, which resolves when the condition improves (Figure 1.2).

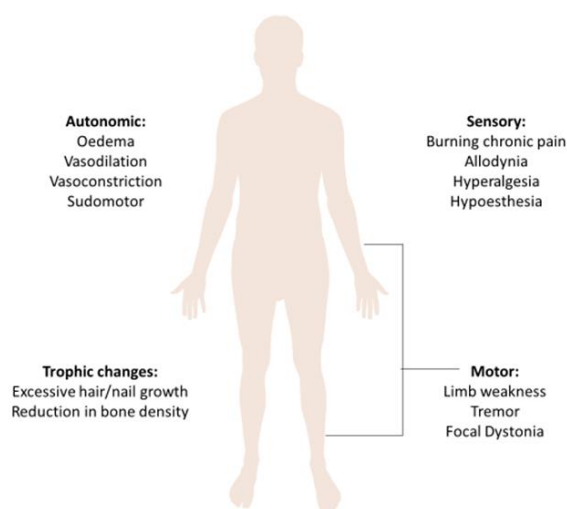


Figure 1.2 CRPS signs.

Characteristic symptoms and signs of CRPS soon after its onset include redness, warmth, swelling and pain (Parkitny et al. (2013)). In particular patients with warm-CRPS present symptoms like changes in skin colour, swelling, (Figure 1.3 a), and changes in sudomotor function (Figure 1.3 b) (McBride and Atkins (2005)). While patients with predominantly cold skin present decreased skin temperature, cyanotic appearance, atrophy and sometimes contracture (Figure 1.3 c) without cardinal signs of inflammation. In 2015 Bruehl provided statistical evidence that patients with warm-CRPS within five months of CRPS onset typically have significantly 'inflammatory' signs which diminish over the following three months. The pain duration is different between patients presenting initially with warm or cold CRPS, it is shorter in warm CRPS sub-type (4.7 months) and longer in cold CRPS sub-type (20 months) (Bruehl (2015)).

A diagnosis of Long-standing or persistent CRPS is given when symptoms do not reduce after 12-18 months (Goebel et al. (2021a)).



Figure 1.3 Signs and symptoms of CRPS.

Patients with warm-CRPS present symptoms like changes in skin colour, swelling. b. Increased sudomotor function in warm CRPS. Patients with warm-CRPS present symptoms like changes in sudomotor function c. Late CRPS with complications affecting, patients with predominantly cold skin, cyanotic appearance, atrophy and sometimes contracture without cardinal signs of inflammation. This complication can likely be prevented by good physiotherapeutic treatment; this is less frequent now. Images taken from McBride et al (McBride and Atkins (2005)).

So far both clinician's clinical experience and use of the IASP Budapest diagnostic criteria are crucial for a correct diagnosis of CRPS. Most patients with CRPS get the correct diagnosis late, probably because CRPS features are very similar to other health conditions or because they need to get advice from different health professionals for the variety of their symptoms (Kessler et al. (2020); Taylor et al. (2021)). Because of their burning pain and clinical signs, patients with CRPS tend to stop working and need support from health care systems. For these reasons, like other chronic pain conditions CRPS is expensive (Scholz-Odermatt et al. (2019)).

1.1.4 Epidemiology

Most relevant studies for the CRPS incidence in the general population were published by Sandroni et al. in 2003 and by De Mos et al. in 2007. The former study assessed the incidence of CRPS in the Olmsted County, USA; for this study the authors without using specific diagnostic criteria documented an incidence rate of CRPS I and CRPS II of 6.28 per 100000 persons-years, where CRPS I was 5.46 per 100,000 person-years and CRPS II was 0.82 per 100,000 persons-years (de Mos et al. (2007)). In the latter study, authors assessed the incidence of CRPS in Netherlands, using diagnostic criteria to classify CRPS. In this study the overall incidence of CRPS was estimated 26.2 per 100000 person-years. These two epidemiology studies estimated different incidence rates likely because of differences in the two populations (the US

study reported from one tertiary care centre whereas the Netherlands study reported all patients registered in GP practices) as well as differential use of diagnostic criteria (Sandroni et al. (2003)). Interestingly in both studies females were more affected than males, in particular postmenopausal woman, aged 55-75 could develop CRPS with higher risk. Further studies confirmed that females are at least three times more susceptible to develop CRPS than males, in particular if they are postmenopausal and that CRPS on upper extremity is more frequent than on lower extremity (de Mos et al. (2007); Sandroni et al. (2003)). There is high evidence that CRPS is associated with surgery in the upper limb and lower evidence for the lower limb. It is also reported that fracture is the most common trigger for the development of CRPS (Birklein et al. (2018)).

1.1.5 Pathophysiology

The aetiology of CRPS remains uncertain and the treatment is therefore empirical and of limited efficacy. Two principle possible group of mechanisms aim to explain pathogenesis and maintenance of CRPS, one involves central nervous system leading to a central sensitization and include altered cortical representation, both somatosensory and motor, of the affected limb, (Pleger et al. (2006)) and central nervous system-mediated abnormal sympathetic activation in this limb (Wasner et al. (2003)). The other mechanism implicates the peripheral nervous system and the immune system at the site of injury and specifically includes facilitated neurogenic inflammation, and aberrant immune responses (Birklein et al. (2001); Huygen et al. (2002)). Both, peripheral and

central mechanisms, together with other possible mechanisms such as psychological and genetic factors contribute to the integrative conceptual model of disease pathology (Figure 1.4).

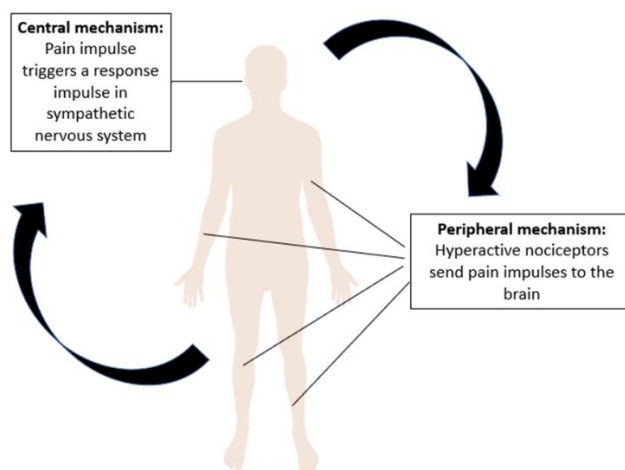


Figure 1.4 Possible mechanisms involved in CRPS.

The peripheral nervous and the immune system mechanism

In recent years, the understanding of CRPS has made significant progress. In 2015 Birklein et al. reviewed CRPS pathophysiology and proposed an initial peripheral inflammatory phenotype after limb trauma and a later central neuroplasticity phenotype. The proposed first phenotype is characterised by an exaggerated inflammatory response to the trauma with CRPS-affected limb revealing the five cardinal signs of inflammation (rubor, calor, dolor, tumor, and functio laesa), this situation is hypothesised to be caused by an increased

release of inflammatory mediators (such as cytokines), growth factors, catecholamines and neuropeptides which in turn activate keratinocytes, fibroblast or osteocytes in injured tissue contributing to trophic changes and sensitised nociceptors inducing persistent pain and heat hyperalgesia. The involvement of inflammatory mechanisms in the acute phase of CRPS has been documented by several studies that reported release of proinflammatory neuropeptides and mediators (substance P, calcitonin gene related peptide, bradykinin) and cytokines such as IL- β , IL-2, IL-6 and TNF- α (Bruehl (2015); Goh et al. (2017)). Other studies have suggested that the non-resolution of inflammatory process in CRPS is caused by downregulation of several microRNA that control inflammation in target cells. (Orlova et al. (2011)). Some studies have also documented abnormalities in the number of various immune cell types in the patients' peripheral blood such as an increased number of proinflammatory monocytes (CD14+ CD16+) and mast cells and depletion of CD20+B cells (Bruehl (2015)).

In recent years, several works have suggested a possible auto-immune component in CRPS pathophysiology where CRPS autoantibodies directly or indirectly sensitise primary sensory neurons. Initial patient trials demonstrated that some CRPS patients experience good pain relief after intravenous immunoglobulins and plasma exchange treatments, technologies which promote auto antibody elimination. Then further studies suggested that aspects of CRPS can be transferred to animals and that patients often have functionally active cell surface autoantibodies (Blaes et al. (2004); Goebel et al. (2010); Goebel and Blaes (2013); Kohr et al. (2011); Kohr et al. (2009); Tékus et al. (2014)).

The central nervous system mechanism

Months after the development of CRPS, a group of patients is suggested to start “centralising” CRPS, i.e. passing from the peripheral phenotype to a central neuroplasticity phenotype. This central phenotype is characterised by central sensitisation (see below), sensory deficit, altered body perceptions and movement disorders (Birklein and Schlereth (2015); Parkitny et al. (2013)).

‘Central sensitisation’ is characterised by a higher sensitivity of spinal neurons with consequent altered sensory transmission and sensorimotor processing in the spinal cord. In CRPS increased neuronal sensitivity is caused by peripheral tissue injury (Van Hilten (2010); Woolf and Salter (2000)). Mechanical allodynia is one hallmark of central sensitization, it is one often present feature which is caused by prolonged inputs to the dorsal horn as a result of sensitization in C fibre nociceptors which in turn can be mediated by neuropeptides in the periphery such as substance P, bradykinin and glutamate (McBride and Atkins (2005); Goh et al. (2017)).

Interestingly, some patients with CRPS present with altered sympathetic nervous system activity, resulting in abnormal nail or hair growth and also contributing to the observed vasomotor changes. Although the causes for such abnormal activity has remained unclear, central effects may play a role including reduced neuronal activity in primary and secondary sensory cortex areas. CRPS patients are also subject to important changes in the motor cortex, and further it is clinically shown that they often feel alienation with their affected limb and that they must concentrate to use it (Birklein and Schlereth (2015)).

Other possible mechanisms particularly genetic and psychological factors are often considered to contribute to the integrative conceptual model of disease pathology, but so far there is a lack of understanding regarding the role of these two factors in CRPS. Recent family studies suggest that genes encoding the human leukocyte antigens (HLA) system and α 1a-adrenoceptors are involved in CRPS development. Other studies demonstrated a mitochondrial inheritance pattern in CRPS that explains the fact that siblings of CRPS patients under fifty years old have a high risk to develop the condition. (Goh et al. (2017)). Finally, psychological factors may play a role in perpetuation of CRPS but, as many studies suggest, these alone do not cause CRPS. (Bruehl (2015)).

1.1.6 Treatments

Like the diagnosis of CRPS, treatment has also proven to be difficult across patients. After diagnosis, medications are commonly used including steroids, analgesics, antidepressants and anti-neuropathic drugs (Kim et al. (2020)) which are typically offered in combination psychological support and physiotherapy. Physical therapy that includes moving the painful limb can improve blood flow and lessen circulatory symptoms such as swelling to increase flexibility strength and function. Although some clinical reports and small trials suggest that additional treatments given early such as ganglion block, spinal cord stimulation and surgical sympathectomy can help to temporarily reduce persistent pain (Crapanzano et al. (2017); Herschkowitz

and Kubias (2018)), there is no evidence that these are curative for any CRPS patients (Bruehl (2015)).

As discussed above, acute CRPS often improves naturally; whether drug treatments such as corticosteroids, anticonvulsant, opioid analgesics can play a role to accelerate such improvement is currently unknown.

In contrast, chronic CRPS is complex and typically won't improve; such chronic/persistent CRPS should be treated with multidisciplinary treatments (medical, psychological and physical) to help patients improve their quality of life (Stanton-Hicks et al. (2002)).

Sometimes patients with persistent CRPS ask clinicians to have their limb amputated as last extreme attempt to reduce their pain when no other treatment was efficient. In this case clinicians should discourage their CRPS patients from considering this operation because there is currently no clear evidence for the beneficial effect of an amputation (Bodde et al. (2011)) (Figure 1.5).

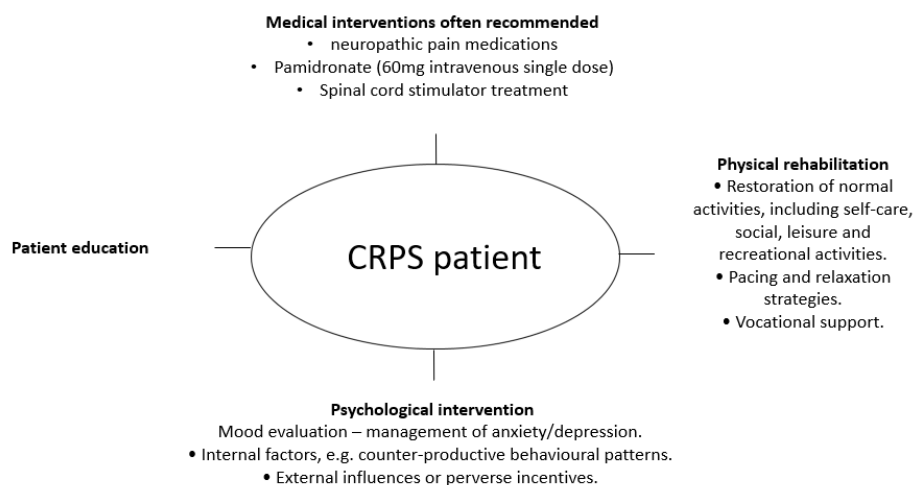


Figure 1.5 The four pillars of care for CRPS.

Adapted from Goebel et al (2018).

A recent review by Birklein et al published in 2018 described an up to date range of biomarkers directly associated with CRPS that may support clinicians in their diagnosis, prognosis and treatment. The most relevant biomarkers that are proposed as promising include: microRNAs, blood and serum. Skin biopsies can be used to measure keratinocyte and mast cell accumulation. Both cell types proliferate in CRPS affected skin in the acute phase but not in the chronic phase (Birklein et al. (2014)). MicroRNAs could be a valuable source of information regarding cellular homeostasis and abnormal gene expression, but so far research on microRNA in CRPS patients is still in his infancy (Birklein et al. (2018)). Blood and serum biomarkers include serum cytokines, Osteoprotegerin (involved in bone turnover) for Early/Acute CRPS (Lenz et al. (2013); Krämer et al. (2014)) and serum autoantibodies identified as biomarkers for both early and persistent CRPS (Kohr et al. (2011); Dubuis et al., (2014)).

One emerging therapy for CRPS patients presenting with autoantibodies as serum biomarkers, could be plasma exchange therapy (PE) or plasmapheresis (figure 1.6). PE is a standard procedure used for autoimmune disorders that separates plasma, containing autoantibodies, from whole blood and replaces plasma with a saline solution before return to the patient. Thereby it substantially reduces blood auto antibody levels by 70-80%.

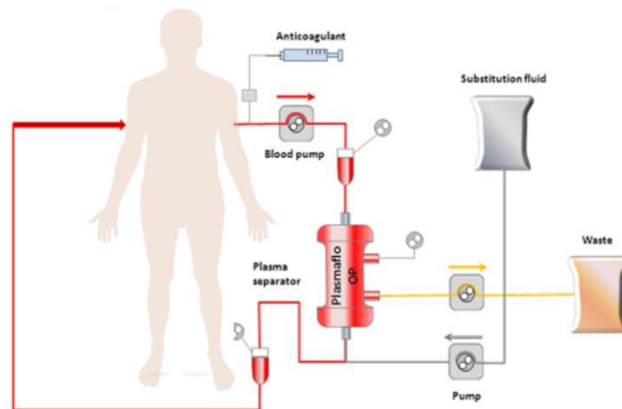


Figure 1.6 Plasma exchange therapy (PE) or plasmapheresis.

PE is a standard procedure used for autoimmune disorders that separates plasma, containing autoantibodies, from whole blood and replaces plasma with a saline solution before returning it into patients.

Together with PE therapy, Intravenous immunoglobulin treatment (IVIg) has been tested for CRPS. IVIg treatment consists in administration of highly purified polyclonal IgG fraction obtained from pooled plasma of thousands of healthy donors. The suggested mechanisms of action of IVIg treatment against autoantibodies involves anti-idiotypic antibodies which bind to the variable region (fab portion) of the autoantibodies preventing its binding to the self-antigen and promoting its elimination (Figure 1.7) (Yu and Lennon (1999); Ballou (2011)). IVIg treatment is currently used as treatment of choice for patients with antibodies deficiencies and for some autoimmune disorders such as Guillain-Barre polyneuropathy, an autoimmune disease where the myelin sheath that surrounds the axons is degraded (Arnson et al., (2009); Kaveri et al., (1991)), or inflammatory disorders such as myopathies including dermatomyositis and polymyositis. (Lünemann et al. (2016); Dalakas (2004); Sherer et al. (2002); Zuercher et al. (2016)).

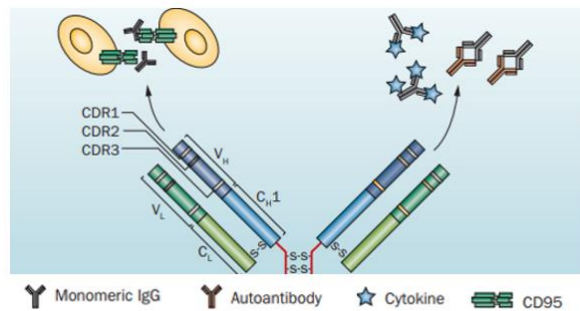


Figure 1.7 Intravenous immunoglobulin treatment (IVIg).

Mechanisms of action of IVIG treatment against autoantibodies includes monomeric antibodies which bind to the variable region (fab portion) of the autoantibodies and to cytokines preventing its binding to the self-antigen and promoting its elimination. Furthermore, monomeric antibodies block cell–cell interactions that are mediated by cell-surface receptors. Figure adapted from (Lünemann et al. (2015))

Preliminary works conducted in a small group of patients suffering from chronic pain conditions, showed that low-dose (0.5g/kg) IVIG treatment can reduce pain in most of these including refractory CRPS (Goebel et al. (2002); Goebel et al. (2010)). In contrast with these works, a recent trial conducted in a group of 108 patients demonstrated that low-dose IVIG treatment had no clinically important effect on pain intensity in patients with moderate to severe CRPS of 1–5 years' duration (Goebel et al. (2017)). This last result suggests that low-dose Intravenous immunoglobulin treatment (IVIg) is very unlikely effective for persistent CRPS, however responses to high-dose IVIG, PE therapy or to immune therapies that target lymphocytes are yet to be assessed.

1.1.7 New Pain Classifications

Chronic pain is a frequent condition that lasts or recurs for more than three months (IASP online terminology); according to the literature, chronic pain affects 20% of people worldwide (Goldberg and McGee (2011)) In the past two decades classification of some of the most common chronic pain conditions has often been considered unclear, and in particular classification of unexplained chronic pains has been difficult and challenging because of a lack of clear understanding about their etiology and because often psychological and social factors also contribute to chronic pain (Nicholas et al. (2019)). In 2015 the IASP Task force began to develop an updated classification of chronic pain for revision of the 11th International Classification of Diseases (ICD) published by World Health Organisation (WHO). The ICD-11 classification comprises of seven groups of chronic pains, the first group is called chronic primary pain and includes common and uncommon chronic pain conditions with an unknown aetiology while all other groups (chronic cancer pain, chronic post-traumatic and post-surgical pain, chronic neuropathic pain, chronic headache and orofacial pain and chronic visceral pain) are secondary pain syndromes (Nicholas et al. (2019)).

Chronic primary pain lasts for more than three months, affects one or more anatomic regions, cannot be identified as any other pain condition, and patients usually show significant emotional distress and significant functional disability. Chronic primary pain can affect any body site in isolation, or when it affects a combination of body sites it is called widespread pain. CRPS is classified as a chronic primary pain condition.

1.2 The human sensory system and pain

The human body uses a highly specialized and interconnected sensory system ('nociceptive system') to rapidly respond to noxious or harmful stimuli and thereby protect the body before tissue damage occurs. This sensory system helps to conduct information from the periphery about noxious stimuli to the brain, where pain is first perceived (Woolf and Ma (2007); Basbaum et al. (2009)). The pain perception network is composed by two main parts: the peripheral nervous system (PNS), formed by all nerves outside the brain and the spinal cord, which responds to noxious stimuli and through the electrical encoding provides a signal to alert the organism to potential injury; and the central nervous system (CNS) which conveys signals from the PNS to the brain and then in the brain processes these signals and coordinates the body's reactions.

According to its duration, pain can be classed into two types: acute and chronic. In clinical terms, acute pain typically lasts up to 3 months, until the acute tissue injury has typically resolved; it is typically proportional to the tissue damage, for this reason it is considered beneficial and protective. (Millan (1999)). On the contrary, chronic pain is characterised by non-transient pain and this is usually a result of abnormal and continuous neuronal activation even if tissue damage is resolved (Wall and Gutnick (1974)).

Pain Pathways

When a nerve or adjacent nerve fibres are damaged, various cells type surrounding the injury release peripheral “sensitizers” like cytokines, growth factors and nitric oxide that cause neuronal cell hyperexcitability. Spontaneous ectopic firing of nociceptors leads to peripheral and central sensitization and consequent pain with alterations in gene expression within neuronal and non-neuronal cells (Uçeyler et al. (2009);Koch et al. (2007)).

In primates and in humans, some sensory information (pain, temperature, non-discriminative touch and pressure) is transmitted throughout three groups of neurons in sequence that orchestrate the pain pathways; the spinothalamic tract (STT) is a well-known pain pathway that takes part in the signalling and perception of touch, pressure and visceral sensation (Mantyh (1983)). The first group of neurons involved in the STT are primary afferent (or sensory dorsal root ganglion, DRG) neurons, which create the signal in response to stimuli in the periphery. DRG neurons innervate sensory organs and transmit a nociceptive signal to the second group of neurons in the dorsal horn of the spinal cord. The second group of neurons connect the spinal cord and the brain, these neurons include the relay neurons and the interneurons that are responsible for signal modification (Millan (1999); Dubin and Patapoutian (2010)). Finally, the third group of neurons terminate in the brain. (Willis and Westlund (1997)). After an injury the first group of neurons trigger various changes in neuronal and biochemical processing such as phosphorylation of transcription factors like nuclear factor kB (NFkB), receptors like kainite receptors and lead to central sensitisation (Basbaum et al. (2009)). These modification lead to the migration of ion channels and receptors to the cellular

membrane (Wang et al. (2006); Woolf and Ma (2007)). Biochemical processing and peripheral “sensitizers” around the injury contribute to the states of peripheral and central injury.

Dorsal Root Ganglia

Primary sensory neurons, which are involved in the transduction of the sensory information from the periphery have their cell bodies in the dorsal root ganglia (DRG). Humans have in total 62 spinal nerves, 31 right and 31 left divided in different groups: cervical (8 right-left pairs), thoracic (12 right-left pairs), lumbar (5 right-left pairs), sacral (5 right-left pairs) and coccygeal (1 right-left pair). Spinal nerves contain afferent sensory axons located dorsally (dorsal root) and motor ventral efferent axons (ventral root). The dorsal root ganglion (DRG) is an enlargement of the dorsal root, in particular the dorsal root forms the DRG when exiting the neural foramina (Krames (2014); Esposito et al. (2019)), so that each spinal nerve has an associated dorsal root ganglion; the only exemption may be C1, as it is a spinal nerve with a purely motor neuron nature so that dorsal root ganglion may be rudimentary or absent (Yabuki and Kikuchi (1996)). Anatomically, DRGs are located outside the blood brain barrier; this ensures good blood supply and also allows both small and large molecules and even cells circulating in the vascular system to directly reach DRGs (Haberberger et al. (2019a)). Each dorsal root ganglion contains spherical cell bodies of up to 15,000 pseudo-unipolar sensory neurons that innervate the corresponding segmental level (Figure 1.8). Considering some dimensions, DRG neurons are a varied population with a diameter range from 20 to 150µm

Esposito et al. (2019) and according to cell body size, they can be divided into three groups: large (>30), medium (23-30) and small (<23) (Djoughri et al. (2006); Djoughri and Lawson (2004)).

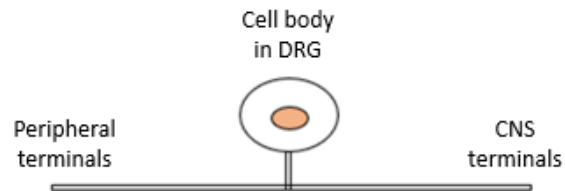


Figure 1.8 Pseudo-unipolar neuron.

The pseudo-unipolar neuron has the cell body in the dorsal root ganglion and the axon is divided in two parts. The proximal one reaches the central nervous system and the distal one reaches its peripheral targets in the skin, muscles, deep tissue.

DRG neurons subgroups

DRG neurons are activated by a variety of sensory stimuli. They extend their afferent nerve fibre axons into the periphery of the body that are responsible for thermo-reception, nociception, mechanoreception and proprioception (Nascimento et al. (2018)). Large and medium DRG neurons are myelinated and have respectively $A\alpha/\beta$ and $A\delta$ fibres with high conduction velocity while small DRG neurons are un-myelinated and have c-fibres with low conduction velocity(McCarthy and Lawson (1990)) (table 1.3).

Table 1.3 Primary afferent nerve fibres.

Adapted from (Julius and Basbaum, (2001)).

Type of fibre:	A α , A β	A δ	C
Myelin:	<ul style="list-style-type: none">• Myelinated	<ul style="list-style-type: none">• Lightly myelinated	<ul style="list-style-type: none">• Unmyelinated
Diameter:	<ul style="list-style-type: none">• large	<ul style="list-style-type: none">• medium	<ul style="list-style-type: none">• small
Responsible for:	<ul style="list-style-type: none">• Proprioception	<ul style="list-style-type: none">• Nociception	<ul style="list-style-type: none">• Nociception

After tissue injury, medium and small DRG neurons (commonly described as nociceptors) release neuropeptides into the injured skin, such as substance P or calcitonin gene related peptide (Schäffer et al. (1998)); these neuropeptides promote a neuro- inflammatory process termed 'neurogenic inflammation' resulting in increasing vasodilatation and extravasation (Knibestöl (1973)) and further nociceptive excitation (Woolf and Wiesenfeld-Hallin (1986)), consequently contributing to the more diffuse and deeper secondary pain.

Nociceptors

Nociceptors are a specialized subgroup of DRG sensory neurons that respond to mechanical, chemical or thermal noxious stimuli (nociception). These are the most abundant type of DRG neurons. Nociceptors can be divided into different subsets according to their conduction velocity and then their stimulus modality. On the basis of their conduction velocity, nociceptors are divided in A-fibres and C-fibres (Pinho-Ribeiro et al., (2017); Dubin et al., (2010)); According with Djouhri et al 73% small c-fibres neurons are nociceptors, 23%

of medium size neurons are nociceptors and 20% of large neurons are nociceptors (Djouhri et al. (2006)) (Table 1.4) (Figure 1.9).

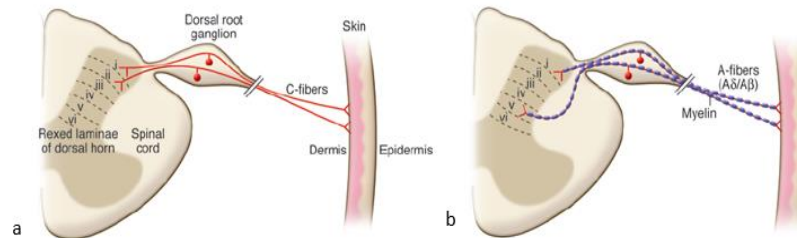


Figure 1.9 Nociceptive fibers in the peripheral sensory system.

a. C-fibers are small unmyelinated fibers that project to laminae I and II of the dorsal horn. b. A-fibers are bigger myelinated fibers that project to the laminae I and V. Figure taken from Dubin et al. 2010 (Dubin et al. (2010)).

On the basis of their responses to stimuli, nociceptors are divided in mechanical, heat and cold. High threshold mechanical nociceptors, or mechanoreceptors, respond to excessive pressure, such as a pinch and pin-prick or mechanical deformation such as a cut (Delmas et al. (2011)). According with Lewin et al., mechanoreceptors are 32% of all DRG neurons, the majority of mechanoreceptors are small C-fibres neurons and only 12% are bigger A-fibres neurons (Lewin and Moshourab (2004)) (table 4). In 1983, Schaible and Schmidt observed for the first time a category of mechanically insensitive nociceptors that can be activated by inflammatory mediators such as bradykinin, protein kinases, prostaglandins, serotonin and histamine. (Schaible and Schmidt (1983); Dray et al. (1988); Schepelmann et al. (1993); Birrell et al. (1993); Davis et al. (1993)). Mechanically insensitive nociceptors could play an important role in maintaining chronic pain because they are

involved in development and maintenance of hyperalgesia or hypersensitive states (Gold and Gebhart (2010)). Thermal nociceptors are medium and small nociceptors that mediate thermal pain responding to noxious heat or noxious cold (Meyer et al. (1994); Julius and Basbaum (2001)). Most of noxious heat thermoreceptors are activated at more than 43°C and a minority are activated at more 50°C (Cesare and McNaughton (1996); Kirschstein et al. (1997)). Noxious cold nociceptors are activated by temperatures below 15°C (Basbaum et al. (2009)). and according to Hensel and Zotterman even by cooling agents such as menthol and eucalyptol (Hensel and Zotterman (1951)). Chemical nociceptors are mainly activated by a variety of chemical stimuli and chemical irritants such as Capsaicin which is the ingredient of hot chili pepper (Frias and Merighi (2016)). Chemical nociceptors are also activated by low pH, lactic acid and inflammatory mediators (Gold and Gebhart (2010)). The most common type of nociceptor is the polymodal nociceptor. Differently from other nociceptor types that are activated by only one specific stimulus, polymodal nociceptors are activated by a several noxious stimuli (mechanical, thermal and chemical) (Perl (1996)).

Table 1.4 Nociceptors subpopulations.

(Djoughri et al (2006); Lawson (2004); Millan (1999); Lewin (2004)).

Nociceptors %	~20%	~23%	~ 73%
Fibre	A α / β -fibre (Large)	A δ -fibre (Medium)	C-fibre (small)
Cell diameter	>30	23-30	<23

stimulus	12% mechanical/ innocuous	Mechanical, thermal, chemical	Mechanical, thermal, chemical
----------	---------------------------------	----------------------------------	----------------------------------

Other cells type in DRGs

DRG not only contain sensory neurons but also a variety of other non-neuronal cell types including a type of glia known as satellite cells (SGC) (Haberberger et al. (2019b)), endothelial and smooth muscles cells that are part of small blood vessels, and some immune cells such as macrophages, t-lymphocytes and few b- lymphocytes (Schmid et al. (2013); Lakritz et al. (2015); Makker et al. (2017)).

SGC are supportive cells surrounding neurons and do not produce any electrical impulse. The cell bodies of the DRG neurons are separated from each other by an envelope of satellite glial cells that are coupled by gap junctions and express connexin 43 which suggest an involvement in cell-to cell communication (Koeppen et al. (2016)). SGC undergo both morphological and biochemical changes in response to nerve injury; they multiply and release inflammatory mediators which regulate neuronal excitability and immune reactions involving white cells, macrophages, T cells, glial cells and Schwann cells within the DRG (Esposito et al. (2019); Matsuka et al. (2020); Esposito et al. (2019)).

Pain treatments targeting the DRG

The DRGs have been specifically targeted by chronic pain treatments; in particular DRG neuro-stimulation can achieve focused and precise therapy to a specific painful area such as part of a foot or hand (Van Buyten et al. (2015); Harrison et al. (2018)). DRGs can be accessed from both the periphery, and from the spinal cord epidural space through the neuroforamina to the outside. DRG neuro-stimulation masks the sensation of pain via delivery of electrical impulses generated by an implanted pulse generator to electrodes placed in the epidural space. Recently, dorsal root ganglion stimulation has been approved as a treatment modality for intractable pain such as CRPS (Crapanzano et al. (2017); Herschkowitz and Kubias (2018)).

1.3 Immune system and pain

1.3.1 Inflammation

Inflammatory response (Inflammation) is a process coordinated by the immune system (innate immune system and adaptive immune system) including the release of inflammatory mediators that aims to a) remove

harmful stimuli of various natures, including infectious agents, cell debris after injury, toxic compounds or irradiation and b) coordinate the healing process (Medzhitov (2010); Ferrero-Miliani et al. (2007)). At tissue level, inflammation is well characterised by five cardinal signs: redness, swelling, heat, pain and dysfunction and by recruitment and accumulation of innate and adaptive immune cells (Libby (2007)), furthermore inflammatory cytokines, proteins and enzymes released by these and other cells play a role and can be used as bio-markers of inflammatory diseases.

Inflammatory cells are part of both the innate and adaptive immune systems. The innate immune system contributes to initiation and amplification of the inflammatory response and it acts through inflammatory cells and proteins. Several inflammatory cells are involved in acute inflammation: neutrophils which are the first and most abundant leukocytes to arrive at the site of injury, macrophages, dendritic cells, natural killer cells, together with inflammatory proteins such as complement and coagulation system (Stramer et al. (2007)). The innate immune system responds quickly to injury and the main effectors are macrophages with their scavengers and toll-like (TLRs) receptors (Fujiwara and Kobayashi (2005)). On the other hand, the adaptive immune system responds slowly, once activated by the innate immune system, targeting precisely and directly antigens through Th1 and Th2 cells. Th1 release cytokines that stimulate macrophages and Th2 stimulate B-cells antibody production (Libby (2007); Chaplin (2010)).

Inflammatory cells of both innate and adaptive immune systems cross-talk with cells in the injured tissue releasing inflammatory mediator molecules divided in cytokines, chemokines, and non-cytokines inflammatory mediators such as eicosanoids, arachidonic acid metabolite, leukotrienes, thromboxane. Cytokines are soluble glycoproteins released by many cell types, in particular by immune cells and are crucial to coordinate the inflammatory response. Cytokines can be divided in pro-inflammatory and anti-inflammatory and include interleukins (IL-1A, IL-1 β , IL-4, IL-6, IL-10, IL-12, and others), growth factors (including TGF- β), interferons (IFN- γ) and haematopoietic factors. IL-1 β , IL-6, IL-12, TNF- α , INF- γ are pro-inflammatory while IL-4, IL-10, TGF- β are anti-inflammatory cytokines (Chen et al. (2018)). Cytokines and other inflammatory mediators activate toll like receptors (TLRs) triggering several intracellular signalling pathways including the mitogen activated protein kinase (MAPK), nuclear factor Kappa-B (NF κ B), Janus kinase (JAK) and signal transducer and activator of transcription (STAT) (Hendrayani et al. (2016); Kyriakis and Avruch (2001)) (Figure 1.10).

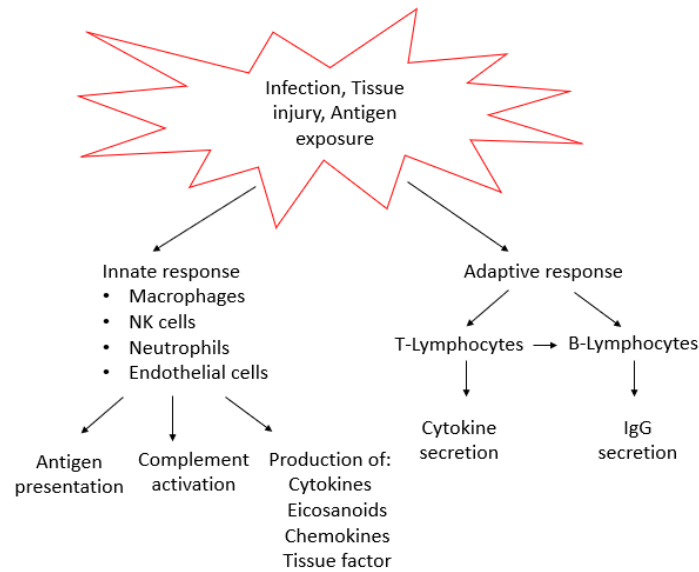


Figure 1.10 The immune response to injury and infection.

The innate immune system contributes to initiation and amplification of the inflammatory response, and it acts through inflammatory cells and proteins. The adaptive immune system targets precisely and directly antigens through Th1 and Th2 cells. Th1 release cytokines that stimulate macrophages, regulatory T cells and Th2 stimulate B-cells antibody production. Figure adapted from Sherwood et al 2004 (Sherwood and Toliver-Kinsky (2004)).

Usually inflammation starts with an acute phase which lasts for 1-3 days when pro-inflammatory mediators and immune cells trigger and maintain inflammatory response. The acute phase is characterised by vasodilatation and oedema; these early signs of inflammation facilitate the movement of inflammatory cells, soluble factors and acute phase proteins (coagulation cascade and complement system) to the site of injury. Within several minutes from the injury, inflammatory mediators such as histamine and bradykinin trigger exudation of protein-rich fluid from vascular compartment to the interstitial space. This environment facilitates innate immune system cells (leukocytes) migration to the site of injury. This process consists of three phases: rolling, adherence and

diapedesis mediated by selectins, integrins (expressed by neutrophils) and intracellular adhesion molecules (ICAM) (expressed by endothelial cells). The acute phase is followed by a sub-acute phase (from 3-4 days to 1 month), characterised initially by an amplification of inflammatory response and cross-talk between immune system and tissue cells. The final part 'sub-acute phase' (resolution phase) leads to restoration of tissue homeostasis and is characterised by inflammation resolution where pro-inflammatory response gradually decreases and anti-inflammatory mediators are released. During the resolution phase neutrophils stop infiltrate tissue, and macrophages stop releasing cytokines (Reville et al. (2006); Serhan and Savill (2005)). If inflammation is not resolved by one month from the sub-acute phase start, then it becomes chronic and can last several months with consequent additional tissue damage. chronic inflammation is probably caused by altered tissue repair or inflammation resolution mechanisms (Lintermans et al. (2014)). Chronic inflammation contributes to a wide range of chronic complex inflammatory diseases causing further tissue damage and fibrosis, such as asthma and diabetes (Zhou et al. (2016)).

1.3.2 Autoimmunity

Autoimmunity consists of an adaptive immune response against self-antigens on the organism's own tissues (Clark et al. (2018)). Autoimmune syndromes are usually chronic and debilitating and many treatments are inadequate. In a study published in 2012 the prevalence of autoimmune diseases in the population was approximately 10% overall with a higher percentage of females affected (6.4%) than males (2.7%) (Hayter and Cook (2012)). Autoimmune disease can be divided according to four categories: largely systemic, such as Rheumatoid Arthritis, largely tissue specific, such as type I diabetes, largely cell mediated, such as multiple sclerosis and largely antibody mediated, such as Myasthenia Gravis (Table 1.5).

Table 1.5 Autoimmune disease classification.

Examples of most common autoimmune diseases divided in four categories a-b) systemic vs. tissue specific, c-d) cell mediated vs antibody mediation.

A. Largely systemic	B. Largely tissue specific
Rheumatoid Arthritis	Type I Diabetes
Systemic Lupus Erythematosus	Grave's Disease
Dermatomyositis	Vitiligo

C. Cell mediated	D. Antibody mediated
Multiple Sclerosis	Myasthenia Gravis

Rheumatoid Arthritis	Rheumatoid Arthritis
Systemic lupus erythematosus	Systemic Lupus Erythematosus

Environmental factors as pollution, diet, smoking and hormonal factors (as most autoimmune diseases are frequent in women) together with polygenic risk factors initiate common human autoimmune diseases (Marson et al. (2015)). The majority of autoimmune diseases are against tissue specific antigens not normally exposed to the immune system.

The observed parallel between an increasing incidence of autoimmune diseases and a declining incidence of most infectious diseases in developed countries has been proposed to suggest that environmental bacterial and parasitic infections contribute to protect against some autoimmune conditions (hygiene hypothesis) (Bach (2018)). On the contrary, there is evidence that viral infection often causes rather than prevent autoimmunity as it triggers pro-inflammatory response, tissue damage and release of self-antigens. Furthermore, molecular mimicry between viral and self-antigens after immune response to virus antigens can cause autoimmunity (Mills (2011)). Molecular mimicry occurs when a foreign (microbial) molecule has a similar structure of a self-molecule of the host. Molecular mimicry is considered one of the leading mechanisms that contribute to the development of an autoimmune disorder, other mechanisms may be a breach in central tolerance and persistent antigenic stimulation (Rojas et al., (2018)).

Several factors influence autoimmune disease development, such as association with the human leukocyte antigen (HLA) region II (Gough and Simmonds (2007)), presence of activated auto-reactive T cells, excessive T cell mediated responses and presence of auto-reactive pathogenic B cells. The pathophysiology of T-cell mediated autoimmune disease is usually related to two mechanisms: an incomplete central or peripheral tolerance of T cells to certain self-antigens which are not highly expressed in thymus, and presence of defective regulatory T cells specific for tissue-specific self-antigens. The initiation phase is followed by a propagation phase in which cytokine production and a disrupted lymphocyte T balance contribute to perpetuate inflammation and tissue damage. Finally, in the resolution phase lymphocyte T cells are activated by self-antigens and contribute to resolve inflammation (Suurmond and Diamond (2015)). Frequently cell mediated autoimmune mechanisms are caused by genetic mutations in key protein-coding genes described below. CTLA-4 (protein expressed in regulatory T cells) mutations are associated with regulatory T cells (involved in suppression of immune and autoimmune responses) altered suppressed function (Marson et al. (2015)). Tyrosine phosphatase gene (PTPN22) mutations are associated with altered thymic development and altered T-cell receptor activation and Toll like receptors signalling (Rawlings et al. (2015)). Activated T cells may produce pro-inflammatory cytokines or attract macrophages or neutrophils which cause tissue damage (Bluestone et al. (2015)). Other common mechanisms across autoimmune diseases involve CD6,

tumour-necrosis-factor receptor (TNFR) AND IL-2 receptor (Marson et al. (2015)).

Auto antibodies

Antibodies (Ab), also known as Immunoglobulins (Ig) are a major component of humoral immunity and are divided in five classes or isotypes: IgG, IgM, IgA, IgE and IgD. They are glycoproteins found in serum and tissue fluids which are produced in large amount by B-cells after contact with immunogenic foreign molecules. Antibodies bind specifically to the antigen that induced their formation and target it for destruction. All antibodies have the same basic structure that can be broken into variable and constant region; the variable region is antigen specific and contains two fragment antigen binding (Fab) sites, while the constant region also known as fragment crystallizable (Fc) is isotype specific and stimulates antigen destruction (Figure 1.11).

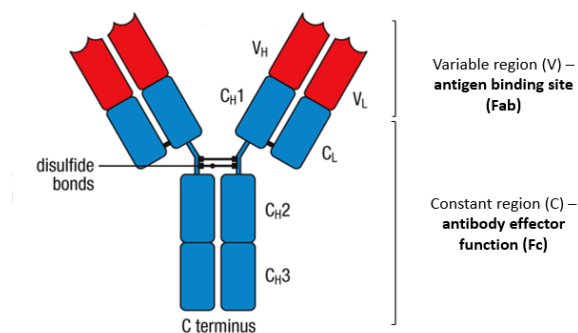


Figure 1.11 Antibody structure.

An antibody is made of two identical Light chains (VL and CL) and two identical heavy chains (VH and CH1, CH2, CH3). The variable region contains the antigen binding site (FC) and the constant region contains the antibody effector site. Image adapted from Janeway's Immunobiology, 9th ed. (Garland Science)

Immunoglobulin G is a type of antibody normally found in blood and extracellular fluid and is predominant in adaptive immune responses (Birrell et al. (1993)). IgG isotype is 75% of normal serum immunoglobulins (14 mg/ml) and is divided in four sub-classes IgG1, IgG2, IgG3, IgG4, which are 70%, 20%, 8% and 2% of the normal serum IgG in humans. Immunoglobulin isotype and glycosylation/sialylation are important properties that modulate auto antibody inflammatory or anti-inflammatory response (Anthony et al. (2011)).

IgG has a basic monomer structure with a molecular mass of 150,000 Da (150kDa) and is involved in antigen neutralisation, opsonisation, and phagocytosis (Figure 1.12).

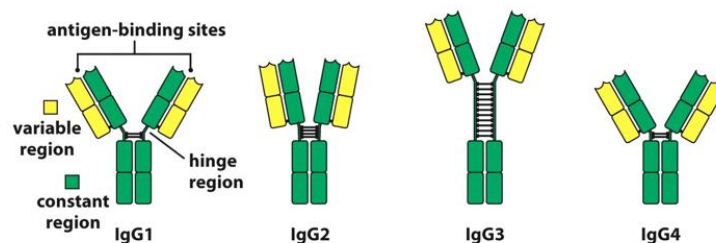


Figure 1.12 IgG isotypes.

IgG1 is responsible for antibody responses to soluble and membrane proteins. IgG2 is responsible for responses to bacterial infections. IgG3 is responsible for pro-inflammatory responses. IgG4 is responsible for immune responses to allergens and therapeutic proteins (Vidarsson et al (2014)). Figure adapted from the Immune System 3ed (Garland Science 2009).

Intravenous IgG is derived from purified IgG antibodies from several thousand blood donors and is used to treat immune deficiencies and as immunomodulatory therapy for some autoimmune disorders.

Auto antibodies are produced by auto-reactive B cells which had not been eliminated. Usually auto-reactive B cells which are highly reactive to self-antigens in the medulla are negatively selected, efficiently eliminated or undergo receptor editing in lymphoid tissues. Sometime some auto-reactive B cells with low binding affinity may escape (Wardemann et al. (2003)).

Auto antibodies can cause tissue damage either as a consequence of binding directly self-antigens on cells, or by forming immuno-complexes circulating in the peripheral blood. Several auto antibodies isotypes are involved in autoimmune diseases. The commonest auto antibody isotypes involved in autoimmunity are Immunoglobulin G and M (Birrell et al. (1993); Suurmond and Diamond (2015)).

Differential mechanisms of auto antibody-mediated autoimmune diseases

As with normal antibodies, the auto antibody mode of action consists of two steps, the first involves the antigen binding site of the F(ab) portions and the second involves the F(c) effector portion. In autoimmune responses that are not dependent on immune complex formation, F(ab) binds to surface membrane antigens such as receptors and ion channels, often altering some physiological functions either directly, or by receptor cross linking and internalisation (Graus et al. (1997); Peers et al. (1993)) (figure 1.13). On the other hand, the F(c) portion binds to F(c) receptors

(F-cR) expressed in different cell types including immune effector cells. F(c) mediated effects can amplify antigen-antibody interaction effects and – dependent on auto antibody class or subclass (which have a critical role) result in either complement, immune complex (involved after epitope binding) or cells activation, or a combination (Figure 1.13). Most anti-inflammatory immunotherapies, such as aspirin and glucocorticoids, reduce also F(c) mediated effects (Rowley and Whittingham (2015)). Some autoantibodies bind intracellular antigens such as nuclear, ribosomal and mitochondrial proteins. Several studies describe auto antibody internalisation through F(c) receptors especially in neuronal tissue which is rich of these receptors (Mohamed et al. (2002); Borges et al. (1985); Yoshimi et al. (2002)). Antibody internalisation might be associated with electrostatic interactions of arginine residues of the auto antibody with polysaccharides of cell membrane (Song et al. (2008)).

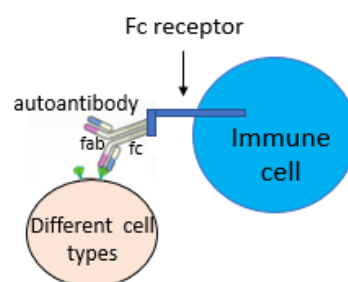


Figure 1.13 Fab and fc mechanism of action.

F(ab) binds to surface membrane antigens such as receptors and ion channels. F(c) binds to F(c) receptors (F-cR) expressed in different cell types including immune effector cells.

Auto antibody binding to cellular antigens secondarily usually causes inflammation and disease through Fc-receptor mediated cellular mechanisms such as mediator release or phagocytosis by Fc-binding cells, or through Fc-receptor mediated complement effects resulting in lysis of the Fab-bound cell such as in Haemolytic anaemia (Figure 1.14 c). As described above auto-antibodies through their Fab portion can also be receptor agonists and act like a hormone that leads to the release of a different hormone such as in Grave's disease (Figure 1.14 a). They can also block receptor function, for example by inhibiting binding of a neurotransmitter to its receptor such as in Myasthenia Gravis, or they can alter synaptic structures like in NMDA encephalitis (Figure 1.14 b). Finally, auto-antibodies circulating in immune-complexes (comprised of autoantibodies bound with their Fab section to the Fc sections of other antibodies) can cause inflammation where they deposit. Some antibodies cause inflammation (through their Fc sections) at their binding site, such as auto-antibodies against citrullinated proteins in Rheumatoid Arthritis (RA) and auto-antibodies against aquaporin-4 in Neuromyelitis Optica (NMO)(Ludwig et al. (2017)) (Figure 1.14 d).

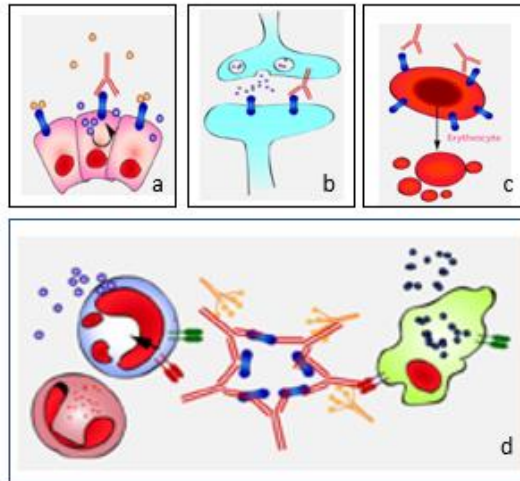


Figure 1.14 Mechanism of auto antibody induced pathology.

a) mimicry of receptor activation by hormone. b) blocking of neuronal transmission. c) direct cell lysis (a)-c) are mediated by binding of cells through the Fab portion). d) induction of inflammation by immune-complexes. Figure adapted from Ludwig et al. (2017).

1.3.3 Inflammation and pain

The immune system is actively involved in causing pain, both as part of physiological responses, and in pathological responses when pain is disproportionate to the cause. During inflammation, inflammatory mediators such as kinins, amines, prostaglandins, growth factors, protons, ATP, chemokine and cytokine released by immune cells and non-neuronal cells, activate directly nociceptors (McMahon et al. (2015); Verri et al. (2006)). The immune system thereby also lowers the nociceptor threshold to noxious stimuli (Woolf and Salter (2000); Schaible et al. (2011)). Peripheral sensitisation leads to a misrepresented

sensory stimulation which results in patient experiencing allodynia, hyperalgesia and 'spontaneous' pain in absence of external stimuli.

Intracellular signalling mechanism in peripheral sensitisation

Peripheral sensitization, describes the process of early post-translational alterations in the peripheral terminals of nociceptors and can be caused by changes in either the transducer molecule (e.g TRPV1 receptor), or the voltage gated ion channels (e.g. sodium channels) secondary to the phosphorylation of membrane bound proteins.

Electrical activity in sensitised nociceptors can increase intra-cellular calcium and activate intra-cellular transcription factors such as Camp-response element-binding protein (CREB). Various kinase families have been implicated as intracellular signalling systems involved in inflammation-mediated peripheral sensitization. Mitogen activated protein (MAP) kinases, including extracellular signal-regulated kinase (ERK) and p3845, cyclic adenosine monophosphate (cAMP) dependent protein kinase A (PKA), calcium dependent protein kinase C (PKC) and c-Jun N-terminal kinase (JNK)C have all been implicated (Hucho et al. (2005); Varga et al. (2006)). Inflammatory proteases, such as mast cell tryptase and trypsin, can also alter the sensitivity of the TRPV1 receptor, through binding of the protease-activated receptor (PAR) 2 expressed on sensory neurones(Dai et al. (2007); Ji et al. (1999)).

The role of inflammatory mediators in peripheral sensitization

Bradykinin (kinin) and prostaglandin E2 (pro-inflammatory prostanoid) are endogenous pain inducing inflammatory mediators that have widely been used to study nociceptive sensitisation during inflammation (Linley et al. (2010)). Both directly sensitise nociceptors by activating G-protein-coupled receptors (Wang et al. (2006); Lin et al. (2006)). Among cytokines, pro-inflammatory TNF- α , IL-1 β and IL-6 have been shown to induce pain or abnormal sensitisation (Uçeyler et al. (2009); Boettger et al. (2010)). In-vitro studies demonstrated that TNF- α increases intracellular calcium in cultured rodent DRG neurons inducing a rapid activation of p38 MAPK and c-jun N-terminal kinase (Pollock et al. (2002)). Another study demonstrated that IL-1 β sensitises murine DRG neurons through p38 MAPK pathway (Inoue et al. (1999)). Furthermore, a study in inflamed joints showed that nociceptors are sensitised by IL-6 in complex with its soluble receptor binding to glycoprotein 130 expressed on sensory neurones (Boettger et al. (2010)). Finally, the pro-inflammatory CC-chemokine ligand 3 (CCL3) has been shown to alter the sensitivity of the TRPV1 receptor (Rosenbaum and Simon (2007)). Among growth factors, granulocyte macrophage colony-stimulating factor (GM-CSF) contribute indirectly to inflammatory pain through an eicosanoid-dependent pathway (Lee et al. (2017)).

In addition to their effects on causing abnormal orthodromic (i.e. peripheral to proximal) electrical transmission in sensory nerves, inflammatory mediators described above also activate nociceptive nerve fibres to release neuronal mediators distally, such as substance P that

are responsible for increasing blood flow, inducing T cells to produce cytokines and stimulating macrophages (Wu et al. (2017); Totsch and Sorge (2017)). Finally, most non-neuronal cells within the DRG are actively involved in inflammatory pain process. DRG satellite glial cells, activated by sensory neurons contribute to nociceptive sensitisation releasing a variety of inflammatory mediators including IL-1 β , ATP, nerve growth factor, metalloproteases and CGRP. T cells, T lymphocytes, macrophages further contribute to sensitisation of nociceptive signalling by releasing chemokines and cytokines (Wu et al. (2017)).

1.3.4 Autoimmunity and chronic pain

Recent works have suggested the existence of chronic pain conditions caused by serum IgG directed against specific pain related components of the peripheral and central nervous systems. Furthermore, *in vivo* and *in vitro* studies have demonstrated that specific serum IgG auto-antibodies can cause nociceptive responses when injected in mice and can bind and activate cells in culture. Recently, several autoantibodies have been identified that bind to antigens which are well known to alter pain pathways: LG11, CASPR1, CASPR2, glycine receptor, amphiphysin and aquaporin-4 channel. Autoantibodies against other antigens, such as β -2 adrenergic receptor, muscarinic-2 receptor and alpha-1

adrenoreceptor have been identified in patients and may be involved in causing pathological pain but any mechanisms are still unclear (Mifflin and Kerr (2017)).

In 2016 Goebel suggested as 'auto antibody pain' conditions a group of chronic painful conditions characterised by absent or minimal regional immune cell infiltration and tissue damage, normal levels of inflammatory mediators and the apparent presence of functionally active autoantibodies that interfere with physiological cell function. Auto antibody pain conditions were suggested to be a subgroup of painful autoimmune diseases. In auto antibody pain conditions, nociception might be directly and completely induced by antigen-IgG binding, but without destructive immune cell or complement involvement and without classical signs of inflammation (Goebel (2016)). Examples of such conditions are joint pains preceding the development of rheumatoid Arthritis (RA) and Voltage Gated Potassium Channels (VGKC) complex disorders such as neuro-myotonia (although some contribution from nerve cell destruction can perhaps not be excluded) (Klein et al. (2012); Krishnamurthy et al. (2016)).

Auto antibody pain mechanisms

Possible auto antibody mediated pain mechanisms include: a) auto antibody-action related pain which is caused after Fab binding to cells or to other antibodies *by the Fc-mediated binding of cells and complement* causing inflammation and cell destruction, or by complex formation and deposition in tissues which again causes inflammation with cell

destruction, b) auto antibody-mediated pain where such a response is absent. This category can be further classified into i) Fab-mediated pains that are caused likely purely through actions of Fab on channels or receptors on neurons which change the way the neuron functions, ii) other, either Fab or Fc mediated mechanisms that work by enhancing mediator release from the bound cell; although this involves the same inflammatory mediators as a) above, this may not activate the same typical cascade of destructive immunity described earlier and which is the hallmark of the a) class of diseases. More research is needed to fully understand why in some conditions no inflammatory cascade is elicited, the exact mechanism how pain is then elicited in these conditions is only begun to be understood; some IgG subtypes are less associated with an inflammatory cascade and additional work need to be done to understand whether IgG antibodies play a role in an auto antibody pain condition such as CRPS.

An example of F(c) mediated painful neurological condition that is caused by autoantibodies is Neuromyelitis Optica (NMO); in this condition, auto antibody actions induce inflammation and lead to painful inflammation, which excites nociceptors through the typical receptors and channels, and nerve damage to spinal cord nerves which then fire abnormally. 75% of patients with NMO have autoantibodies associated with aquaporin-4 (AQP4) channel in central nervous system. There are probably several distinct mechanisms; autoantibodies cross link AQP4 channel with consequent channel internalisation and down regulation of glutamate transporters (Pittock et al. (2021)). This triggers inflammation with

production of inflammatory mediators such as chemokines and cytokines which may directly excite their respective receptors and additionally also cause tissue damage which can lead to abnormal, painful nociceptor electrical discharges, although the exact mechanisms are not fully understood. *In vitro* studies demonstrated that NMO autoantibodies induce death of cultured somatosensory neurons and axonal damage. (Mifflin and Kerr (2017); Xu et al. (2020)).

An example of a F(ab) mediated painful auto antibody related condition are VGKC complex disorders. VGKCC autoimmune disorders are a group of neurological diseases associated with autoantibodies against the VGKCC. Autoantibodies bind not directly to the ion channel but to proteins which form the subunit of the VGKC macro-molecular complex, such as leucine rich glioma inactivated 1 (LGI1) and contactin-associated protein-like 2 (CASPR2) which is the main target of VGKC antibodies (Plantone et al. (2015)). Patients with neuro-myotonia that present with pain among their clinical features are usually seropositive for CASPR-2 autoantibodies. In 2018 Patterson et al demonstrated that anti-CASPR-2 antibodies prevent neuronal cells adhesion inhibiting interaction between CASPR-2 (a cell adhesion molecule) and contactin-2 but these do not cause CASPR-2 internalisation unlike other autoantibodies targeting ionotropic receptors (Patterson et al. (2018)). In the same year, Dawes et al demonstrated that passive transfer of human CASPR-2 autoantibodies to mice causes pain related hypersensitivity in mice but no sign of inflammation or nerve damage; the authors suggested that CASPR2 auto antibody reduce Kv1 Membrane Expression on DRG

Neurons enhancing neuronal excitability and hypersensitivity (Dawes et al. (2018)). In Rheumatoid Arthritis (RA) some patients are seropositive for ACPA-autoantibodies. Recent research has suggested that these antibodies can activate osteoclasts (through either Fab or Fc mechanisms) to release the pronociceptive chemokine IL-8 that induces pain and directly sensitises nociceptors, but there is no activation of an inflammatory cascade. ACPA-autoantibodies appear to induce pain before development of the RA-typical joint inflammation (Krishnamurthy et al. (2016); Wigerblad et al. (2016)). Neuro-myotonia and pre-RA pains are therefore both good examples of ‘auto antibody pain’ conditions because auto-antibodies induce pain directly without overt inflammation. An overview of confirmed and purported mechanisms by which autoantibodies may cause pain is given in (Table 1.6).

Table 1.6 Mechanism of auto antibody pain.

(Dawes and Vincent (2016))

Antibody region involved	Pain mechanism
Fc	1)Sensitization/activation of nociceptors by inflammatory mediators with possible damage of nociceptors as result of inflammation
Fc	2)Complement activation and inflammation leading to neuronal damage
Fab	1) Binding site blockade
Fab	2) Alteration in target conformation
Fab	3) Target activation
Fab	4) Target crosslinking with internalization
Fab	5) Altered neuropeptide secretion from the nociceptor
Fab	6)Change in cell signalling such as increased mediator secretion consequently activating or sensitizing nociceptors

It is interesting to note that auto antibody pain mechanisms appear sometimes specific for chronic pain conditions that arise after a trauma. For example, in the ‘passive-transfer-trauma’ mouse model for CRPS,

physical injury to the hind-paw appears to trigger a transition of auto antibody action to become pathological (Tékus et al. (2014)). Here, either trauma may cause the presentation of new antigens to the immune system, or induce alterations of immunological tolerance. Whether the adaptive immune system releases new autoantibodies as a result of trauma, or whether pre-existing antibodies now become pathogenic is yet unknown (Goebel (2016)). Recent studies have suggested that in addition to persistent CRPS autoimmunity (likely IgM mediated) may also play a role early after trauma in cases that later resolve (Eldufani et al. (2020); David Clark et al. (2018)). Inflammation and in particular inflammatory mediators which are released after limb injury may promote the binding of pathogenic IgG to receptors on the surface of peripheral sensory neurons causing central sensitisation (Dawes and Vincent (2016); Goebel (2016)). However, it has also been suggested that CRPS antibodies may not be the cause of the syndrome but just a biomarker of the process (Birklein et al. (2018)).

1.3.5 Autoimmunity in CRPS

CRPS had long been understood as a sympathetically maintained pain condition with a neurogenic inflammatory process that contributes to the pathogenesis of the early phase (Wasner et al. (2003)). Only recently an

increasing number of works have suggested a possible auto-immune component in CRPS pathophysiology. In 2002 Goebel et al. demonstrated that some patients with CRPS appear to experience good pain relief with intravenous immunoglobulins. Then further studies suggested: i) aspects of CRPS can be transferred to animals, ii) patients often have functionally active cell-surface-directed autoantibodies and iii) Plasma Exchange therapy (PE) appear effective in a subgroup of patients with severe longstanding CRPS (Goebel (2011); Aradillas et al. (2015); Goebel et al. (2017); (Blaes et al. (2004); Goebel et al. (2010); Goebel and Blaes (2013); Kohr et al. (2011); Kohr et al. (2009); Tékus et al. (2014)).

In 2013 Goebel suggested a conceptual model for an antibody-mediated CRPS pathophysiology; in this model patient's autoantibodies exert an important role in sensitizing primary sensory neurons in the injured limb and in perpetuating the perception of pain. In particular, in the auto antibody model inflammation triggered after limb injury might facilitate the binding of circulating pathogenic IgG autoantibodies to antigens on primary sensory neurons (or cells close to these) and this could lead to a central sensitization in the spinal cord dorsal horn. (Goebel and Blaes (2013)) (Figure 1.15).

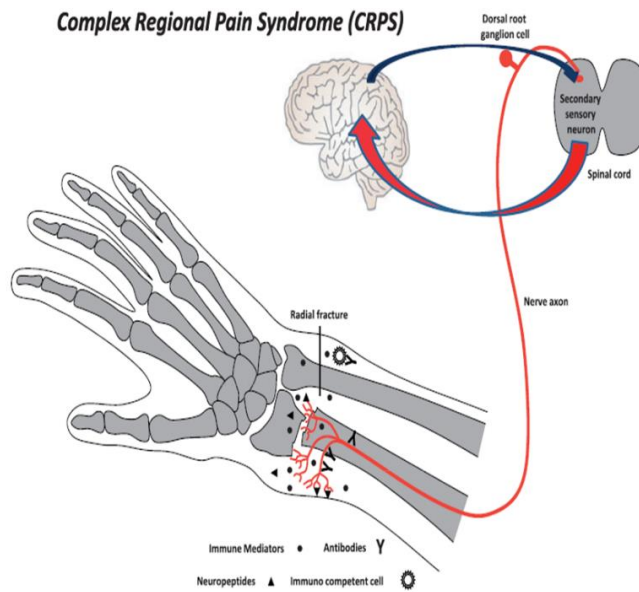


Figure 1.15 Antibody mediated model for CRPS

After radial fracture sensory nerve endings secrete neuropeptides (\blacktriangle) that enhance release of immune mediators (\bullet) from adjacent cells and from immuno competent cells (\odot). Such inflamed tissue may trigger the binding between CRPS autoantibodies (γ) and antigens on primary sensory nerves. (Goebel and Blaes (2013))

Mechanism of action of CRPS autoantibodies have not yet been determined and epitope specificities of the pathogenic autoantibodies remain unknown and require further research. However, more recently a significant improvement has been made in understanding the role of CRPS autoantibodies, both *in vivo* and *in vitro* (Tékus et al. (2014); Kohr et al. (2011)).

According with the Witebsky's postulates, a human autoimmune disease is defined following three steps: 1) recognition of an autoimmune response (auto antibody or cell mediated immunity) 2) identification of the antigen 3) induction of analogous autoimmune response in an experimental animal and the animal should develop a similar disease

(Rose and Bona (1993)). Following Witebsky's postulates, *in vivo* passive immunoglobulin transfer studies have been used in the past to demonstrate antibody involvement in autoimmune disease (Toyka et al. (1975)). *In vivo* studies are useful tools to study the pathophysiology of autoimmune diseases and candidate therapies. Mice are used for these studies because cell surface epitopes between mice and humans are structurally often well preserved (Rose and Bona (1993)).

In initial passive transfers models for CRPS IgG, authors injected CRPS IgG intraperitoneally in *normal* mice and this didn't induce CRPS clinical sign in mice (Goebel (2011)). The first passive transfer animal model using injured mice was published in 2014 by Tekus et al. In this model (lasting 8 days) mice were firstly injected with CRPS-IgG and then incised in one hind limb to resemble CRPS patient clinical features after trauma. At day 0, just after CRPS-IgG injection, plantar skin and muscle were incised, mice were then injected other two times on day 5 and day 6 and then sacrificed on day 8. Between day 0 and day 8 researchers performed a series of measures on injured paw including inflammatory neuropeptides (such as substance P) and cytokines (such TNF- α , IL-1 and IL-6). This animal model did not reproduce all CRPS clinical signs but did reflect some key features as limb swelling mechanical hyperalgesia and increased concentration of substance P in the injured paw. It successfully demonstrated that a combination of trauma and serum IgG triggers clinical disease (Tékus et al. (2014)). In 2019 the same research group developed an enhanced passive transfer model that confirmed previous findings that CRPS IgG induce an abnormally

increased sensitivity to pain (hyperalgesia) and a slowed resolution of limb swelling (oedema). Then the new model demonstrated that CRPS IgG increases Neutrophil Myeloperoxidase activity (MPO) but don't alter plasma extravasation and don't trigger a systemic or localized inflammatory response (mediators were not specifically raised early after surgery in animals injected with CRPS vs healthy IgG). Additionally, the authors demonstrated that CRPS IgG induces central nervous system glial activation along pain pathways, suggesting that inflammatory mechanism in the central nervous system are associated with the observed mechanical hypersensitivity in this model. Since glial cells are known to contribute to pain hypersensitivity responses through pro-inflammatory cytokines and among these IL-1, the authors then studied the effects of treating CRPS induced mice with an antagonist of IL-1 receptor (anakinra) and compared this with treatment with a glucocorticoid treatment (prednisolone). Anakinra treatment alone blocked all CRPS signs included microglia activation in the dorsal horn. To further confirm the role of IL-1 induced mechanisms in CRPS, the authors created an IL-1 knockout mouse line and found that knockout mice treated with CRPS IgG showed a significant reduction in mechanical hyperalgesia, paw oedema and microglia activation. In summary this study suggested that CRPS IgG contribute to activate microglia and astrocytes which through secretion of IL-1 are involved in maintaining persistent pain (Helyes et al. (2019)).

Recently, another study described electrophysiological investigation of neuronal hypersensitivities in the passive transfer-trauma model of

CRPS; in particular, by using a skin saphenous nerve preparation the authors demonstrated for the first time that CRPS autoantibodies actively induce increased sensitivity in mechanosensitive nociceptors (Cuhadar et al. (2019)). In line with previous passive transfer studies, this study confirmed that IgG from patients with long-standing CRPS induce clinical features such as mechanical hypersensitivity in mice and that specific minimal IgG doses are required (8mg per day) for to achieve successful CRPS passive transfer. Furthermore, the authors showed that IgG from patients with different pain intensities induce a different degree of hyperalgesia in mice and that pain intensity correlates with IgG mass transferred (Cuhadar et al. (2019)).

The CRPS passive transfer animal model described above explained a relevant number of mechanisms of CRPS pathophysiology, nevertheless cellular and molecular targets of CRPS IgG are still unclear and need to be investigated. In 2009 Kohr et al published an initial flow cytometry analysis of CRPS IgG binding to primary autonomic neurons demonstrating CRPS IgG specificity for a neuronal surface marker (Kohr et al. (2009)). In further studies the beta2 adrenergic receptor and the M2 muscarinic acetylcholine receptor were identified as antigens of CRPS auto-antibodies intracellular Ca (2+) concentration measures on cell lines (over-expressing these receptors) incubated with CRPS IgG (Kohr et al. (2011)). Interestingly, other intracellular Ca⁺² concentration studies on DRGs (that express alpha-1 adrenoceptors) showed a reduction of intracellular calcium levels in sensory neurons that have been pre-incubated with inflammatory mediators (Reilly et al. (2016)).

Another study analysed proteins obtained from dorsal hind-paw skin in mice with limb fracture and cast immobilisation. Proteins were analysed with mass spectrometry, and Keratin-16 (KRT-16) which is involved as a target in some autoimmune conditions, was identified as a possible autoantigen reactive with CRPS sera and consequently a possible biomarker for CRPS. This study suggested that skin related autoantigens may contribute together with neural tissue autoantigens to CRPS autoimmune mechanisms, further underpinning the complexity of CRPS (Tajerian et al. (2017)).

A very recent study identified P29ING4 as a possible biomarker for early-stage CRPS type I. P29ING4 belongs to the tumour suppressor proteins family and it activates apoptosis and is involved in inflammation in particular in joints (Baerlecken et al. (2019)).

1.4 Hypothesis and Aims

In vivo and *in vitro* studies described in this chapter have made important and fundamental initial efforts in identifying molecular targets for CRPS IgG but mechanism of action and relevant specific epitopes involved in CRPS pathophysiology are still unclear.

It is hypothesised that inflammation in CRPS may trigger the binding between pathogenic IgG and DRG cells. In this project I used the following research methods to qualitatively and quantitatively assess

DRG surface binding by CRPS serum IgG, ultimately aiming to identify the molecular targets for CRPS IgG.

- a) Flow cytometry, Immunocytochemistry and Western Blot to locate and identify the epitope involved in the binding between CRPS-IgG and primary neurons and any role of inflammatory mediators in triggering or enhancing IgG binding.
- b) Use IHC and IF staining to provide proof of concept for the detection of specific binding between CRPS-IgG and DRG tissue from injured mice compared to binding between HC-IgG and DRG tissue; I used immunohistochemistry (IHC) for a preliminary histological examination of human IgG binding to DRG tissue and then I used IF to more precisely locate and quantify the IgG involved in binding.
- c) Use IHC and IF staining to provide proof of concept for the detection of specific binding between CRPS-IgG and DRG tissue from injected and then injured mice compared to binding between HC-IgG and DRG tissue; I used immunohistochemistry (IHC) for a preliminary histological examination of human IgG binding to DRG tissue and then I used IF to more precisely locate and quantify the IgG involved in binding.

Chapter 2 – MATERIALS AND METHODS

2.1. Materials

2.1.1 Antibodies and solutions

Below is a table documenting all materials for IgG purification (Table 2.1)

Table 2.1 Details of materials for IgG purification.

Materials	Catalogue number	Source
Protein G Sepharose, Fast Flow	P3296-5ML	Sigma Aldrich
HiTrap® Protein G High Performance (1ml)	GE17-0404-01	Sigma Aldrich
Bradford Reagent for 0.1-1.4 mg/ml protein	B6916-500ML	Sigma Aldrich
Sucrose, Molecular Biology Grade	J65148.A1	AlfaAesar by Thermo Fisher Scientific
Ethanol, lab grade	E7023	Sigma Aldrich
SnakeSkin™ Dialysis Tubing, 10K MWCO, 22 mm	68100	ThermoFisher
Baxter 1000 ml Compound Sodium Lactate Solution for Infusion BP (Hartmann's Solution for infusion) in Viaflo	FKE2324	Baxter

Tris Base, C ₄ H ₁₁ NO ₃	BP152-1	Thermo Fisher Scientific
Glycine	G7126-100G	Sigma Aldrich
Hydrochloric acid (HCl)	20252.244	VWR International (Leicestershire, UK)

Below is a table documenting all materials for Flow Cytometry, IHC and immunofluorescence (IF) (Table 2.2).

Table 2.2 Details of all materials for Flow Cytometry, IHC and immunofluorescence (IF).

Materials	Catalogue number	Source
Bovine Serum Albumin (BSA)	A9418	Sigma Aldrich
Normal Goat Serum	ab7481	ABCAM
Fetal bovine serum (FBS) heat inactivated	10500056	Invitrogen
Liquid DAB+, 2-component system, Immunohistochemistry Visualization	K346811-2	Agilent Technologies
PFA (pH 7.4)	158127	Sigma Aldrich
Xylene	15618420	Thermo Fisher
Ethanol, lab grade	E7023	Sigma Aldrich

OCT embedding cryo-embedding Matrix	12678646	Thermo Fisher
ProLong™ Gold Antifade Mountant	P10144	Thermo Fisher
Isopentane (2-Methylbutane anhydrous), ≥99%	277258	Sigma Aldrich

All medias used for cell culture, flow cytometry, immunocytochemistry (ICC), ICH and immunofluorescence (IF) are detailed in the table below, alongside their composition (table 2.3).

Table 2.3 Details of the media used for cell culture, flow cytometry, IHC and immunofluorescence

Media	Components
Dissociation solution	500 ml of HBSS (Thermo Fisher Scientific, Gibco™, catalog number: 14175-053), 3.5 ml of HEPES (1 M, pH 7.25) (AppliChem GmbH, catalog number: A3268), 1% penicillin-streptomycin (sigma catalog number: P0781)
DRG culture media	Neurobasal A medium (10888, Life Technologies), 1x B27 (17504-044, Life Technologies), 1% Glutamax (35050-061, Life Technologies), 1% penicillin-streptomycin (P0781, Sigma).
Collagenase solution	10 mg of collagenase-II (Worthington Biochemical Corporation, catalog number: LS004176) in 3 ml of dissociation solution Solution was freshly prepared for each experiment
Trypsin solution	Trypsin-EDTA (0.05%), phenol red (Catalog number: 25300062 Thermo Fisher)
Flow cytometry staining buffer (FACS buffer)	500 ml of HBSS (Thermo Fisher Scientific, Gibco™, catalog number: 14175-053), 50ml Fetal bovine serum (FBS) heat inactivated (catalog number: 10500056, Invitrogen). 0.1% Sodium Azide (catalog number: S2002, Sigma Aldrich) was added to prevent bacterial contamination, photo-bleaching of fluorochromes and block antibody shedding
Blocking solution for IHC	5% BSA (Reference number: A9418 Sigma-Aldrich) in distilled water

Blocking solution for immunofluorescence (IF)	5% BSA (Reference number: A9418 Sigma-Aldrich) in distilled water
30% Sucrose	30% (w/v) sucrose (S/8600/53, Fisher Scientific) in 1x PBS.
0.3% Triton in PBS	0.3% (v/v) Triton X-100 (BP151-500, Fisher Bioreagents) in 1x PBS.
1x Phosphate-Buffered saline (PBS)	10% (v/v) 10x Phosphate-Buffered saline (1.37 M Sodium chloride, 0.027 M Potassium Chloride and 0.119 M Phosphate buffer) (BP399-20, Fisher Scientific) in distilled water (pH 7.4).
Permeabilization buffer (ICC)	0.2 % Tween-20 (1 ml), 0.5 % Triton-X-100 (2.5 ml) PBS (1x) (46.5 ml)

Below is a table documenting secondary antibodies used for flow cytometry IHC and immunofluorescence (Table 2.4).

Table 2.4 Details of secondary antibodies used for flow cytometry IHC and immunofluorescence.

Secondary antibody	Species raised in	Dilution	Catalogue number	Source
APC anti-human IgG Fc Antibody	rat	1:40	410712	Bio Legend
Anti-Human IgG (H+L) Cross-Adsorbed Secondary Antibody, Alexa Fluor 488	Goat	1:500	A-11013	Thermo Fisher Scientific
Anti-human IgG (H+L) (HRP) pre-adsorbed (AB97175)	Goat	1:100	AB97175	ABCAM

Below is a table documenting inflammatory mediators used for flow cytometry (Table 2.5).

Table 2.5 Details of inflammatory mediators used for flow cytometry.

Mediators	Final concentration	Catalogue number	Source
Serotonin	1 μ M	14927	Sigma Aldrich
Bradykinin	1 μ M	B3259	Sigma Aldrich
Prostaglandin E2	1 μ M	2296	Tocris
Histamine	1 μ M	H7125	Sigma Aldrich
Recombinant murine IL-6	50ng/ml	216-16	PreProtech
Recombinant Murine IL-1 β	50ng/ml	211-11B	PreProtech
Recombinant Murine TNF- α	50ng/ml	315-01A	PreProtech

2.1.2 Animals

Experiments were performed using tissue harvested from C57Bl/6J young adult (9-10 weeks old) mice (Charles River, UK). We used female mice to

match sex of CRPS patients and healthy control donors. Mice were housed in a temperature-controlled environment on a 12h light/dark cycle with access to food and water ad libitum. All experiments involving rodents performed in the University of Liverpool were approved by the United Kingdom Home Office, while procedures performed in the University of Pecs were approved by The Ethics Committee on Animal Research of the University of Pecs.

2.1.3 Human sera

Plasma samples used for experiments discussed in this thesis were obtained from two female donors (P1 and P2) that received plasma exchange treatment for persistent CRPS at the Walton Centre NHS Foundation Trust. Both donors provided individual written informed consent; no ethics approval was required for the use of waste plasma (15/NW/0467, North West – Haydock Research Ethics Committee). Both donors had signs in all four Budapest diagnostic categories (Harden et al. (2010)) and a pain specialist, a rheumatologist and a consultant neurologist had excluded alternative causes for their pain (Table 2.6).

Table 2.6 Plasma CRPS samples.

NRS=11-point numeric rating scale rating the average pain over the past 24h, with 0=no pain, 10=pain as bad as you can imagine

Patient	Age	Sex	Affected limb	Disease duration (years)	Pain intensity (NRS)	CRPS type
P1	42	Female	lower	10	8-9	1
P2	40	Female	lower	9	9-10	1

For experiments on pooled IgG, serum samples available from participants in the LIPS-trial (Goebel et al. (2017)) were divided in either moderate (NRS 5-7) or high (NRS 7.5-9) baseline pain intensity. I randomly chose 27 high intensity samples from anonymized list of all sample available (n=111) created by the trial statistician. I then mix 1 ml serum of each of the 27 samples to get a final volume of 27ml of serum for IgG purification. Serum samples for pool HC IgG were chosen following the same method from an anonymized list of all sample available (n=50).

All patients participating in the LIPS trial had persistent CRPS with 1 to 5 years duration and fulfilled the international research criteria for the diagnosis of CRPS (Goebel et al. (2017)). Sera were used under ethical permission and individual consent for auto antibody research (12/EE/0164, East of England). Pooled CRPS and HC IgG used for tissue staining were processed from the

same serum of as the High intensity pain group used in (2019 Cuhadar et al. (2019)) (Table 2.7).

Table 2.7 Pooled CRPS and HC serum samples used for staining.

pain intensity: 24h NRS average pain intensity, averaged over 10 days screening period.

Patient code (CRPS H.I)	Sample	Gender	Age at Consent date	pain intensity
CRPS-1	serum	male	47	8.4
CRPS -2	serum	male	54	8.5
CRPS -3	serum	female	43	7.5
CRPS -4	serum	male	39	7.8
CRPS -5	serum	male	41	8.1
CRPS -6	serum	female	35	8.8
CRPS -7	serum	female	39	8.5
CRPS -8	serum	female	49	7.8
CRPS -9	serum	female	20	8.5
CRPS -10	serum	female	31	8.1
CRPS -11	serum	male	49	8.5
CRPS -12	serum	female	21	7.5

CRPS -13	serum	male	44	8.7
CRPS -14	serum	male	34	9.1
CRPS -15	serum	male	28	7.5
CRPS -16	serum	male	29	8.1
CRPS -17	serum	female	41	8.5
CRPS -18	serum	female	56	10
CRPS -19	serum	female	24	7.5
CRPS -20	serum	male	33	8.1
CRPS -21	serum	female	40	7.5
CRPS -22	serum	female	43	8.8
CRPS -23	serum	female	27	9.8
CRPS -24	serum	male	32	8.1
CRPS -25	serum	female	51	8
CRPS -26	serum	male	47	8.4
CRPS -27	serum	female	41	7.5

healthy controls codes	Sample Type	Gender	Age at Consent date
HC-1	Serum	female	25
HC -2	Serum	female	30
HC -3	Serum	female	25
HC -4	Serum	female	45
HC -5	Serum	female	49

The positive control used in experiments described in chapters 4 and 5 was collected from a patient suffering from a CASPR2 associated neurological disorder with a high antibody level and was kindly provided by Prof. Sarosh Irani, Oxford. CASPR2 autoantibodies bind to the surface of small nerves and reduce Kv1 Membrane Expression on DRG Neurons enhancing neuronal excitability and hypersensitivity (Dawes et al. (2018)).

According with the Human Tissue Act (2004), serum and cell-free plasma are not considered as “relevant material” (2004 c 30, England).

2.2. Methods

2.2.1 Serum Isolation and storage

Blood taken for serum isolation was drawn into golden top vacutainers (BD Vacutainer™ SST™ II Advance Tubes) with an inert, stable gel that separates the serum from blood during centrifugation, and a clotting activator comprised of silica particles which facilitates blood clotting. Tubes were centrifuged at 2000 g for 15 min to separate blood cells and the serum was removed from the top of the tube. Isolated serum was then stored frozen in small aliquots at -80oC for later IgG purification to avoid multiple freeze/thaw.

2.2.2 IgG purification

Developing a fit for purpose IgG purification protocol was a milestone for this research project. Several IgG purification methods are available such as protein G Sepharose, polyethylene glycol and caprylic acid ammonium sulphate precipitation but according to the literature the best method to obtain

high quality IgG is affinity purification with Protein G (Bergmann-Leitner et al. (2008);Roque et al. (2007)). The protocol used for this thesis consisted of four steps (column preparation, serum running, wash and elution) and two extra steps (protein dialysis and concentration) described below (Figure 2.1) (Sensi and Goebel (2022)).

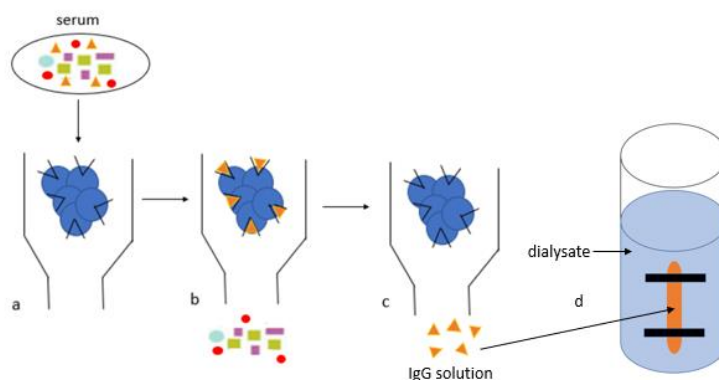


Figure 2.1 IgG purification protocol.

IgG purification protocol consisted of three main steps (serum running, wash and elution) and two extra steps (protein dialysis and concentration). a. Diluted serum was added to the protein G beads and IgG bind to FC receptors on protein G beads. b. Beads were washed in Hartman's solution to fully remove complex protein mixture (multicolour shapes). c. IgG (orange triangles) were removed from protein G with Glycine and collected in Tris buffer. d. IgG put into semi-permeable membrane ('snake skin') and left in dialysis overnight to allow buffer exchange with a physiological solution (Hartmann's) (Sensi and Goebel (2022)).

Where a large amount of human serum/plasma (20ml) was available, usually where plasma was obtained as waste plasma from plasma exchange treatment, IgG fractions were purified using 10ml of Protein G Sepharose Fastflow beads (Sigma-Aldrich, Gillingham, UK). When only small amounts of serum were available (0.5ml to max 2ml) IgG fractions were purified using 1ml HiTrap® Protein G High Performance (Sigma-Aldrich, Gillingham, UK) with an adapted protocol. HiTrap® Protein G High Performance enabled to obtain

between 1ml and 2ml of IgG with a concentration of 8mg/ml thanks to the small bead size (34µm) and high binding capacity of 25 mg IgG/mL resin. Differently from protein G Sepharose, protein G High performance are already packed and just need to be connected to a syringe before use (Figure 2.2) (Table 2.8).



Figure 2.2. HiTrap® Protein G High Performance.

Protein G High performance are already packed and just need to be connected to a syringe before use

Table 2.8 Protein G specifications

Protein G	Bead size	Binding capacity	Serum purified
Sepharose	34 µm	20 mg IgG/mL resin	20ml per run
HighTrap	90 µm	25 mg IgG/mL resin	500 µl-2ml per run

Column preparation

20ml of 100% ethanol was added into a chromatography column (Bio rad #7321010) to remove any contamination, and then 20ml of binding buffer (HS) were added to equilibrate the column. The protein G Sepharose slurry was removed from the vial, washed twice in HS to remove ethanol, and poured into the column in a single, continuous motion. At this point the two-way stopcock at the end of the column was turned on diagonal position to let HS drain slowly and allow protein G deposit at the bottom of the column. Before and after each step listed below the column was always left with 2ml of solution to completely cover the protein G, this step was extremely important to preserve protein G integrity and performance. According with the manufacturer's instructions, the column flow rate was always kept at 11cm/h (Table 2.8).

Serum running

Before purification, serum was always spun down at 2000G x15min to remove any particulate matter that can prevent binding between the IgG and the protein G and/or block the flow-through. After centrifugation, serum was diluted 1:3 in the Binding buffer (Hartmann's solution, Baxter, UK) to maintain a neutral pH. Diluted serum was applied to the column and thereafter the first flow-through was passed once more through the protein G to retain excess antibody

that didn't bind in the first run. Finally, flow-through from the second run was discarded or stored in a freezer to examine any un-bound antibodies (Figure 2.3). According with the manufacturer's instructions, the column flow rate was always kept at 11cm/h (Figure 2.3) during serum running.

Column washing

Protein G were then washed in 100ml binding buffer to remove unbound proteins from the column. A Bradford assay was used to confirm removal of un-bound proteins (Figure 2.3) I washed until Bradford did not show any more protein was present.

Elution

Elution step is the final and critical step in antibody purification, I used Glycine pH 2.30 and TRIS pH 8 as in the protocol established by Koneczny et al (Koneczny et al. (2013)). Both buffers were left on ice during elution and weren't older than three months.

The bound IgG fraction was eluted by adding 20ml of 100 mM Glycine pH 2.3 to the column and the flow-through which now contained the eluted IgG was

collected in 20 tubes (1.5 ml Eppendorf tubes) containing 100µl of Tris pH 8 before elution, each receiving about 900µl of Glycine pH 2.3 to adjust to a neutral pH of 7.4 on ice (figure 3). A Bradford assay was again used to identify tubes containing IgG fractions (the first five tubes always had no IgG and were discarded) and these were collected and pooled together in a 50ml tube. For a 20ml serum volume, typically 20 such tubes (the highest concentration) were collected, with a typical final IgG concentration of 7mg/ml (Figure 2.3).

Column storage

After elution the residual Glycine was removed and the column was washed in HS (approx. 60 ml). As recommended by the supplier the column was stored at 4 °C filled with 20% ethanol to avoid contaminations. Each column was used up to five times for 20ml serum diluted 1:3 (Figure 2.3).

Protein dialysis and concentration

For animal injection experiments, purified IgG was dialysed overnight at 4°C in Hartmann's solution using a 10 kDa dialysis membrane (Fisher Scientific, Loughborough, UK) to remove electrolytes and salts (Figure 2.3).

After dialysis, the IgG concentration was measured using a Nanodrop 2000 spectrophotometer for protein concentration measurements and adjusted to 8mg/mL concentration used for *in vivo* passive transfer (Tékus et al. (2014)). This was achieved either through concentration by dialysis achieved through embedding the overnight-dialysed IgG-containing solution in sucrose. Sucrose removes Hartmann's solution through the dialysis membrane (Snakeskin™ Dialysis Tubing Thermo Fisher #68100) as the solution seeks to equalise the solute concentrations (osmosis); alternatively, the sample was diluted using Hartmann's solution.

Purified IgG solution was finally filtered using a 0.2µM filter (Millipore, Watford, UK), stored at 4°C and used within 3 months. Purified CRPS IgG shouldn't be frozen as repeated freeze-thaw cycles may damage IgG.

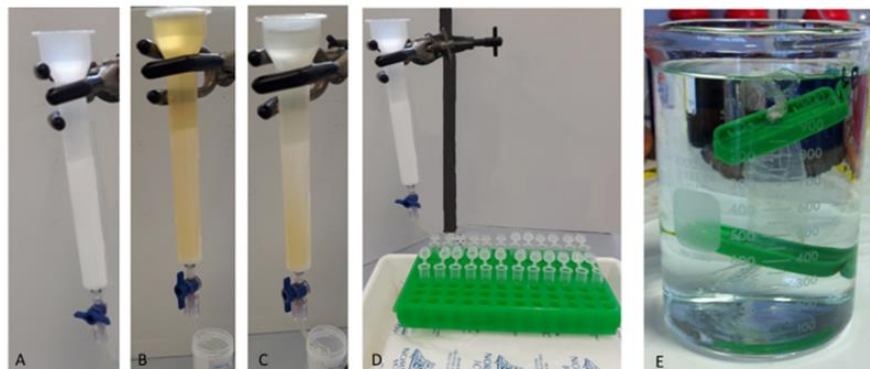


Figure 2.3 IgG purification steps.

A. Column preparation. 20ml of 100% ethanol and then 20ml of binding buffer (HS) were added to the column and then the protein G Sepharose slurry was added to the vial. B. serum running. Diluted serum was slowly applied to the column twice. C. column washing. Protein G were then washed in 100ml binding buffer. D. The bound IgG fraction was eluted adding 20ml of 100 mM Glycine pH 2.3 to the column and was collected in 20 tubes (1.5 ml Eppendorf tubes). E. protein dialysis. Purified IgG was dialysed overnight at 4°C in Hartmann's solution using a 10 kDa dialysis membrane (Sensi and Goebel (2022)).

Factors affecting IgG binding and stability

Due to issues relating to the laboratory temperature regulation during summer (defect in the air-conditioning), serendipitously initially IgG used for this project were purified either at high room temperature (30 °C) or at standard room temperature (20 °C). Subsequently, IgG purified solution at 30 °C was not found to be active by collaborating groups when used either *in vivo* experiments, suggesting that the very high room temperature may have negatively affected either IgG binding to protein G or IgG stability as the manufacturer recommended room temperature (20°C) as optimal.

Another factor that affects IgG binding and stability is pH. Low pH (2.5-3.0) is commonly used during Protein G elution to break the ionic and hydrogen bonds between the antigen and antibody (McMahon and O'Kennedy (2000); Darcy et al. (2017); Grodzki and Berenstein (2010); Hnasko and McGarvey (2015)). IgG used for this project were eluted at a lower pH 2.3 accordingly with Koneczny et al. (Koneczny et al. (2013)); such lower pH was found by collaborating groups to achieve a more complete elution yield (Prof. Vincent, personal communication).

Other factors that may negatively affect IgG binding to protein G include protein G beads freezing (freezing may cause detachment of the protein G from the agarose beads) and column flow rate (too high flow rate lead to IgG loss as IgG won't has not sufficient time to bind to Fc receptors on protein G) (Hnasko and McGarvey (2015)). Finally, according with the manufacturer's instructions, any element of drying of the protein G resin will result in a detachment of the protein G from agarose beads with consequent loss of IgG yield.

2.2.3 Animal incision protocol for tissue staining

For all experiments involving use of ex vivo lumbar DRGs from injured and uninjured paws for tissue staining, on day 0 female C57Bl/6 mice (8-12 weeks old; 18-23 g) were weighted and a small skin-muscle incision was applied to the right hind paw under general anaesthesia.

The skin muscle incision was applied as previously described by Tekus et al (Tékus et al. (2014)). Briefly, on day 0 (day of the limb injury) mice were anaesthetized with 100mg/kg of ketamine and 5mg/kg of xylazine intraperitoneally, then a 0.5 cm long incision (involving skin, fascia and muscle) was applied to the right hind paw and finally the wound was opposed with two mattress sutures of 5-0 nylon on an FS-2 needle according to the Brennan model of mice incisional pain (Brennan et al. (1996)) (Figure 2.4).

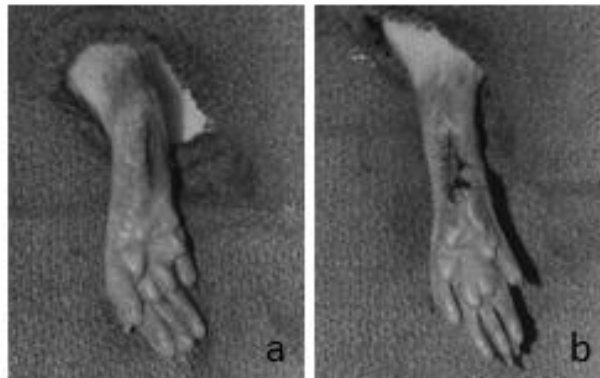


Figure 2.4 The Brennan model of rat incisional pain.

a) plantar incision. b) wound with two mattress sutures. Figure adapted from Brennan et al (Brennan et al. (1996)).

In this model wound healing is very quick, and sutures are typically removed by the animal by one day after the operation. Incision was performed by Nikolett Szentes in the University of Pecs. Mice were then subjected to repeated daily injections (1ml at 8mg/ml per day) for a variable length of time

2.2.4 IgG injection protocol for tissue staining

For experiments involving the examination of DRGs harvested from mice that had been subjected to the passive transfer model, mice were injected daily intra-peritoneally with either affinity-purified plasma-IgG from a patient with persistent CRPS (P1-CRPS), or with IgG derived from healthy controls as described by Tekus et al. (Tékus et al. (2014)) (Figure 2.5).

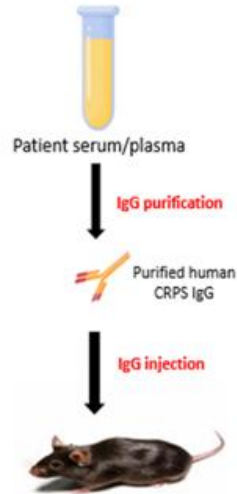


Figure 2.5 IgG Injection protocol.

IgG were purified from patient and healthy control and then injected in a mouse (with an incised paw) 1ml at 8mg/ml per day.

On day 0 a small skin-muscle incision was applied to the right hind paw under general anaesthesia as described above. Mice were then subjected to repeated daily injections for a variable length of time (Table 2.9).

Table 2.9 IgG injection protocols.

Experiment 1 had four injection days and DRG harvest on day 2. Experiment 2 had six injection days and DRG harvest on day 8. Experiment 3 had six injection days and DRG harvest on day 13.

Protocol	Injections (days)	Sacrifice (day)
Experiment 1	-1, 0, 1, 2	Day 2
Experiment 2	-1, 0, 1, 2, 3, 4	Day 8
Experiment 3	-1, 0, 1, 2, 3, 4	Day 13

2.2.5 Tissue harvest and fixation

DRGs (L3, L4, L5) receiving input from the incised (right) and intact (left) paws (Bala et al. (2014); Shi et al. (2018); Laedermann et al. (2014); Zimmermann et al. (2009); Walcher et al. (2018)) were harvested either on day 2 or day 8 or day 13 and fixed with several different method listed below (Table 2.10). DRG harvest and DRG fixation were performed by Nikolett Szentes in the University of Pecs, Hungary, who kindly then provided these tissues to me.

On the day of sacrifice, three different protocols were used to prepare and fix DRGs:

a) Tissue perfusion with 4% PFA and post fixation in 4% PFA

After mice terminal perfusion with 4%PFA DRGs were harvested, then post-fixed in 4% PFA overnight at 4 degrees and stored in 4% PFA until use.

b) Tissue harvest without perfusion, followed by post fixation in 4% PFA

Mice were sacrificed and DRGs were harvested immediately, fixed in 4% PFA overnight at 4 degrees and stored in 4% PFA.

c) Snap-freezing tissue fixation

Mice were sacrificed, DRGs were harvested immediately and snap-frozen in cool isopentane. Briefly Optimal Cutting Temperature (OCT) compound was added into an embedding mould containing a DRG in one corner, then the mould was immersed into a glass bucket containing isopentane chilled by liquid nitrogen (-150°C) for 20-50 seconds (Figure 2.6). After freezing in isopentane, frozen DRGs were left on dry ice for 10 minutes and were then stored in -80°C until use. Adapted from Schäfers M. et al., 2003 (Schäfers et al. 2003).

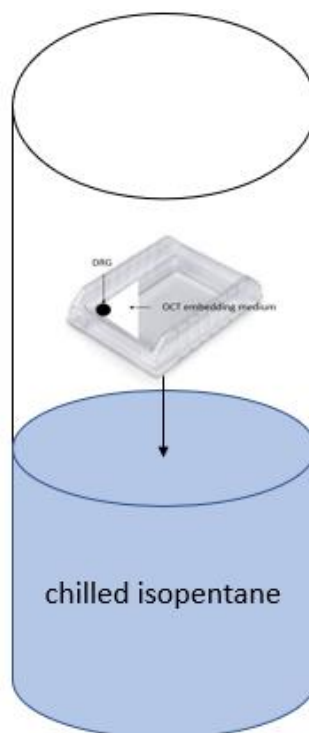


Figure 2.6 DRG snap-freezing.

OCT was added into the embedding mould containing a DRG in one corner, then the mould was immersed into a glass bucket containing isopentane chilled by liquid nitrogen.

Table 2.10 Fixation methods

Fixation method	Fixative
Perfusion	4% PFA (perfusion and post fixation)
Fixation after harvest	4% PFA (post fixation)
Snap-freezing after harvest	Cool isopentane

2.2.6 Dissection of Dorsal Root Ganglion

Animals were killed by cervical dislocation, and DRGs were removed using the method described previously (Heinrich et al. (2016); Malin et al. (2007); Shi et al. (2018)). For neuronal cell culture and flow cytometry staining DRGs were removed from all levels of the spinal cord; for IHC and immunofluorescence, only L3, L4 and L5 were removed, right and left separately, as these are the DRGs which receive sensory input from the injured paws. As the DRG harvest protocol is up to one hour per mouse, mice were culled individually to prevent loss of protein expression during the time interval between harvest and preparation. A brief description of the DRG dissection procedure is provided below.

The mouse was decapitated, then the spinal cord was immediately dissected with incisions on the ventral side of the mouse. All tissue was largely removed using spring scissors and then the spinal cord was exposed and removed with horizontal incisions at the neck opening of the spinal column and at the same time lifting the ventral side away with medical forceps. Using a dissection microscope, the DRG were carefully pulled from their sockets and cut at the base, mirror finish tweezers were used to reduce tissue damage. Finally, for cell cultures DRG were washed in dissociation solution before dissociation to obtain neurons (Figure 2.7). DRG dissection was kindly performed by Sarah Roper and Katie Gibson in the Biomedical Services Unit in the University of Liverpool.

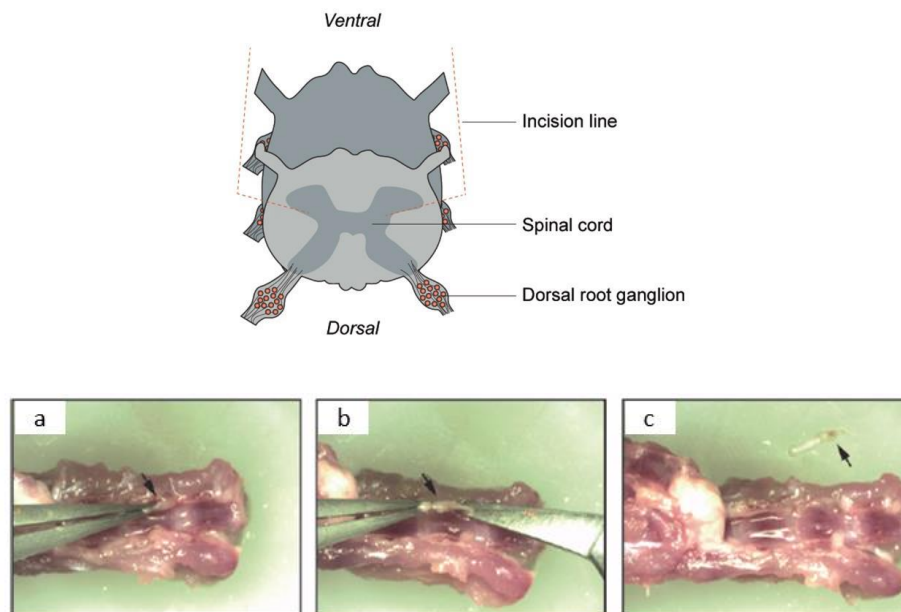


Figure 2.7 DRG dissection.

a. DRG exposition. b. DRG (arrow) isolation from tissue. c. DRG (arrow) was completely removed from tissue. Image taken from www.bio-protocol.org/e1785

2.2.7 Dorsal Root Ganglion dissociation and cell culture

Isolated DRGs (approximately 40 per mouse) were collected in a 15ml tube, were washed three times in dissociation solution and after the last washing step 2 ml of dissociation solution were left and 1 ml of Collagenase-II solution (Worthington Biochemical Corporation, catalogue number: LS004176) was added to reach a final concentration of 10 mg of collagenase-II in 3 ml of dissociation solution. DRGs were then left at 37°C in a humidified incubator gassed with 5% CO₂ for 1 hour. This was followed by 20-minute incubation with 0.05% trypsin-EDTA solution (Shi et al. (2018)). Trypsin was removed and DRGs were washed with 5 ml of dissociation solution twice; after the last washing step 1.5 ml of dissociation solution were left. The DRGs were then dissociated mechanically via trituration with flame polished Pasteur pipettes with an original opening diameter of 1.1-1.3 mm. The diameter was modified by inserting a needle into a Pasteur pipette pore and holding this over a flame to shrink the pore around the needle. I found it was important to avoid making bubbles while resuspending as bubbles caused cell death. The cell suspension was then centrifuged at ~168 x g for 10 minutes, DRG cells were resuspended in Neurobasal media supplemented with 10% FBS and 1% penicillin-streptomycin (P0781, Sigma), then centrifuged and finally resuspended in DRG neuronal culture medium with a 1,000µl pipette (Heinrich et al. (2016); Shi et al. (2018)). After dissociation, DRG cells obtained from one mouse were placed at 37°C in a humidified incubator gassed with 5% CO₂ for two hours to let neurons settle and adhere to the flask, then all media was removed and

fresh media was added to the flask now containing a neuron-enriched culture (approximately 50,000 to 100,000 cells). Neurons were cultured for flow cytometry for 24 to allow recovery after dissociation and exposure of all antigens. After 24 hours neurons were then easily harvested (using a cell scraper) as their processes were still small. Furthermore, preliminary experiments showed that IgG had a very low staining when neurons were stained just after dissociation.

2.2.8 Immunocytochemistry staining

After dissociation, DRG cells were plated on a 24 well plate on coverslips coated with poly-D-lysine to allow cell adhesion for later staining; cells were left in culture for 4 days to allow complete development of DRG neuronal processes in culture (Heinrich et al. (2016)). Cells on coverslips were washed in 1 ml/well fresh permeabilization buffer for 15 minutes twice; then cells were blocked at room temperature for 1 hour in blocking buffer (5 % BSA in permeabilization buffer (0.5 ml/well)). Cells were incubated overnight in primary antibody in blocking buffer at 4°C (300 µl/well). Following staining with primary, cells were washed 3 times with 1 ml/well at room temperature in permeabilization buffer (used for intracellular markers PGP9.5 and Phalloidin) (Table 2.3) (15 minutes each wash) and then incubated with secondary antibody in blocking buffer (300 µl/well) for 1 hour at room temperature in the dark. Cells were then stained with DAPI (1:5000)/Phalloidin (1:250) mix to each well and incubate for 20 minutes and washed twice with 1 ml/well PBS for

15 minutes each wash. Finally, coverslips were mounted on glass slide using mounting media Pro-Long gold and coverslips were sealed onto slide using nail varnish. Stained cells were left in fridge for at least 24 hours for Pro-long gold and nail varnish to dry before visualising cells.

2.2.9 Flow cytometry and data analysis

Flow cytometry overview

Flow cytometry is a powerful technology used to measure multiple parameters of single cells in solution and quantify fluorescence intensities. This technology is mostly used in immunology to analyse populations of immune cells from blood (immunophenotyping), but it can be also used to characterize mixed populations of cells derived from solid tissues by dissociation (McKinnon (2018)) Furthermore, the fluorescent activated cell sorter (FACS) is a specific type of flow cytometer commonly to allows selection of a population of cells and to separate these from the total population (McKinnon (2018)).

In flow-cytometry, cell samples are stained with fluorescent-labelled antibodies, then samples passed through a capillary, through a laser beam, and a fluorescent light signal is captured and analysed by a detector. The characteristics of cell populations are presented in a dot plot and fluorescent histogram (Figure 2.8).

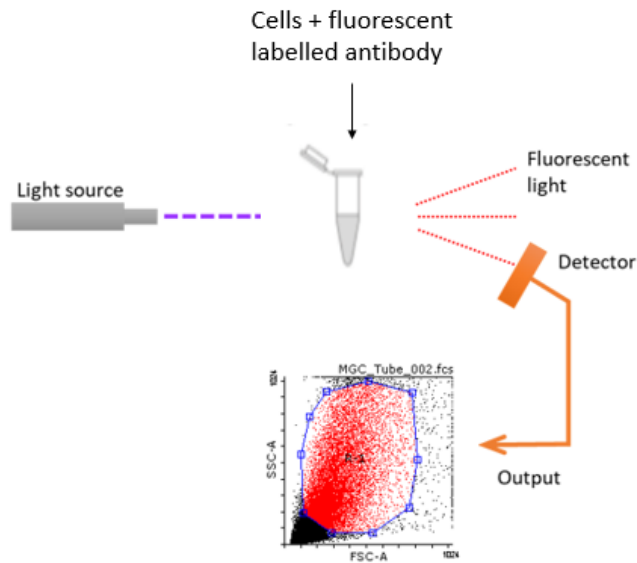


Figure 2.8 Diagram of flow cytometric analysis.

The fluorescent light signal emitted by the samples was captured and analyzed by a detector. The cell population was presented in a dot plot.

While flow cytometry is an established and very effective tool for the study of the immune system, the use of this technology to analyse neuronal populations is less common and presents several challenges and limits such as the requirement of genetically labelled cells. It can be very challenging to distinguish neurons from debris without a transgenic marker. (Martin et al. (2017)). Only recently several works used flow cytometric sorting of neuronal populations (neuro-cytometry) to analyse mixed DRG neuronal populations and select neuronal sub-populations for microarray analysis and RNA sequencing (Chiu et al. (2014); Lopes et al. (2017)).

Flow cytometry analysis to assess autoantigen bound by CRPS autoantibodies was firstly introduced by Kohr et al. in 2009, who also reported that CRPS

autoantibodies bind to an inducible autonomic nervous system autoantigen (Kohr et al. (2009)). Further to that study, a flow cytometry technique aiming to identify the primary neuronal population was used; this was thought to later allow investigating the cell surface epitope(s) involved in the antibody binding to DRG neurons and to investigate whether or not the binding is enhanced by inflammation.

Flow cytometry with inflammatory mediators and cytokines

In order to recreate inflammation *in vitro*, I used either an inflammatory mediator soup (serotonin, bradykinin, prostaglandin E2, histamine 1 μ M) or cytokines (IL-6, IL-1 β , TNF- α 50ng/ml), or both (Reilly et al. (2016)).

Cytokines are a group of inflammatory mediators released in injured tissue that can bind to neuronal receptors and actively regulate nociceptive ion channels. In the last decade several *in vitro* works reported evidence that classic pro-inflammatory cytokines such as TNF- α , IL-1 beta and IL-6 directly act on nociceptors by activating intracellular signalling mechanisms (protein kinases p38/MAPK and PKC) that lead to inflammatory hypersensitivity to both heat and mechanical stimuli (Kress et al. (1997); Kress (2010); Cunha et al. (2000); Loram et al. (2007); Pinho-Ribeiro et al. (2017)). TNF- α is generally considered as the prototypic proinflammatory cytokine due to its principal role in inducing production of other cytokines including IL-1 beta and IL-6. Furthermore, IL-1 β

is associated with pain and hyperalgesia in many conditions including autoinflammatory diseases (Kress (2010)).

Recent studies on CRPS pathophysiology identified the pro-inflammatory cytokines TNF- α , IL-1 β and IL-6 in patients affected skin as potential biomarker for the syndrome (Birklein et al. (2001); Huygen et al. (2002); Parkitny et al. (2013)) . The TNF- α receptor antibody infliximab was tested on CRPS patients in a clinical trial, it reduced TNF- α and IL-6 levels in blister fluids and increased pain relief in some patients; however, in a later trial the biologic infliximab wasn't effective (Huygen et al. (2004)).

Staining

To confirm the role of inflammation in facilitating the patient IgG binding to neuronal cells, three different experimental series were designed respectively featuring incubation of DRG cells with i) inflammatory mediators, ii) cytokines and iii) a combination of both; experimental details including mediators used and mediator concentrations achieved are listed in (Table 2.11). Immediately after dissociation cultured DRG cells were incubated with mediators for 24 hours at 37 °C. Plated neuronal cell cultures were then detached from the flask with a cell scraper, moved to a flow cytometry tube and stained with purified serum-IgG (diluted 1:100) from CRPS patients or healthy volunteers (Figure 2.9). Briefly, Cells were split in 100 μ l aliquots of FACS buffer (staining buffer)

containing approximately 20,000 cells and 1 μ l of human IgG was added to each tube for 1 hour at room temperature. Cells were then washed in 500 μ l of FACS buffer twice to remove unbound IgG. After last wash, 100 μ l of fresh FACS buffer containing 2.5 μ l of APC directly conjugated secondary antibody were added to each sample for 1 hour at room temperature protected from light. Cells were then washed in 500 μ l of FACS buffer twice to remove unbound secondary antibody. After the last wash each sample was fixed in 300 μ l of 4% PFA. Samples were stored in at 4 degrees until flow cytometry analysis.

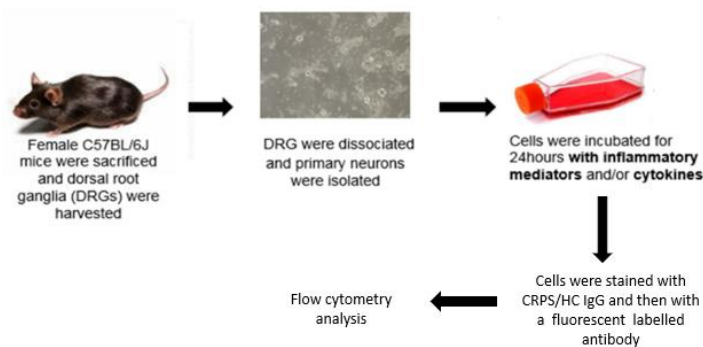


Figure 2.9 Flow cytometry staining.

Cultured cells were incubated with mediators for 24 hours at 37 °C. Plated neuronal cell culture was detached from the flask with a cell scraper, moved to a flow cytometry tube and stained with purified serum-IgG (diluted 1:100) from CRPS patients or healthy volunteers

Table 2.11 Flow cytometry inflammatory factors pre-incubation experiments.

The table summarises three experimental series for incubation of DRG cells. IL: interleukin, TNF: tumour necrosis factor.

Experiment	Mediators used
Flow cytometry analysis with inflammatory mediators	Serotonin (1 μ M), bradykinin(1 μ M), prostaglandin E2 (1 μ M), histamine (1 μ M)
Flow cytometry analysis with cytokines	IL-6 (50ng/ml), IL-1 β (50ng/ml), TNF- α (50ng/ml)
Flow cytometry analysis with inflammatory mediators and cytokines	Serotonin (1 μ M), bradykinin(1 μ M), prostaglandin E2 (1 μ M), histamine (1 μ M), IL-6 (50ng/ml), IL-1 β (50ng/ml), TNF- α (50ng/ml)

Forward and side scatter

A flow cytometer provides two independent parameters, a visible light scatter and one (or multiple) fluorescence parameter. The light scatter is measured in a forward direction (Forward Scatter or FSC) and at 90° (Side Scatter or SSC); FSC detects the size of each cell while SSC detects cell granularity. Flow cytometry results in this thesis are presented in the traditional dot plot histogram with two parameters (FCS and SSC). Forward and side scatters were adjusted as described below.

While cells passed through the flow cytometry capillary, scatters levels were set on flow cytometry software; forward scatter levels were increased to exclude debris and dead cells as much as possible while side scatter levels were adjusted to include all different cells in the heterogeneous DRG cell population. All experiments were performed with same forward and side scatters values.

Gates and plots

The first step of flow cytometry analysis is gating. Gating consists in selecting a region of interest (ROI) containing the cell population on a 'dot plot' where each dot is a single cell (Figure 2.10) and cells are distinguished based on their size and granularity (forward and side scatter). Gating is commonly used to exclude residual debris and dead cells from the ROI; in my analysis debris and dead cells were at the bottom left corner of the density plot because they have low forward and side scatters; it is important to exclude these from the analysis as they feature both increased autofluorescence and unspecific binding to antibodies.

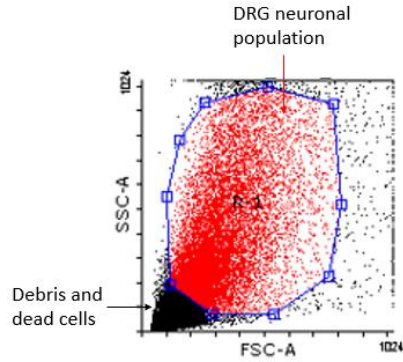


Figure 2.10 Gating on dot plot.

The neuronal cell population (R-1) was selected drawing a ROI on the dot plot (blue circle); debris and dead cells were excluded from the region.

A staining pattern can be confirmed by back-gating. Back-gating consists of analysing cells identified within the original gate on a dot plot or histogram with different parameters (Figure 2.11).

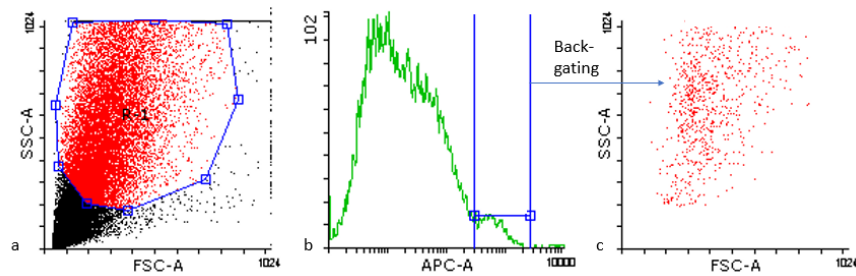


Figure 2.11 Back-gating.

a. dot plot of the DRG neuronal cell population. In order to identify high fluorescence population, a region of the fluorescence intensity histogram (b) was back gated in the original dot plot (c) confirming that only few cells in the whole population had high staining intensity

Single parameter histograms

In this project a fluorescence parameter was measured in addition to the light scatter; in particular, samples were stained with a fluorescent dye (APC) anti-human IgG to identify auto-antibodies bound to the DRG cell population. Flow cytometry results in this thesis are presented in a single parameter histogram with fluorescent intensity and cell count values for the selected population (Figure 2.12). A histogram with fluorescent intensity values was obtained from the population selected on the dot plot. Unstained cells were used, and their staining pattern defined as 'baseline fluorescence'; Unstained cells usually have no fluorescence and consequently a leftward shift; on the contrary, cells with high fluorescence usually have a rightward shift.

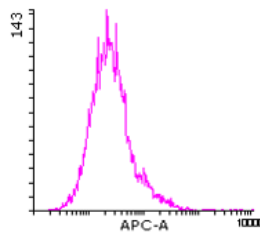


Figure 2.12 fluorescence intensity histogram.

X axis. Fluorescence intensity, fluorescent dye: APC Y axis. Cell numbers. Cells stained in this example had low-medium fluorescence intensity as the fluorescence peak is in the middle of the histogram.

Data acquisition

Data were acquired running cells through CANTO II flow cytometer Lintermans et al. (2014) and analysis of data obtained was completed using Flowing

Software a flow cytometry data analysis software for Windows. Flow cytometry data files had the “fcs” file extension that allows the files to be read by any flow cytometry analysis program.

Fluorescence activated cell sorting (FACS) data analysis

When P1-CRPS cell population was sorted to separate cell sub-population with higher staining intensity for CRPS IgG, cells were presented on a dot-plot based on granularity and dimension, and gating was used to identify cells of interest and to exclude debris. A forward scatter height versus forward scatter area density plot was created for doublet exclusion; a small number of doublets was found to curve out from the linearity of the main cluster and these were excluded from the analysis; doublets are frequently responsible for false brightness of fluorescence and for this reason were excluded from the analysis. A side scatter versus fluorescence intensity plot was created to present cells based on granularity and fluorescence intensity. A single-parameter histogram was created to identify cells with a particular marker expression.

2.2.10 Western Blot of DRG homogenates

Lumbar DRG harvested from native mice C57BL/6J were immediately lysed in 1 mL of NP40-lysis buffer with protease inhibitor (the volume was calculated to achieve roughly 2000 ug protein /mL), using a homogeniser. The lysis solution was then transferred in a 2 ml tube and placed on a rotating plate at 4°C for 2 hours. Then the lysed sample was centrifuged for 20 min at 14000 rpm at 4°C. The supernatant was kept, and the pellet was discarded. The final sample protein concentration was assessed with a BCA assay.

This protein lysis sample was then mixed with Laemmli buffer 2x (1 volume sample + 1 volume Laemmli buffer) and 20 ug of protein were loaded per well. Gels were placed in the running container which was then filled with running buffer. The sample ran for the first 11 min at 70 mV then at 110 mV for an hour, and during this time transfer cassettes were prepared. Sponges, blotting paper nitrocellulose membrane and SDS phage gel were soaked in transfer buffer at 4°C and the Western blot "sandwich" was prepared as in (Figure 2.13). After protein transfer was completed, nitrocellulose was placed in Ponceau solution for 10 min and washed with water to allow visualisation of the protein bands. The membrane was then placed in 10% milk in PBS +0.05% tween 20 for two hours on a shaker to block unspecific binding. A 50ml tube was then filled with 5ml of 5% milk in PBS+0.05 Tween 20 and 1:100 CRPS-IgG and the membrane was delicately placed in it, the tube was then placed on a roller for 1hour and a half at room temperature. After the staining the

membrane was washed 3 times 10 min in PBS +0.05% Tween 20. Then 5 ml of 5% milk in PBS +0.05% Tween 20 with 1:10 000 secondary antibody (goat anti Human IgG) were added for 2 hours on the roller at room temperature. After staining the membrane was washed 3 times 10 min in PBS +0.05% Tween 20 and then was prepared for imaging.

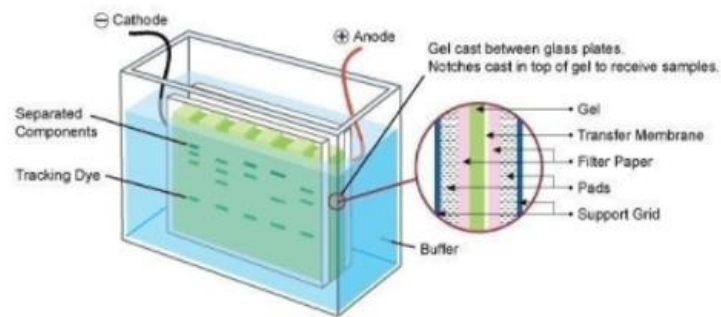


Figure 2.13 Western blot sandwich.

Image taken from www.antibodies-online.com

2.2.11 Immunohistochemistry

2.2.11.1 Tissue embedding

Immunohistochemical staining is widely used to identify specific molecular markers and for histological examination of many tissues including DRGs, but despite its common use, few protocols are published in literature and I found none which explained DRGs embedding. Below is detailed an embedding protocol used for the first time to my knowledge for DRG embedding. DRGs are very small tissues compared with other tissues commonly used for immunohistochemical staining (e.g. brain). For this reason, it is easy to lose DRGs during tissue processing. The main aim of this protocol was to protect and preserve DRGs during the whole tissue processing, before staining.

DRG agar embedding

For IHC staining I used only DRGs harvested and immediately post-fixed in 4%PFA and stored in 4% PFA (no PFA perfusion, see section 2.2.4). DRGs fixed in 4% PFA were washed twice with PBS to remove excess of fixative and were then transferred to a 2ml conical ended tube (only one DRG per tube). A drop of hot liquid 1% agar was added to the bottom of the tube and the DRG

was guided to the tip by means of gentle tapping. The tube was then placed on ice for 10 minutes to let the agar solidify, then the conical base of the tube was cut off using a sharp scalpel. With the aid of a small spatula, the agar-embedded DRG was carefully removed from the tube, wrapped in cigarette paper, and placed in a pencil-labelled tissue processing cassette (Figure 2.14), before the cassette was transferred to 70% ethanol for processing and consequent paraffin embedding.

Tissue processing

Tissue cassettes holding agar embedded DRG were placed in a basket and processed on a Shandon 2LE tissue processor with vacuum unit according to the following timed 16 hours schedule (Table 2.12).

Table 2.12 Tissue processing schedule.

Tissue processing is essential to make fixed tissue suitable for paraffin embedding. This is a long process that is usually performed overnight and consists of dehydration in ethanol (step 1-6), clearing in xylene (step 7-10) and tissue infiltration with hot paraffin wax (step 11-12).

STEP	SOLVENT	DURATION (HOURS)
1	70% ethanol	1
2	100% ethanol	2
3	100% ethanol	2
4	100% ethanol	1.30
5	100% ethanol	1.30

6	100% ethanol	1.30
7	Xylene	2
8	Xylene	1.30
9	Xylene	1.30
10	Xylene	1
11	Wax	2
12	Wax	2.30

Tissue paraffin embedding

After processing, the tissue cassettes were placed in a pre-warmed Histocentre 2 automated embedding centre. The agar embedded DRGs were removed from the cassettes and carefully unwrapped. Hot wax was dispensed into a small mould and the point of the conical agar (where the DRG is located) was orientated centrally and face-down. The labelled plastic cassette was placed on top of the mould, and both were transferred to the cold plate to solidify for at least 30min. When completely cold, paraffin embedded DRG blocks were ejected from their mould (figure 2.14).

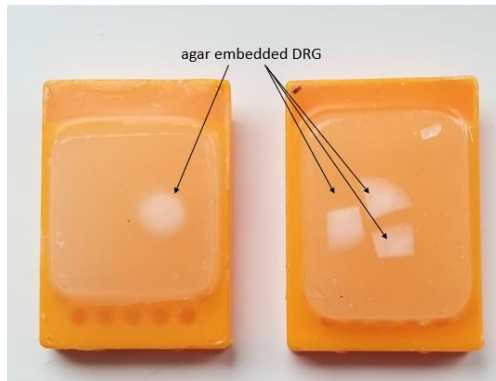


Figure 2.14 Agar embedded DRGs.

The figure shows paraffin cassette containing one or three DRGs embedded in agar. Agar embedding with its white colour was essential to find DRG in paraffin block as DRGs had same colour as paraffin.

2.2.11.2 Sectioning of tissue

DRG tissue sections were cut from the paraffin blocks using an Anglia Scientific Rotary Microtome with disposable blades. Excess paraffin was first removed from around each block which was then clamped into the microtome block holder. The untrimmed block was cooled on a block of ice for 60min, then it was cut at a thickness of 4 μ m. As soon as a ribbon of sections was achieved, 6-8 sections were floated onto a warm water bath (55 $^{\circ}$) as wet warm sections easily adhere to the glass slide. The last section was removed from the water onto a microscope slide and was placed under a light microscope to check for evidence of agar or DRG tissue. If no tissue was seen, then the remaining floating sections were discarded. This procedure was repeated until evidence of tissue could be seen under the microscope. If necessary, the block was periodically removed and re-cooled between ribboning. As soon as evidence

of DRG tissue could be seen in a tissue section, all the subsequent sections were kept and labelled serially. Each paraffin block yielded between 30 and 70 x 4µm sections. Sections were transferred to racks and placed in a 42°C drying oven overnight, then these were stored at room temperature.

2.2.11.3 Antigen retrieval

A heat induced epitope retrieval (HIER) protocol was tested to unmask antigenic sites and facilitate IgG binding (Figure 2.15). Briefly, Sodium citrate buffer was added to a microwaveable vessel containing de waxed tissue slides and let boil for 20 minutes. Slides were then placed under running cold tap water for 10 minutes.

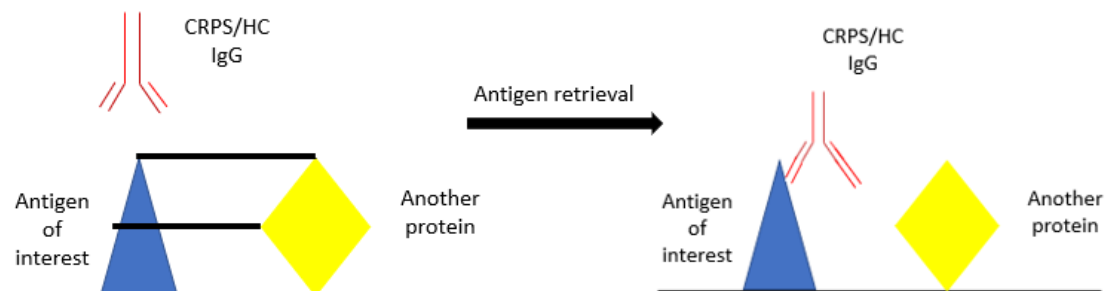


Figure 2.15 Antigen retrieval mechanism.

2.2.11.4 Immunohistochemical staining for paraffin slides

For histological examinations DRG sections were dewaxed (see below) because paraffin wax prevents the aqueous solutions from penetrating the fixed tissue and stained with haematoxylin and eosin (H&E) according to standard protocols (Bancroft and Gamble (2008)).

The protocol for CRPS/HC IgG staining was as follows. Paraffin slides embedded as described above were stained first with affinity purified CRPS/HC-IgG (see Chapter 4 section 4A) and then with anti-human-IgG-HRP (Figure 2.16).

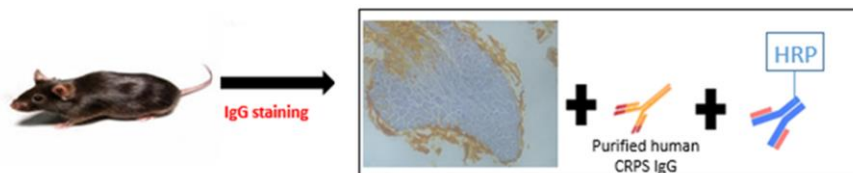


Figure 2.16 IHC staining protocol.

DRGs were harvested, fixed, paraffin embedded, cut and stained with CRPS/HC IgG and then with HRP-conjugated secondary antibody (Bluestone et al. (2015)). Yellow colour of the rim of the tissue was obtained with a yellow dye and used for a first attempt to localize DRG in a paraffin block

Briefly slides were dewaxed in 4x changes of Xylene (hydrophobic compound) for 5 min each and then rehydrated through 4x changes of graded ethanol (hydrophilic compound) 70%-80%-90%-100% for 1 min each; ethanol increased concentration of water preparing the sample for staining in hydrous media. Sections were then rinsed in water and placed in methanol containing 2ml of hydrogen peroxide for 20 minutes to block endogenous peroxidase.

Sections were rinsed in water and blocked for 30 minutes in 5% BSA (blocking solution) at room temperature to prevent nonspecific binding of human IgG. Blocking solution was then drained off slides and purified human IgG were added to the slides at a final concentration of 5µg/mL in blocking solution in 5% BSA and incubated overnight at 4 degrees. The following day slides were washed in 3X changes of PBS and were stained with secondary antibody, anti-human HRP-conjugated, at a dilution of 1:100 for 1 hour at room temperature; in addition to HRP-directly conjugated antibody HRP polymer, conjugated secondary antibody (Figure 2.17) was tested once in an attempt to improve staining. The HRP polymer conjugated antibody had a polymer backbone that can bind several HRP molecules with consequently proposed higher assay sensitivity.

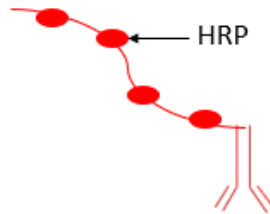


Figure 2.17 HRP polymer.

HRP polymer conjugated antibody had a polymer backbone that can bind several HRP molecules (black arrow).

After staining, slides were washed in 3X changes of PBS and the chromogen solution in substrate buffer (DAB) was added for 5 minutes at room temperature. Slides were washed in 3X changes of PBS and counterstained in Haematoxylin (deep blue-purple staining for nucleic acids) for 1 minute and

then moved in Scott's water. Slides were then washed in water, dehydrated in 4X changes of graded ethanol 70%-80%-90%-100% 5min in each and cleared in 4X charges of Xylene for 5 minutes each to replace ethanol with xylene and completely remove water droplets (that can interfere with tissue visualisation) from the tissue. Slides were then cover-slipped using DPX mounting media and dried for 24 hours at room temperature before imaging.

2.2.11.5 Imaging of sections

Sections were imaged on VWR Inverted Trinocular Microscope IT415 PH with VWR Visicam TC20 Plus Microscope Camera at 20x and 40x magnifications.

2.2.11.6 Image analysis

Staining intensity was determined by asking a colleague to look at the images in a blinded way and rate the overall binding intensity between 0-3, allowing half points (Goebel et al. (2005b)).

2.2.12 Immunofluorescence

2.2.12.1 Tissue embedding

Immunofluorescence staining (IF) is usually performed on cryo-embedded tissue differently from IHC that is performed on paraffin embedded tissue consequently tissue embedding for IF differs from IHC.

There are two different protocols in the literature for embedding/preparing of tissue for IF staining, i) snap-freezing and ii) post fixation embedding. Snap-freezing is usually used when fresh tissue is available; in this method the tissue is embedded in OCT and immediately snap frozen before cutting. The second method is the most commonly used for DRGs embedding and consist of a fixation in PFA immediately after harvest, then cryo-protection in sucrose (to avoid cell shrinkage during cutting at low temperatures) at 4 degrees and finally embedding in OCT before cutting.

Snap freezing

The protocol used for fixed tissue in this study was adapted from Schäfers M. et al., 2003 (Schäfers et al. (2003)) Mice were terminated and DRGs were harvested immediately, and firstly placed in a corner of a plastic embedding mould (separately L3, L4, L5), then OCT embedding compound was added and DRGs were snap-frozen in cool isopentane (Figure 2.18) as described in section 2.2.5c. The mould with the frozen DRGs was then stored in -80°C until

cryo-sectioning, sections were then stored again at -80°C until staining. Before staining snap-frozen DRGs were thawed and post fixed in acetone.

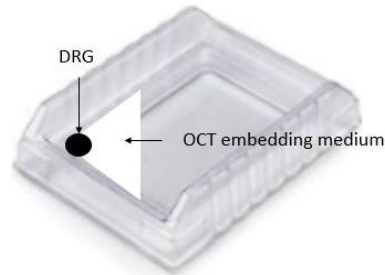


Figure 2.18 DRG snap-freezing.

A DRG placed in a corner of a plastic embedding mould with OCT embedding compound.

PFA fixation and cryoprotection

The protocol used for fixed tissue in this study was adapted from the one published by Mallat et al. 1999, similar to Yanik et al. 2020 and Wu H. et al. 2017 (Mallat et al. (1999); Yanik et al. (2020); Wu et al. (2017)). Briefly, following either perfusion in 4% PFA followed by post fixation in 4% PFA, or post-fixation in 4% PFA alone without PFA perfusion, DRGs were washed twice in PBS and transferred to 30% sucrose solution (cryoprotection buffer) and stored 24 hours at 4°C as described in section 2.2.5; sucrose was used as cryoprotection buffer as it maintains the osmolarity of the tissue and prevents cells from shrinking. The DRGs were first placed in a corner of a plastic embedding mould (Figure 17) and then were embedded in OCT (ThermoFisher) one per block and stored in the mould at -80°C until use.

Before sectioning, the corner with DRGs was cut from the block of OCT-embedded DRG (with the DRG on top of the corner) and put on top of the cryostat chuck and secured with extra OCT.

2.2.12.2 Sectioning of tissue (same protocol after snap freezing or PFA-fixation/cryoprotection)

Frozen sections were prepared using a manual cryostat (CM1850, Leica). Before sectioning, frozen blocks were removed from the -8°C freezer and were left at -20°C for 20 minutes, the OCT corner containing the DRGs was then cut with a blade and placed on the cryostat chuck with OCT on it at -20°C and left for 10 minutes then the chuck was secured for cutting (Figure 2.19). Sections were cut at $10\mu\text{m}$ and mounted directly onto SuperFrost plus slides (ThermoFisher) and stored at -80°C until staining.

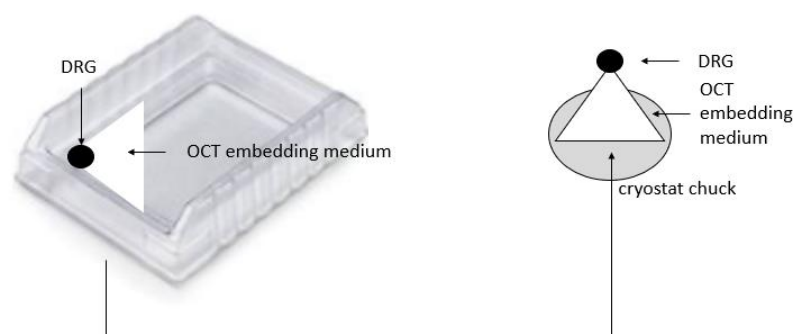


Figure 2.19 Sectioning of tissue.

The corner containing the DRG was cut with a blade, placed on the cryostat chuck and secured on the base of the chuck with fresh OCT.

2.2.12.3 Immunofluorescence staining

DRGs were stained directly according to the following protocol adapted from Schäfers M. et al, 2003. Tissue slides were thawed for 20 minutes at room temperature, and before staining washed in PBS to remove excess of OCT. Sections were then first incubated in blocking solution for 30 min, and then for 1 hour at room temperature with purified human IgG at 5µg/mL in blocking solution (Table 13). After this staining with primary antibody, sections were washed three times in PBS for 10 minutes. Sections were then incubated with anti-human secondary antibodies FITC conjugated 1:500 for 1 hour in blocking solution in the dark (Figure 2.20) (

Table 2.13). Sections were washed three times for 10 minutes in PBS and were left air drying in the dark. As last step, 2µl of Prolong Gold mounting medium were applied to each coverslip before mounting on top of the tissue slide. Slides were stored at 4°C in the dark covered with foil before imaging.

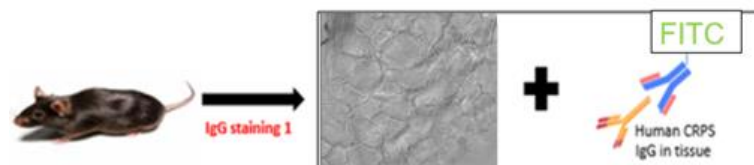


Figure 2.20 IF staining protocol.

DRGs embedded in OCT and cut were stained with CRPS/HC IgG (yellow) and then with FITC-conjugated secondary antibody Bluestone et al. (2015).

Table 2.13 Blocking solution for IF staining

	Snap-frozen DRGs	PFA fixed DRGs
Blocking solution for primary antibody	5% BSA	10% FBS
Blocking solution for secondary	5% BSA	5% goat normal serum

2.2.12.4 Imaging of sections

Sections were imaged on a Zeiss LSM780 confocal microscope at 20x and 40x magnifications, using Zen Black (Zeiss) software in the Centre for cell imaging (CCI) in the University of Liverpool. Images were taken with a pinhole of one airy unit using the green channel.

2.2.12.5 Quantitative electronic analysis

Quantitative immunofluorescence image analysis was performed only on tissue harvested from human IgG injected and injured mice because this protocol provided superior staining patterns. Image analysis and quantification was performed using FIJI (ImageJ v2.0.1) software. The FIJI 'analyse' function was then used to generate an outline and calculate the area contained within the marked outline.

Human IgG intensity fluorescence was measured by drawing a region of interest around each neuron within the neuron rich area of the DRG. Intensity

fluorescence was measured applying a minimum pixel intensity threshold, and then the percent positive area above the threshold and the average pixel intensity above the threshold were evaluated as described by Goebel et al. (Goebel et al. (2021a)). Larger cells had a bright area near the cell membrane and a dark central cell body, while smaller cells were comparatively bright throughout (Figure 2.21).

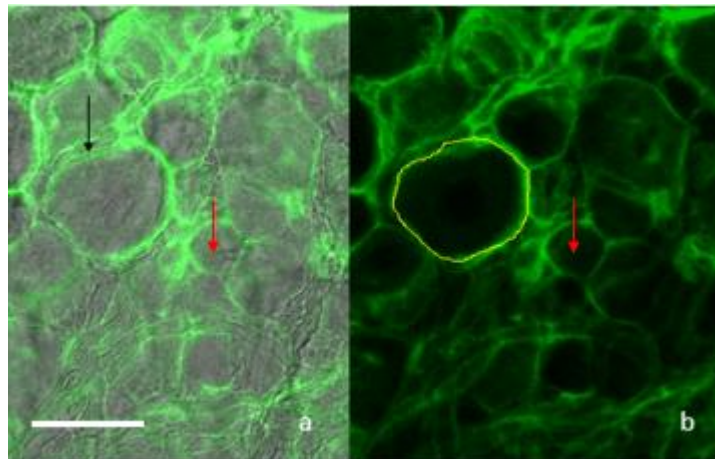


Figure 2.21 DRG neuron-rich area.

a) Brightfield and green fluorescence merged channels: big neuron (black arrow) and small neuron (red arrow). b) Fluorescence channel: big neuron (yellow circle), small neuron (red arrow). Scale bar 100 μ m

Integrated density (Mean intensity \times area) is commonly used for fluorescence microscopy analysis of tissues. The integrated density calculates how much signal there is in the region of interest. A small but bright cell (with a higher mean/median intensity) might have a lower integrated density, i.e. less IgG, than a large but dimmer cell (lower mean/median intensity), i.e. more total IgG. Integrated density allows a representative analysis of a heterogeneous cell population such as DRG neuronal cells and it is usually recommended when comparing samples with discrepancies of size within the sample or between different samples.

2.2.12.6 Statistical analysis

For IHC statistical analysis, I tested statistical significance using a paired T-test to compare two samples (healthy control-right vs healthy control-left and CRPS-right vs CRPS-left). I calculated the mean and standard deviation of the right and left data and using a 95% confidence interval I obtained the p values. P values were then compared with a significant level α of 0.05 in order to determine whether the difference between the means was statistically significant or not.

Statistical significance between HC-right and CRPS-right was calculated with Mann-Whitney tests for unpaired data and adjusted for multiple comparisons ($p < 0.05$).

Chapter 3 – RESULTS: ASSESSMENT OF CRPS IgG

BINDING TO DRG NEURONAL CELLS

3.1 Introduction

Several works suggest that in some patients with CRPS there is an auto antibody response against surface markers on rodent primary neurons, but cellular and molecular targets are unknown. Furthermore, according with the conceptual model of auto antibody mediated CRPS (Goebel and Blaes (2013)Goebel A. *et al.*), inflammatory mediators, released after trauma, may trigger the binding of circulating pathogenic IgG autoantibodies.

In this chapter I describe the assessment by *in vitro* staining, of surface binding of CRPS-serum-IgG to murine dorsal root ganglion neurons taken from intact (non-injured) animals. I have utilized a number of established assessment methods (flow cytometry, western blot, mass spectrometry and immunocytochemistry).

Flow cytometry analysis was used for a simultaneous *characterization* of the mixed neuronal DRG population and for quantitative detection of the neuronal sub-population involved in binding with CRPS and HC IgG.

Immunocytochemistry and Western blot were used for a qualitative and quantitative assessment of CRPS and HC IgG binding to neuronal cells; the prior technique was used to locate IgG binding on neuronal cells while the

latter was used to quantify and detect IgG binding in DRG protein homogenates.

3.2 Aim

The first aim of this project part was to investigate the feasibility of detecting the binding between CRPS-IgG and primary neurons and any role of inflammatory mediators in triggering or enhancing IgG binding. The second aim was to locate and identify the epitope involved in the binding (Figure 3.1).

The first objective was to isolate murine primary DRG cells and assess the binding by CRPS/HC-IgG to these cells using flow cytometry analysis. Then, the second objective was to validate a protocol to incubate isolated DRG neurons with a mixture of inflammatory mediators and then assess the IgG binding again using flow cytometry, to establish any role of inflammatory mediators in activating the patient IgG binding. The final objective was to use protocols for Immunocytochemistry and Western blot staining of neuronal cells and proteins in order to detect a specific binding between CRPS-IgG on primary neurons.

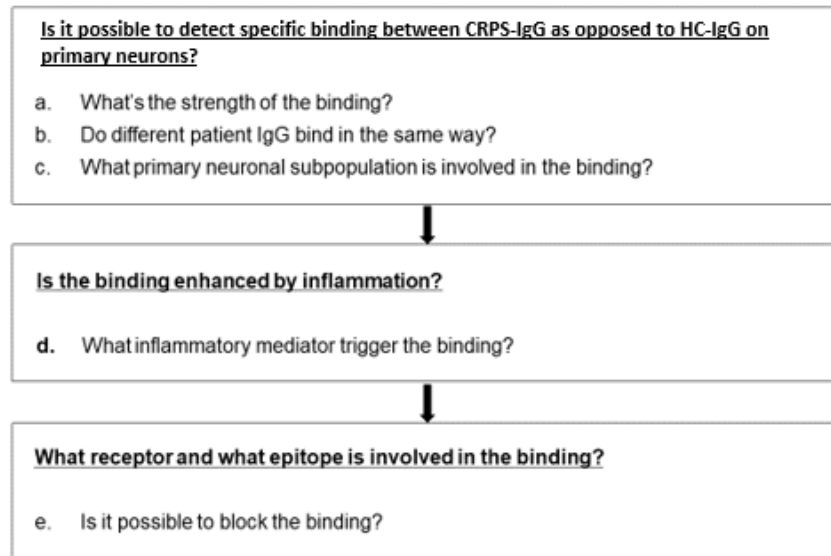


Figure 3.1 Chapter aims.

The first aim of this project part was to investigate the binding between CRPS-IgG and primary dorsal root ganglion neurons and any role of inflammatory mediators in triggering or enhancing IgG binding. The second aim was to locate and identify the epitope involved in the binding. This second aim was pursued using several methods: flow cytometry, Immunocytochemistry and Western blot staining.

3.3 Results

3.3.1 Flow cytometry analysis of DRG neuronal population

3.3.1.1 Assessment of neuronal cell surface binding by CRPS-IgG

Plasma samples used for experiments discussed in this chapter were obtained from two female donors (P1 and P2) that had received plasma exchange treatment for persistent CRPS at the Walton Centre NHS Foundation Trust. Both donors had signs in all four Budapest diagnostic categories (Harden et

al. (2010)) and had high pain intensity; demographics are reported in chapter 2 (Table 2.6).

When I initially stained neuronal cells with human IgG directly after DRG dissociation and assessed binding using flow cytometry, I found that the cell population involved in the binding seemed to vary dependent on the overall dissociated cell numbers, as indicated by both varying neuronal sub-populations and non-neuronal populations. In order to standardize flow cytometry staining, DRG neuronal cells were therefore left in culture for 24 hours with neuronal medium (Neurobasal media, Thermo Fisher); this step allowed to select neurons and remove non-neuronal cells (Figure 3.2).

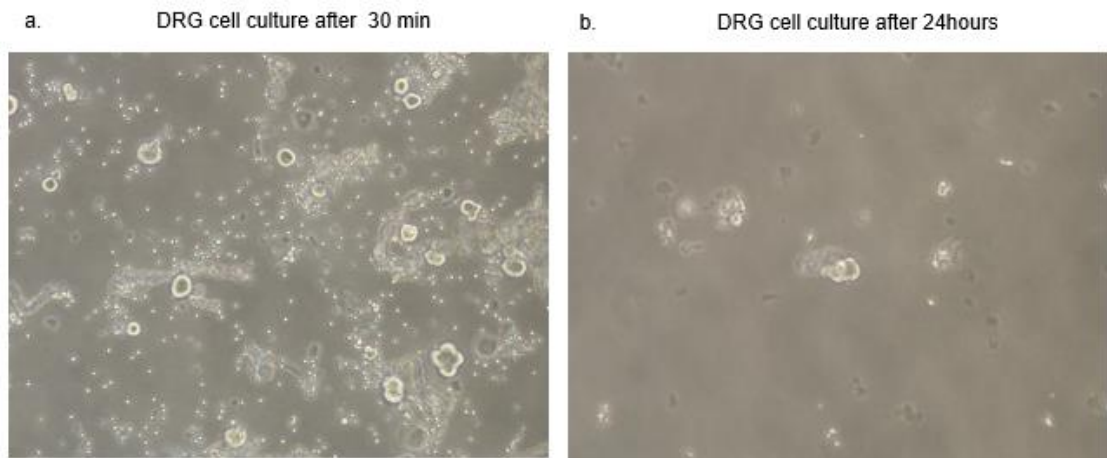


Figure 3.2 DRG cell culture.

a. After 30 min in culture the DRG cells were a mixture of different cell populations including primary neurons, satellite glial cells, other non-neuronal cells and debris. b. After 24 hours in cell culture with Neurobasal media only adherent neurons remained in the flask.

After 24 hours cell culture, stained neurons had a very homogeneous histogram patterns between each experiment (not shown). CRPS samples

consistently had higher main fluorescence values than healthy volunteer, indicating that CRPS IgG recognised one or several DRG neuronal antigen(s) not or less recognised by HC IgG (Figure 3.3 and Figure 3.4). While this was common to both examined samples, P1 and P2 had very different staining histograms (Figure 3.4), and three different HCs had similar staining histograms (Figure 3.3).

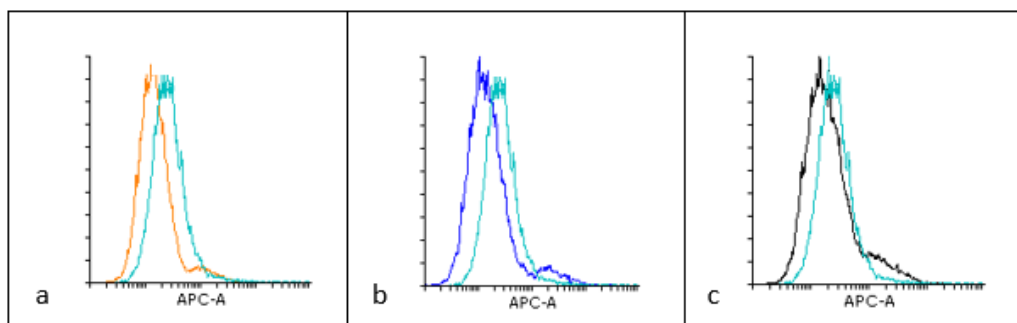


Figure 3.3 HC IgG staining after 24 hours of neuronal cell culture.

Fluorescence intensity histograms. x axis: fluorescence intensity, y axis: cell number. HC1 (orange), HC2 (blue), HC3 (black) and P2 (light blue). a HC1 and P2. b HC2 and P2. c HC1 and P2 three different HCs had similar staining histograms.

P1 IgG bound to a consistently higher number of neurons, and with stronger staining than HC IgG, while P2 had a staining pattern similar to the healthy control but with slightly higher fluorescence intensity (Figure 3.4).

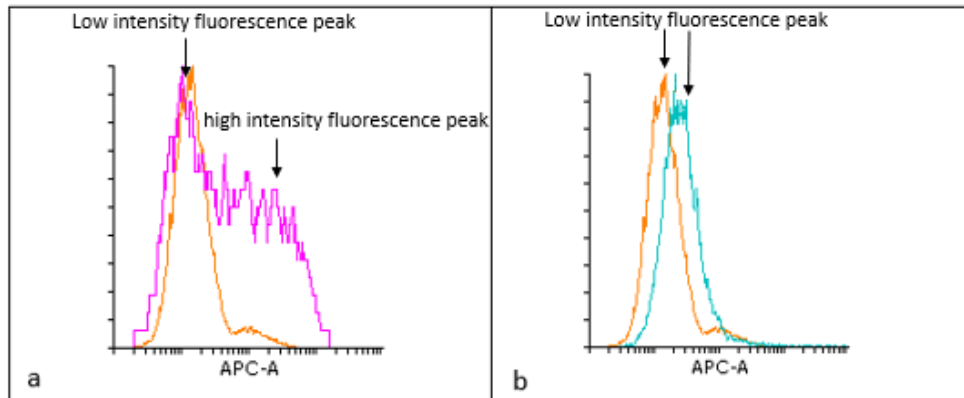


Figure 3.4 CRPS IgG staining after 24 hours of neuronal cell culture.

Fluorescence intensity histograms. x axis: fluorescence intensity, y axis: cell number. P1 (pink), P2 (light blue) and HC1 (orange). HC1 had a low fluorescence intensity as the peak of fluorescence is on the left part of the histogram while P1-CRPS stained a sub population of cells with high staining intensity b. P2-CRPS HC1 fluorescence histogram; P2-CRPS and HC1 had both a relatively low intensity fluorescence peak. Number of cells stained can be seen on the y axis, a high and narrow peak on the left (like the HC peak) represents a large cell number with very low fluorescence intensity, while a smaller peak on the right (like P1 subpopulation) represents a small cell number with high fluorescence intensity.

3.3.1.2 Flow cytometry of cultured neurons with inflammatory mediators

Experiments with inflammatory mediators were triggered by the finding that peripheral soft tissue injury, which involves peripheral inflammation facilitates the behavioural effects of human IgG in rodents; this might suggest that the injury-associated inflammation induces a differential expression of relevant epitopes in the neurons allowing IgG binding (Tékus et al. (2014); Helyes et al. (2019)). Furthermore, it is well documented that inflammatory mediators can increase primary neurons excitability (Michaelis et al. (2000); Ma et al. (2006); Kress et al. (1997); Kessler et al. (1992)). In 2016 Reilly *et al.* tested the effect of CRPS-IgG on the CaV1-induced calcium entry in DRG neurons incubated with and without an inflammatory soup. The authors found that one

CRPS patient's serum- IgG significantly reduced the K⁺ response of primary neurons pre-incubated for 24 hours with an inflammatory mediator soup (1 μ M histamine, 5-hydroxytryptamine, bradykinin and PGE₂) (Reilly et al. (2016)). These results highlight the additional possibility that ongoing peri-neuronal inflammation might synergise with the effect of neuron-bound pathogenic IgG. Considering these interesting results, I used flow cytometry to investigate whether or not inflammatory mediators trigger CRPS IgG binding to a neuronal surface antigen.

Briefly, neurons were dissociated from DRGs, placed in two different flasks (inflammatory mediators with cells, and cells only) and were left in culture for 24 hours. I had initially tested incubation with inflammatory mediators for 12 and 24 hours and best staining was obtained after 24 hours incubation. An inflammatory mediator soup was added (1 μ M histamine, 1 μ M Prostaglandin E₂, 1 μ M Bradykinin, 1 μ M Serotonin) only to the first flask while the second flask contained only media. Then cells from both flasks were stained with CRPS/HC IgG. I found that neurons incubated with inflammatory mediators and then stained with CRPS/HC IgG did not display any significant increase of mean fluorescence upon flow cytometry when compared with cells only samples (Figure 3.5).

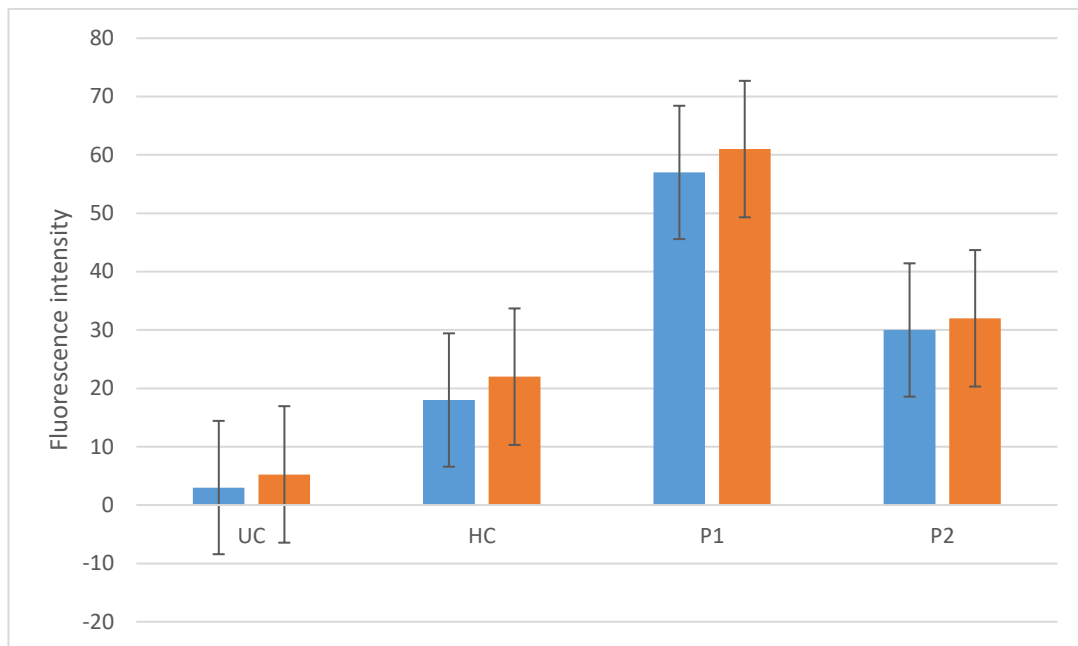


Figure 3.5 Incubation with inflammatory mediators for 24 hours.

From left to right: unstained cells (UC), healthy control (HC), CRPS patient 1 (P1) and CRPS patient 2 (P2). Blue: cells without inflammatory mediators, orange: cells incubated with inflammatory mediators. Incubation with inflammatory mediators did not increase flow cytometry fluorescence values. Statistical significance was calculated with t- tests for paired data ($p < 0.05$).

Interestingly, these results confirmed that pre-incubation of DRG cells in inflammatory soup did not, per se, appear to modify IgG staining to DRG cells with the two CRPS-IgG preparations that were used. I also noted quite high variability in the staining intensities between cells.

3.3.1.3 Flow cytometry of cultured neurons with cytokines

Cytokines are a group of inflammatory mediators released in injured tissue that can bind to neuronal receptors and actively regulate neuronal excitability and sensitivity to external stimuli. In the last decade several works have suggested

that classic pro-inflammatory cytokines such as TNF- α , IL-1 beta and IL-6 are associated with inflammatory hypersensitivity. (Sommer and Kress (2004); Kress (2010); Cunha et al. (2000); Loram et al. (2007)). Several studies identified pro-inflammatory cytokines TNF- α , IL-1 β and IL-6 as potential biomarker for CRPS (Birklein et al. (2001); Huygen et al. (2002);Parkitny et al. (2013)) . I therefore also used flow cytometry to investigate whether cytokines trigger CRPS IgG binding to DRG neurons. Neurons were dissociated from DRGs, placed in different flasks and were left in culture for 24hours neurons with either TNF- α or IL-1 beta or IL-6 or a pool of these three cytokines, or medium only.

Cytokine pool treatment

I found that unlike with the inflammatory mediator setup described above, cytokine pool treatment significantly increased either main fluorescence or bound cell percentage with a prominent effect in P1 and a possible very minor effect in P2 (Figure 3.6).

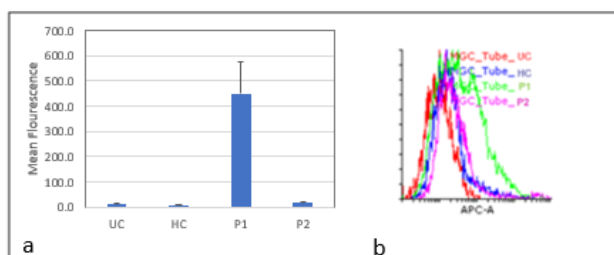


Figure 3.6 Cytokine pool treatment.

Unstained cells (UC), healthy control (HC), CRPS patient 1 (P1) and CRPS patient 2 (P2). **a.** Cytokine pool treatment mean staining intensity. **b** Cytokine pool treatment fluorescence histogram UC (red), HC (blue), P1-CRPS (green) and P2-CRPS (pink). In both a and b P1-CRPS had higher fluorescence intensity. Statistical significance was calculated with Mann-Whitney tests for unpaired data ($p < 0.05$)

Single cytokine treatment

Following incubation with a pool of cytokines, neurons were incubated with each cytokine (TNF- α , IL-1 β and IL-6) separately to investigate whether a single cytokine could trigger CRPS IgG binding to DRG neurons and whether there was a difference in staining intensity between these three cytokines. Neurons incubated with single cytokine were then stained either with P1 and P2 CRPS IgG preparations; P1-CRPS IgG seemed sensitive to all cytokines, IL-1 β and IL-6 to a higher degree and slightly less to TNF- α . While P2-CRPS seemed not sensitive to either TNF- α or IL-1 β or IL-6 (Figure 3.7).

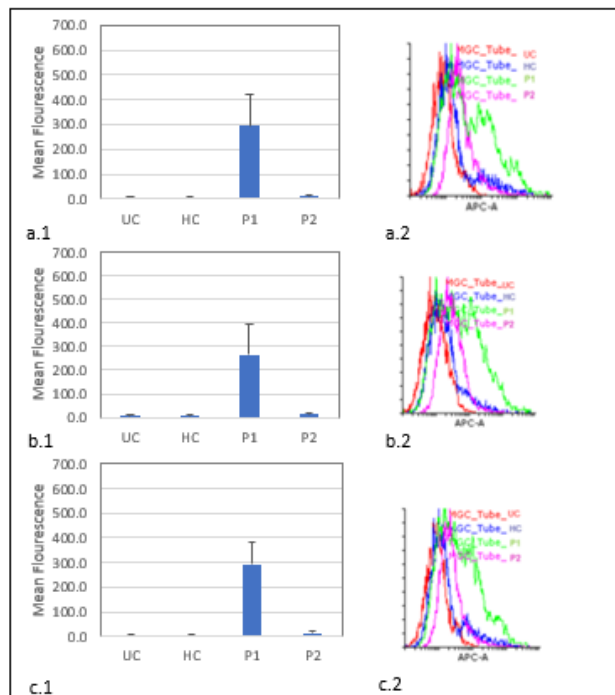


Figure 3.7 Single cytokine treatment.

Unstained cells (UC), healthy control (HC), CRPS patient 1 (P1) and CRPS patient 2 (P2). a1 and a2. IL-1 β . b1 and b2 TNF- α . c1 and c2 IL-6. a1, b1, c1. Single cytokine treatment mean staining intensity. a2, b2, c2. Single cytokine fluorescence histogram UC (red), HC (blue), P1-CRPS (green) and P2-CRPS (pink). In a and b P1-CRPS had higher fluorescence intensity. Statistical significance was calculated with Mann-Whitney tests for unpaired data ($p < 0.05$)

Cytokine pool and single cytokine treatment

Overall, I found that the higher fluorescence intensity values were obtained when DRG cells were stained with a pool of cytokines (IL-1 β , IL-6 and TNF- α) with a prominent effect in P1 and a possible very minor effect in P2 (Figure 3.8). For P1-CRPS, single cytokines treatment when compared with pooled treatment had a lower effect on IgG binding and consequent fluorescence intensity especially for IL-1 β ; IL-6 incubation causes comparatively higher fluorescence intensity values. For P2-CRPS no particular difference in fluorescence intensity was obtained between pool of cytokines and single cytokines treatment.

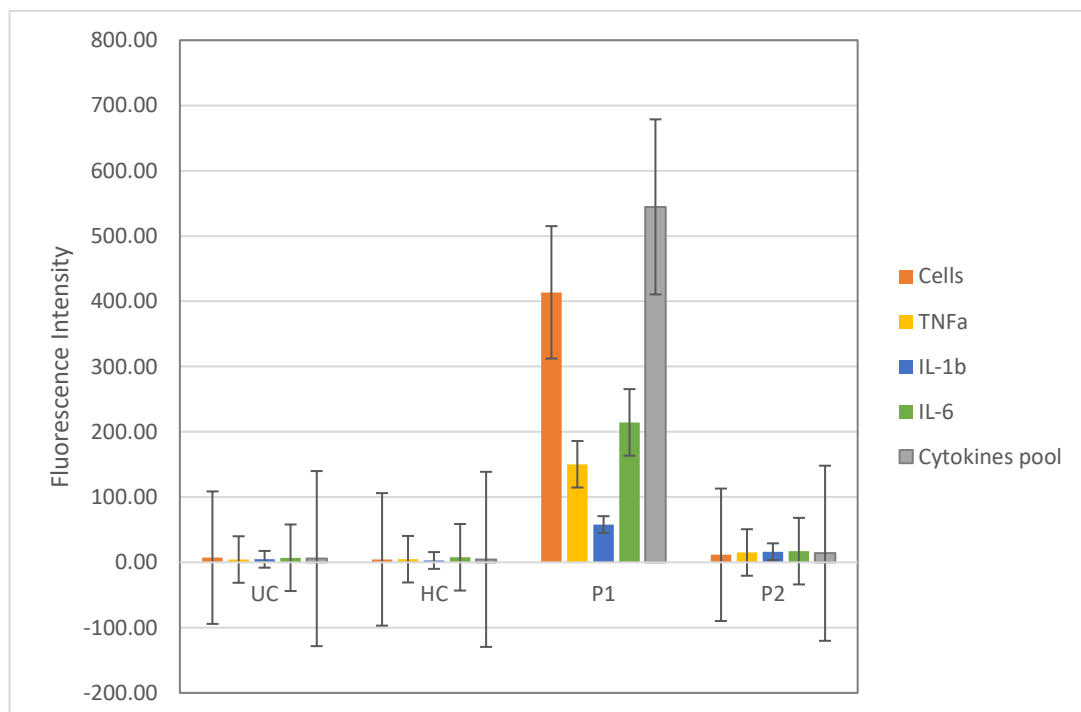


Figure 3.8 Fluorescence staining of DRG primary neurons after cytokines treatment.

Orange: cells only, yellow: TNF- α , blue: IL-1 β , green: IL-6, grey: pooled cytokines, UC: unstained cells, HC: healthy control. Cytokines treatment significantly increased either main fluorescence or cell

percentage involved in IgG binding. P1 has a strong fluorescence increase when treated with TNF- α , IL-1 β and IL-6 together. Statistical significance was calculated with Mann-Whitney tests for unpaired data ($p < 0.05$)

3.3.1.4 Flow cytometry of cultured neurons after concomitant incubation with both cytokines and inflammatory mediators

Several works have documented a synergistic role of inflammatory mediators and cytokines in the development of inflammatory hyperalgesia. Both inflammatory mediators and cytokines can bind directly on primary neurons activating a complex signalling cascade with secondary production of additional mediators and cytokines. IL-1 β , for example, induces secondary production of nitric oxide, bradykinin or prostaglandins by primary sensory neurons (Poole et al. (1999)) while bradykinin stimulates the release of cytokines (TNF- α , IL-6, IL-1 β , IL-8) (Cunha et al. (2000)).

To further investigate the role of the combined effects of mediators and cytokines on CRPS-IgG binding to primary DRG neuronal cells, I repeated experiments above with neurons pre-incubated with a pool of inflammatory mediators and cytokines (1 μ M histamine, 1 μ M Prostaglandin E2, 1 μ M Bradykinin, 1 μ M Serotonin, TNF- α , IL-1 β and IL-6).

Interestingly, when P1-CRPS was stained with neurons pre-incubated with both inflammatory mediators and cytokines, mean fluorescence values were higher than pre-incubation with only inflammatory mediators and lower than

pre-incubation with cytokines only (Figure 3.9) CRPS P2 staining remained not significantly different from HC.

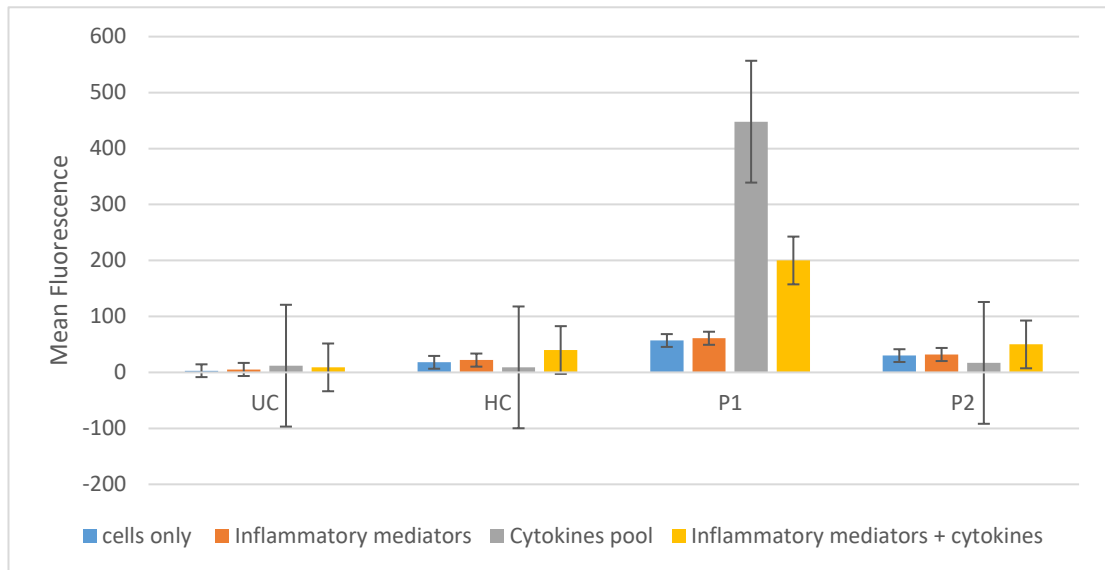


Figure 3.9 Staining of DRG primary neurons after combined inflammatory mediator and cytokine treatment.

Blue: cells only, orange: inflammatory mediators, grey: cytokine pool, yellow: inflammatory mediators and cytokine pool, P1-CRPS has a stronger fluorescence increase when treated with cytokines than with either inflammatory mediators or individual cytokines. P2-CRPS IgG may not be sensitive to inflammatory mediators neither to cytokines. Statistical significance was calculated with Mann-Whitney tests for unpaired data ($p < 0.05$)

Taken together these results suggested that the interaction between inflammatory mediators and cytokines exerts a complex effect on the binding of some CRPS IgG primary neurons.

3.3.1.5 Fluorescence activated cell sorting of P1-CRPS stained population

Following staining with inflammatory mediators and cytokines, I was interested to find out what neuronal subpopulations bound particularly strongly to CRPS IgG. When neurons were stained only with cytokine pool, I was able to identify a bimodal cell distribution following P1-CRPS IgG staining and a unimodal cell distribution following P2-CRPS IgG staining. Nearly half of cells stained with P1-CRPS had a substantial fluorescence increase only when incubating with either the cytokine pool or with IL-6 and IL-1 β ; (Figure 3.10).

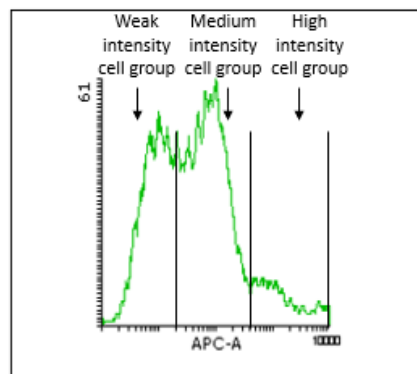


Figure 3.10 P1 CRPS Patient staining pattern.

P1 had bimodal distribution with three groups of cells with different intensity fluorescence involved in the binding.

The identification of a bimodal cell distribution following P1-CRPS IgG staining, suggested that it may be interesting to analyse binding to the inflammation-induced sub-population.

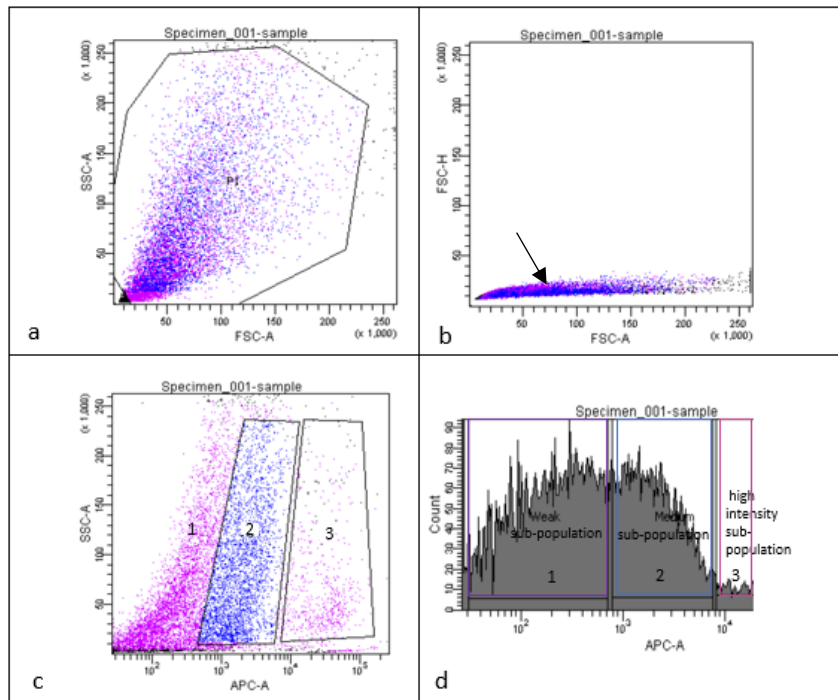


Figure 3.11 P1-CRPS cell sorting.

A. Cells are presented based on granularity and dimension and gating is used to identify cells of interest and exclude debris; the P1 population is heterogeneous as it is spread across the plot. **b.** a small number of doublets curved out from the linearity of the main cluster (arrow); doublets are frequently responsible for false brightness of fluorescence and hence were subsequently excluded from the analysis. **c.** cells are presented based on granularity and fluorescence intensity, differently from plot a in plot c. it is possible to see cells distributed according to their fluorescence intensity and select the three different population represented in d; 1: weak intensity population, 2: medium intensity population 3: s high intensity population. **d.** Traditional fluorescence intensity histogram x axis: fluorescence intensity y axis: cell numbers. The weak population contains the majority of the cells, medium contains a smaller number of cells with relatively high staining intensity while strong contains a few cells with very strong fluorescence intensity.

Using fluorescence activated cell sorting (FACS) I was able to isolate the high binding sub population, the medium population and the weak subpopulation. The weak and medium subpopulations were very heterogeneous in terms of cells morphology and fluorescence intensity, while the high subpopulation consisted in a small subgroup of very high intensity cells without specific granules in the cytoplasm that might be neurons (Figure 3.11). After sorting,

the medium-high subpopulation was stored for following mass spectrometry analysis.

Cells in the medium-high population isolated with FACS analysis were then lysed to extract immune complexes and then identify the bound surface antigen by mass spectrometry (Littleton et al. (2009)). Unfortunately, because a relatively low number of cells were isolated (10,000 per sample) it wasn't possible to collect enough protein required for a mass spectrometry analysis (20 µg of cell lysate per well) from these samples.

3.3.2 Western Blot with DRG neuronal cell homogenates

As an alternative approach, which might provide higher protein yields, to investigate whether particular DRG-neuronal proteins are bound by CRPS-IgG (instead of using FACS sorted cells), I utilized Western Blot methodology. For this approach I prepared DRG homogenates instead of DRG lysates in order to achieve a consistent protein amount. A tissue homogenate is a solution containing tissue solids, proteins and fluids obtained after tissue disruption (mechanical, sonication, bead-beating and enzymatic). A lysate is obtained directly from cells lysis (sonication or enzymatic). I chose to use tissue homogenates to avoid the process of DRG dissociation that reduced cells number.

Western blot is a very common technique that allows a qualitative and semi-quantitative estimation of proteins and consists in transferring protein bands from a gel to a membrane and then stain with a specific primary antibody and secondary antibody; size and color intensity of the band are used to identify and quantify protein detected.

Briefly, DRG homogenates were stained with HC and CRPS IgG and human IgG were detected using an HRP- anti human antibody. I found a weak band in both CRPS samples and no band for HC samples (Figure 3.12). This suggested that an antigen specifically bound by CRPS IgG may be present in DRG homogenates.

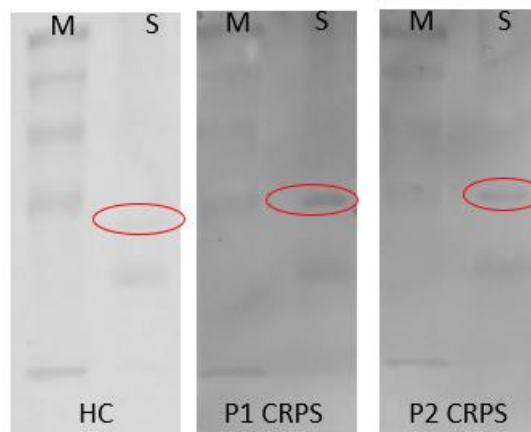


Figure 3.12 Western Blot of protein homogenates of DRG ganglia incubated with HC P1-CRPS and P2-CRPS.

M: protein marker HC: healthy control. DRGs were homogenated immediately after harvest, black protein bands (red circle) are IgG bound to tissue proteins.

It is important to say that DRGs were harvested from wild type mice (without a tissue injury to recreate inflammation in the paw) whereas the behavioral effects by IgG in the model were observed only after tissue injury. It may be

possible to obtain a stronger signal if mice were injured before DRG collection; injury and subsequent inflammation may trigger pertinent antigen expression in DRG tissue. For the experiments in the next chapters I used mice which had sustained a tissue injury.

3.3.3 Immunocytochemistry staining with DRG neuronal cells

In order to further assess CRPS IgG binding to DRG neurons I used immunocytochemistry (ICC) staining on DRG primary neurons cultures. ICC is a well- established and robust staining method used to detect target antigens in cells through protein labelling with fluorescent markers (Griffiths (1993)). Similar to flow cytometry and Western blot, ICC relies on the principle of the antibody-antigen interaction and in addition this technique allows exact antigen location. I used immunocytochemistry to qualitatively assess CRPS and HC IgG binding to dorsal root ganglion neuronal cells and to locate IgG on neuronal cell membrane. Briefly, DRG neurons were dissociated, plated on a 24 well plate on coverslips coated with poly-D-lysine and left in culture for 4 days to allow complete development of DRG neuronal processes in culture (Heinrich et al. (2016)). Cells were then fixed in 4% PFA for later staining and permeabilized.

In order to validate the staining protocol, neurons were firstly stained with the neuronal marker PGP9.5 1:500 (ab72910, ABCAM Cambridge) and Phalloidin for F-actin (Figure 3.13). Two samples were imaged, stained with DAPI, Phalloidin and only the secondary antibody for PGP9.5 stained with DAPI, Phalloidin primary and secondary antibody for PGP9.5. As expected, only the second sample stained for PGP9.5- FITC; this result confirmed that the secondary antibody had a specific staining and that our staining protocol was working fine. Interestingly, only few medium-big cells stained with the neuronal marker while some smaller cells were stained only with DAPI and Phalloidin. This staining pattern confirmed that the DRG cell population is very heterogeneous and consist of neurons of different sizes (small, medium, high) and nonneuronal cells like satellite glial cells.

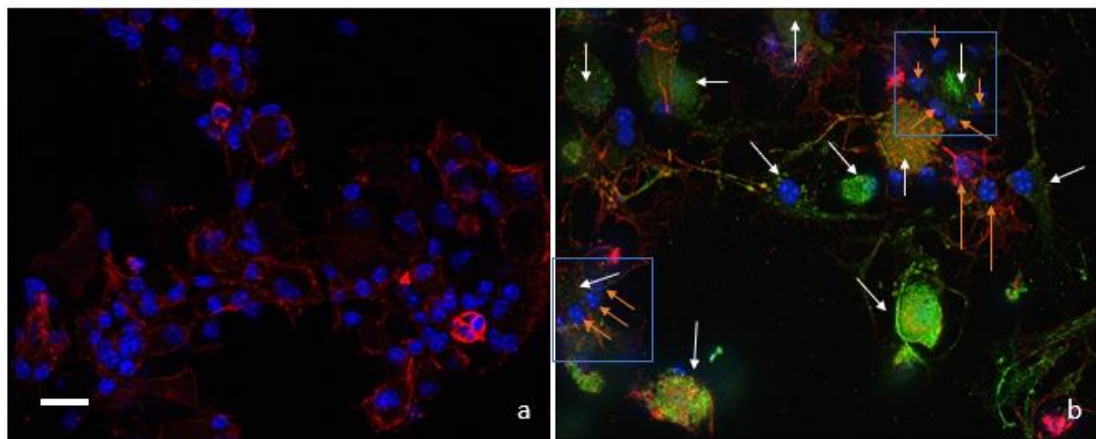


Figure 3.13 PGP9.5 staining (1:500).

Nuclei: blue, Phalloidin staining for F-actin: red. PGP9.5: green. **a.** DRG neuronal population stained with DAPI Bluestone et al. (2015) and Phalloidin (red). **b** neuronal population stained with DAPI Bluestone et al. (2015) and Phalloidin (red) and PGP9.5 (green). The stained DRG cell population is heterogeneous and consist of neurons of different sizes (with arrows) and nonneuronal cells such as satellite glial cells (orange arrows); two neurons are shown surrounded by satellite glial cells (blue squares). Scale bar represents 100 μ m

Dissociated DRG neuronal population cultured for 1 week were then stained with CRPS P1, P2 and HC IgG diluted 1:100 at 4 degrees overnight followed by a FITC anti-human IgG secondary antibody (1:500) for 1 hour at room temperature. There was no difference in staining between CRPS and HC IgG preparation. P2-CRPS had a stronger staining than P1-CRPS (Figure 3.14).

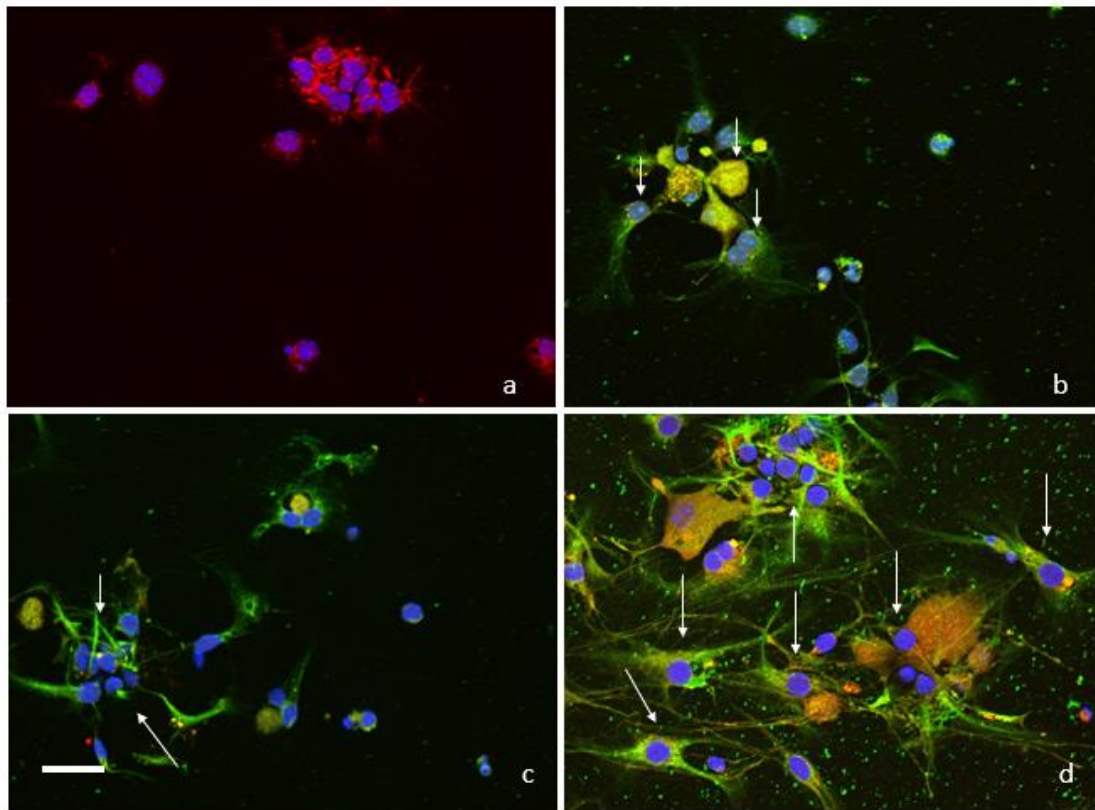


Figure 3.14 CRPS/HC IgG staining (1:100)

Nuclei: blue, Phalloidin staining for F-actin: red. IgG: green. **a.** Unstained cells **b.** healthy control **c.** P1-CRPS **d.** P2-CRPS. Neurons (arrows) were stained by both healthy control and CRPS IgG. P1-CRPS and P2-CRPS IgG stained selectively DRG population cell bodies (arrows), P2-CRPS IgG had some unspecific binding. Scale bar represents 100µm

Furthermore, as the HC and CRPS IgG had staining in the same location as Phalloidin (dye used to stain F-actin in the cytoplasm) I assumed that the IgG bound on an epitope in the cytoplasm (Figure 3.15).

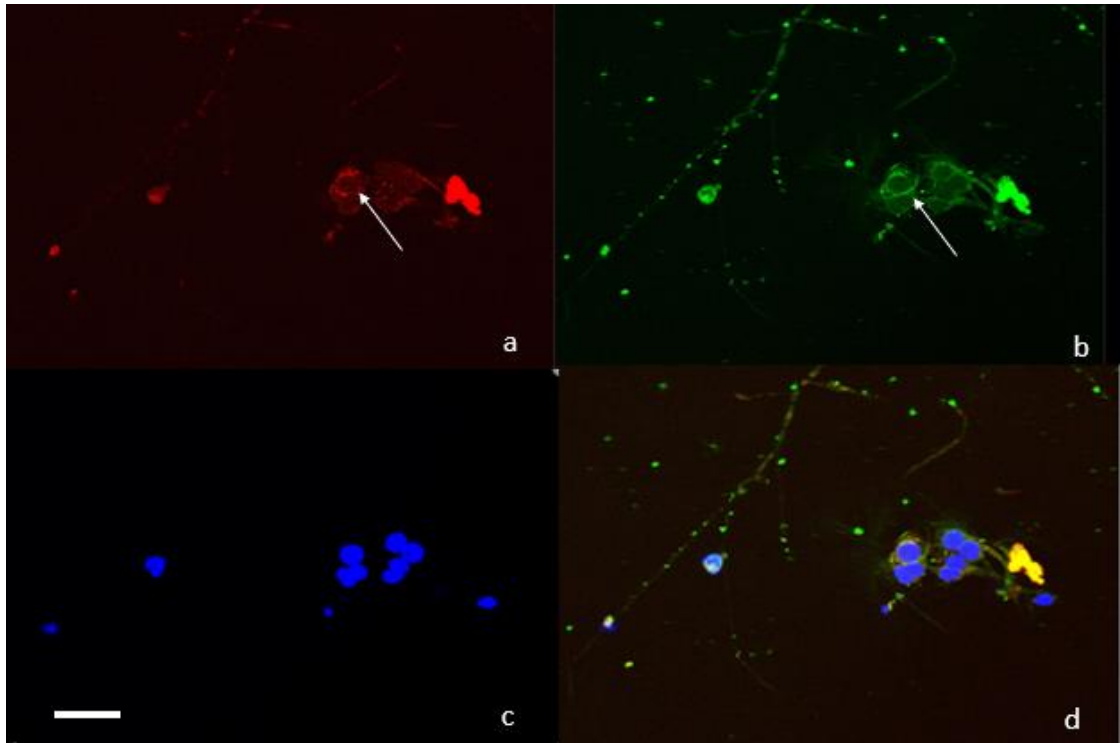


Figure 3.15 P1-CRPS IgG (1:100) staining on the cytoplasm.

a Phalloidin staining for F-actin: red. **b.** P1 CRPS IgG: green. **c.** Nuclei: blue **d.** merge. (a, b) P1-CRPS IgG (green) had staining in the same location as Phalloidin (red), dye used to stain F-actin in the cytoplasm (arrows), for this reason I supposed that P1-CRPS IgG (green) had staining in the cytoplasm. Scale bar represents 100µm

Results obtained with different methods (WB and FC) confirmed that CRPS and HC IgG have dissimilar staining intensity on neuronal population; while ICC staining showed no relevant difference between HC and CRPS IgG. In order to confirm that CRPS IgG could bind specifically only neuronal cells, I tested another cell population present in the injured limb (fibroblast) and I expected no binding. I stained a mouse embryonic fibroblast cell line (3T3) (kindly gifted by Dr Janet Risk, University of Liverpool) with CRPS and HC IgG. Briefly cells were cultured for one week in Dulbecco's Modified Eagle Medium (DMEM) and 10% FBS at 37°C in 5% CO₂. Cells were sub-cultured every

three days. Before staining medium was removed, cells were washed in PBS, fixed in 4% PFA and permeabilized with Triton X-100. Cells were then stained with Phalloidin (Alexa Fluor™ 568 Phalloidin) diluted 1:500, DAPI diluted (1:10000) and CRPS/HC IgG diluted 1:100. Phalloidin was used as a positive control for the staining protocol. I didn't see any IgG staining on fibroblast but just some background in HC and CRPS stained slides (Figure 3.16).

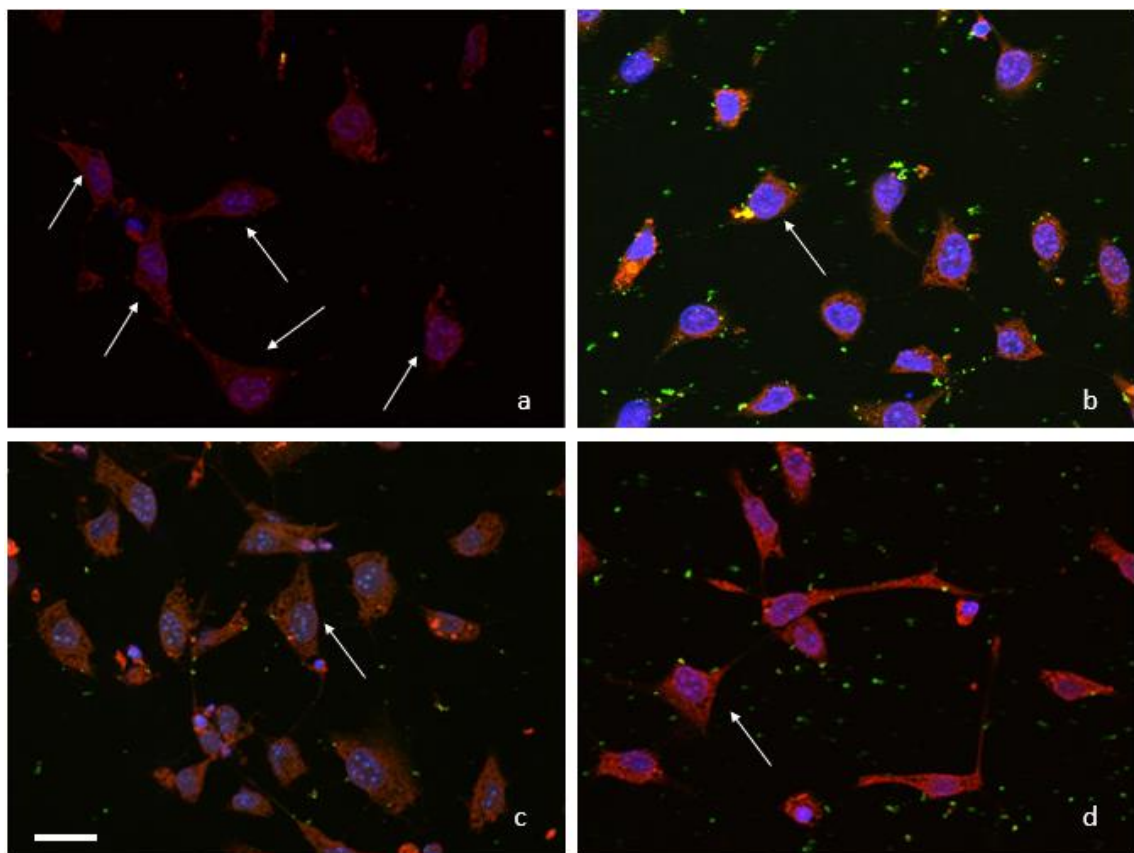


Figure 3.16 Fibroblast staining with CRPS and HC IgG (1:100).

F -actin: red, IgG: green, nuclei: blue. **a.** staining with F-actin only. **b.** healthy control staining **c.** P1-CRPS **d.** P2-CRPS. CRPS and HC IgG didn't stain 3T3 mouse embryonic fibroblast cell line (arrows). Scale bar represents 100µm

Discussion

This chapter presented results for a first assessment of DRG surface binding by CRPS serum IgG using a well-established and robust staining method used to detect target antigens in cells (flow cytometry, mass spectroscopy, western blot and Immunocytochemistry). The results obtained *in vitro* indicate that CRPS IgG bind on a neuronal surface receptor on DRG neurons only when cells are cultured with cytokines, whereas no relevant binding was detected when neurons were stained without incubation with cytokines, or with only inflammatory mediators.

My results thus demonstrate that cytokines in the inflamed limb may play a critical role in triggering the binding of CRPS IgG to an antigen on DRG neuronal cell surface, as suggested by the conceptual model of auto antibody-mediated CRPS (Goebel and Blaes (2013)).

For experiments in this chapter I used IgG purified from two single CRPS donors (described in chapter 2 section 2.1) which would have allowed me to begin to relate the staining pattern directly to the patient phenotype. Experiments with cytokines demonstrated that IgG from different patients have different effects.

Experiments with inflammatory mediators were triggered by the finding that peripheral soft tissue injury, which involves peripheral inflammation facilitates the behavioral effects of human IgG in rodents; this might suggest that the injury-associated inflammation induces a differential expression of relevant epitopes in the neurons allowing IgG binding (Tékus et al. (2014); Helyes et al. (2019)).

When neurons were incubated with inflammatory mediators the pre-incubation did not increase the surface expression of CRPS IgG target protein contrary to what was previously indicated by the results obtained with a different preparation by Reilly et al. Previous studies suggested that the inflammatory soup induces changes in neuronal excitability so it may be possible either that inflammatory mediators contribute to the sensitization of channels through intracellular signaling mechanisms that are not interfering with IgG binding to surface autoantigen, or that other mechanisms influence intracellular calcium regulation (Reilly et al. (2016)). These mechanisms are difficult to be detected with a flow cytometry analysis.

Several studies identified pro-inflammatory cytokines TNF- α , IL-1 β and IL-6 as potential biomarker for CRPS (Birklein et al. (2001); Huygen et al. (2002); Parkitny et al. (2013)). I therefore used flow cytometry to investigate whether cytokines trigger CRPS IgG binding to DRG neurons. Depending on CRPS patient IgG, cytokines treatment significantly increased either the mean fluorescence or cell percentage involved in IgG binding. When neurons were stained only with cytokine pool, nearly half of cells stained with P1-CRPS had a substantial fluorescence increase, and this was also observed after incubation of IL-6 or IL-1 β separately; on the contrary cells stained with P2-CRPS displayed only a small fluorescence increase. The identification of a bimodal cell distribution following P1-CRPS IgG staining, suggested the utility of mass spectrometry analysis to identify the cell membrane receptor bound to CRPS (Littleton et al. (2009)), but I found that the FACS preparation did not yield sufficient mass of protein to allow such mass spectrometry analysis. Since both P1 and P2 had Budapest CRPS and their serum had previously

been shown to contain pathogenic autoantibodies which induced abnormal behavior in mice, yet only P1 showed a marked apparent induction of binding following incubation with inflammatory mediators, it appeared that this induction may not be essential to the functional effect of these antibodies in all patients. At the same time, no clear increase of binding was seen in P1 over HC, highlighting either that the pertinent bound cell sub-population is small, or that methods to identify CRPS-IgG cell surface binding using mouse primary neurons (i.e. neurons not derived from injured animals) are not suitable. My initial experiment had also shown me that it would not be possible to use cells from injured animals (DRGs L3-L5) as the number of cells extracted would be even smaller than with these completed experiments.

As an alternative approach, which might provide higher protein yields than the use of FACS sorted cells, I sought to investigate whether particular homogenized DRG-neuronal proteins are bound by CRPS-IgG, utilizing Western Blot methodology. When DRG homogenates were stained in a Western Blot I found a weak band in both CRPS samples and no band for HC samples. A possible explanation for the presence of a weak band is that in Western blotting proteins are denatured in order to facilitate the charge-mass separation. Denaturation may impede the contribution of quaternary protein structure to epitope antigenicity.

I finally used immunocytochemistry to qualitatively assess CRPS and HC IgG binding to dorsal root ganglion neuronal cells and to locate IgG on neuronal cell membrane. When cells were stained with a fluorescent dye I couldn't see a significant difference in staining between CRPS and HC IgG preparations.

P2-CRPS had a stronger staining than P1-CRPS differently from what one would have expected from the flow cytometry staining results. Furthermore, I found no staining at all when either HC or CRPS were incubated with a fibroblasts line.

Overall these results suggest that in CRPS patients after injury some cells, such as fibroblast, may contribute to release inflammatory mediators and cytokines that may trigger the binding to an antigen expressed on a DRG neuronal cell surface. The binding between antigen and CRPS IgG may be very strong only *in vivo* as additional inflammatory factors or yet unexplained other factors might contribute to facilitate it.

Chapter 4 – STAINING OF DRGS HARVESTED

FROM INJURED MICE

4.1 Introduction to CRPS murine trauma model

Results in a passive transfer-trauma murine model which involves unilateral hind-paw injury suggest that persistent CRPS is caused by IgG autoantibodies (Tékus et al. (2014)), but the binding targets are unknown.

Since previous CRPS passive transfer model studies demonstrated no evidence for any enhanced inflammatory response in the periphery of the model (Tékus et al. (2014); Helyes et al. (2019)), but strong central nervous system activation along cells involved in pain-related signaling pathways, and without any evidence for IgG binding centrally (Helyes et al. (2019)), the missing link between peripheral trauma and strong central activation could be the binding of the IgG to DRG tissue. Earlier staining studies in whole foetal mouse tissue failed to identify specific cellular IgG auto antibody targets including in DRGs (Goebel et al. (2005b)). Since CRPS is a post-traumatic condition, one possible limitation of that earlier study was that dorsal root ganglion (DRG) cell binding may not have reliably been identified in DRGs from non-injured mice. Furthermore, the IHC method used may lack sensitivity to detect pertinent DRG binding, and since CRPS is very rare in young children it is also possible that foetal tissues do not express the pertinent antigens. Here I used both IHC and IF staining methods to investigate surface epitope binding

of CRPS-serum-IgG to murine dorsal root ganglion tissue harvested from hind-paw injured mice. I hypothesized that DRG harvested following limb trauma would have undergone changes in response to trauma and now present the antigen recognized by CRPS autoantibodies and would therefore constitute a promising substrate for further studies.

I used DRGs derived from the same mouse hind paw plantar incision model that was utilized by Tekus et al. (Tékus et al. (2014)) described in chapter 2. Briefly, on day 0 (day of the limb injury) mice were anaesthetized, then a 0.5 cm long incision (involving skin, fascia and muscle) was applied to the right hind paw in accordance with the Brennan model of rat incisional pain (Brennan et al. (1996)) adapted for mouse models (Tékus et al. (2014)). On day 2 mice were sacrificed (without terminal PFA perfusion) and DRGs (L3, L4, L5) receiving input from the incised (right) or intact (left) paws were then harvested and post-fixed in 4% PFA with the exception of DRG used for the last experiment in this chapter that were both perfused and then post fixed in 4% PFA (Figure 4.1). Incision, DRG harvest and DRG fixation were performed by Nikolett Szentes in the University of Pecs, Hungary, who kindly then provided these tissues to me.

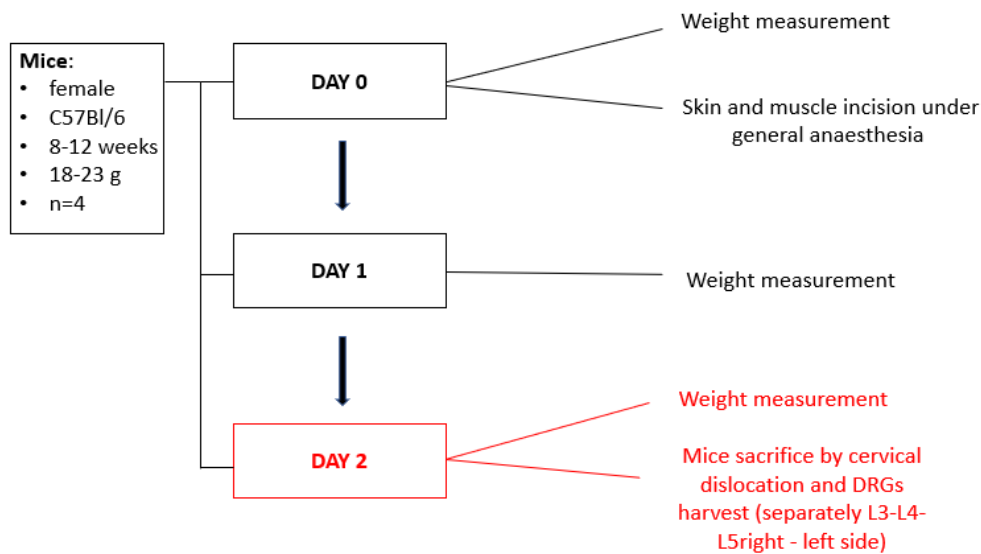


Figure 4.1 Hind paw plantar incision model.

On day 0, (day of the limb injury) mice were anaesthetized then a 0.5 cm long incision (involving skin, fascia and muscle) was applied to the right hind paw and finally the wound was opposed with two mattress sutures of 5-0 nylon. On day 2, mice were sacrificed and DRGs (L3, L4, L5) receiving input from the incised (right) and intact (left) paws were harvested and fixed in 4% PFA with the exception of DRG used for last experiment in this chapter that were first 4% PFA perfused and then post fixed in 4% PFA.

Results presented in this chapter were obtained from staining of L3, L4, L5 DRG tissue because these DRGs contain the neuronal soma of neurons that innervate the hind limb of C57BL/6 mice (Rigaud et al. (2008)). In both mouse and human, L3 contains the soma of neurons in the Saphenous nerve that innervates hind-paw hairy skin, while L4 and L5 contain the soma of neurons in the sciatic nerve that through the peroneal nerve (divided in plantar and sural nerve) innervates the sole of the paw and all muscle innervation in the lower part of the paw and the leg (Figure 4.2) (Bala et al. (2014); Shi et al. (2018); Laedermann et al. (2014); Zimmermann et al. (2009); Walcher et al. (2018)).

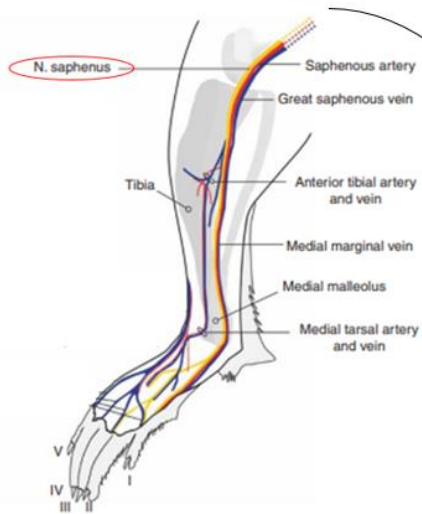


Figure adapted from Zimmermann et al 2009

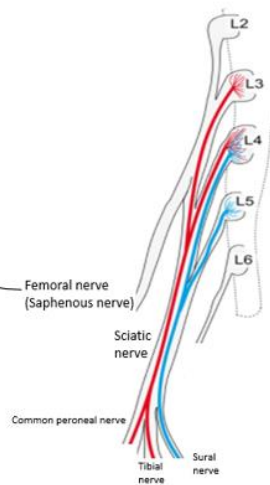


Figure adapted from Laedermann et al 2014



Figure adapted from Walcher and et al 2018

Figure 4.2 L3, L4, L5 spinal nerves in mouse hind-paw skin

A. Hind-paw hairy skin B. Hind-paw glabrous skin. (adapted from(Birklein et al. 2014); Shi et al. (2018); Laedermann et al. (2014);Zimmermann et al. (2009);Walcher et al. (2018))

A comparison between mouse and human innervation of L3, L4, L5 neurons is presented in the table (Table 4.1).

Table 4.1 Comparison between mouse and human innervation of L3, L4, L5 neurons.

Vertebral body	Spinal root	Mouse Root exit	Human Root exit	Mouse nerve	Human nerve	Mouse hind-paw skin innervation	Human foot skin innervation
L3	L3	L3/L4	L3	Femoral nerve (Saphenous nerve)	Femoral nerve (Saphenous nerve)	Hind-paw hairy skin	hairy skin
L4	L4	L4/L5	L4	Sciatic nerve	Sciatic nerve	Hind-paw Glabrous skin	Glabrous skin
L5	L5	L5/L6	L5	Sciatic nerve	Sciatic nerve	Hind-paw Glabrous skin	Glabrous skin

Staining Methods

Histological examination of DRGs is frequently used to study pathophysiological mechanisms involved in chronic pain conditions; both IHC and immunofluorescence (IF) allow visualization of IgG on DRG tissue.

IHC paraffin embedding is the gold standard technique for preparing and preserve tissue for histological staining and examination because it is thought to best preserve morphological details. It also allows long term storage at room temperature. IHC is often used to study the level of defined, known proteins in a tissue through protein labelling with the 3,3'-diaminobenzidine (DAB) chromogen detection system; I used this method to identify whether CRPS IgG binds to any structure in DRG tissue.

Immunofluorescence staining allows protein-binding quantification and identification of cellular location through protein labelling with fluorescent markers; IF is frequently used to study the levels of bound proteins in DRG neurons.

In this chapter I describe how I employed both techniques (IHC and IF) to stain ipsilateral and contralateral L3, L4, L5 DRGs from mice with right-sided hind paw injury.

4.2 Aim

The first aim was to provide proof of concept for the detection of specific binding between CRPS-IgG and DRG tissue from injured mice compared to binding between HC-IgG and DRG tissue; I planned to first use IHC for a preliminary histological examination of human IgG binding to DRG tissue and then to use IF to more precisely locate and quantify the IgG involved in binding. The second aim was to compare DRGs from the right (injured) side to the left (non-injured) side. I expected to detect stronger binding on the right side, likely in both CRPS and HC. Hypothesizing that on the injured side, DRG neurons receiving input from the injured tissue may express either new or higher numbers of existing epitopes that can be bound as suggested by the 'IgG pain' passive transfer in the animal model (Tékus et al. (2014)).

The first objective to achieve these aims was to establish a protocol to initially positioning and embedding DRGs for IHC and IF staining, because no protocol was available in the literature and DRGs were extremely difficult to process due to their very small dimension. Then, the second objective was to validate a protocol to process DRGs for IF and then to validate a protocol for staining snap frozen tissue and PFA fixed tissue.

The research questions evaluated in this chapter were: i. Which if any cells are specifically bound by CRPS IgG? ii. Is the binding intracellular/extracellular? iii. Do different patient IgG preparations bind in the same or in different ways? iv) are there any differences in binding between right and left sides (for either HC or CRPS).

4.3 Results

4.3.1 IHC Staining of DRG harvested from injured mice

4.3.1.1 Histological presentation of DRG from injured mice

Histological examination of DRGs is frequently used for neuropathological evaluation of the peripheral nervous system and to study pathophysiological mechanisms involved in chronic pain conditions. Paraffin embedding tissue preparation is well described for most tissues but no protocol is available in the

literature for DRG paraffin embedding. Published IHC protocols only provide information regarding fixation strategy (immersion or perfusion) or fixative type (neutral buffered formalin or formaldehyde) (Pardo et al. (2020)).

DRG sections were dewaxed and stained with haematoxylin and eosin (H&E) according to standard protocols (Bancroft and Gamble (2008)). I prepared a paraffin block containing L3, L4, L5-right and a paraffin block containing L3, L4, L5-left embedded together respectively, for each of the 10 mice sacrificed; this allowed a direct comparison between right and left part and identification of staining variability between different mice. For each block I cut 40-50 tissue slides (4µm thick) and initially I stained with haematoxylin and eosin (H&E) the slides number 1, 10, 20, 40 (in order of cuts, with '1' being the first usable tissue cut) for histological examination (Figure 4.3). Staining these slides at different depth into the DRG tissue was relevant to comprehensively evaluate tissue morphology and integrity of all DRGs.

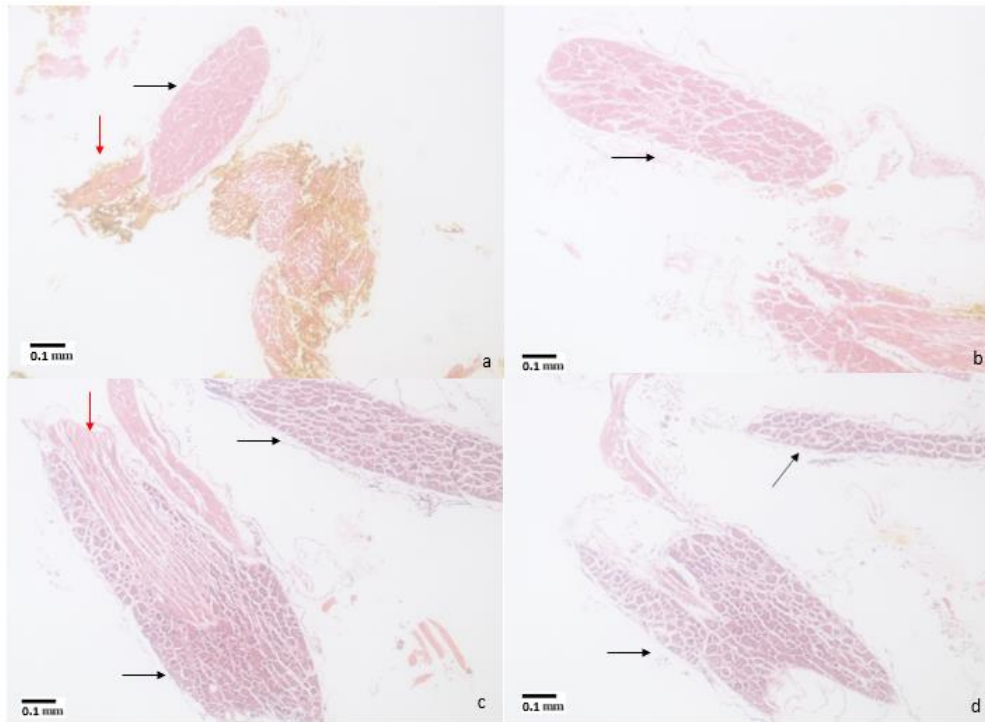


Figure 4.3 Different sections from the same DRG block.

L3, L4, L5 DRGs from same mice (right sided) were embedded in the same paraffin block, and for each paraffin block 40-50 tissue sections were cut, each section was 5 μm thick. **a**= Slide number 1. **b**= Slide number 10. **c**= Slide number 20 **d**= Slide number 40. Black arrows: large and well-preserved neuron rich areas. Red arrow: fibres. Slide bar indicates 100 μm .

I then stained with CRPS/HC IgG only slides with a large and well-preserved neuron rich area (Figure 4.4), usually these were present in slides from 10 to 40.

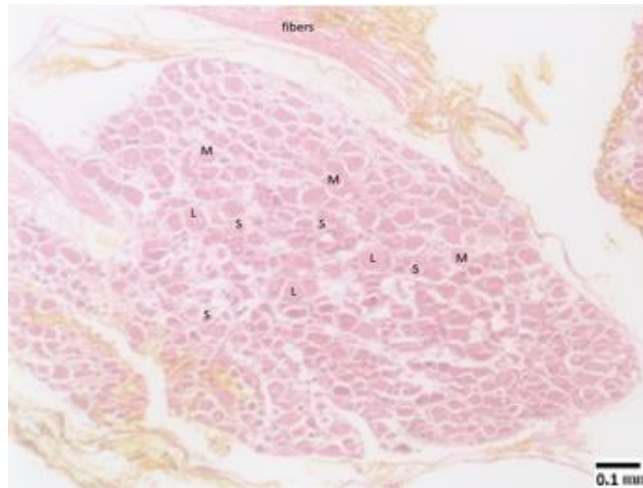


Figure 4.4 Lumbar dorsal root ganglion H&E staining.

The DRG is composed of a mixed neuronal population of large (L) diameter ($>30\mu\text{m}$), medium size (M) ($23\text{-}30\mu\text{m}$), and small diameter (S) ($<23\mu\text{m}$), neurons. The Neurons have been sectioned tangentially as the nucleus can't be observed within the cell body (Pardo et al. (2020)). Slide bar indicates $100\mu\text{m}$.

Some slides presented general cell shrinkage probably due to tissue dehydration or over-fixation in PFA (Pardo et al. (2020)), and were discarded.

4.3.1.2 Right DRGs staining

I chose IHC staining to investigate binding of CRPS-serum-IgG to murine primary dorsal root ganglion cells. For the IHC experiment described below, DRGs corresponding to the incised right paw were fixed in 4% PFA immediately after harvest (animals were not perfused) and then paraffin embedded. Then three consecutive paraffin slides were stained with either affinity purified CRPS, HC-IgG or no IgG (negative control) followed by anti-human-IgG-HRP. The three DRGs (L3, L4, L5) were embedded at slightly different levels in the paraffin block; we stained initial slides (1-10), middle

slides (15-25) and final slides (30-40) in order to achieve an overview of staining pattern in all DRGs.

For an initial tissue staining overview (using slides 1-10), slides were stained with pooled HC IgG and pooled CRPS IgG preps derived respectively from 5 healthy volunteers and 27 CRPS patients with high pain intensities (NRS 7.5-9) and disease durations between 1 to 5 years diagnosed according to international research criteria for the diagnosis of CRPS (Goebel et al. (2017)). Patients demographics are reported in the second chapter.

Overall there appeared a slight difference in staining intensity between HC and CRPS, irrespective of the blocks of embedded tissues (n=10) or DRG-level (L3-L5) investigated while there was no obvious difference between initial, middle and final slides. CRPS staining was uniformly stronger and, interestingly, particularly strong staining appeared to affect some neurons. This observed apparent neuronal selectivity staining didn't appear to be determined by size (Figure 4.5). I have not quantified this staining as this was a screening test, but quantification of individual staining is described further below.

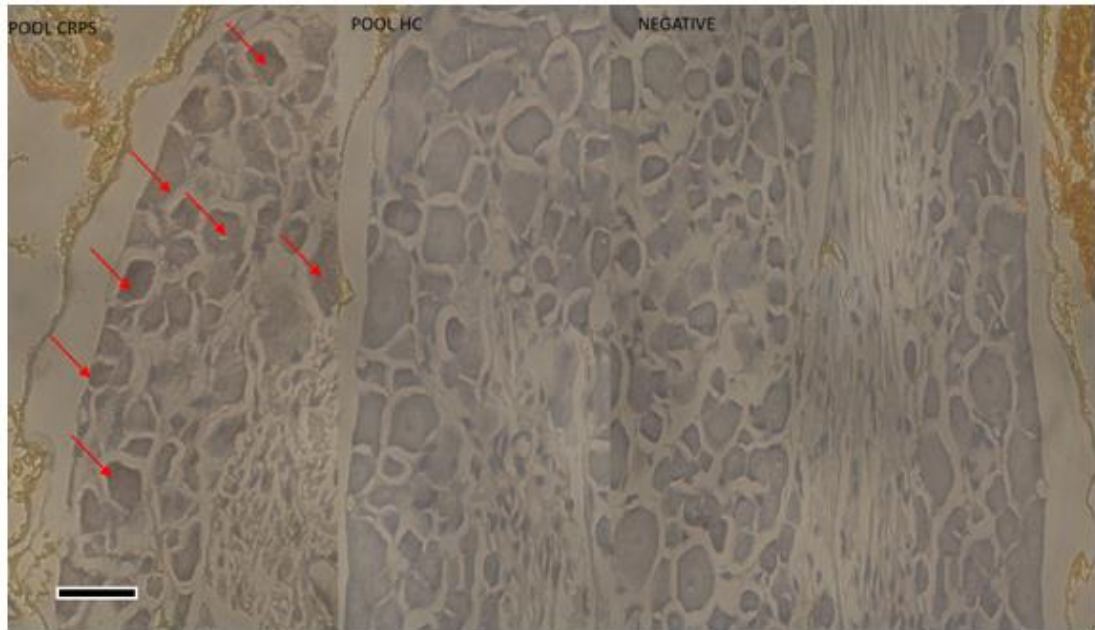


Figure 4.5 Example of right side DRG staining with pool HC/CRPS IgG.

CRPS staining was stronger and selective for some neurons (red arrows). The staining did not appear to be selective for a specific neuronal sub-population, as small, medium and large neurons were stained equally. Scale bar represent 100 μ m.

I hypothesised that the fact that there was only a relatively small difference between patient and control pooled preparations was related to the PFA fixation method I had used. It is understood that PFA fixation can mask some epitopes by cross-linking peptides near the epitope or by altering conformation of the electrostatic charge of the epitopes (Stanly et al. (2016); Im et al. (2019); Arecco et al. (2016); Lettau et al. (2020); Sawano et al. (2016)). In an attempt to enhance staining, I tested both heat-induced epitope retrieval (HIER) and an HRP polymer; the prior is an established method to restore the immunoreactivity of an epitope after PFA fixation while the latter is a signal amplification method used in IHC for detection of rare epitopes and low abundance antigens. Both these methods increased unspecific binding,

especially in the nuclei, but did not enhance specific IgG staining (Figure 4.6, Figure 4.7).

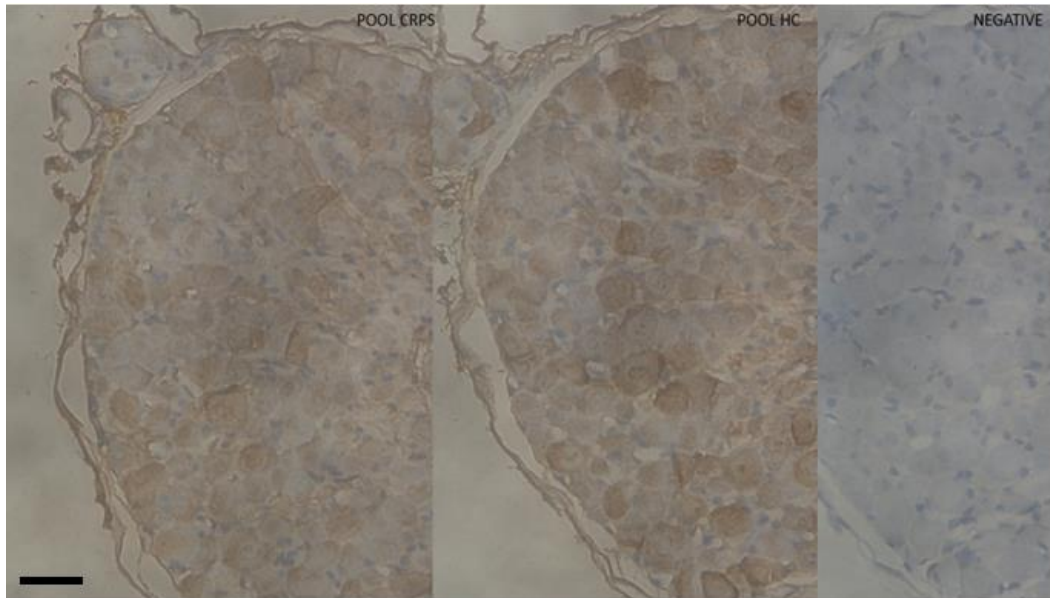


Figure 4.6 Antigen retrieval staining.

Antigen retrieval staining increased unspecific binding, but did not specifically enhance CRPS IgG staining. Scale bar represents 100 μ m.

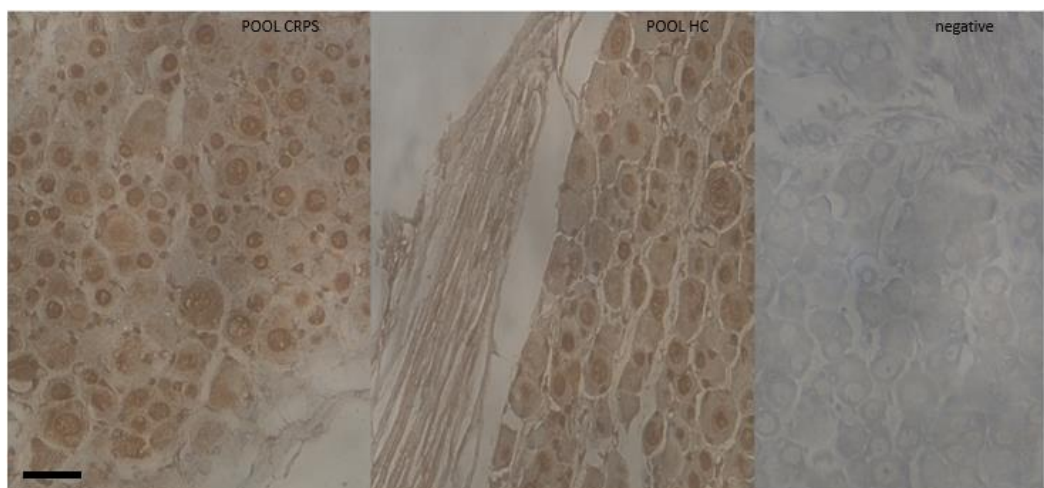


Figure 4.7 HRP polymer staining.

HRP polymer staining appeared to increase binding globally, most evident in the nuclei. Scale bar represents 100 μ m.

Finally, I harvested a second batch of DRGs. I fixed tissue with buffered formalin and it was post-fixed it in 70% ethanol instead of PFA in order to avoid epitope masking and tissue damaging common with over-fixation in PFA. However, tissue processed with this alternative method did appear to neither stain pooled CRPS or HC IgG, and there was overall only weak unspecific binding (Figure 4.8). These experiments, although in the absence of clearly specific CRPS staining confirmed that fixation with PFA was a relatively more promising choice for this kind of staining in our setting.

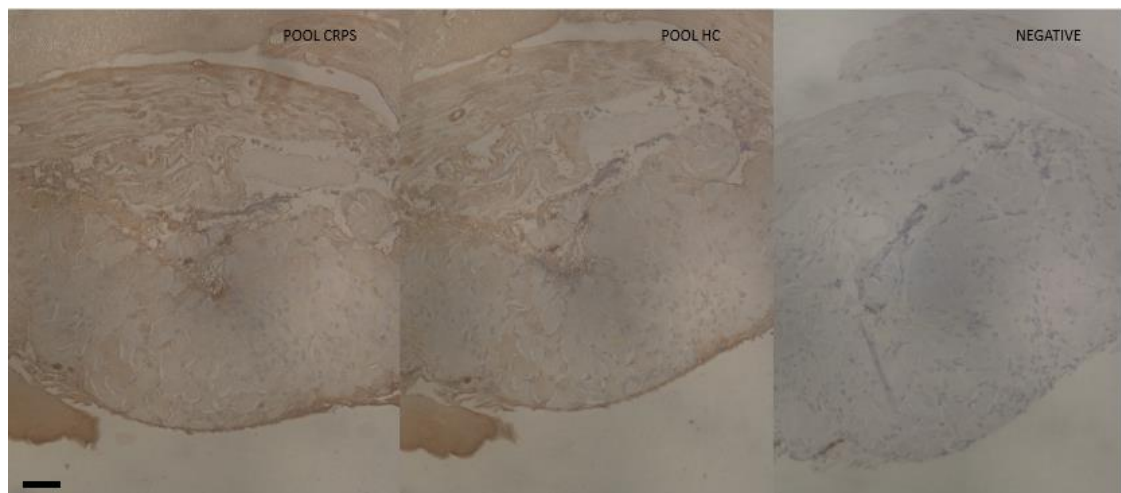


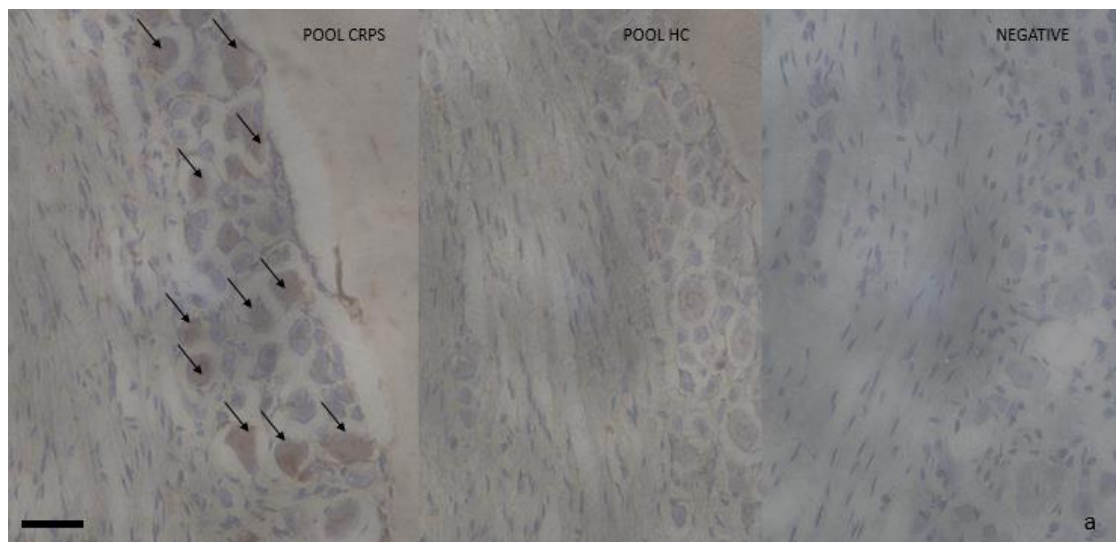
Figure 4.8 Tissue fixed with Buffered formalin.

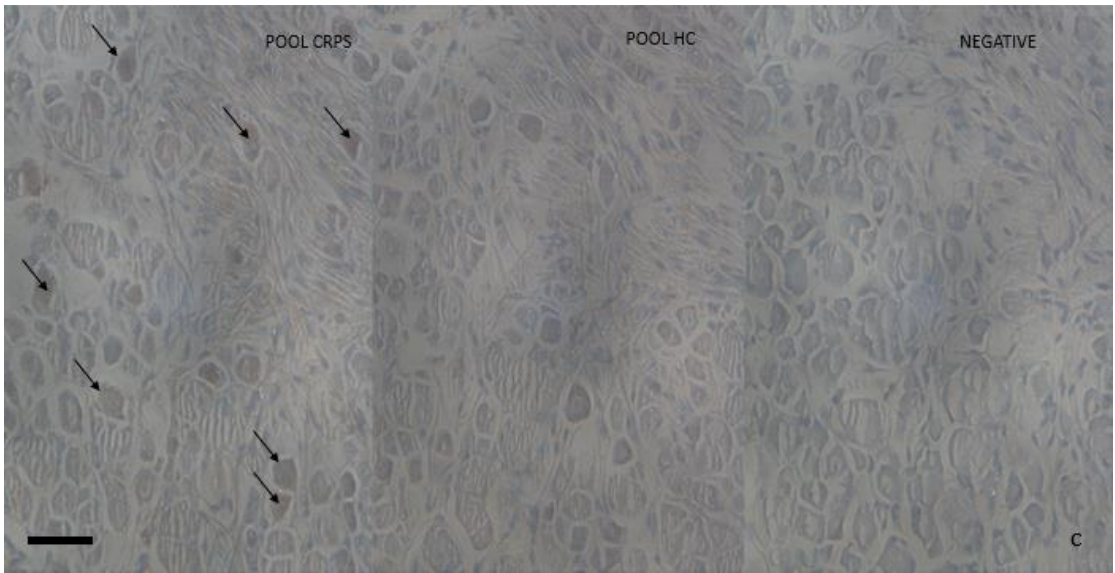
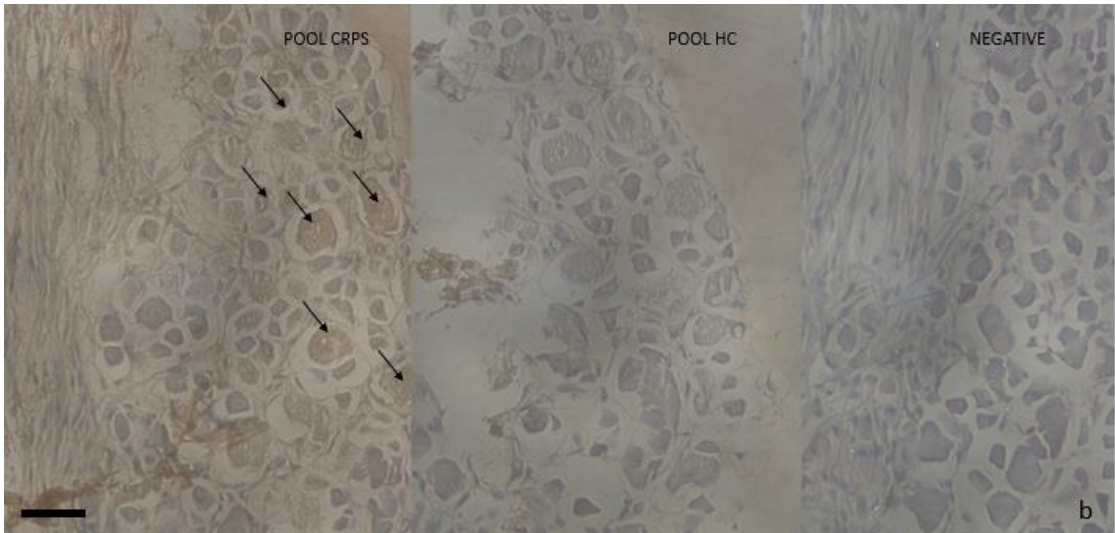
Tissue fixed with Buffered formalin instead of 4% PFA did not stain for pooled preparations. Scale bar represent 100 μ m.

4.3.1.3 Patients staining pattern

I then stained slides number 51-53 per each right block using pool HC and CRPS IgG. When compared to slides number 1-10 the staining of four blocks was stronger (Figure 4.9). I hypothesized that either different DRGs had different staining intensity level or that stronger staining may be observed in when deeper tissue, perhaps due to some variation in expressed epitopes.

I observed that there was staining variability between different blocks and that generally CRPS preparation stained stronger than HC. I have not quantified this staining as this was another screening test, but quantification of individual staining is described further below.





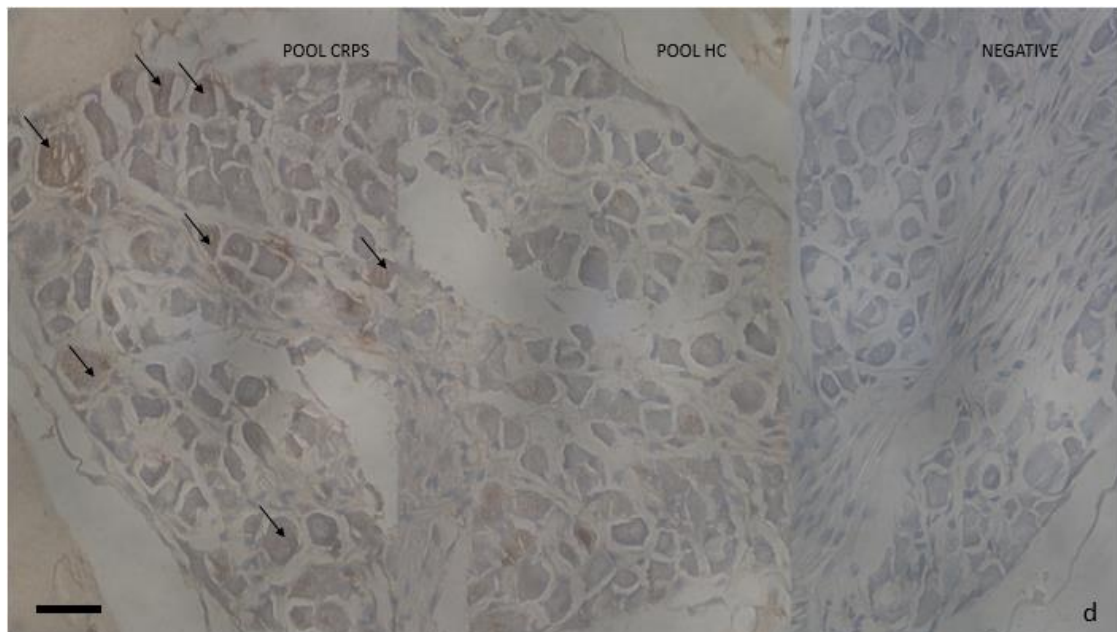


Figure 4.9 Staining of slides 51-53.

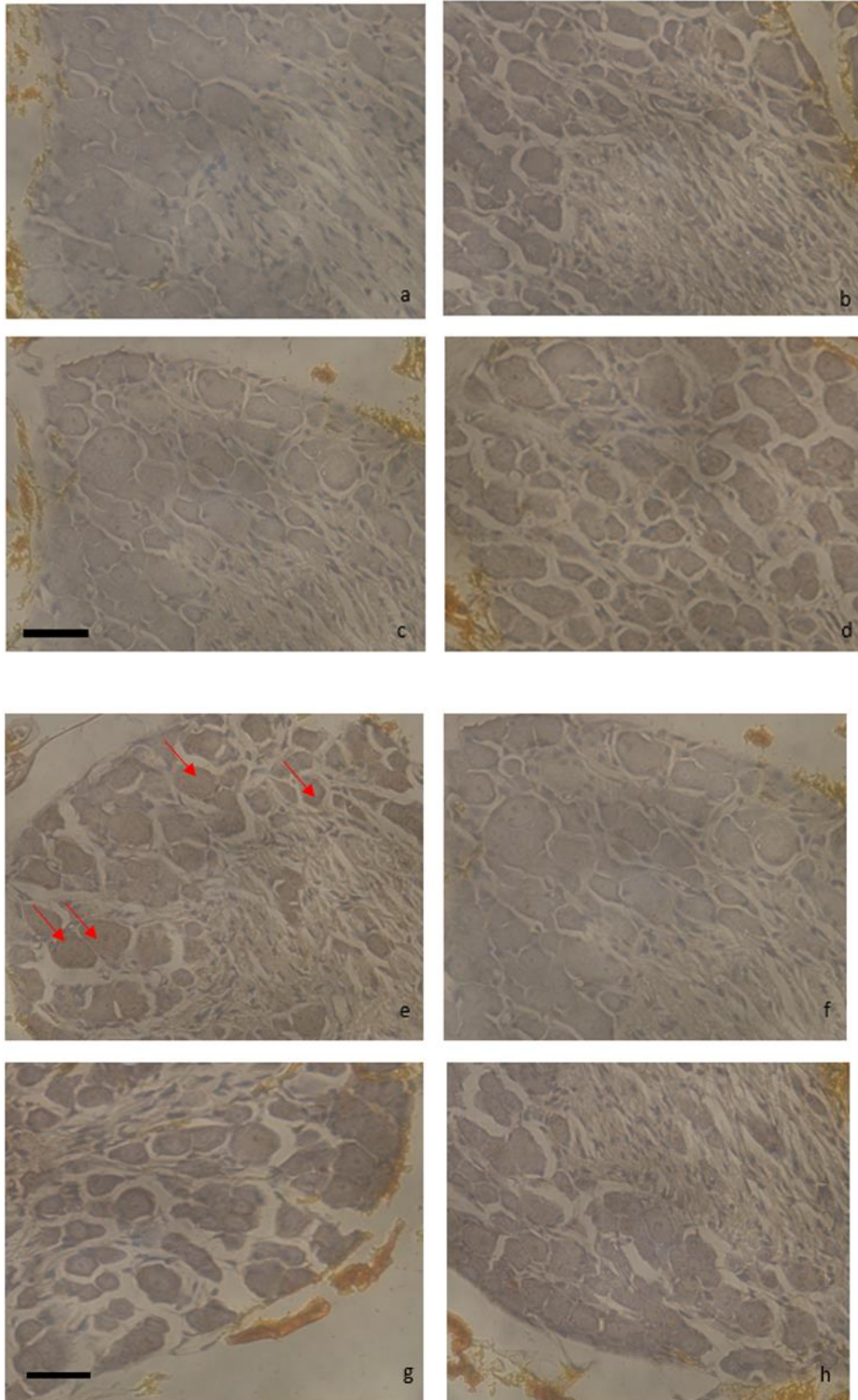
Pool HC and pool CRPS staining in lumbar DRGs harvested from 4 different mice, a. mouse 1, b. mouse 2, c. mouse 3, d. mouse 4. Slides had variability in staining pattern, and additionally in mouse 1,2,4, there is stronger CRPS staining (although the types of staining differ). Whereas staining appears similar in mouse 3. This preliminary staining with a pool of CRPS/HC IgG showed standardized cytoplasmatic or selective nuclear staining of CRPS of some neurons in DRG tissue while pool HC IgG did not stain. Scale bar represent 100µm.

The pooled CRPS IgG stained selectively some neurons, and no other cell types appeared to be stained. DRGs from different mice had a different staining intensity; in particular mice 1 and 3 had a dark brown staining while mice 2 and 4 had a light brown staining indicating presence of CRPS IgG. This preliminary staining with a pool of CRPS/HC IgG showed standardized cytoplasmatic or selective nuclear staining of CRPS of some neurons in DRG tissue while pool HC IgG did not stain.

Slides stained represent any of the DRGs (either L3, L4, L5) as these were paraffin embedded in the same block. It was not feasible to individually examine these three types of DRGs because of lack of tissue.

Additional experiments with single patient IgG were carried out to evaluate staining heterogeneity between different CRPS patients.

Blocks 1,2,3,4 were stained individually with IgG from four different healthy control and eight different CRPS patients selected respectively from those samples that had formed the CRPS and HC pools respectively. Briefly, serum from selected patients and controls was purified and twelve consecutive paraffin slides were stained with affinity purified CRPS patient and HC-IgG and then with anti-human-IgG-HRP. The individual patient IgG's selectively stained neuronal DRG cells, sparing nuclei, and no other cell types appeared to be stained (Figure 4.10). Within these cells, the majority of patient IgG's selectively stained the cytoplasm with varied staining intensity; varied staining intensity was also present among controls however most HC preparations were not obviously different from CRPS. Some patient IgG's caused an unspecific staining pattern either for cell membrane or nuclei. I additionally stained the same DRGs with patient P1 and P2 used in previous chapter and found that P1 had a strong staining involving a mixed neuronal population while P2 had a light staining involving only one neuronal subpopulation of medium-large neurons.



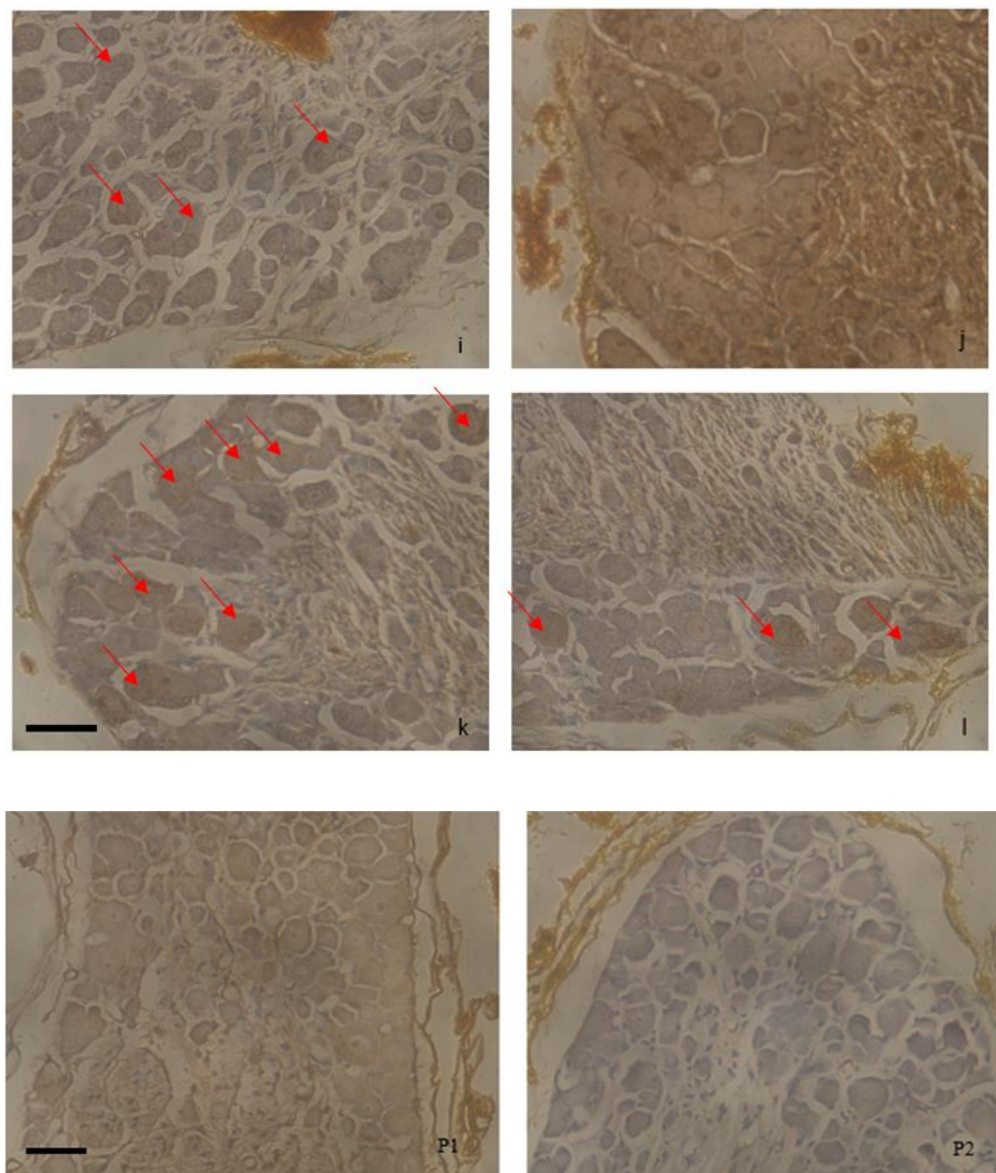


Figure 4.10 Right part individual control's and patient's staining patterns.

Same slides were stained with four different HC (a. b. c. d.) and eight different CRPS IgG (e. f. g. h. i. j. k. l.). CRPS staining was stronger overall and was selective for some neurons (red arrows). The majority of neurons were stained and these had high IgG staining only in the cytoplasm. Few patient IgG's stained both for membranes and nuclei. P1 had a strong staining involving a mixed neuronal population while P2 had a light staining similar to control staining. Scale bar represent 100µm.

Staining intensity for each slide was then also quantified by asking a colleague to look at each image in a blinded way and rate the overall staining intensity across each respective slide between 0-3, allowing half points, irrespective of

the staining pattern such as nuclear staining) (Figure 4.11) (Goebel et al. (2005b)). I found that there was a trend for overall stronger staining by the CRPS serum group when compared to the HC group, however this did not reach statistical significance (Figure 4.11)

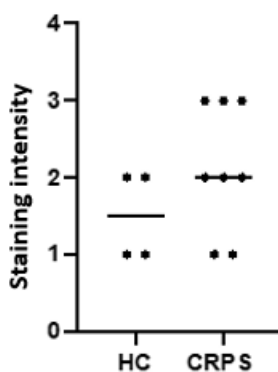


Figure 4.11 Right paw-injured individual healthy control's and patient's L3-L5 DRG staining patterns.

Maximal staining intensity was rated for each affinity-purified serum-IgG preparation by a blinded observer. Statistical significance was calculated with Mann-Whitney tests for unpaired data ($p < 0.05$). HC median staining intensity: 1.5, CRPS median staining intensity: 2. The difference between the value of HC and CRPS was statistically significant ($p = 0.3245$) ($n = 4$).

4.3.1.4 Left DRGs staining

When left sided DRGs, which receive input from left not-injured paws were stained with pool sample preparation, no specific strong staining was found for pool CRPS and no particular difference from pool CRPS and HC (Figure 4.12). I have not quantified this staining as this was a screening test, but quantification of individual staining is described further below.

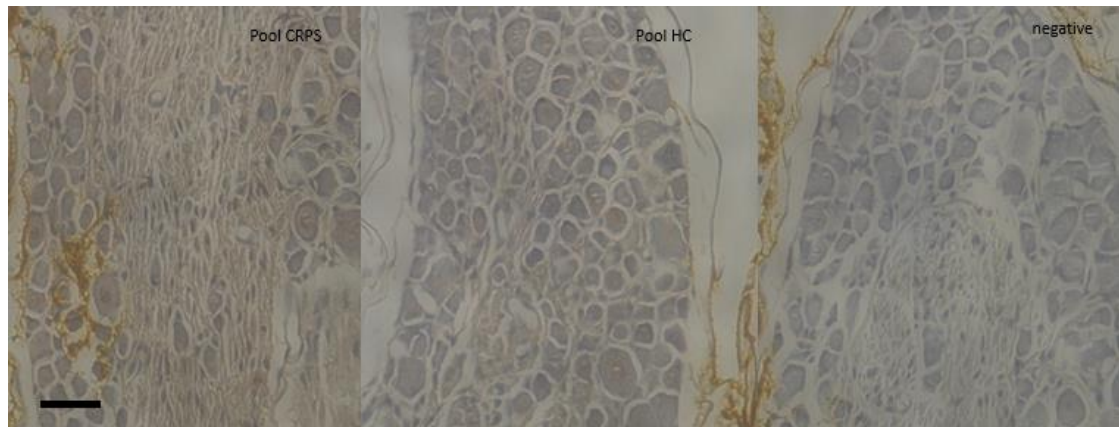
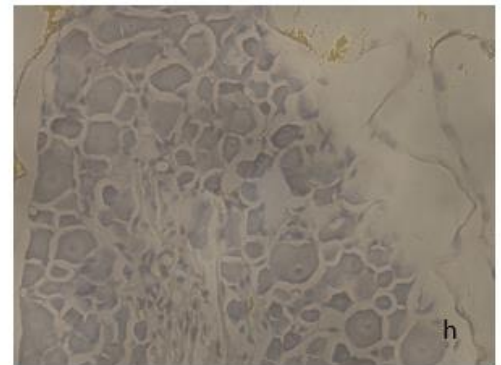
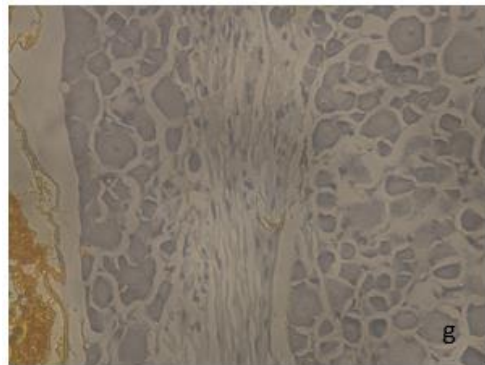
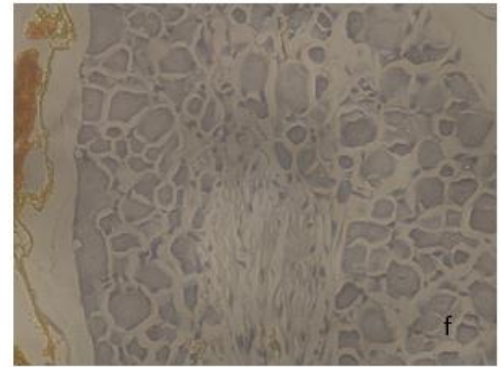
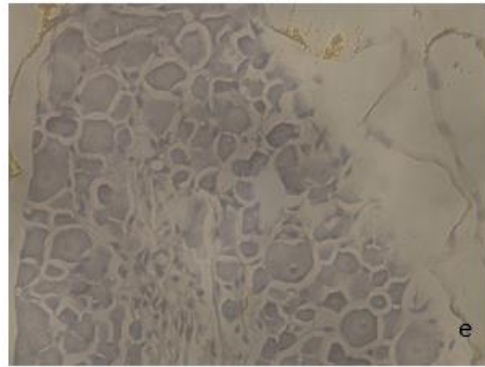
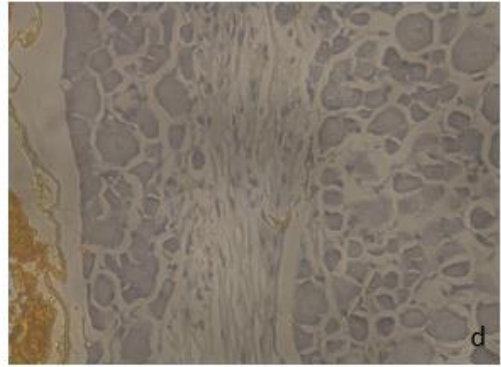
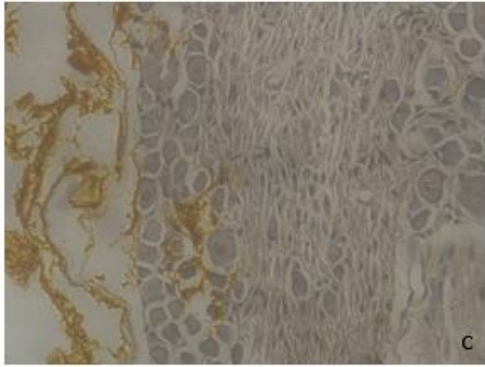
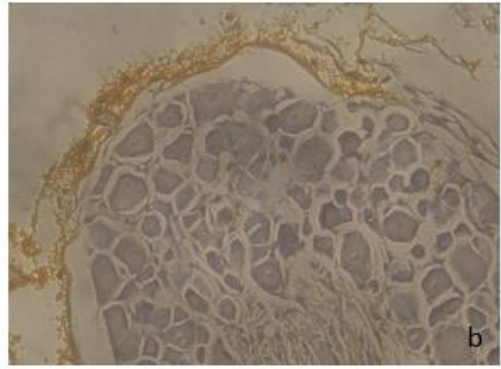
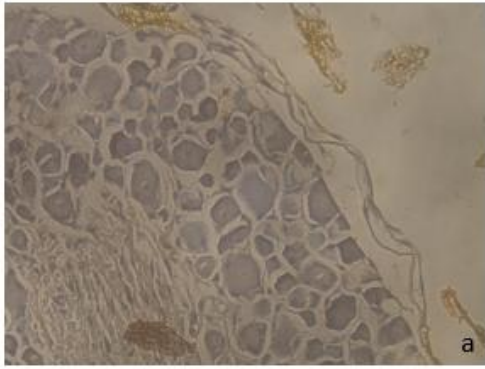


Figure 4.12 Left part staining of pool preparation.

Right sided DRG staining with pooled IgG preparations are copied from Figure X above for comparison. Scale bar represent 100 μ m.

I then stained left DRG blocks 1,2,3,4 individually with IgG from four different healthy control and eight different CRPS patients selected respectively from those samples that had formed CRPS and HC pool as I did for the right blocks. Staining for left side CRPS and HC was lighter than right side CRPS and HC at every slide number (Figure 4.10) (Figure 4.13). In addition to samples selected from pool preparations we also stained the same DRGs with patient P1 and P2 used in previous chapter for flow cytometry, immuno-cytochemistry and Western Blot. Both P1 and P2 had a light staining on the left part. (Figure 4.13)



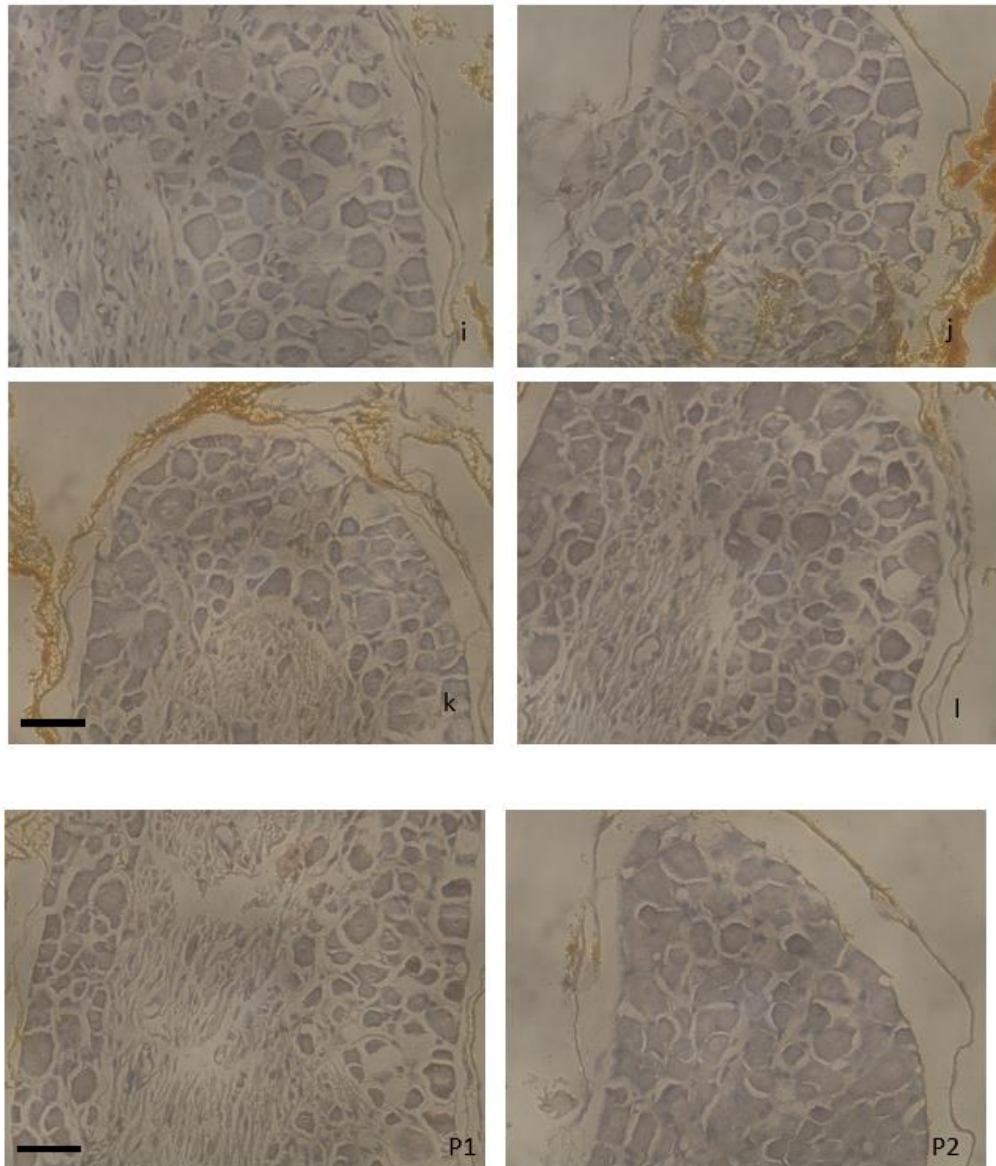


Figure 4.13 Left part Individual control's and patient's staining patterns.

Same slides were stained with four different HC (a. b. c. d.) and eight different CRPS IgG (e. f. g. h. i. j. k. l.). No specific strong staining was found for CRPS and no particular difference from CRPS and HC. Staining for left side CRPS and HC was lighter than right side CRPS and HC at every slide number. Both P1 and P2 had a light staining on the left part. Scale bar represent 100 μ m.

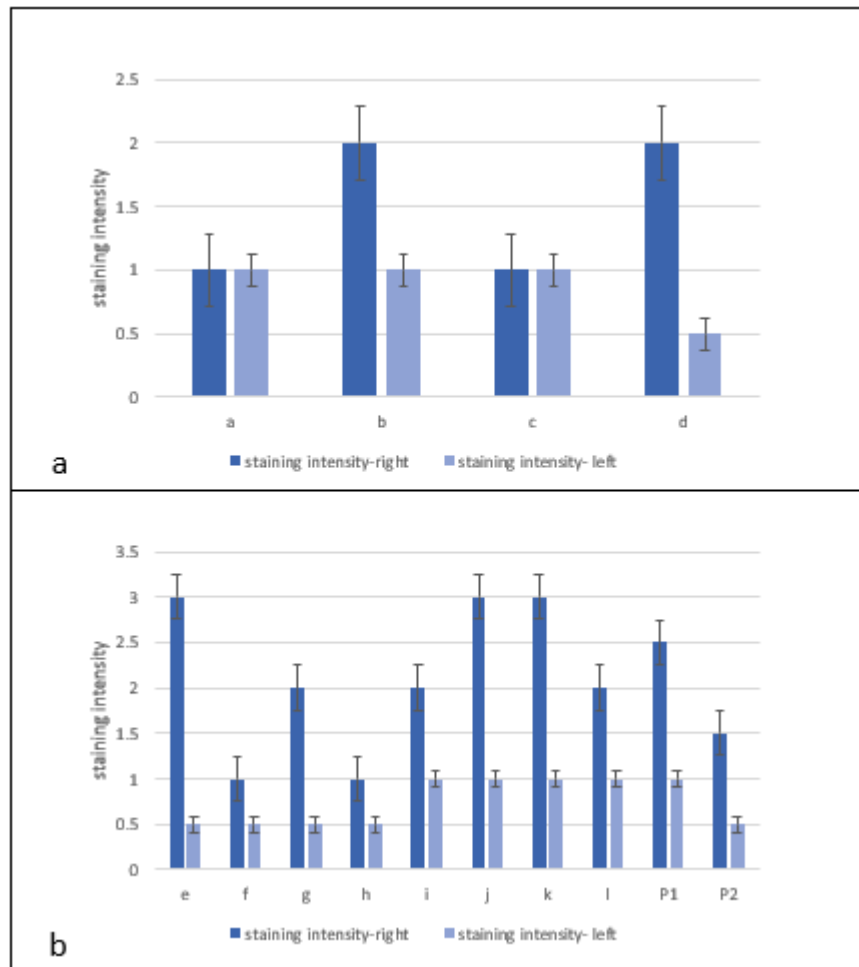


Figure 4.14 HC-right vs. HC-left and CRPS-right vs CRPS left.

a. HC, b. CRPS. Left part had very light/no staining when stained with both CRPS and HC single preparations while right part had stronger staining when stained with both CRPS and HC single preparations. Statistical significance was calculated with t- tests for paired data ($p < 0.05$). HC-right mean value=1.5, HC-left mean value=0.875, CRPS-right=2.1, CRPS-left=0.75. The difference between HC-right and HC-left was not statistically significant (p value=0.194), while the difference between CRPS-right and CRPS-left was statistically significant ($P < 0.0001$).

When the DRGs from the left paw were stained with pool and single sample preparations, staining intensities were generally very low and similar between CRPS and HC. The difference between left and right sided staining intensities

was highly significant for the CRPS when compared with the HC group (Figure 4.14). These observed differential staining intensities between the right (injured) and left (not injured) sides are consistent with a critical role of tissue injury in allowing enhanced binding of autoimmune IgG and consequently in facilitating the development of CRPS (Goebel and Blaes (2013)).

In conclusion, we used IHC for a preliminary histological examination and staining of human IgG on DRG tissue. For an initial tissue staining overview, slides were stained with pooled HC IgG and pooled CRPS IgG preps derived respectively from 5 healthy volunteers and 27 CRPS patients. CRPS staining was stronger and appeared selective for some neurons, and this was uniformly observed across all DRGs and blocks. The staining did not appear to be selective for a size-determined neuronal sub-population.

We then stained blocks 1,2,3,4 individually with IgG from four different healthy control and eight different CRPS patients selected from HC and CRPS pools respectively. The individual patient IgG's selectively stained neuronal DRG cells, sparing nuclei, but no other cell type appeared to be stained. The majority of patient IgG's selectively stained the cytoplasm with varied staining intensity. Varied staining intensity was also present among controls but these appeared to have a less intense staining when compared with CRPS IgG. Few patient IgG's had a staining either for cell membranes or nuclei. When DRG from left paw were stained with pool and single sample preparation, no specific strong staining was found for CRPS and no particular difference between CRPS and

HC (figures 4.12 and 4.13). Overall tissue slides from the right part stained with CRPS single preparation had a stronger staining than slides from the left part. We quantified the seeming difference between right and left sides, following blinded assessment by an independent observer and found that there was a clear numerical difference between groups, which did not quite reach significance for HC-IgG but was statistically significant for CRPS-IgG (Figure 4.14).

4.3.2 IF Staining of DRG harvested from injured mice

4.3 2.1 IF staining of snap-frozen sections

According to the literature, immunofluorescence (IF) staining is usually done on snap-frozen tissues because in frozen tissues molecular structures are usually very well preserved due to the absence of 4% PFA that can cross-link epitopes and can interfere with the staining (Stanly et al. (2016); Im et al. (2019); Arecco et al. (2016); Lettau et al. (2020); Sawano et al. (2016)). . Furthermore, IF staining might be more sensitive than IHC especially for cell membrane antigens staining as it is less harsh than IHC (that requires long tissue processing times, fixation in PFA and passages in strong solvents) (Stanly et al. (2016); Im et al. (2019)). IHC is not possible on snap frozen tissues; frozen tissue is not suitable for IHC because this method is designed

to use paraffin embedded tissue that can be processed at room temperature, frozen tissue would be highly damaged with this method.

Since I had only detected very subtle differences between CRPS and HC IHC staining patterns in PFA fixated tissues (see part A), I now wished to examine whether tissue staining without PFA might allow for a clearer picture to emerge. Even if snap-freezing is frequently used to rapidly fix fresh tissues, it also presents some disadvantages including distortion of the normal shape, making it challenging to identify individual cells and relevant tissue structures.

I stained L3, L4, L5 right blocks with the same pool of 27 CRPS patient IgG and 5 HC IgG, as described in the IHC staining part. As described above DRGs were harvested on day 2 from injured mice (Brennan et al. (1996)) and instead of being fixed in 4% PFA these were immediately snap-frozen in isopentane cooled in liquid nitrogen at -150°C and then stored at -80°C . Furthermore, the preserved DRGs were then also processed differently from IHC. I placed L3, L4, L5 one per block and cut them separately, both for right part and left sided DRGs as I hoped that this would make it easier to examine any differences between the DRGs. Snap-frozen DRGs were then thawed and post fixed in acetone (which has less known adverse effect on epitope presentation) and stained following a protocol adapted from Schäfers et al. (Schäfers et al. (2003)). Briefly, tissues slides were incubated in blocking solution for 30 min and then 1 hour at room temperature with purified human IgG at $5\mu\text{g}/\text{mL}$ in blocking solution. Sections were then incubated with anti-human secondary antibodies FITC conjugated for 1 hour in blocking solution.

In order to further validate my staining results, I now used a positive control. I obtained CASPR2 IgG; CASPR2-associated conditions are autoimmune conditions associated with autoantibodies against small sensory nerves and can be accompanied by neuropathic pain. CASPR2 IgG appears to regulate DRG neuronal excitability; most CASPR2 patients have Morvan's syndrome which also has an important central element. The details of the patient donor for this sample are reported in the second chapter. Samples were kindly gifted by Prof Irani (University of Oxford, UK). IF has recently been used successfully to locate human IgG on DRGs in a mouse animal model of CASPR2 (Dawes et al. (2018)) (Figure 4.15).

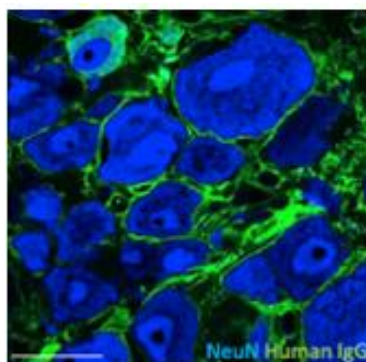


Figure 4.15 CASPR2 IgG staining in a mouse animal model.

Image taken from Dawes et al (Dawes et al. (2018)).

Dawes et al. injected an IgG solution in mice before tissue perfusion with PFA and harvest, as previously discussed, but I decided to directly snap-freeze tissue to avoid any epitopes masking. I then used the same protocol to stain snap-frozen DRGs with pooled CRPS and pooled HC IgG (Figure 4.16 and 4.17).

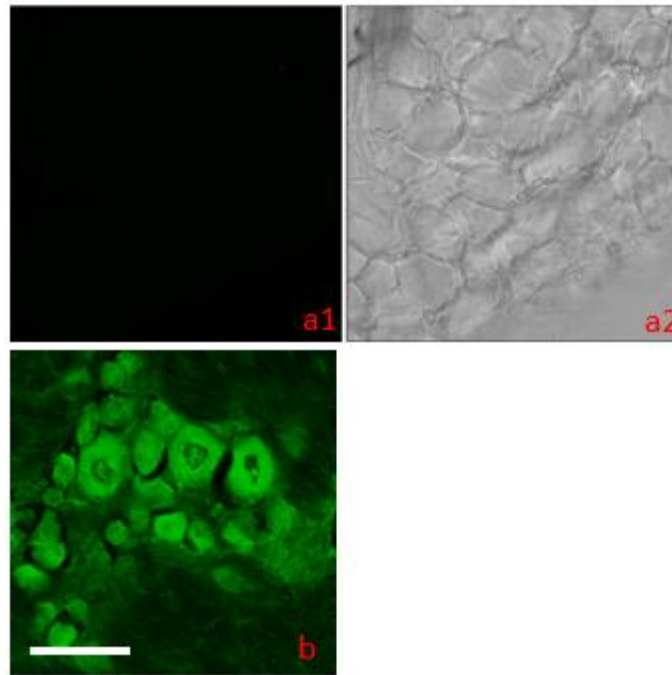


Figure 4.16 Snap-frozen right DRG staining.

Negative (n) and positive control (pc). a1. Fluorescent image of the negative control (no primary added) a2. Brightfield image of the negative control b. Positive control staining with CASPR IgG used by Dawes *et al* Dawes et al. (2018). Scale bar represent 100 μ m.

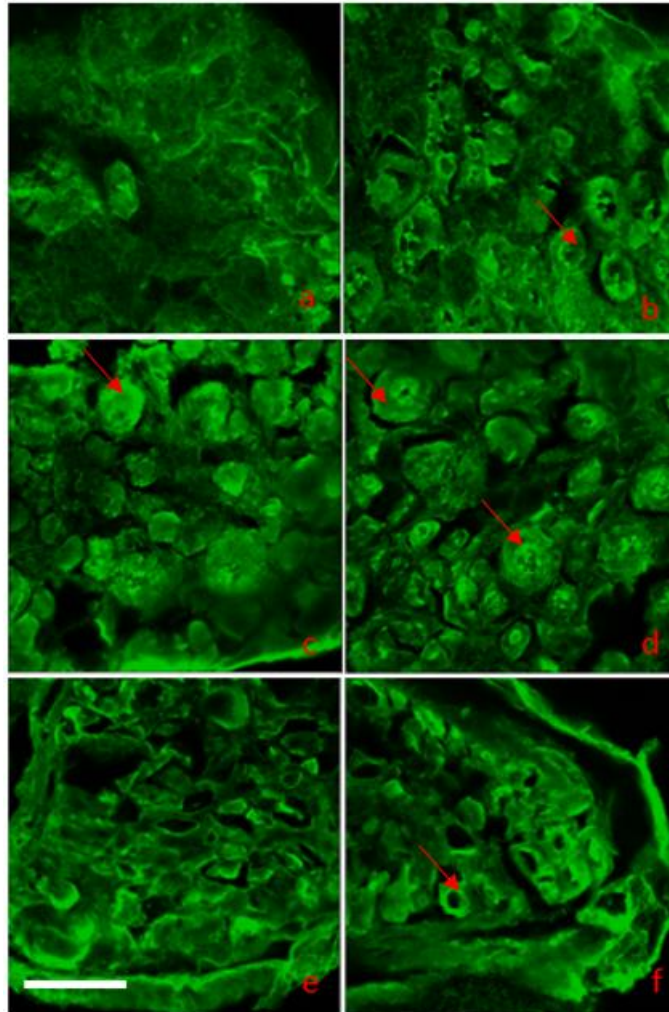


Figure 4.17 Staining of right sided DRG harvested from hind-paw injured mice on day 2 after injury (1:100 dilution of IgG).

Left column HC, right column CRPS, a, b, L3, c, d L4, e, f, L5. Red arrows indicate cytoplasmic staining. Scale bar represent 100 μ m.

Tissue had a strong, general unspecific staining. Neurons were mostly stained in the cytoplasm and there was no difference in staining between HC and CRPS IgG. I repeated the staining for almost all the slides obtained from each DRG and we always observed a similar staining pattern. Epitopes recognised by CRPS IgG may be damaged in the freezing/thawing process or may not be effectively fixed and degrade during long term storage or, most likely, the

unspecific staining was so strong that any specific staining was overshadowed. (Figure 4.16 and 4.17).

4.3.2.2 IF staining of PFA fixed sections and perfused sections

Snap-freezing is considered a gold standard technique for protein preservation in tissue samples because this method allows rapid tissue fixation and preservation (fixation was obtained by just freezing) without using PFA that is toxic and can mask some of epitopes, however some epitopes may also be damaged in the freezing/thawing process or may not be effectively fixed and degrade during long term storage. Additionally, fast freezing might not be the right fixation method for DRGs as the macro-structure of DRG tissue got disrupted by snap freezing and was hard to exactly locate the binding.

Alternative methods to Snap-freezing are: i. post fixation or immersion fixation in PFA, ii. perfusion of fixative through the vascular system. Perfusion fixation is the method of choice for animal models because it provides a very rapid fixation (similar to snap-freezing) before tissue harvest and it is considered effective for some receptors with rapid diffusion or breakdown following harvest that therefore require immediate fixation to prevent this. After tissue harvest, tissue is usually stored in the same fixative for 4 to 24 hours before being cryoprotected with 30% sucrose in 1xPBS and cut; sucrose is usually used as cryoprotection buffer as it maintains the osmolarity of the tissue and

prevents cells from shrinking. (Mallat et al. (1999); Yanik et al. (2020);Wu et al. (2017); Dawes and Vincent (2016); Marone et al. (2018)).

In studies where, vascular perfusion is not possible (such as studies with human samples), small tissues like DRGs can be fixed by immersion fixation overnight and then processed similarly as perfused tissue. We used immersion fixation for IHC experiments, and for the IF experiments presented below . Perfusion fixation was later kindly performed by Nikolett Szentes in the University of Pecs, Hungary.

In this chapter I investigated i. post fixation in PFA and ii. PFA perfusion fixation as an alternative method for IF experiments. I stained L3, L4, L5 right blocks with the same pool of 27 CRPS patient IgG and 5 HC IgG, as used for IHC staining. Fixed DRGs were first cryo-protected in sucrose to avoid cell shrinkage (as the freezing without cryo-protection is associated with dehydration) during later cutting at low temperatures, and then embedded in OCT (Optimal Cutting Temperature embedding matrix designed for storage and cutting at -20°C, while paraffin is optimal for room temperature) before cutting. The protocol used for fixed tissue was adapted from the one published by Mallat et al., Yanik et al., Wu et al. (Mallat et al. (1999); Yanik et al. (2020); Wu et al. (2017)). Briefly, frozen sections were incubated in blocking solution for 30 min and then 1 hour at room temperature with purified human IgG at 5µg/mL in blocking solution. Sections were then incubated with anti-human secondary antibodies FITC conjugated for 1 hour in blocking solution.

I found that our positive control now displayed membrane staining. I then used the same protocol to stain PFA fixed DRGs with pool CRPS and pool HC IgG (Figure 4.18). I observed much reduced intracellular staining.

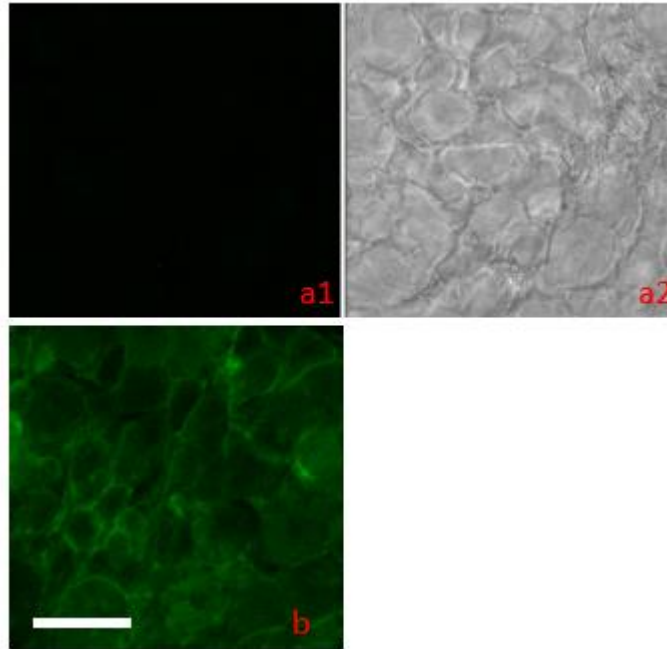


Figure 4.18 PFA post fixation right DRG staining

a1. Florescent image of the negative control (no primary added) **a2.** Brightfield image of the negative control **b.** Positive control staining with CASPR IgG similar as used by Dawes et al. (Dawes et al. (2018)). Scale bar represent 100 μ m.

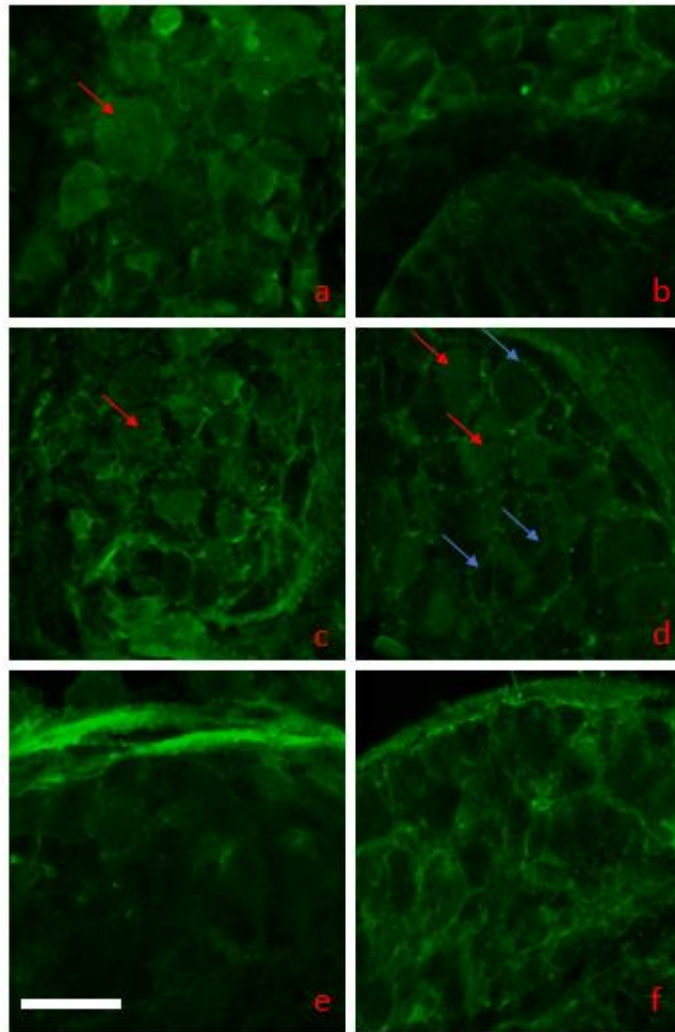


Figure 4.19 Staining of right sided DRG (post-fixed) harvested from hind-paw injured mice on day 2 after injury (1:100 dilution of IgG).

Left column HC, right column CRPS; **a.**, **b.**, L3; **c.**, **d.** L4; **e.**, **f.**, L5. Red arrows indicate cytoplasmic staining, blue arrows indicate examples of membrane staining. Staining seemed mostly to display neuronal membranes with some intracellular staining and pool HC and CRPS IgG appeared to have similar fluorescence intensity and no difference between staining patterns. Scale bar represent 100 μ m.

Tissue structure was generally very well preserved, improved from the snap-frozen tissues (Figure 4.16 and Figure 4.19). Staining seemed mostly to display neuronal membranes with some intracellular staining, and pool HC and CRPS IgG appeared to have similar same fluorescence intensity and no discernible difference between staining patterns. I repeated the staining for

almost all the slides obtained from each DRG and I always observed comparable staining patterns (Figure 4.19).

I finally stained DRGs in 4% PFA perfused animals then post fixed with 4% PFA. In this last preparation tissue was therefore both perfused with PFA and additionally post fixed in PFA in order to maximise epitope fixation and tissue preservation. In terms of tissue preservations, perfused and then post fixed DRGs were the best preparation obtained as tissue and cell appeared well preserved without shrinkage (Figure 4.20 and 4.21). On the other hand, in terms of staining, there was a general unspecific binding and it now was not possible to distinguish between membrane staining and intracellular staining. I hypothesized that an increased intracellular staining observed after PFA perfusion and post fixation may have been caused by tissue over-fixation.

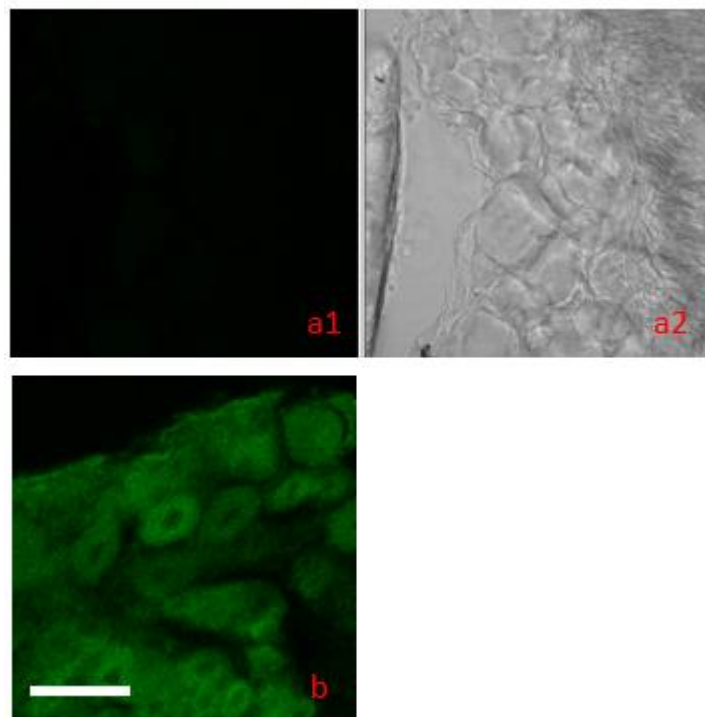


Figure 4.20 PFA perfusion and post fixation right DRG staining. Negative (n) and positive control (pc).

a1. Fluorescent image of the negative control (no primary added) a2. Brightfield image of the negative control b. Positive control staining with CASPR IgG used by Dawes et al. (Dawes et al. (2018)). Scale bar represent 100 μ m.

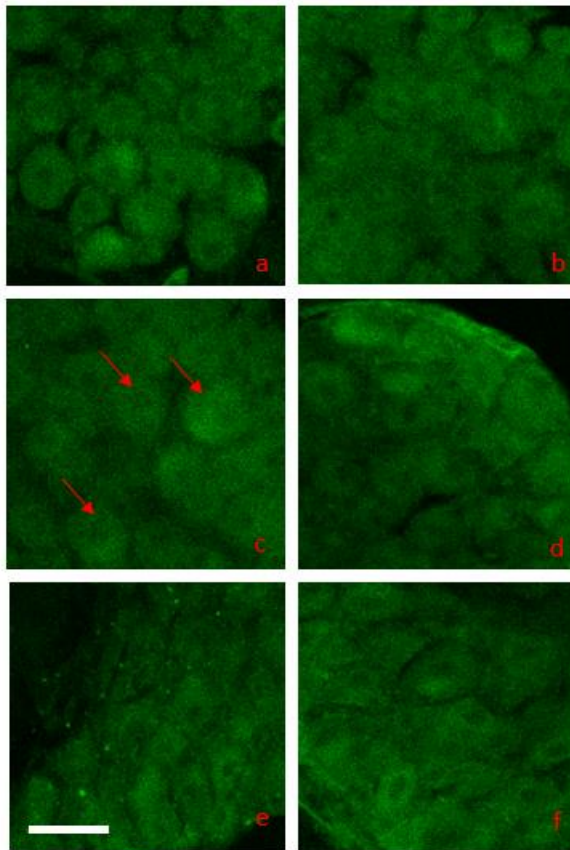


Figure 4.21 Staining of right sided DRG harvested from hind-paw injured mice on day 2 after injury (1:100 dilution of IgG).

Left column HC, right column CRPS, **a, b**, L3, **c, d** L4, **e, f**, L5. In terms of tissue preservations, perfused and then post fixed DRGs were the best preparation obtained as tissue and cell; furthermore, this preparation allowed best tissue preservation during cutting. On the other hand, in terms of staining, there was a general unspecific binding (red arrows) and wasn't possible to distinguish between membrane staining and intracellular staining. Scale bar represent 100 μ m.

In conclusion, even though snap-freezing is considered the method of choice for the majority of tissues, I observed that this method resulted in increased intracellular staining with a blurring of any membrane staining, which was possibly due to a disruption of the membrane due to cell dehydration and shrinkage. For this reason, this method may not be the right method for DRG fixation and staining purpose. On the other hand, the use of 4% PFA as post

and intravenous fixative improved tissue preservation and, consequently staining; it is important to note that tissue fixed with double fixation (such as perfusion and post fixation) produced even superior structure preservation, but may lead to over-fixation which might compromise staining especially when IgG are added after tissue fixation “*in vitro*” as done in these experiments. In the next chapter I present results for IgG “*in vivo*” staining where IgG and tissue are fixed after binding in the mouse (PFA perfusion) and then are harvested and post fixed in PFA as described by Dawes et al. (Dawes et al. (2018)).

4.4 Discussion

In this chapter I presented results for a second assessment of DRG surface binding by CRPS serum IgG using well-established tissue staining methods (IHC and immunofluorescence) commonly employed to detect target antigens in fixed tissue. I used both IHC and IF in order to compare these different tissue processing and staining methods, in particular I used IF after snap freezing in order to avoid or reduce the fixation in PFA that can cross-link epitopes and can interfere with the staining; additionally, IF is more sensitive and precise than IHC, particularly for the investigation of membrane staining, and it allows easier quantification of staining strength.

Results in a passive transfer-trauma murine model suggest that persistent CRPS is caused by IgG autoantibodies (Tékus et al. (2014)) but the binding

targets are unknown. Furthermore, earlier studies in whole fetal mouse tissue failed to identify specific cellular targets (Goebel et al. (2005a)) indicating that epitopes recognized by CRPS IgG might be exposed only after tissue injury.

The aim of this chapter was to investigate the feasibility of detecting the binding of CRPS-IgG to DRG tissue from injured mice. Differently from other studies which after *in vivo* passive transfer of IgG stained harvested DRGs (Goebel et al. (2021b); Dawes et al. (2018)) for the first time I tested *in vitro* staining of tissue harvested from injured mice. I chose *in vitro* staining because this is a gold standard technique used for many tissues and because this requires very low amount of IgG compared with the passive transfer *in vivo* staining.

IHC results presented in this chapter indicate that DRGs corresponding to the incised (right) paw are stained better, perhaps because a neuronal epitope recognized by CRPS IgG is better expressed, but it was not possible to obtain similar results with IF staining.

For experiments presented in this chapter I used pooled IgG (described in chapter 2, section 2.1) for an initial staining overview and then single donor IgG preparations chosen from samples in the original pool. Single preparation had varying staining intensities and pattern confirming that IgG from different CRPS patients have different effects.

I used DRGs derived from the same mouse hind paw plantar incision model that was utilized by Tekus et al. (Tékus et al. (2014)) to develop their passive-transfer trauma model described in chapter 2. On day 2 mice were sacrificed and DRGs (L3, L4, L5) receiving input from the incised (right) or intact (left) paws were harvested and fixed in 4% PFA with the exception of DRGs used

for last experiment in this chapter that were perfused and then post fixed in 4% PFA.

IHC

I used IHC for a preliminary histological examination and staining of human IgG on DRG tissue. For an initial tissue staining overview, slides were stained with pooled HC IgG and pooled CRPS IgG preps derived respectively from 5 healthy volunteers and 27 CRPS patients. The pooled patient IgG staining was light but selective for some neurons for all DRGs and different blocks had similar intensity staining.

Following staining with pool CRPS and HC IgG, blocks 1,2,3,4 were stained individually with IgG from four different healthy control and eight different CRPS patients selected respectively from HC and CRPS pool. The majority of individual patient IgG's selectively stained the cytoplasm with varied staining intensity; varied staining intensity was also present among controls but these had typically a less intense staining when compared with CRPS IgG. Finally, when DRG from left paw were stained with pool and single sample preparation, no specific strong staining was found for either CRPS or HC, and no particular difference between CRPS and HC. Different staining intensity between the right (injured) and left (not injured) side appeared to demonstrate the critical role of tissue injury for antibody binding as a hypothesized basis for the pathophysiology of CRPS (Goebel and Blaes (2013)).

IF (snap-freezing, post fixation and perfusion fixation)

I then used IF in order to obtain a more sensitive and precise staining, particularly for the investigation of membrane staining and to more easily quantify staining.

I used Immunofluorescence staining on snap-frozen and PFA fixed tissue to locate and quantify the IgG involved in binding. My results suggest that snap-freezing can damage neuronal tissue, in particular neuronal membranes and may not be a suitable fixation method for experiments involving membrane staining. The subsequent alternative use of 4% PFA as fixative immediately after tissue harvest improved tissue preservation and staining quality. Furthermore, double-fixed tissue (perfused and post-fixed) had best structure preservation (without cell shrinkage) but over-fixation can compromise staining especially when IgG are added after tissue fixation *in vitro*. We found no difference in IF staining intensities between pool HC and CRPS or between right and left parts. It is important to note that a limitation in my protocol was that not all epitopes required may be expressed by day 2, and some might only be expressed later.

Overall these results suggested that the skin-muscle incision triggers an inflammatory response that induces an increased expression of antigens or the expression of new antigens in the right DRG receiving input from the injured site. Indeed, in a neuropathic pain model injured DRG neurons showed increased expression of antigens on some neurons (Berta et al. (2017)).

In CRPS, after injury, some neurons at DRG level might present antigens on cell surface that that may activate autoimmune IgG. The binding between

antigen and CRPS IgG may be very strong only *in vivo* during inflammation, potentially going some way to explain why I found no convincing differences between CRPS and HC staining in IF *in vitro* experiments. While there might be some differences between HC and CRPS IgG staining in IHC *in vitro* experiments.

Since no convincing staining differences were found I hypothesized that *in vivo* processes requiring the presence of autoreactive antibodies may be pertinent for the establishment of robust DRG staining. I concluded that IgG DRG cell binding cannot reliably be identified with *in vitro* staining of injured mice. I therefore next repeated IHC and immunofluorescence staining, however this time using tissue derived from *in vivo* IgG injected and hind-paw injured animals.

In the next chapter I presented results for IgG *in vivo* staining where IgG and tissue are fixed after binding in the mouse (PFA perfusion) and then are harvested and post fixed in PFA as described by Dawes et al. (Dawes et al. (2018))

Chapter 5 – STAINING OF DRGS HARVESTED

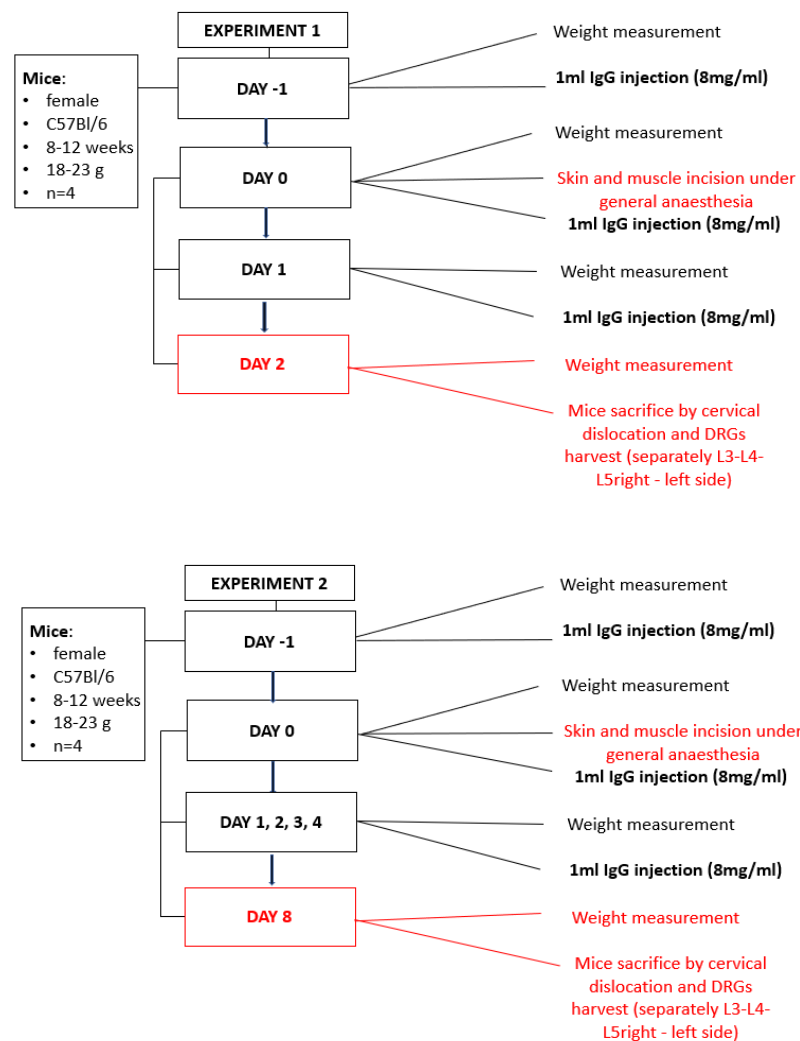
FROM INJECTED AND INJURED MICE

5.1 Introduction

Results in the previous chapter suggest that human IgG, but not specifically patient IgG bind structures in DRGs harvested from mice with a hind paw plantar incision. Some neurons appeared to be bound strongly with human IgG, either on cell surface or in the cytoplasm. Importantly such staining was detected predominantly or exclusively in DRGs corresponding to the injured side (right paw). There was substantial variability between slides, and as we had embedded three DRGs in each paraffin block we had been unable to securely identify whether differences between slides corresponded to the depth within the DRG or to the particular DRG investigated, L3 L4, L5.

Results described in the current chapter were obtained by staining L3, L4, L5 separately in order to allow identification of any differences between these three DRGs. We used IHC and IF staining to investigate binding of CRPS/HC-serum-IgG to murine dorsal root ganglion tissue harvested from injured mice; differently from the previous chapter, rather than staining *in vitro*, mice were injected with purified patient and control IgG (8mg/ml) on day -1 for several consecutive days; the hind paw incision was applied on day 0 as described in previous chapter.

Injection and incision protocols were performed as described by Tekus et al. (Tékus et al. (2014)). Briefly, in the morning mice were treated intraperitoneally with patient or control purified serum-IgG preparations (1ml at a concentration of 8mg/ml) from day -1 to day 1 or day 4; then mice were sacrificed at either of three different time points, day 2, day 8, or day 13 (Figure 5.1). IgG injection, incision, DRG harvest and DRG fixation were performed by Nikolett Szentes in the University of Pecs, Hungary.



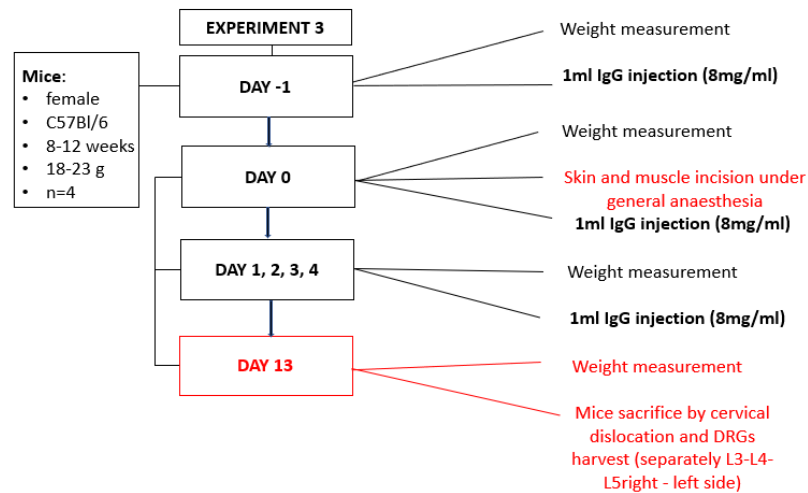


Figure 5.1 Experiment 1, 2, 3 Flow-chart.

In the morning mice were treated intraperitoneally with case and control purified IgG preparations (1ml at a concentration of 8mg/ml) from day -1 to day 2 or day 4. DRG=dorsal root ganglion, IgG=immunoglobulin G

Ex vivo staining using anti-human IgG antibodies conjugated with a fluorescent dye has recently been successfully used in animal pain models to detect human IgG bound to neuronal tissue such as DRGs; human serum-IgG was located on DRGs in a mouse animal model of CASPR2-related conditions and in a fibromyalgia passive transfer mouse model (Goebel et al. (2021b); Dawes et al. (2018)).

Ex vivo staining allows fixation of the antigen-IgG complex throughout animal perfusion with 4%PFA *in vivo*, followed by histological tissue examination; IF is preferred to IHC as the staining process is easier and allows fluorescence quantification (see chapter 4). It is important to note that this method requires manipulation (i.e. injection) of the rodents *in vivo*, and use of a much higher volume of IgG solution compared to *in vitro* staining (e.g. for 4 days injections

we used 4ml IgG at 8mg/ml per mouse, while for *in vitro* staining we only used 1-4µl per experiment). For these reasons, I used IgG injections as the last method aiming to investigate IgG location on DRG neurons.

In this chapter I used two different techniques to stain L3, L4, L5 DRGs right and left sided tissues harvested from mice after *in vivo* IgG injection and hind limb injury. I used IHC for a first histological assessment of DRG tissue and preliminary staining, followed by IF for more precise location of staining and quantification of the staining strength. I used a protocol of *ex vivo* histological examination of DRG tissue as described by Dawes et al. and Goebel et al. (Goebel et al. (2021b);Dawes et al. (2018)) .

All experiments described in this chapter were performed on DRGs harvested from PFA perfused mice which were then post fixed in 4%PFA.

5.2 Aim

The first aim of experiments described in this chapter was to investigate whether binding between CRPS-IgG and DRG tissue from injected and injured mice can be detected; we used IHC for a preliminary histological examination. The second aim was to localize and quantify the IgG binding; we used IF staining because this method is more sensitive and precise than IHC, particularly for the investigation of membrane staining; additionally, IF allows

easier quantification of staining strength. The third aim was to compare DRGs from the right (injured) side to the left (non-injured) side. Based on the results presented in the previous chapter we expected to detect stronger patient-IgG when compared to control-IgG binding on the right-sided DRGs as behavioral abnormalities in the model are only detected on the right side, and presumably the pertinent binding epitopes presenting for IgG-binding might be expressed after injury.

The research questions evaluated in this chapter were: i. Which cells are bound by CRPS IgG? ii. Is the binding intracellular/extracellular? iii. Do different patient IgG bind in the same or in different ways?

5.3 Results

5.3 1 IHC Staining of DRG harvested from injected and injured mice

5.3.1.2 Experiment 1 right and left DRGs staining

We used IHC staining to investigate epitope binding of CRPS-serum-IgG to murine primary dorsal root ganglion cells. On day 2, DRGs corresponding to the incised right paw were perfused with 4% PFA, harvested, post-fixed in 4%

PFA, and paraffin embedded (table 1). One paraffin slide per each block was stained directly with anti-human IgG-HRP. The three DRGs (L3, L4, L5) were embedded at slightly different levels in the paraffin block; middle slides (15-25) in order to get an overview of staining pattern in all DRGs.

Table 5.1 IHC experiment 1 experimental design.

Day -1	Day 0	Day 1	Day 2
Injection 1ml IgG at 8mg/ml	Injection 1ml IgG at 8mg/ml	Injection 1ml IgG at 8mg/ml	Injection 1ml IgG at 8mg/ml
	Paw incision		Mice sacrifice

For this initial tissue staining overview, four mice were injected with pooled CRPS IgG and four with pooled HC IgG preparations derived respectively from 27 CRPS patients and from 5 healthy volunteers and (same used in chapter 4). DRGs were harvested from PFA perfused mice and then post fixed in 4% PFA; L3, L4, L5-right/left DRGs from all mice were paraffin embedded in two blocks (one block for each side). When right blocks were examined, only one slide (in the middle of the block) per block was stained for either HC and CRPS. I found no difference in staining intensity between both preparations (Figure

5.2). CRPS IgG preparation stained some medium-sized neurons mostly in the cytoplasm. Large neurons had a dark brown staining while medium-size neurons had a light brown staining; HC IgG preparation had cytoplasmic staining on some neurons on the left side of the neuron rich area.

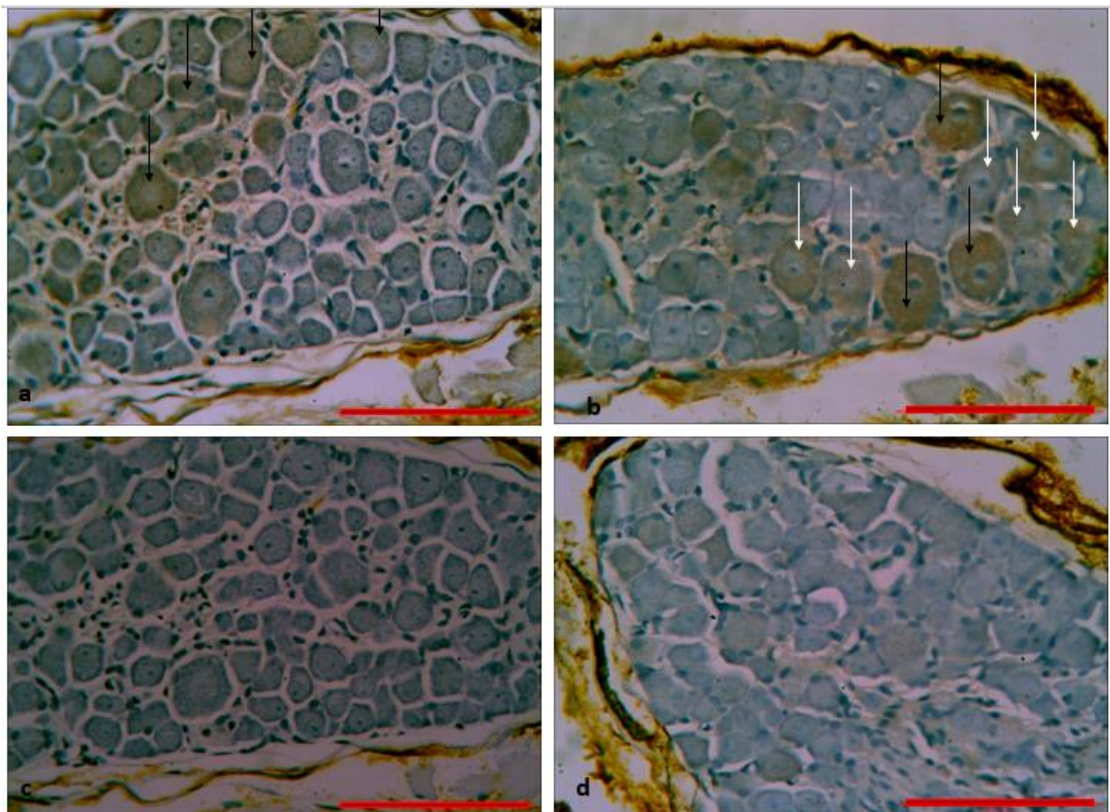


Figure 5.2. Experiment 1. IHC DRGs staining right and left.

a. Pool HC IgG right side b. Pool CRPS IgG right side c. Pool CRPS IgG left side d. Pool CRPS IgG left side. a and b Some neurons were stained and these had high IgG concentration only in the cytoplasm c and d. In left side DRGs from mice injected with pool HC-IgG and pool CRPS-IgG there was no staining. Scale bar represents 100µm

When DRG from left paw were stained with pool and single sample preparation, no specific strong staining was found for CRPS and no particular

difference from CRPS and HC (figure 5.2). Staining for left side CRPS and HC was lighter than right side CRPS and HC at every slide number, this confirmed that tissue from the right injured side was more sensitive to IgG binding than non-injured tissue. Overall perfused and post fixed tissue had less cells shrinkage and looked less damaged than just post fixed tissue (shown in chapter 4). I have not quantified this staining as this was a screening test, but quantification of individual staining is described further below. From this preliminary experiment I learned that I can detect some IgG binding from the injected mice, and hence I then moved on to try to localise and quantifying the binding using immunofluorescence staining.

5.3.2 IF Staining of DRG harvested from injured and injected mice

5.3.2.1 Experimental design

Immunofluorescence localization of human IgG in mouse tissue has been successfully used to study several auto antibody-pain syndromes such Myasthenia Gravis, CASPR2 and recently fibromyalgia (Wu et al. (2001); Goebel et al. (2021b); Dawes et al. (2018)). Differently from *in vitro* staining of

tissue, ex vivo staining allows quick fixation of IgG in the tissue directly in the animal. In this chapter I present results from three different experiments that differ in injection day number and sacrifice day; injections protocols were adapted from Tekus et al. 2014 (Tékus et al. (2014)).

For all experiments I used IgG purified from one single healthy control and one single CRPS patient (P1) as described in chapter 3 and chapter 4 (patient demographics are reported in chapter 2). We chose this patient because injection experiments require large amount of purified IgG and we had a sufficient amount of plasma available after plasma exchange from this patient. Negative controls images presented in this chapter are the same as in chapter 4 (IF staining of injured tissue part B) because the primary antibody (CRPS patient/HC IgG) was injected in tissue before DRG harvest and staining only with secondary antibody wasn't possible. No positive control experiments were performed because we had only small amount of PC serum available, not enough for animal injection for several days.

The first experiment involved 4 injection days, and sacrifice was on day 2 (Table 5.2), the second experiment had 6 injection days and sacrifice was on day 8 (Table 5.3) and the third experiment had 6 injection days and sacrifice was on day 13 (Table 5.4). Experiments flow charts are reported in (Figure 5.1) and in material and methods chapter (chapter 2).

Table 5.2 IF experiment 1 experimental design. The first experiment had 4 injection days and sacrifice was on day 2

Day -1	Day 0	Day 1	Day 2
Injection 1ml IgG at 8mg/ml	Injection 1ml IgG at 8mg/ml	Injection 1ml IgG at 8mg/ml	Injection 1ml IgG at 8mg/ml
	Paw incision		Mice sacrifice

Table 5.3 IF experiment 2 experimental design. The second experiment had 6 injection days and sacrifice was on day 8

Day -1	Day 0	Day 1	Day 2	Day 3	Day 4	Day 8
Injection 1ml IgG at 8mg/ml	Injection 1ml IgG at 8mg/ml	Injection 1ml IgG at 8mg/ml	Injection 1ml IgG at 8mg/ml	Injection 1ml IgG at 8mg/ml	Injection 1ml IgG at 8mg/ml	
	Paw incision					Mice sacrifice

Table 5.4 IF experiment 1 experimental design. The third experiment had 6 injection days and sacrifice was on day 13

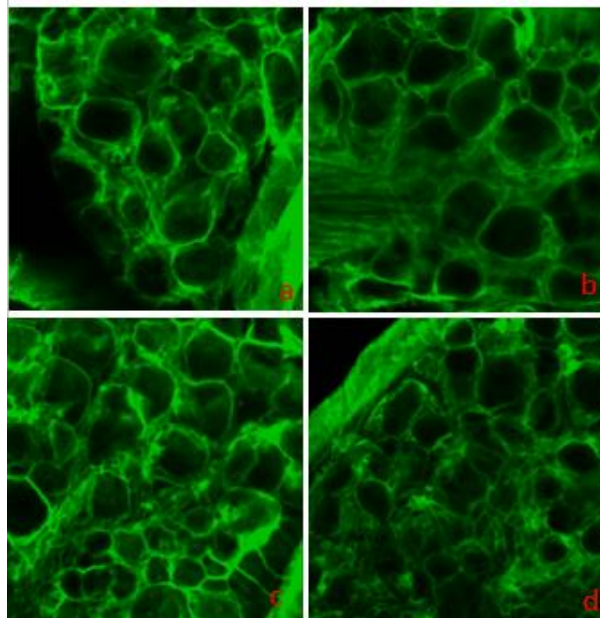
Day -1	Day 0	Day 1	Day 2	Day 3	Day 4	Day 13
Injection 1ml IgG at 8mg/ml	Injection 1ml IgG at 8mg/ml	Injection 1ml IgG at 8mg/ml	Injection 1ml IgG at 8mg/ml	Injection 1ml IgG at 8mg/ml	Injection 1ml IgG at 8mg/ml	
	Paw incision					Mice sacrifice

5.3.2.2 Evaluation of DRGs staining

Experiment 1

The first experiment had 4 injection days and sacrifice was on day 2. I found that all lumbar DRGs (L3, L4, L5) had staining on neuronal cell membrane, with similar staining intensities between individual ganglia. Staining was strong for all samples (HC-R, HC-L, CRPS-R, CRPS-L). (figure 5.3). While staining strongly, fluorescence was almost exclusively restricted to cell membranes, more selectively than in all previously employed methods. Since small satellite

glial cells (SGC) surround neuronal cells almost entirely Hanani (2005) the observed pattern did not allow to securely distinguish between neuronal and glial membrane staining. However, some small cell bodies appeared to have stained (arrows) indicating that mouse SGC were stained by human IgG. After this initial staining, we tested IgG binding on DRG harvested at later time points (days 8 and 13), aiming to reduce any control IgG unspecific binding; we hypothesised that as the mice metabolise the human IgG, the reduction of control-IgG concentrations would be accompanied by parallel reduction of unspecific DRG staining, whereas patient-IgG might bind specifically, with higher affinity so that a reduction in serum titre would lead to a less rapid reduction in staining intensity and hence a difference between healthy and patient preparations might emerge.



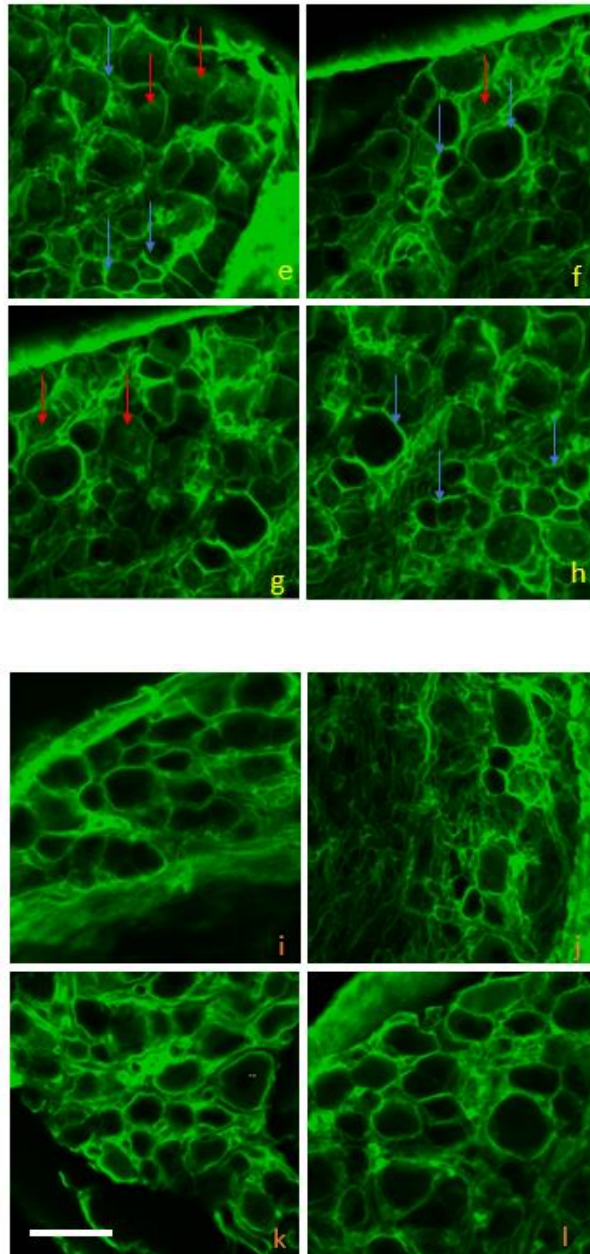
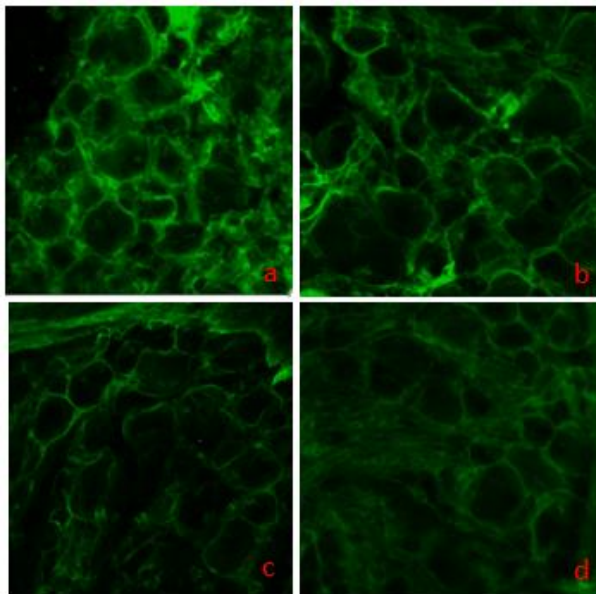


Figure 5.3 Experiment 1.

Staining of right and left sided L3, L4, L5 DRG harvested from injected and injured mice on day 2 after injury (1:100 dilution of human IgG). Left column HC, right column CRPS, within each set of four the two top slides are from the right side, bottom slides left side. First set of four L3, then L4, L5. Red arrows indicate examples cytoplasmic or next layer membrane staining, blue arrows indicate membrane staining which was much more abundant. Scale bar represent 100µm.

Experiment 2

The second experiment had 6 injection days and sacrifice was on day 8. I observed a similar staining pattern as with experiment 1, however, as expected staining was overall weaker; when compared with experiment 1, in experiment 2 the last IgG injection had been four days prior to sacrifice). There was no discernible difference between HC and CRPS or between the three ganglia, however in a weaker staining intensity for the left part when compared with the right part appeared obvious in L4 (Figure 5.4).



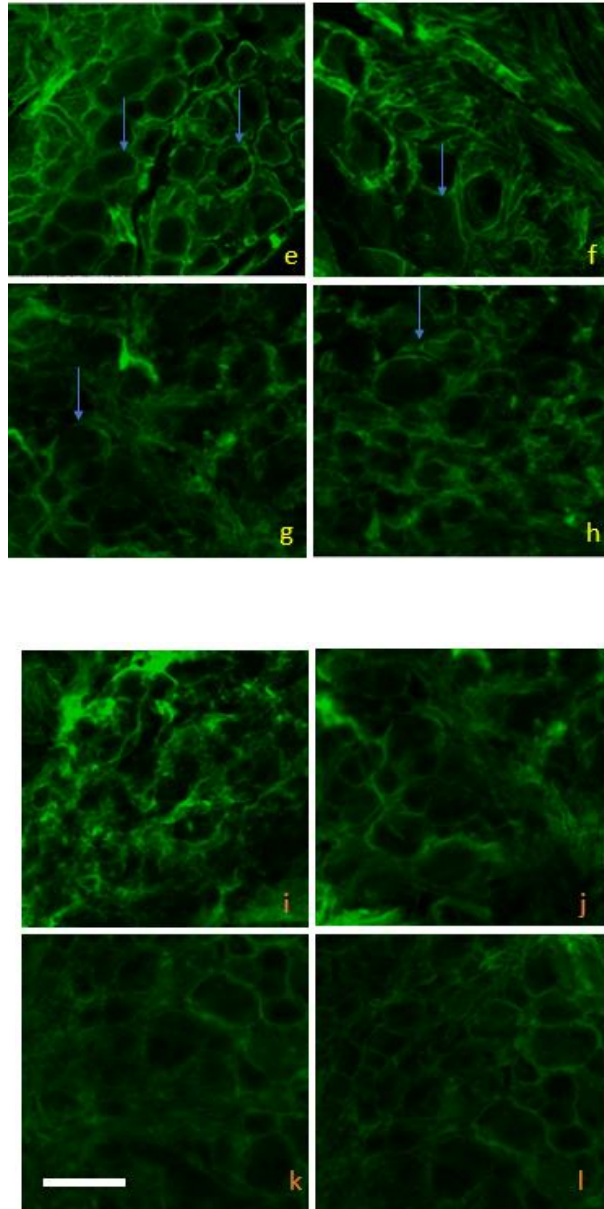
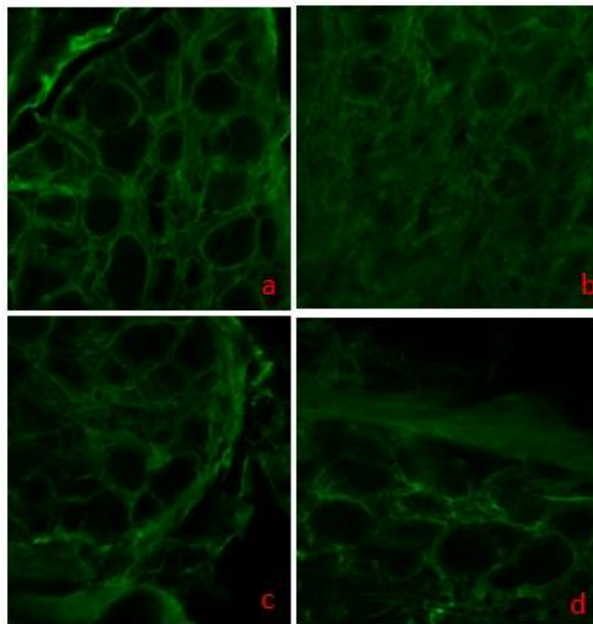


Figure 5.4 Experiment 2.

Staining of right and left sided L3, L4, L5 DRG harvested from injected and injured mice on day 2 after injury (1:100 dilution of IgG). Left column HC, right column CRPS, within each set of four the two top slides are from the right side, bottom slides left side. First set of four L3, then L4, L5. Red arrows indicate cytoplasmic or next membrane layer staining, blue arrows indicate membrane staining. Scale bar represent 100µm.

Experiment 3

The third experiment had 6 injection days and sacrifice was on day 13. I observed a similar staining pattern as with experiment 1 and 2, however, as expected staining intensities were overall weaker; when compared with experiment 1 and experiment 2 the last IgG injection had been nine days prior to sacrifice). There was no discernible difference between HC and CRPS or between the three ganglia (Figure 5.5).



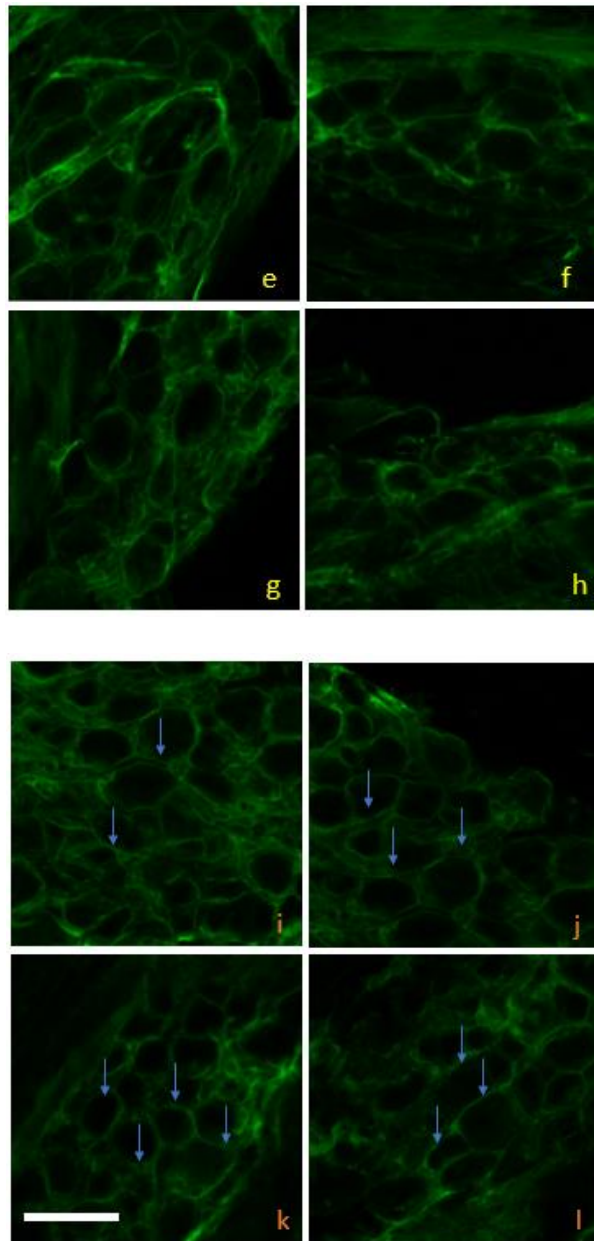


Figure 5.5 Experiment 3.

Staining of right and left sided L3, L4, L5 DRG harvested from injected and injured mice on day 2 after injury (1:100 dilution of IgG). Left column HC, right column CRPS, within each set of four the two top slides are from the right side, bottom slides left side. First set of four L3, then L4, L5. Red arrows indicate cytoplasmic or next membrane layer staining, blue arrows indicate membrane staining. Scale bar represent 100 μ m.

I selected four images per experiment (L4 HC-R, L4 HC-L, L4 CRPS-R, L4 CRPS-L) to compare staining intensity between different experiments and right and left parts and also used negative control from chapter 4 (Figure 5.6).

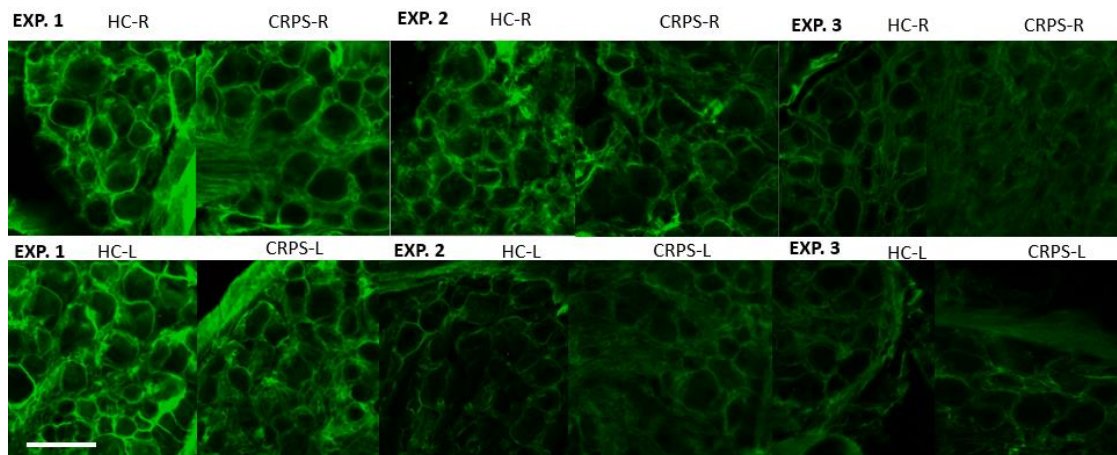
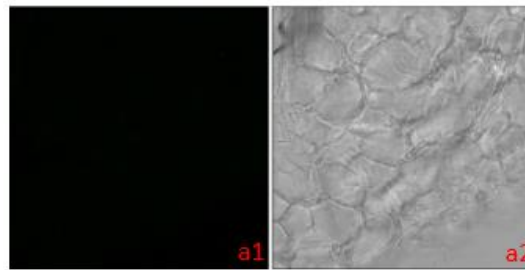


Figure 5.6 Experiment 1,2,3 comparison.

Staining of right and left sided L3, L4, L5 DRG harvested from injected and injured mice on day 8 after injury (1:100 dilution of IgG). a1. Fluorescent image of the negative control (no primary added) a2. Brightfield image of the negative control. Overall, staining of injected tissue was on neuronal or SGC cell membranes, in particular it was similar to positive control staining of PFA fixed tissue and different from positive control staining of perfused tissue from chapter 4. Staining intensity decreased from experiment 1 to experiment 3. Scale bar represent 100 μ m.

Experiment 1 staining was very strong and sometimes unspecific for both CRPS and HC, right and left parts. The reason for this strong and unspecific staining might be that DRGs were harvested on the same day as the last injection and control IgG unspecific binding wasn't properly reduced. Experiment 2 was the only experiment where the left part had a weaker staining than the right part but in this experiment the control IgG still had a similar or even stronger intensity than CRPS. Similar as experiment 2, experiment 3 was designed to allow reduction of background from HC staining; both CRPS and HC displayed light staining but CRPS was not seemingly stronger than HC (Figure 5.6).

Overall, staining of injected tissue was membrane focused, in particular it was similar to positive control *in vitro* staining of PFA fixed tissue (chapter 4 figure 18) and different from positive control staining of perfused tissue (chapter 4, figure 20).

5.3.2.3 Quantitative analysis of DRGs staining

In order to measure fluorescence intensity, we selected four images (HC-R, HC-L, CRPS-R, CRPS-L) for L4 staining. Image analysis and quantification was performed using FIJI ImageJ software as detailed in chapter 2. Briefly, for a first intensity overview, human IgG intensity fluorescence was measured by drawing a region of interest around each neuron within the neuron rich area of

the DRG, applying a minimum pixel intensity threshold, and then the percent positive area above the threshold and the average pixel intensity above the threshold were evaluated as described by Goebel et al. (Goebel et al. (2021b)).

Our quantitative analysis confirmed what was previously observed in the qualitative analysis. Experiment 1 staining was very strong and sometimes unspecific for both CRPS and HC, right and left part (figure 5.7). Experiment 2 was the only experiment where the left part had a weaker staining than the right part but in this experiment the control IgG still had a stronger intensity than CRPS (Figure 5.7). In experiment 3 both CRPS and HC had a light staining but CRPS wasn't stronger than HC (Figure 5.7). Furthermore, right and left part had similar fluorescence intensity.

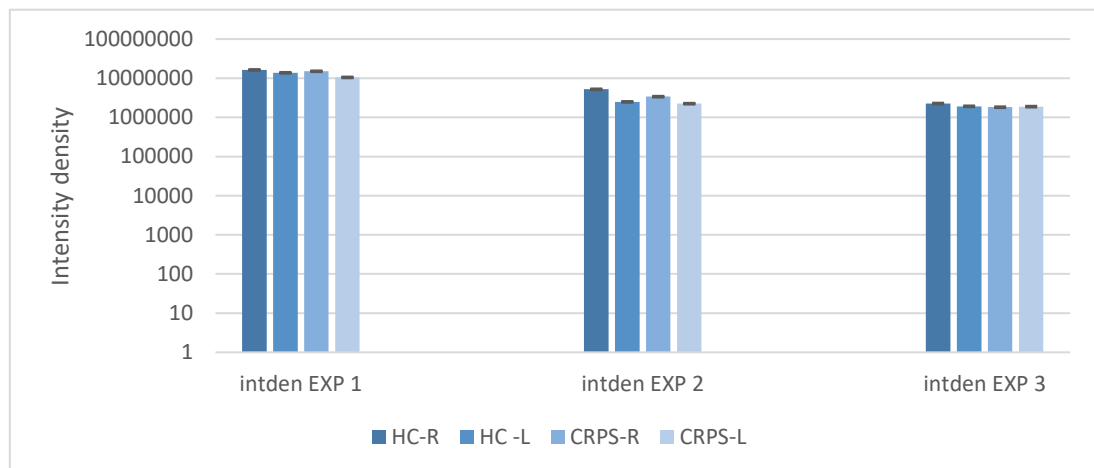


Figure 5.7 Experiment 1,2, 3 comparison.

In all experiments CRPS IgG staining wasn't stronger than HC and only in experiment 2 was the only experiment where the left part had a weaker staining than the right part. Statistical significance was calculated with t- tests for paired data ($p < 0.05$).

Overall this quantitative analysis confirmed what previously observed in tissue images; in all experiments CRPS IgG staining wasn't stronger than HC and only in experiment 2 was the only experiment where the left part had a weaker staining than the right part (Figure 5.7).

5.4 Discussion

In this chapter I presented results for a third assessment of DRG surface binding by CRPS serum IgG using IHC and immunofluorescence commonly employed to detect target antigens in fixed tissue. The aim of this chapter was to investigate the feasibility of detecting the binding of CRPS-IgG to DRG tissue in mice injected with purified IgG and then injured.

I stained DRG harvested from mice receiving the passive transfer of IgG as described previously (Goebel et al. (2021b);Dawes et al. (2018)). Following results obtained with *in vitro* staining, I chose this *in vivo* staining method because this is a gold standard technique successfully used for auto antibody pain syndrome studies previously. (Goebel et al. (2021b);Dawes et al. (2018)).

For experiments presented in this chapter I used pooled IgG (described in chapter 2, section 2.1) for an initial staining overview and then I used IgG purified from one single CRPS donor P1 (described in chapter 2 section 2.1).

As in chapter 4, I used two different techniques to stain L3, L4, L5 DRGs right and left sided tissues harvested from mice after *in vivo* IgG injection and hind limb injury. I used IHC for a first histological assessment of DRG tissue and preliminary staining, followed by IF for more precise location of staining and quantification of the staining strength. I used a protocol of *ex vivo* histological examination of DRG tissue as described by Dawes et al. and Goebel et al. (Goebel et al. (2021b);Dawes et al. (2018)).

IHC

IHC results presented in this chapter indicate that DRGs (from injected mice) corresponding to the incised paw may present a neuronal epitope recognized by CRPS IgG but it was not possible to reproduce such results with IF staining.

Differently from chapter 4, in this chapter I stained DRGs from injected and injured mice, the staining appeared similar to DRG from just injured mice (Chapter 4). For an initial tissue staining overview, slides were stained with pooled HC IgG and pooled CRPS IgG preps derived respectively from 5 healthy volunteers and 27 CRPS patients. Some neurons were stained (mostly medium-large) and these had high IgG concentration only in the cytoplasm (figure 5.2); The staining did not appear to be selective for a specific neuronal sub-populations as small, medium and large neurons were stained equally. In DRGs from mice injected with pool HC-IgG there was no staining. When DRG

from left paw were stained with pool and single sample preparation, no specific strong staining was found for CRPS and no particular difference from CRPS and HC

IE

I used Immunofluorescence staining on perfused and post fixed tissue to locate and quantify the IgG involved in binding. In this chapter I presented three different experiments that differ in injection days number and sacrifice day adapted from the one used in the CRPS passive transfer model described by Tekus et al (Tékus et al. (2014)). For all experiments we used IgG purified from one single CRPS healthy control and one single CRPS patient (P1) previously used for experiments in chapter 3. Experiment 1 staining was very strong and sometimes unspecific for both CRPS and HC, right and left part. The reason for this strong and unspecific staining might be that DRGs were harvested on the same day as last injection and control IgG unspecific binding wasn't properly reduced. Experiment 2 was the only experiment where the left part had a weaker staining than the right part but in this experiment the control IgG still had a stronger intensity than CRPS. As experiment 2, experiment 3 was designed to allow reduction of background from HC staining; both CRPS and HC had a light staining but CRPS wasn't stronger than HC. These observations were confirmed by a subsequent quantitative analysis.

In conclusion, as previously shown in chapter 4, these results confirm that the injury might play a crucial role in triggering the binding between CRPS IgG and an epitope on neuronal cell surface; this was confirmed by results obtained in

IHC and IF (experiment 2) where staining in the right DRGs appeared stronger than staining on the left DRGs. From the methodological point of view, IgG injection improved staining quality but it did not help to distinguish between CRPS and HC staining. A limitation in IgG injection is the high volume of serum required for each experiment and a very limited number of patients can be tested. In addition, a relevant difference in staining might be seen only *in vivo* in the animal where CRPS IgG, the peripheral nervous system and the central nervous system might be simultaneously involved in triggering and maintaining CRPS 'burning' pain.

Chapter 6 - DISCUSSION AND CONCLUSION

CRPS is a painful, usually post-traumatic, condition characterized by sympathetic, sensory and motor dysfunction in the affected limb and its most important symptom is incapacitating pain. The persistence of CRPS beyond six months typically leads to the development of a chronic condition with patient experiencing extremely poor quality of life (Veldman et al. (1993)). The pathophysiology of CRPS is incompletely understood and the treatment is therefore still of limited efficacy. CRPS is caused by several mechanisms including altered cortical representation, both somatosensory and motor, of the affected limb (Pleger et al. (2006)), central nervous system-mediated abnormal sympathetic activation in this limb (Wasner et al. (2001)), facilitated neurogenic inflammation, and aberrant immune responses (Birklein et al. (2001);Huygen et al. (2002)).

Recent works suggest that there is an auto-immune component, in that some patients experience good pain relief with intravenous immunoglobulin, aspects of the condition can be transferred to animals, and patients often have functionally active cell-surface-directed autoantibodies (Blaes et al. (2004);Goebel et al. (2010); Goebel and Blaes (2013); Kohr et al. (2011); Kohr et al. (2009); Tékus et al. (2014)).

Investigation of surface epitope binding of CRPS-serum-IgG is now required, to better understand the disease mechanism and to facilitate the study of drug treatments directed at auto antibody-induced abnormalities.

This PhD project aimed to assess the binding by CRPS-serum-IgG to epitopes on primary mouse neurons in DRGs. For this purpose, I used several gold standard research techniques used in pharmacology research such as: flow cytometry, Western blot, immuno-cytochemistry (ICC), immuno-histochemistry (IHC) and Immuno-fluorescence. I used flow cytometry, the cutting-edge technique for antibody interaction analysis to be able to measure multiple parameters and quantify fluorescence intensities. Then I used Western blot, immuno-cytochemistry (ICC), immuno-histochemistry (IHC) and Immuno-fluorescence in order to measure binding intensities and identify the epitopes recognized by CRPS IgG.

In chapter 3 I presented results from a first assessment of DRG surface binding by CRPS serum IgG, using a well-established and robust staining method used to detect target antigens in cells (flow cytometry, western blot and Immunocytochemistry). The results obtained *in vitro* indicate that CRPS IgG bind stronger than controls to membrane structures on DRGs neurons only when cells are cultured with cytokines; no relevant binding was detected when neurons were stained without incubation with cytokines and inflammatory mediators.

When neurons were incubated with inflammatory mediators the pre-incubation did not increase the surface expression of CRPS IgG target protein; this result

appear to be at variance with those previously reported by Reilly et al who used different serum-IgG preparations. These previous studies had suggested that the inflammatory soup induces changes in neuronal excitability and it was thought that it may be possible that inflammatory mediators contribute to the sensitization of neuronal CaV channels through intracellular signaling mechanisms. It is worth noting, though that such mechanisms would not necessarily be requiring stronger surface binding (Reilly et al. (2016)).

Several studies identified pro-inflammatory cytokines TNF- α , IL-1 β and IL-6 as a potential biomarker for CRPS (Birklein et al. (2001); Huygen et al. (2002); Parkitny et al. (2013)). I therefore also wished to use flow cytometry to investigate whether cytokines trigger CRPS IgG binding to DRG neurons. For some CRPS patient IgG preparations, cytokines treatment significantly increased either the mean fluorescence or cell percentage involved in IgG binding. When neurons were incubated with cytokine pool only, nearly half of cells stained with P1-CRPS showed substantial fluorescence increase and this was similarly observed after incubation with IL-6 and IL-1 β separately; in contrast, all cells stained with P2-CRPS had only a small fluorescence increase. My results thus demonstrate that increased cytokine concentrations either in the inflamed limb or DRG may play a critical role in triggering the binding to an antigen on DRG neuronal cell surface as suggested by the conceptual model of auto antibody-mediated CRPS (Goebel and Blaes (2013)).

The identification of a bimodal cell distribution following P1-CRPS IgG staining, allowed further mass spectrometry analysis required to identify the cell membrane receptor bound to CRPS (Littleton et al. (2009)), but mass spectrometry analysis was not conclusive. Since both P1 and P2 had Budapest CRPS and their serum had previously been shown to contain pathogenic autoantibodies which induced abnormal behavior in mice, yet only P1 showed a marked apparent induction of binding following incubation with inflammatory mediators, it appeared that this induction may not be essential to the functional effect of these antibodies in all patients. At the same time, no clear increase of binding was seen in P1 over HC, highlighting either that the pertinent bound cell sub-population is small, or that methods to identify CRPS-IgG cell surface binding using mouse primary neurons (i.e. neurons not derived from injured animals) are not suitable. My initial experiment had also shown me that it would not be possible to use cells from injured animals (DRGs L3-L5) as the number of cells extracted would be even smaller than with these completed experiments.

As an alternative approach, which might provide higher protein yields, to investigate whether particular DRG-neuronal proteins are bound by CRPS-IgG (instead of using FACS sorted cells), I utilized Western Blot methodology. When DRG homogenates were stained for Western Blot I found a weak band in both CRPS samples and no band for HC samples. A drawback of this method is that in Western blotting proteins are denatured in order to facilitate the charge-mass separation. Denaturation may impede the contribution of

quaternary protein structure to epitope antigenicity, because of this limitation I stopped using this method.

I finally used immunocytochemistry to qualitatively assess CRPS and HC IgG binding to dissociated dorsal root ganglion neuronal cells and to locate IgG on their neuronal cell membrane. When cells were stained with a fluorescent dye I couldn't see a significant difference in staining between CRPS and HC IgG preparation as previously observed in flow cytometry and Western blot staining. P2-CRPS had a stronger staining than P1-CRPS, differently from what previously observed in flow cytometry staining (Chapter 3 section 3.3.1). Furthermore, I found no staining when both HC and CRPS were incubated with fibroblasts.

Overall these negative or inconclusive results suggest that in CRPS patients after injury some cells, such as fibroblast, can contribute to release inflammatory mediators and cytokines that may activate autoimmune IgG and trigger the binding to an antigen on DRG neuronal cell surface. The binding between antigen and CRPS IgG may be very strong only *in vivo* during inflammation; the *in vivo* environment may differ from the *in vitro* environment and my cytokine incubations cannot properly mimic the required environment. This can explain why there is no difference between CRPS and HC staining *in vitro* experiments.

In chapter 4 I presented results for a second assessment of DRG surface binding by CRPS serum IgG using well-established tissue staining methods (IHC and immunofluorescence) commonly employed to detect target antigens

in fixed tissue. I used both IHC and IF in order to explore and compare these different tissue processing and staining methods for their utility, in particular I used IF in order to avoid or reduce the fixation in PFA underpinning IHC that can cross-link epitopes and can interfere with the staining; additionally, IF is more sensitive and precise than IHC, particularly for the investigation of membrane staining and allows easier quantification of staining strength.

Results in a passive transfer-trauma murine model suggest that persistent CRPS is caused or contributed to by IgG autoantibodies (Tékus et al. (2014)) but the binding targets are unknown. Furthermore, earlier studies in naïve fetal mouse tissue failed to identify specific cellular targets (Goebel et al. (2005a)) indicating that epitopes recognized by CRPS IgG might be exposed only after tissue injury.

The aim of experiments in this chapter was to investigate the feasibility of detecting the binding of CRPS-IgG to DRG tissue from injured mice. Differently from other studies performing *in vivo* passive transfer of IgG (Tékus et al. (2014); Cuhadar et al. (2019); Goebel et al. (2021b); Dawes et al. (2018)). for the first time I tested *in vitro* staining of tissue harvested from injured mice. I chose *in vitro* staining because this is a gold standard technique used for many tissues and because this requires a very low amount of IgG compared with the passive transfer *in vivo* staining.

IHC results presented in this chapter showed increased staining in the injured versus intact paws, and an impression of further enhanced staining with CRPS vs. control IgG; this means that these results may indeed indicate that specifically those DRGs that correspond to the incised paw may present a

neuronal epitope recognized by CRPS IgG but further work is needed to confirm this. It was not possible, however to obtain similar results with IF staining.

For experiments presented in this chapter I used pooled IgG (described in chapter 2, section 2.1) to obtain an initial staining overview, and then single donor IgG preparations chosen from samples in the original pool. Single preparation had different staining intensities confirming that IgG from different CRPS patients have different staining effects.

I used DRGs derived from the same mouse hind paw plantar incision model that was utilized by Tekus et al. (Tékus et al. (2014)) to develop their passive-transfer trauma model described in chapter 2. On day 2 mice were sacrificed and DRGs (L3, L4, L5) receiving input from the incised (right) or intact (left) paws were harvested and fixed in 4% PFA with the exception of DRG used for last experiment in this chapter that were perfused and then post fixed in 4% PFA.

The pooled patient IgG staining was light but selective for some neurons for all DRGs and different blocks had similar intensity staining. Pooled CRPS IgG appeared stronger than pooled HC staining.

Following staining with pool CRPS and HC IgG, blocks 1,2,3,4 were stained individually with IgG from four different healthy control and eight different CRPS patients selected respectively from HC and CRPS pool. The majority of individual patient IgG's selectively stained the cytoplasm with varied staining intensity; varied staining intensity was also present among controls but these had typically a less intense staining when compared with CRPS IgG. I found

that there was a trend for overall stronger staining by the CRPS serum group when compared to the HC group, however this did not reach statistical significance. Finally, when DRG from left paw were stained with pool and single sample preparations, staining intensities were generally very low and similar between CRPS and HC. The difference between left and right sided staining intensities was highly significant and the difference between left and right was numerically larger for the CRPS when compared with the HC group. These observed differential staining intensities between the right (injured) and left (not injured) sides are consistent with a critical role of tissue injury in allowing enhanced binding of autoimmune IgG and consequently in facilitating the development of CRPS (Goebel and Blaes (2013)).

I then used IF in order to get a more sensitive and precise staining, particularly for the investigation of membrane staining and to more easily quantify the staining.

I first used Immunofluorescence staining on snap-frozen and PFA fixed DRG tissue to locate and quantify the IgG involved in binding. My results suggest that snap-freezing can damage neuronal tissue in particular neuronal membranes which appeared disrupted (Figure 4.18). DRG snap-freezing may not be a suitable fixation method for experiments involving membrane staining because a quick transfer to cold temperatures may induce cell dehydration and consequent shrinkage that damages cell membrane. Indeed, a freezing-induced dehydration and consequent membrane hydraulic permeability changes had been reported during cooling of mammalian cells (Akhondi et al. (2011)). The subsequent use of 4% PFA as fixative immediately after tissue

harvest, appeared to improve tissue preservation and consequently staining. Furthermore, double-fixed tissue (perfused and post-fixed) had best structure preservation but this appeared to compromise a later *in vitro* staining, likely due to over-fixation so that IgG added after tissue fixation stained un-specifically either the membrane and cytoplasm. I found no difference in staining between pool HC and CRPS or between right and left part. It is important to note that a limitation in my protocol was that not all epitopes required may be expressed by day 2 after injury, the time of tissue harvest, some might only be expressed later.

Results in this chapter showed that IF did not reproduce the IHC findings, a possible reason is that for IF and IHC methods tissue is processed and stored in a completely different way and at different temperatures respectively -80 and 20°C. The antigen recognized by CRPS IgG might be sensitive to long term storage at cold temperatures, especially fixed cell membrane antigens might be internalized or degrade after long term storage at cold temperatures. For these reasons results in this chapter suggested that the best method to use for CRPS IgG staining might be IHC as it allowed better antigen preservation thanks to storage and preservation at room temperature.

Overall IHC results suggested that the skin-muscle incision triggers a process, perhaps involving an inflammatory response, that induces an increased expression of antigens or the expression of new antigens on paw-injury corresponding DRGs. These results are consistent with earlier findings in studies in neuropathic pain, where injured DRG neurons showed increased expression of antigens in some neurons (Berta et al. (2017)), however I have

shown here for the first time that such an expression change after injury also causes enhanced binding of serum-IgG, and further, that this type of enhancement may appear larger after staining with patient-IgG when compared with control-IgG.

In CRPS, after injury, some neurons at DRG level might present antigens on their cell surface that that may allow binding of autoimmune IgG. I hypothesized that the absence of clear differences between HC and CRPS in my experiments may be explained by the need for the presence of a dynamic interaction between the consequences of antibody binding and the consequences of injury which may produce enhanced molecular changes.

I concluded that DRG cell binding cannot reliably be identified with *in vitro* staining of injured mice. I therefore next repeated IHC and immunofluorescence staining, however this time using tissue derived from *in vivo* IgG injected and hind-paw injured animals.

In chapter 5 I presented results for a third assessment of DRG surface binding by CRPS serum IgG using IHC and immunofluorescence commonly employed to detect target antigens in fixed tissue. The aim of the experiments in this chapter was to investigate the feasibility of detecting the binding of CRPS-IgG to DRG tissue injected with purified IgG and then injured.

I stained DRG harvested from mice receiving the passive transfer of IgG as described by Goebel et al. and Dawes et al. (Goebel et al. (2021b);Dawes et al. (2018)). Following results obtained with *in vitro* staining, I chose *in vivo*

staining because this is a gold standard technique successfully used for auto antibody pain syndrome studies. (Goebel et al. (2021b);Dawes et al. (2018)).

For experiments presented in this chapter I used pooled IgG (described in chapter 2, section 2.1) for an initial staining overview and then I used IgG purified from one single CRPS donor P1 (described in chapter 2 section 2.1) this allowed me to correlate the staining directly to the patient clinical observation. Experiments with cytokines demonstrated that IgG from different patient have different effects.

As in chapter 4, I used two different techniques to stain L3, L4, L5 DRGs right and left sided tissues harvested from mice after *in vivo* IgG injection and hind limb injury. I used IHC for a first histological assessment of DRG tissue and preliminary staining, followed by IF for more precise location of staining and quantification of the staining strength. I used a protocol of *ex vivo* histological examination of DRG tissue as described by Dawes *et al* and Goebel *et al* (Goebel et al. (2021b);Dawes et al. (2018)) .

IHC results obtained from experiments described in this chapter again indicated that only DRGs corresponding to the incised paw may be more strongly recognized by CRPS IgG, however, again it was not possible to confirm these results with IF staining. Furthermore, in this chapter the staining location was different when using these two different staining methods; for IHC staining was mainly cytoplasmic while for IF staining was mainly on neuronal membrane. For an initial tissue staining overview, IHC slides were stained with pooled HC IgG and pooled CRPS IgG preps derived respectively from 5

healthy volunteers and 27 CRPS patients. Some neurons were stained (mostly medium-large neurons) and these had high IgG concentration only in the cytoplasm (*Figure 5.2*); The staining didn't appear to be selective for a specific neuronal sub-populations as small, medium and large neurons were stained equally. In DRGs from mice injected with pool HC-IgG there was no staining. When DRG from left paw were stained with pool and single sample preparation, no specific strong staining was found for CRPS and no particular difference from CRPS and HC.

I used Immunofluorescence staining on perfused and post fixed tissue to locate and quantify the IgG involved in binding. In this chapter I presented three different experiments that differ in injection days number and sacrifice day adapted from the one used in the CRPS passive transfer model described by Tekus *et al* (Tékus et al. (2014)). For all experiments I used IgG purified from one single CRPS healthy control and one single CRPS patient (P1) previously used for experiments in chapter 3. Experiment 1 staining was very strong and sometimes unspecific for both CRPS and HC, right and left part. The reason for this strong and unspecific staining might be that DRGs were harvested on the same day as last injection and control IgG unspecific binding wasn't properly reduced. Experiment 2 was the only experiment where the left part had a weaker staining than the right part but in this experiment the control IgG appeared to be stronger intensity than CRPS. As experiment 2, experiment 3 was designed to allow reduction of background from HC staining; both CRPS and HC had a light staining but CRPS was not stronger than HC. These

observations were confirmed by a subsequent quantitative analysis. The lack of relevant difference in staining between CRPS and HC and between right and left side can be explained by a possible internalisation by the neuron of the antigen-IgG complex *in vivo* just after binding. In this case, if the majority of IgG were internalized by an epitope-specific mechanism the membrane staining could appear lower and similar to the healthy control staining. Auto antibody binding on neuronal cell surface epitopes and consequent internalisation had already been documented in other studies with anti-amphysin-IgG and anti-CASPR2-IgG (Dawes et al. (2018)). Experiments described in chapter 5 did not investigate intracellular staining as no permeabilization buffer was used.

In conclusion results presented in this thesis supports the observation that the inflammation facilitates the binding of circulating IgG autoantibodies as suggested by Goebel in the conceptual model of auto antibody-mediated CRPS (Goebel and Blaes (2013)). The role of the inflammation (in particular cytokines) in the pathophysiology of CRPS was first demonstrated *in vitro* using DRG cell cultures incubated with inflammatory mediators and later *ex vivo* using DRG tissue from animals with hind limb injury (Tékus et al. (2014)). My results demonstrate that increased IL-6 and IL-1 β concentrations either in the inflamed limb or DRG may play a critical role in triggering the binding to an antigen on DRG neuronal cell surface confirming that these could be potential biomarkers for CRPS as suggested by other studies (Birklein et al. (2001); Huygen et al. (2002); Parkitny et al. (2013))

Furthermore, my results confirm that the injury might play a crucial role in triggering the binding between CRPS IgG and an epitope on DRG cells. The role of the injury in CRPS was firstly demonstrated by IHC staining and then by IF staining. IHC staining appears to demonstrate enhanced DRG IgG binding on the right compared to left, with some indication that this effect is stronger in CRPS IgG. While IF staining does not confirm this probably because tissue preparation at cold temperatures might affect the epitope recognised by CRPS IgG or might be that *in vivo* antibody binding might down regulate the pertinent receptor with consequent low staining intensity. On the other hand, IF *in vivo* showed that injection days and DRG harvest time play a crucial role in reducing staining unspecific binding.

Given the results described in this thesis that i. cytokines successfully enhance the binding of CRPS IgG to DRG neuronal cells and ii. tissue from injured mice present antigens recognised by CRPS IgG, additional immunocytochemistry (ICC) staining of DRG cells enriched with other cell types (e.g. satellite glial cells, fibroblast, endothelial cells, macrophages) and CRPS IgG may be an interesting avenue for future investigations. The cells could be either from naïve mice cultured with cytokines or from incised mice. A co-culture with different cells types and cytokines present in the inflamed limb could trigger complex interactions between cells and consequent enhance IgG binding.

Additionally, further experiments investigating IgG internalisation would be required to confirm that no difference in binding between CRPS and HC IgG was caused by *in vivo* neuronal internalisation as suggested further above.


Finally, future efforts should be focused on improving the understanding of the role of different IgG subclasses (IgG1, IgG2, IgG3 and IgG4) involved in the binding. IgG1, IgG2, IgG3 subclasses induce inflammatory responses (Dekkers et al. (2017)). Different subclasses should be purified and stained individually, this would help to reduce unspecific binding, maybe caused by not active subclasses, that was frequently observed in this project.

Chapter 7 – APPENDIX

In this chapter are listed all the conference proceedings and publications to date obtained from this PhD. I had the opportunity to present my work to other researchers in the field of pain, neurological and immune disorders.

Published journal articles

Bio Protoc. , 2022 Dec 5; 12(23): e4562 .	PMCID: PMC9729856
Published online 2022 Dec 5. doi: 10.21769/BioProtoc.4562	PMID: 36561118
Human Auto-IgG Purification from High Volume Serum Sample by Protein G Affinity Purification	
Serena Sensi ^{III*,#} and Andreas Goebel ^{III#}	
▶ Author information ▶ Article notes ▶ Copyright and License information Disclaimer	

Pharmacological Research 182 (2022) 106347	
	Contents lists available at ScienceDirect
Pharmacological Research	
journal homepage: www.elsevier.com/locate/yphrs	
	
	
Discovery of novel targets in a complex regional pain syndrome mouse model by transcriptomics: TNF and JAK-STAT pathways	
Krisztina Pohóczky ^{a,b,c,1} , József Kun ^{b,d,1} , Nikolett Szentes ^{b,c,j,1} , Tímea Aczél ^{b,c} , Péter Urbán ^d , Attila Gyenesei ^d , Kata Bölcskei ^{b,c} , Éva Szóke ^{b,c,j} , Serena Sensi ^{f,g} , Ádám Dénes ^e , Andreas Goebel ^{f,g} , Valéria Tékus ^{b,c,h,i,1} , Zsuzsanna Helyes ^{b,c,i,j,1}	

Passive transfer of fibromyalgia symptoms from patients to mice

Andreas Goebel,^{1,2} Emerson Krock,³ Clive Gentry,⁴ Mathilde R. Israel,⁴ Alexandra Jurczak,³ Carlos Morado Urbina,³ Katalin Sandor,³ Nisha Vastani,⁴ Margot Maurer,⁴ Ulku Cuhadar,⁴ Serena Sensi,² Yuki Nomura,³ Joana Menezes,³ Azar Baharpoor,³ Louisa Brieskorn,³ Angelica Sandström,⁵ Jeanette Tour,⁵ Diana Kadetoff,^{5,6} Lisbet Haglund,⁷ Eva Kosek,^{5,8} Stuart Bevan,⁴ Camilla I. Svensson,³ and David A. Andersson⁴

Authorship note: AG and E Krock are co-first authors. CIS and DAA are co-senior authors.

Published July 1, 2021 - [More info](#)

RESEARCH PAPER





Autoantibodies produce pain in complex regional pain syndrome by sensitizing nociceptors

Cuhadar, Ulku^a; Gentry, Clive^a; Vastani, Nisha^a; Sensi, Serena^b; Bevan, Stuart^a; Goebel, Andreas^b; Andersson, David A.^{a,*}

[Author Information](#)

PAIN 160(12):p 2855-2865, December 2019. | DOI: 10.1097/j.pain.0000000000001662

Transfer of complex regional pain syndrome to mice via human autoantibodies is mediated by interleukin-1-induced mechanisms

Zsuzsanna Helyes , Valéria Tékus, Nikolett Szentes, , and Andreas Goebel   [Authors Info & Affiliations](#)

Edited by David Julius, University of California, San Francisco, CA, and approved May 13, 2019 (received for review December 1, 2018)

June 10, 2019 | 116 (26) 13067-13076 | <https://doi.org/10.1073/pnas.1820168116>

Conference posters

British pain society annual scientific meeting 2020

Investigating IgG mediated autoimmunity in Complex Regional Pain Syndrome (CRPS) using primary mouse cells

Serena Sensi^a, Andreas Goebel^a, Angela Platt-Higgins^b, Claudia Barnes^a, Dean Naisbitt^a, Philip Rudland^b,

[a] Department of Molecular and Clinical Pharmacology, University of Liverpool, Liverpool, UK

[b] Department of Biochemistry, University of Liverpool, Liverpool, UK

Recent works suggest that some CRPS may be caused by an autoantibody response against surface markers on sensory neurons, but cellular and molecular targets are unknown, and staining experiments in naïve rodent Dorsal Root Ganglia (DRG) were non-conclusive. Using IHC staining we investigated binding of CRPS-serum-IgG to primary DRG derived from hind paw injured mice.

A small skin-muscle incision was applied to the right hind paw of each mouse under general anaesthesia on day 0. On day 2 mice were perfused with 4% Paraformaldehyde and DRG corresponding to the incised paw (L3, L4, L5) were harvested, fixed in 4% Paraformaldehyde, immersed in 3% agar, paraffin embedded together and cut with a microtome for IHC staining. Paraffin slides were stained with affinity purified CRPS/HC-IgG and then with anti-human-IgG-HRP. We firstly stained slides with a pool of 27 CRPS patient IgG and a pool of 7 HC, then we stained with three different CRPS patient IgG chosen from the pool.

We found consistent difference between HC and CRPS IgG staining, in particular slides cut deeper in paraffin block showed consistent strong staining only on certain large-diameter neurons when stained by pooled and single CRPS preparation, and not by controls. The staining pattern was mostly membrane.

In conclusion, in this initial assessment of DRG binding by CRPS serum IgG, certain large-diameter neurons showed membrane binding.

Assessment of Dorsal Root Ganglia surface binding by Complex Regional Pain Syndrome (CRPS)-serum-IgG using primary mouse cells

Serena Sensi^a, Andreas Goebel^a, Dean Naisbitt^a, Philip Rudland^b, Angela Platt-Higgins^b.

[a] Department of Molecular and Clinical Pharmacology, University of Liverpool, Liverpool, UK

[b] Department of Biochemistry, University of Liverpool, Liverpool, UK

Recent works suggest that some CRPS may be caused by an autoantibody response against surface markers on sensory neurons, but cellular and molecular targets are unknown, and staining experiments in naïve rodent Dorsal Root Ganglia (DRG) were non-conclusive. Using IHC staining we investigated binding of CRPS-serum-IgG to primary DRG derived from hind paw injured mice.

Mice were injected daily intra-peritoneally (for up to 13 days) with either affinity-purified plasma-IgG from patients with persistent CRPS, or with IgG derived from healthy controls; a small skin-muscle incision was applied to the right hind paw under general anaesthesia on day 0. Finally mice were perfused with 4% Paraformaldehyde and DRG corresponding to the incised paw were harvested, fixed in 4% Paraformaldehyde, paraffin embedded and cut with a microtome for IHC staining. Paraffin slides were firstly stained with goat anti-human-IgG-HRP to detect CRPS/HC IgG in tissue and in case of no staining slides were then stained with affinity purified CRPS/HC-IgG and then with anti-human-IgG-HRP.

We found inconsistent staining in slides stained directly with anti-human-IgG-HRP, but when slides were incubated with affinity purified CRPS/HC IgG, certain large-diameter neurons were consistently stained by tested CRPS preparations, and not by controls. The staining pattern was exclusively cytoplasmic, and sparing the nucleus.

In conclusion, in this initial assessment of DRG binding by CRPS serum IgG, certain large-diameter neurons showed intracellular binding.

Research abstract

Assessment of DRG surface binding by CRPS-serum-IgG using primary mouse cells

Serena Sensi^a, Andreas Goebel^a, Dean Naisbitt^a

^aDept. of Molecular and Clinical Pharmacology, University of Liverpool, L69 3GE, UK

Recent works suggest that in some patients with CRPS there is an autoantibody response against surface markers on primary neurons, but cellular and molecular targets are unknown. Using FACS analysis we investigate surface epitope binding of CRPS-serum-IgG to murine primary dorsal root ganglion cells.

Dorsal root ganglia (DRGs), harvested from female C57Bl/6J mice, were dissociated. Isolated primary sensory neurons were either directly stained or plated and placed at 37 °C under a 5% CO₂ atmosphere for 24 hours; plated cells were scraped and incubated with purified serum-IgG from CRPS patients or healthy volunteers and then stained. To confirm the role of inflammation in activating the patient IgG, isolated DRG neurons were also incubated with inflammatory mediators and cytokines before assessing the IgG binding.

Directly stained neurons had variable histogram patterns and only in rare cases the mean fluorescence values were higher for CRPS patients than for healthy volunteers. On the contrary, plated neurons had more repeatable histogram patterns and CRPS samples always had higher mean fluorescence values than healthy volunteers. When neurons were incubated with inflammatory mediators there was no significant increase of mean fluorescence. Depending on CRPS patient IgGs, cytokines treatment significantly increased either the mean fluorescence or cell percentage involved in IgG binding.

In this assessment of DRG surface binding by CRPS serum IgG, the majority of plated neurons have a stronger and standardised binding with human IgGs than directly stained neurons. This effect appears to be increased only by cytokines and not by inflammatory mediators.

Chapter 8 - REFERENCES

- Akhoondi M, Oldenhof H, Stoll C, Sieme H, Wolkers WF (2011) Membrane hydraulic permeability changes during cooling of mammalian cells. *Biochim Biophys Acta* 1808 (3):642-648. doi:10.1016/j.bbamem.2010.11.021
- Anthony RM, Kobayashi T, Wermeling F, Ravetch JV (2011) Intravenous gammaglobulin suppresses inflammation through a novel T(H)2 pathway. *Nature* 475 (7354):110-113. doi:10.1038/nature10134
- Aradillas E, Schwartzman RJ, Grothusen JR, Goebel A, Alexander GM (2015) Plasma Exchange Therapy in Patients with Complex Regional Pain Syndrome. *Pain Physician* 18 (4):383-394
- Arecco N, Clarke CJ, Jones FK, Simpson DM, Mason D, Beynon RJ, Pisconti A (2016) Elastase levels and activity are increased in dystrophic muscle and impair myoblast cell survival, proliferation and differentiation. *Sci Rep* 6:24708. doi:10.1038/srep24708
- Bach JF (2018) The hygiene hypothesis in autoimmunity: the role of pathogens and commensals. *Nat Rev Immunol* 18 (2):105-120. doi:10.1038/nri.2017.111
- Baerlecken NT, Gaulke R, Pursche N, Witte T, Karst M, Bernateck M (2019) Autoantibodies against P29ING4 are associated with complex regional pain syndrome. *Immunol Res* 67 (6):461-468. doi:10.1007/s12026-020-09114-y
- Bala U, Tan KL, Ling KH, Cheah PS (2014) Harvesting the maximum length of sciatic nerve from adult mice: a step-by-step approach. *BMC Res Notes* 7:714. doi:10.1186/1756-0500-7-714
- Ballow M (2011) The IgG molecule as a biological immune response modifier: mechanisms of action of intravenous immune serum globulin in autoimmune and inflammatory disorders. *J Allergy Clin Immunol* 127 (2):315-323; quiz 324-315. doi:10.1016/j.jaci.2010.10.030
- Bancroft JD, Gamble M (2008) *Theory and practice of histological techniques*. Elsevier health sciences,
- Basbaum AI, Bautista DM, Scherrer G, Julius D (2009) Cellular and molecular mechanisms of pain. *Cell* 139 (2):267-284. doi:10.1016/j.cell.2009.09.028
- Bergmann-Leitner ES, Mease RM, Duncan EH, Khan F, Waitumbi J, Angov E (2008) Evaluation of immunoglobulin purification methods and their impact on quality and yield of antigen-specific antibodies. *Malar J* 7:129. doi:10.1186/1475-2875-7-129
- Berta T, Perrin FE, Pertin M, Tonello R, Liu YC, Chamesian A, Kato AC, Ji RR, Decosterd I (2017) Gene Expression Profiling of Cutaneous Injured and Non-Injured Nociceptors in SNI Animal Model of

- Neuropathic Pain. *Sci Rep* 7 (1):9367. doi:10.1038/s41598-017-08865-3
- Birklein F, Ajit SK, Goebel A, Perez R, Sommer C (2018) Complex regional pain syndrome - phenotypic characteristics and potential biomarkers. *Nat Rev Neurol* 14 (5):272-284. doi:10.1038/nrneurol.2018.20
- Birklein F, Drummond PD, Li W, Schlereth T, Albrecht N, Finch PM, Dawson LF, Clark JD, Kingery WS (2014) Activation of cutaneous immune responses in complex regional pain syndrome. *J Pain* 15 (5):485-495. doi:10.1016/j.jpain.2014.01.490
- Birklein F, Schlereth T (2015) Complex regional pain syndrome-significant progress in understanding. *Pain* 156 Suppl 1:S94-s103. doi:10.1097/01.j.pain.0000460344.54470.20
- Birklein F, Schmelz M, Schifter S, Weber M (2001) The important role of neuropeptides in complex regional pain syndrome. *Neurology* 57 (12):2179-2184. doi:10.1212/wnl.57.12.2179
- Birrell GJ, McQueen DS, Iggo A, Grubb BD (1993) Prostanoid-induced potentiation of the excitatory and sensitizing effects of bradykinin on articular mechanonociceptors in the rat ankle joint. *Neuroscience* 54 (2):537-544. doi:10.1016/0306-4522(93)90273-i
- Blaes F, Schmitz K, Tschernatsch M, Kaps M, Krasenbrink I, Hempelmann G, Bräu ME (2004) Autoimmune etiology of complex regional pain syndrome (M. Sudeck). *Neurology* 63 (9):1734-1736. doi:10.1212/01.wnl.0000143066.58498.ba
- Bluestone JA, Bour-Jordan H, Cheng M, Anderson M (2015) T cells in the control of organ-specific autoimmunity. *J Clin Invest* 125 (6):2250-2260. doi:10.1172/jci78089
- Bodde MI, Dijkstra PU, den Dunnen WF, Geertzen JH (2011) Therapy-resistant complex regional pain syndrome type I: to amputate or not? *J Bone Joint Surg Am* 93 (19):1799-1805. doi:10.2106/jbjs.J.01329
- Boettger MK, Leuchtweis J, Kümmel D, Gajda M, Bräuer R, Schaible HG (2010) Differential effects of locally and systemically administered soluble glycoprotein 130 on pain and inflammation in experimental arthritis. *Arthritis Res Ther* 12 (4):R140. doi:10.1186/ar3079
- Borges LF, Elliott PJ, Gill R, Iversen SD, Iversen LL (1985) Selective extraction of small and large molecules from the cerebrospinal fluid by Purkinje neurons. *Science* 228 (4697):346-348. doi:10.1126/science.2580350
- Brennan TJ, Vandermeulen EP, Gebhart GF (1996) Characterization of a rat model of incisional pain. *Pain* 64 (3):493-502. doi:10.1016/0304-3959(95)01441-1
- Bruehl S (2015) Complex regional pain syndrome. *Bmj* 351:h2730. doi:10.1136/bmj.h2730
- Cesare P, McNaughton P (1996) A novel heat-activated current in nociceptive neurons and its sensitization by bradykinin. *Proc Natl Acad Sci U S A* 93 (26):15435-15439. doi:10.1073/pnas.93.26.15435
- Chen L, Deng H, Cui H, Fang J, Zuo Z, Deng J, Li Y, Wang X, Zhao L (2018) Inflammatory responses and inflammation-associated diseases in organs. *Oncotarget* 9 (6):7204-7218. doi:10.18632/oncotarget.23208

- Crapanzano JT, Harrison-Bernard LM, Jones MR, Kaye AD, Richter EO, Potash MN (2017) High Frequency Spinal Cord Stimulation for Complex Regional Pain Syndrome: A Case Report. *Pain Physician* 20 (1):E177-e182
- Cuhadar U, Gentry C, Vastani N, Sensi S, Bevan S, Goebel A, Andersson DA (2019) Autoantibodies produce pain in complex regional pain syndrome by sensitizing nociceptors. *Pain* 160 (12):2855-2865. doi:10.1097/j.pain.0000000000001662
- Cunha JM, Cunha FQ, Poole S, Ferreira SH (2000) Cytokine-mediated inflammatory hyperalgesia limited by interleukin-1 receptor antagonist. *Br J Pharmacol* 130 (6):1418-1424. doi:10.1038/sj.bjp.0703434
- Dai Y, Wang S, Tominaga M, Yamamoto S, Fukuoka T, Higashi T, Kobayashi K, Obata K, Yamanaka H, Noguchi K (2007) Sensitization of TRPA1 by PAR2 contributes to the sensation of inflammatory pain. *J Clin Invest* 117 (7):1979-1987. doi:10.1172/jci30951
- Dalakas MC (2004) Intravenous immunoglobulin in autoimmune neuromuscular diseases. *Jama* 291 (19):2367-2375. doi:10.1001/jama.291.19.2367
- Darcy E, Leonard P, Fitzgerald J, Danaher M, Ma H, O'Kennedy R (2017) Purification of Antibodies Using Affinity Chromatography. *Methods Mol Biol* 1485:305-318. doi:10.1007/978-1-4939-6412-3_15
- David Clark J, Tawfik VL, Tajerian M, Kingery WS (2018) Autoinflammatory and autoimmune contributions to complex regional pain syndrome. *Mol Pain* 14:1744806918799127. doi:10.1177/1744806918799127
- Davis KD, Meyer RA, Campbell JN (1993) Chemosensitivity and sensitization of nociceptive afferents that innervate the hairy skin of monkey. *J Neurophysiol* 69 (4):1071-1081. doi:10.1152/jn.1993.69.4.1071
- Dawes JM, Vincent A (2016) Autoantibodies and pain. *Curr Opin Support Palliat Care* 10 (2):137-142. doi:10.1097/spc.0000000000000211
- Dawes JM, Weir GA, Middleton SJ, Patel R, Chisholm KI, Pettingill P, Peck LJ, Sheridan J, Shakir A, Jacobson L, Gutierrez-Mecinas M, Galino J, Walcher J, Kühnemund J, Kuehn H, Sanna MD, Lang B, Clark AJ, Themistocleous AC, Iwagaki N, West SJ, Werynska K, Carroll L, Trendafilova T, Menassa DA, Giannoccaro MP, Coutinho E, Cervellini I, Tewari D, Buckley C, Leite MI, Wildner H, Zeilhofer HU, Peles E, Todd AJ, McMahon SB, Dickenson AH, Lewin GR, Vincent A, Bennett DL (2018) Immune or Genetic-Mediated Disruption of CASPR2 Causes Pain Hypersensitivity Due to Enhanced Primary Afferent Excitability. *Neuron* 97 (4):806-822.e810. doi:10.1016/j.neuron.2018.01.033
- de Mos M, de Bruijn AG, Huygen FJ, Dieleman JP, Stricker BH, Sturkenboom MC (2007) The incidence of complex regional pain syndrome: a population-based study. *Pain* 129 (1-2):12-20. doi:10.1016/j.pain.2006.09.008
- Dekkers G, Treffers L, Plomp R, Bentlage AEH, de Boer M, Koeleman CAM, Lissenberg-Thunnissen SN, Visser R, Brouwer M, Mok JY, Matlung H, van den Berg TK, van Esch WJE, Kuijpers TW, Wouters D, Rispens T, Wuhrer M, Vidarsson G (2017) Decoding the Human Immunoglobulin

- G-Glycan Repertoire Reveals a Spectrum of Fc-Receptor- and Complement-Mediated-Effector Activities. *Front Immunol* 8:877. doi:10.3389/fimmu.2017.00877
- Delmas P, Hao J, Rodat-Despoix L (2011) Molecular mechanisms of mechanotransduction in mammalian sensory neurons. *Nat Rev Neurosci* 12 (3):139-153. doi:10.1038/nrn2993
- Dirckx M, Stronks DL, van Bodegraven-Hof EA, Wesseldijk F, Groeneweg JG, Huygen FJ (2015) Inflammation in cold complex regional pain syndrome. *Acta Anaesthesiol Scand* 59 (6):733-739. doi:10.1111/aas.12465
- Djoughri L, Koutsikou S, Fang X, McMullan S, Lawson SN (2006) Spontaneous pain, both neuropathic and inflammatory, is related to frequency of spontaneous firing in intact C-fiber nociceptors. *J Neurosci* 26 (4):1281-1292. doi:10.1523/jneurosci.3388-05.2006
- Djoughri L, Lawson SN (2004) Abeta-fiber nociceptive primary afferent neurons: a review of incidence and properties in relation to other afferent A-fiber neurons in mammals. *Brain Res Brain Res Rev* 46 (2):131-145. doi:10.1016/j.brainresrev.2004.07.015
- Dray A, Bettaney J, Forster P, Perkins MN (1988) Bradykinin-induced stimulation of afferent fibres is mediated through protein kinase C. *Neurosci Lett* 91 (3):301-307. doi:10.1016/0304-3940(88)90697-0
- Dubin AE, Patapoutian A (2010) Nociceptors: the sensors of the pain pathway. *J Clin Invest* 120 (11):3760-3772. doi:10.1172/jci42843
- Egloff N, Sabbioni ME, Salathé C, Wiest R, Juengling FD (2009) Nondermatomal somatosensory deficits in patients with chronic pain disorder: clinical findings and hypometabolic pattern in FDG-PET. *Pain* 145 (1-2):252-258. doi:10.1016/j.pain.2009.04.016
- Eldufani J, Elahmer N, Blaise G (2020) A medical mystery of complex regional pain syndrome. *Heliyon* 6 (2):e03329. doi:10.1016/j.heliyon.2020.e03329
- Esposito M, Malayil R, Hanes M, Deer T (2019) Unique Characteristics of the Dorsal Root Ganglion as a target for Neuromodulation. *Pain Medicine*:S23-S30
- Ferrero-Miliani L, Nielsen OH, Andersen PS, Girardin SE (2007) Chronic inflammation: importance of NOD2 and NALP3 in interleukin-1beta generation. *Clin Exp Immunol* 147 (2):227-235. doi:10.1111/j.1365-2249.2006.03261.x
- Frias B, Merighi A (2016) Capsaicin, Nociception and Pain. *Molecules* 21 (6). doi:10.3390/molecules21060797
- Fujiwara N, Kobayashi K (2005) Macrophages in inflammation. *Curr Drug Targets Inflamm Allergy* 4 (3):281-286. doi:10.2174/1568010054022024
- Goebel A (2011) Complex regional pain syndrome in adults. *Rheumatology (Oxford)* 50 (10):1739-1750. doi:10.1093/rheumatology/ker202
- Goebel A (2016) Autoantibody pain. *Autoimmun Rev* 15 (6):552-557. doi:10.1016/j.autrev.2016.02.011
- Goebel A, Baranowski A, Maurer K, Ghiai A, McCabe C, Ambler G (2010) Intravenous immunoglobulin treatment of the complex regional pain

- syndrome: a randomized trial. *Ann Intern Med* 152 (3):152-158.
doi:10.7326/0003-4819-152-3-201002020-00006
- Goebel A, Birklein F, Brunner F, Clark JD, Gierthmühlen J, Harden N, Huygen F, Knudsen L, McCabe C, Lewis J, Maihöfner C, Magerl W, Moseley GL, Terkelsen A, Thomassen I, Bruehl S (2021a) The Valencia consensus-based adaptation of the IASP complex regional pain syndrome diagnostic criteria. *Pain* 162 (9):2346-2348.
doi:10.1097/j.pain.0000000000002245
- Goebel A, Bisla J, Carganillo R, Cole C, Frank B, Gupta R, James M, Kelly J, McCabe C, Milligan H, Murphy C, Padfield N, Phillips C, Poole H, Saunders M, Serpell M, Shenker N, Shoukrey K, Wyatt L, Ambler G (2017) Efficacy and Mechanism Evaluation. In: A randomised placebo-controlled Phase III multicentre trial: low-dose intravenous immunoglobulin treatment for long-standing complex regional pain syndrome (LIPS trial). NIHR Journals Library
- Copyright © Queen's Printer and Controller of HMSO 2017. This work was produced by Goebel et al. under the terms of a commissioning contract issued by the Secretary of State for Health. This issue may be freely reproduced for the purposes of private research and study and extracts (or indeed, the full report) may be included in professional journals provided that suitable acknowledgement is made and the reproduction is not associated with any form of advertising. Applications for commercial reproduction should be addressed to: NIHR Journals Library, National Institute for Health Research, Evaluation, Trials and Studies Coordinating Centre, Alpha House, University of Southampton Science Park, Southampton SO16 7NS, UK., Southampton (UK). doi:10.3310/eme04050
- Goebel A, Blaes F (2013) Complex regional pain syndrome, prototype of a novel kind of autoimmune disease. *Autoimmun Rev* 12 (6):682-686.
doi:10.1016/j.autrev.2012.10.015
- Goebel A, Krock E, Gentry C, Israel MR, Jurczak A, Urbina CM, Sandor K, Vastani N, Maurer M, Cuhadar U, Sensi S, Nomura Y, Menezes J, Baharpoor A, Brieskorn L, Sandström A, Tour J, Kadetoff D, Haglund L, Kosek E, Bevan S, Svensson CI, Andersson DA (2021b) Passive transfer of fibromyalgia symptoms from patients to mice. *J Clin Invest* 131 (13). doi:10.1172/jci144201
- Goebel A, Netal S, Schedel R, Sprotte G (2002) Human pooled immunoglobulin in the treatment of chronic pain syndromes. *Pain Med* 3 (2):119-127. doi:10.1046/j.1526-4637.2002.02018.x
- Goebel A, Stock M, Deacon R, Sprotte G, Vincent A (2005a) Intravenous immunoglobulin response and evidence for pathogenic antibodies in a case of complex regional pain syndrome 1. *Ann Neurol* 57 (3):463-464. doi:10.1002/ana.20400
- Goebel A, Vogel H, Caneris O, Bajwa Z, Clover L, Roewer N, Schedel R, Karch H, Sprotte G, Vincent A (2005b) Immune responses to *Campylobacter* and serum autoantibodies in patients with complex regional pain syndrome. *J Neuroimmunol* 162 (1-2):184-189.
doi:10.1016/j.jneuroim.2005.01.018

- Goh EL, Chidambaram S, Ma D (2017) Complex regional pain syndrome: a recent update. *Burns Trauma* 5:2. doi:10.1186/s41038-016-0066-4
- Gold MS, Gebhart GF (2010) Nociceptor sensitization in pain pathogenesis. *Nat Med* 16 (11):1248-1257. doi:10.1038/nm.2235
- Goldberg DS, McGee SJ (2011) Pain as a global public health priority. *BMC Public Health* 11:770. doi:10.1186/1471-2458-11-770
- Gough SC, Simmonds MJ (2007) The HLA Region and Autoimmune Disease: Associations and Mechanisms of Action. *Curr Genomics* 8 (7):453-465. doi:10.2174/138920207783591690
- Graus YF, de Baets MH, van Breda Vriesman PJ, Burton DR (1997) Anti-acetylcholine receptor Fab fragments isolated from thymus-derived phage display libraries from myasthenia gravis patients reflect predominant specificities in serum and block the action of pathogenic serum antibodies. *Immunol Lett* 57 (1-3):59-62. doi:10.1016/s0165-2478(97)00046-1
- Griffiths G (1993) Fixation for fine structure preservation and immunocytochemistry. In: *Fine structure immunocytochemistry*. Springer, pp 26-89
- Grodzki AC, Berenstein E (2010) Antibody purification: affinity chromatography - protein A and protein G Sepharose. *Methods Mol Biol* 588:33-41. doi:10.1007/978-1-59745-324-0_5
- Haberberger RV, Barry C, Dominguez N, Matusica D (2019a) Human Dorsal Root Ganglia. *Front Cell Neurosci* 13:271. doi:10.3389/fncel.2019.00271
- Haberberger RV, Barry C, Dominguez N, Matusica D (2019b) Human Dorsal Root Ganglia. *Frontiers in Cellular Neuroscience* 13:1-17
- Hanani M (2005) Satellite glial cells in sensory ganglia: from form to function. *Brain Res Brain Res Rev* 48 (3):457-476. doi:10.1016/j.brainresrev.2004.09.001
- Harden NR, Bruehl S, Perez R, Birklein F, Marinus J, Maihofner C, Lubenow T, Buvanendran A, Mackey S, Graciosa J, Mogilevski M, Ramsden C, Chont M, Vatine JJ (2010) Validation of proposed diagnostic criteria (the "Budapest Criteria") for Complex Regional Pain Syndrome. *Pain* 150 (2):268-274. doi:10.1016/j.pain.2010.04.030
- Harden RN, Bruehl S, Stanton-Hicks M, Wilson PR (2007) Proposed new diagnostic criteria for complex regional pain syndrome. *Pain Med* 8 (4):326-331. doi:10.1111/j.1526-4637.2006.00169.x
- Harrison C, Epton S, Bojanic S, Green AL, FitzGerald JJ (2018) The Efficacy and Safety of Dorsal Root Ganglion Stimulation as a Treatment for Neuropathic Pain: A Literature Review. *Neuromodulation* 21 (3):225-233. doi:10.1111/ner.12685
- Hayter SM, Cook MC (2012) Updated assessment of the prevalence, spectrum and case definition of autoimmune disease. *Autoimmun Rev* 11 (10):754-765. doi:10.1016/j.autrev.2012.02.001
- Heinrich T, Hübner CA, Kurth I (2016) Isolation and primary cell culture of mouse dorsal root ganglion neurons. *Bio-protocol* 6 (7):e1785-e1785
- Helyes Z, Tékus V, Szentes N, Pohóczky K, Botz B, Kiss T, Kemény Á, Környei Z, Tóth K, Lénárt N, Ábrahám H, Pinteaux E, Francis S, Sensi

- S, Dénes Á, Goebel A (2019) Transfer of complex regional pain syndrome to mice via human autoantibodies is mediated by interleukin-1-induced mechanisms. *Proc Natl Acad Sci U S A* 116 (26):13067-13076. doi:10.1073/pnas.1820168116
- Hendrayani SF, Al-Harbi B, Al-Ansari MM, Silva G, Aboussekhra A (2016) The inflammatory/cancer-related IL-6/STAT3/NF- κ B positive feedback loop includes AUF1 and maintains the active state of breast myofibroblasts. *Oncotarget* 7 (27):41974-41985. doi:10.18632/oncotarget.9633
- Hensel H, Zotterman Y (1951) The effect of menthol on the thermoreceptors. *Acta Physiol Scand* 24 (1):27-34. doi:10.1111/j.1748-1716.1951.tb00824.x
- Herschkowitz D, Kubias J (2018) Wireless peripheral nerve stimulation for complex regional pain syndrome type I of the upper extremity: a case illustration introducing a novel technology. *Scand J Pain* 18 (3):555-560. doi:10.1515/sjpain-2018-0014
- Hnasko RM, McGarvey JA (2015) Affinity Purification of Antibodies. *Methods Mol Biol* 1318:29-41. doi:10.1007/978-1-4939-2742-5_3
- Hucho TB, Dina OA, Levine JD (2005) Epac mediates a cAMP-to-PKC signaling in inflammatory pain: an isolectin B4(+) neuron-specific mechanism. *J Neurosci* 25 (26):6119-6126. doi:10.1523/jneurosci.0285-05.2005
- Huygen FJ, De Bruijn AG, De Bruin MT, Groeneweg JG, Klein J, Zijlstra FJ (2002) Evidence for local inflammation in complex regional pain syndrome type 1. *Mediators Inflamm* 11 (1):47-51. doi:10.1080/09629350210307
- Huygen FJ, Ramdhani N, van Toorenenbergen A, Klein J, Zijlstra FJ (2004) Mast cells are involved in inflammatory reactions during Complex Regional Pain Syndrome type 1. *Immunol Lett* 91 (2-3):147-154. doi:10.1016/j.imlet.2003.11.013
- Im K, Mareninov S, Diaz MFP, Yong WH (2019) An Introduction to Performing Immunofluorescence Staining. *Methods Mol Biol* 1897:299-311. doi:10.1007/978-1-4939-8935-5_26
- Inoue A, Ikoma K, Morioka N, Kumagai K, Hashimoto T, Hide I, Nakata Y (1999) Interleukin-1 β induces substance P release from primary afferent neurons through the cyclooxygenase-2 system. *J Neurochem* 73 (5):2206-2213
- Ji RR, Baba H, Brenner GJ, Woolf CJ (1999) Nociceptive-specific activation of ERK in spinal neurons contributes to pain hypersensitivity. *Nat Neurosci* 2 (12):1114-1119. doi:10.1038/16040
- Julius D, Basbaum AI (2001) Molecular mechanisms of nociception. *Nature* 413 (6852):203-210. doi:10.1038/35093019
- Kessler A, Yoo M, Calisoff R (2020) Complex regional pain syndrome: An updated comprehensive review. *NeuroRehabilitation* 47 (3):253-264. doi:10.3233/nre-208001
- Kessler W, Kirchoff C, Reeh PW, Handwerker HO (1992) Excitation of cutaneous afferent nerve endings in vitro by a combination of

- inflammatory mediators and conditioning effect of substance P. *Exp Brain Res* 91 (3):467-476. doi:10.1007/bf00227842
- Kim K-J, Choi SH, Jang J-S, Jang I-T (2020) Complex regional pain syndrome following lumbar discectomy: A case report. *Interdisciplinary Neurosurgery* 19:100587
- Kirschstein T, Büsselberg D, Treede RD (1997) Coexpression of heat-evoked and capsaicin-evoked inward currents in acutely dissociated rat dorsal root ganglion neurons. *Neurosci Lett* 231 (1):33-36. doi:10.1016/s0304-3940(97)00533-8
- Klein CJ, Lennon VA, Aston PA, McKeon A, Pittock SJ (2012) Chronic pain as a manifestation of potassium channel-complex autoimmunity. *Neurology* 79 (11):1136-1144. doi:10.1212/WNL.0b013e3182698cab
- Knibestöl M (1973) Stimulus-response functions of rapidly adapting mechanoreceptors in human glabrous skin area. *J Physiol* 232 (3):427-452. doi:10.1113/jphysiol.1973.sp010279
- Koch A, Zacharowski K, Boehm O, Stevens M, Lipfert P, von Giesen HJ, Wolf A, Freynhagen R (2007) Nitric oxide and pro-inflammatory cytokines correlate with pain intensity in chronic pain patients. *Inflamm Res* 56 (1):32-37. doi:10.1007/s00011-007-6088-4
- Koeppen AH, Ramirez RL, Becker AB, Mazurkiewicz JE (2016) Dorsal root ganglia in Friedreich ataxia: satellite cell proliferation and inflammation. *Acta Neuropathol Commun* 4 (1):46. doi:10.1186/s40478-016-0288-5
- Kohr D, Singh P, Tschernatsch M, Kaps M, Pouokam E, Diener M, Kummer W, Birklein F, Vincent A, Goebel A, Wallukat G, Blaes F (2011) Autoimmunity against the β_2 adrenergic receptor and muscarinic-2 receptor in complex regional pain syndrome. *Pain* 152 (12):2690-2700. doi:10.1016/j.pain.2011.06.012
- Kohr D, Tschernatsch M, Schmitz K, Singh P, Kaps M, Schäfer KH, Diener M, Mathies J, Matz O, Kummer W, Maihöfner C, Fritz T, Birklein F, Blaes F (2009) Autoantibodies in complex regional pain syndrome bind to a differentiation-dependent neuronal surface autoantigen. *Pain* 143 (3):246-251. doi:10.1016/j.pain.2009.03.009
- Koneczny I, Cossins J, Waters P, Beeson D, Vincent A (2013) MuSK myasthenia gravis IgG4 disrupts the interaction of LRP4 with MuSK but both IgG4 and IgG1-3 can disperse preformed agrin-independent AChR clusters. *PLoS One* 8 (11):e80695. doi:10.1371/journal.pone.0080695
- Krämer HH, Hofbauer LC, Szalay G, Breimhorst M, Eberle T, Zieschang K, Rauner M, Schlereth T, Schreckenberger M, Birklein F (2014) Osteoprotegerin: a new biomarker for impaired bone metabolism in complex regional pain syndrome? *Pain* 155 (5):889-895. doi:10.1016/j.pain.2014.01.014
- Krames ES (2014) The role of the dorsal root ganglion in the development of neuropathic pain. *Pain Med* 15 (10):1669-1685. doi:10.1111/pme.12413
- Kress M (2010) Nociceptor sensitization by proinflammatory cytokines and chemokines. *The open pain journal* 3 (1)

- Kress M, Reeh PW, Vyklicky L (1997) An interaction of inflammatory mediators and protons in small diameter dorsal root ganglion neurons of the rat. *Neurosci Lett* 224 (1):37-40. doi:10.1016/s0304-3940(97)13450-4
- Krishnamurthy A, Joshua V, Haj Hensvold A, Jin T, Sun M, Vivar N, Ytterberg AJ, Engström M, Fernandes-Cerqueira C, Amara K, Magnusson M, Wigerblad G, Kato J, Jiménez-Andrade JM, Tyson K, Rapecki S, Lundberg K, Catrina SB, Jakobsson PJ, Svensson C, Malmström V, Klareskog L, Wähämaa H, Catrina AI (2016) Identification of a novel chemokine-dependent molecular mechanism underlying rheumatoid arthritis-associated autoantibody-mediated bone loss. *Ann Rheum Dis* 75 (4):721-729. doi:10.1136/annrheumdis-2015-208093
- Kyriakis JM, Avruch J (2001) Mammalian mitogen-activated protein kinase signal transduction pathways activated by stress and inflammation. *Physiol Rev* 81 (2):807-869. doi:10.1152/physrev.2001.81.2.807
- Laedermann CJ, Pertin M, Suter MR, Decosterd I (2014) Voltage-gated sodium channel expression in mouse DRG after SNI leads to re-evaluation of projections of injured fibers. *Mol Pain* 10:19. doi:10.1186/1744-8069-10-19
- Lakritz JR, Bodair A, Shah N, O'Donnell R, Polydefkis MJ, Miller AD, Burdo TH (2015) Monocyte Traffic, Dorsal Root Ganglion Histopathology, and Loss of Intraepidermal Nerve Fiber Density in SIV Peripheral Neuropathy. *Am J Pathol* 185 (7):1912-1923. doi:10.1016/j.ajpath.2015.03.007
- Lee MC, McCubbin JA, Christensen AD, Poole DP, Rajasekhar P, Lieu T, Bunnett NW, Garcia-Caraballo S, Erickson A, Brierley SM, Saleh R, Achuthan A, Fleetwood AJ, Anderson RL, Hamilton JA, Cook AD (2017) G-CSF Receptor Blockade Ameliorates Arthritic Pain and Disease. *J Immunol* 198 (9):3565-3575. doi:10.4049/jimmunol.1602127
- Lenz M, Üçeyler N, Frettlöh J, Höffken O, Krumova EK, Lissek S, Reinersmann A, Sommer C, Stude P, Waaga-Gasser AM, Tegenthoff M, Maier C (2013) Local cytokine changes in complex regional pain syndrome type I (CRPS I) resolve after 6 months. *Pain* 154 (10):2142-2149. doi:10.1016/j.pain.2013.06.039
- Lettau M, Wiedemann A, Schrezenmeier EV, Giesecke-Thiel C, Dörner T (2020) Human CD27+ memory B cells colonize a superficial follicular zone in the palatine tonsils with similarities to the spleen. A multicolor immunofluorescence study of lymphoid tissue. *PLoS One* 15 (3):e0229778. doi:10.1371/journal.pone.0229778
- Lewin GR, Moshourab R (2004) Mechanosensation and pain. *J Neurobiol* 61 (1):30-44. doi:10.1002/neu.20078
- Libby P (2007) Inflammatory mechanisms: the molecular basis of inflammation and disease. *Nutr Rev* 65 (12 Pt 2):S140-146. doi:10.1111/j.1753-4887.2007.tb00352.x
- Lin CR, Amaya F, Barrett L, Wang H, Takada J, Samad TA, Woolf CJ (2006) Prostaglandin E2 receptor EP4 contributes to inflammatory pain

- hypersensitivity. *J Pharmacol Exp Ther* 319 (3):1096-1103.
doi:10.1124/jpet.106.105569
- Linley JE, Rose K, Ooi L, Gamper N (2010) Understanding inflammatory pain: ion channels contributing to acute and chronic nociception. *Pflugers Arch* 459 (5):657-669. doi:10.1007/s00424-010-0784-6
- Lintermans LL, Stegeman CA, Heeringa P, Abdulahad WH (2014) T cells in vascular inflammatory diseases. *Front Immunol* 5:504.
doi:10.3389/fimmu.2014.00504
- Littleton E, Dreger M, Palace J, Vincent A (2009) Immunocapture and identification of cell membrane protein antigenic targets of serum autoantibodies. *Mol Cell Proteomics* 8 (7):1688-1696.
doi:10.1074/mcp.M800563-MCP200
- Loram LC, Themistocleous AC, Fick LG, Kamerman PR (2007) The time course of inflammatory cytokine secretion in a rat model of postoperative pain does not coincide with the onset of mechanical hyperalgesia. *Can J Physiol Pharmacol* 85 (6):613-620.
doi:10.1139/y07-054
- Ludwig RJ, Vanhoorelbeke K, Leypoldt F, Kaya Z, Bieber K, McLachlan SM, Komorowski L, Luo J, Cabral-Marques O, Hammers CM, Lindstrom JM, Lamprecht P, Fischer A, Riemekasten G, Tersteeg C, Sondermann P, Rapoport B, Wandinger KP, Probst C, El Beidaq A, Schmidt E, Verkman A, Manz RA, Nimmerjahn F (2017) Mechanisms of Autoantibody-Induced Pathology. *Front Immunol* 8:603.
doi:10.3389/fimmu.2017.00603
- Lünemann JD, Nimmerjahn F, Dalakas MC (2015) Intravenous immunoglobulin in neurology--mode of action and clinical efficacy. *Nat Rev Neurol* 11 (2):80-89. doi:10.1038/nrneurol.2014.253
- Lünemann JD, Quast I, Dalakas MC (2016) Efficacy of Intravenous Immunoglobulin in Neurological Diseases. *Neurotherapeutics* 13 (1):34-46. doi:10.1007/s13311-015-0391-5
- Ma C, Greenquist KW, Lamotte RH (2006) Inflammatory mediators enhance the excitability of chronically compressed dorsal root ganglion neurons. *J Neurophysiol* 95 (4):2098-2107. doi:10.1152/jn.00748.2005
- Makker PG, Duffy SS, Lees JG, Perera CJ, Tonkin RS, Butovsky O, Park SB, Goldstein D, Moalem-Taylor G (2017) Characterisation of Immune and Neuroinflammatory Changes Associated with Chemotherapy-Induced Peripheral Neuropathy. *PLoS One* 12 (1):e0170814.
doi:10.1371/journal.pone.0170814
- Malin SA, Davis BM, Molliver DC (2007) Production of dissociated sensory neuron cultures and considerations for their use in studying neuronal function and plasticity. *Nat Protoc* 2 (1):152-160.
doi:10.1038/nprot.2006.461
- Mallat Z, Heymes C, Ohan J, Faggini E, Lesèche G, Tedgui A (1999) Expression of interleukin-10 in advanced human atherosclerotic plaques: relation to inducible nitric oxide synthase expression and cell death. *Arterioscler Thromb Vasc Biol* 19 (3):611-616.
doi:10.1161/01.atv.19.3.611

- Mantyh PW (1983) The spinothalamic tract in the primate: a re-examination using wheatgerm agglutinin conjugated to horseradish peroxidase. *Neuroscience* 9 (4):847-862. doi:10.1016/0306-4522(83)90273-7
- Marone IM, De Logu F, Nassini R, De Carvalho Goncalves M, Benemei S, Ferreira J, Jain P, Li Puma S, Bunnett NW, Geppetti P, Materazzi S (2018) TRPA1/NOX in the soma of trigeminal ganglion neurons mediates migraine-related pain of glyceryl trinitrate in mice. *Brain* 141 (8):2312-2328. doi:10.1093/brain/awy177
- Marson A, Housley WJ, Hafler DA (2015) Genetic basis of autoimmunity. *J Clin Invest* 125 (6):2234-2241. doi:10.1172/jci78086
- Martin D, Xu J, Porretta C, Nichols CD (2017) Neurocytometry: Flow Cytometric Sorting of Specific Neuronal Populations from Human and Rodent Brain. *ACS Chem Neurosci* 8 (2):356-367. doi:10.1021/acscchemneuro.6b00374
- Matsuka Y, Afroz S, Dalanon JC, Iwasa T, Waskitho A, Oshima M (2020) The role of chemical transmitters in neuron-glia interaction and pain in sensory ganglion. *Neurosci Biobehav Rev* 108:393-399. doi:10.1016/j.neubiorev.2019.11.019
- McBride A, Atkins R (2005) Complex regional pain syndrome. *Current Orthopaedics* 19 (2):155-165
- McCarthy PW, Lawson SN (1990) Cell type and conduction velocity of rat primary sensory neurons with calcitonin gene-related peptide-like immunoreactivity. *Neuroscience* 34 (3):623-632. doi:10.1016/0306-4522(90)90169-5
- McKinnon KM (2018) Flow Cytometry: An Overview. *Curr Protoc Immunol* 120:5.1.1-5.1.11. doi:10.1002/cpim.40
- McMahon MJ, O'Kennedy R (2000) Polyreactivity as an acquired artefact, rather than a physiologic property, of antibodies: evidence that monoreactive antibodies may gain the ability to bind to multiple antigens after exposure to low pH. *J Immunol Methods* 241 (1-2):1-10. doi:10.1016/s0022-1759(00)00196-4
- McMahon SB, La Russa F, Bennett DL (2015) Crosstalk between the nociceptive and immune systems in host defence and disease. *Nat Rev Neurosci* 16 (7):389-402. doi:10.1038/nrn3946
- Medzhitov R (2010) Inflammation 2010: new adventures of an old flame. *Cell* 140 (6):771-776. doi:10.1016/j.cell.2010.03.006
- Merskey H, Bogduk N International Association for the Study of the Pain, Classification of Chronic Pain: Descriptions of Chronic Pain Syndromes and Definitions of Pain Terms 1994 2nd edn Seattle. Washington IASP Press,
- Meyer R, Campbell J, Raja S (1994) Textbook of pain. McMahon, SB:3-34
- Michaelis M, Liu X, Jänig W (2000) Axotomized and intact muscle afferents but no skin afferents develop ongoing discharges of dorsal root ganglion origin after peripheral nerve lesion. *J Neurosci* 20 (7):2742-2748. doi:10.1523/jneurosci.20-07-02742.2000
- Mifflin KA, Kerr BJ (2017) Pain in autoimmune disorders. *J Neurosci Res* 95 (6):1282-1294. doi:10.1002/jnr.23844

- Millan MJ (1999) The induction of pain: an integrative review. *Prog Neurobiol* 57 (1):1-164. doi:10.1016/s0301-0082(98)00048-3
- Mills KH (2011) TLR-dependent T cell activation in autoimmunity. *Nat Rev Immunol* 11 (12):807-822. doi:10.1038/nri3095
- Mitchell SW, Morehouse GR, Keen WW (2007) Gunshot wounds and other injuries of nerves. 1864. *Clin Orthop Relat Res* 458:35-39. doi:10.1097/BLO.0b013e31803df02c
- Mohamed HA, Mosier DR, Zou LL, Siklós L, Alexianu ME, Engelhardt JI, Beers DR, Le WD, Appel SH (2002) Immunoglobulin Fc gamma receptor promotes immunoglobulin uptake, immunoglobulin-mediated calcium increase, and neurotransmitter release in motor neurons. *J Neurosci Res* 69 (1):110-116. doi:10.1002/jnr.10271
- Nascimento AI, Mar FM, Sousa MM (2018) The intriguing nature of dorsal root ganglion neurons: Linking structure with polarity and function. *Progress in Neurobiology*:86-103
- Nicholas M, Vlaeyen JWS, Rief W, Barke A, Aziz Q, Benoliel R, Cohen M, Evers S, Giamberardino MA, Goebel A, Korwisi B, Perrot S, Svensson P, Wang SJ, Treede RD (2019) The IASP classification of chronic pain for ICD-11: chronic primary pain. *Pain* 160 (1):28-37. doi:10.1097/j.pain.0000000000001390
- Orlova IA, Alexander GM, Qureshi RA, Sacan A, Graziano A, Barrett JE, Schwartzman RJ, Ajit SK (2011) MicroRNA modulation in complex regional pain syndrome. *J Transl Med* 9:195. doi:10.1186/1479-5876-9-195
- Pardo ID, Weber K, Cramer S, Krinke GJ, Butt MT, Sharma AK, Bolon B (2020) Atlas of Normal Microanatomy, Procedural and Processing Artifacts, Common Background Findings, and Neurotoxic Lesions in the Peripheral Nervous System of Laboratory Animals. *Toxicol Pathol* 48 (1):105-131. doi:10.1177/0192623319867322
- Parkitny L, McAuley JH, Di Pietro F, Stanton TR, O'Connell NE, Marinus J, van Hilten JJ, Moseley GL (2013) Inflammation in complex regional pain syndrome: a systematic review and meta-analysis. *Neurology* 80 (1):106-117. doi:10.1212/WNL.0b013e31827b1aa1
- Patterson KR, Dalmau J, Lancaster E (2018) Mechanisms of Caspr2 antibodies in autoimmune encephalitis and neuromyotonia. *Ann Neurol* 83 (1):40-51. doi:10.1002/ana.25120
- Peers C, Johnston I, Lang B, Wray D (1993) Cross-linking of presynaptic calcium channels: a mechanism of action for Lambert-Eaton myasthenic syndrome antibodies at the mouse neuromuscular junction. *Neurosci Lett* 153 (1):45-48. doi:10.1016/0304-3940(93)90073-t
- Perl ER (1996) Cutaneous polymodal receptors: characteristics and plasticity. *Prog Brain Res* 113:21-37. doi:10.1016/s0079-6123(08)61079-1
- Pinho-Ribeiro FA, Verri WA, Jr., Chiu IM (2017) Nociceptor Sensory Neuron-Immune Interactions in Pain and Inflammation. *Trends Immunol* 38 (1):5-19. doi:10.1016/j.it.2016.10.001

- Pittock SJ, Zekeridou A, Weinshenker BG (2021) Hope for patients with neuromyelitis optica spectrum disorders - from mechanisms to trials. *Nat Rev Neurol* 17 (12):759-773. doi:10.1038/s41582-021-00568-8
- Plantone D, Renna R, Koudriavtseva T (2015) Neurological diseases associated with autoantibodies targeting the voltage-gated potassium channel complex: immunobiology and clinical characteristics. *Neuroimmunology and Neuroinflammation*:0
- Pleger B, Blankenburg F, Bestmann S, Ruff CC, Wiech K, Stephan KE, Friston KJ, Dolan RJ (2006) Repetitive transcranial magnetic stimulation-induced changes in sensorimotor coupling parallel improvements of somatosensation in humans. *J Neurosci* 26 (7):1945-1952. doi:10.1523/jneurosci.4097-05.2006
- Pollock J, McFarlane SM, Connell MC, Zehavi U, Vandenabeele P, MacEwan DJ, Scott RH (2002) TNF-alpha receptors simultaneously activate Ca²⁺ mobilisation and stress kinases in cultured sensory neurones. *Neuropharmacology* 42 (1):93-106. doi:10.1016/s0028-3908(01)00163-0
- Poole S, Lorenzetti BB, Cunha JM, Cunha FQ, Ferreira SH (1999) Bradykinin B1 and B2 receptors, tumour necrosis factor alpha and inflammatory hyperalgesia. *Br J Pharmacol* 126 (3):649-656. doi:10.1038/sj.bjp.0702347
- Rawlings DJ, Dai X, Buckner JH (2015) The role of PTPN22 risk variant in the development of autoimmunity: finding common ground between mouse and human. *J Immunol* 194 (7):2977-2984. doi:10.4049/jimmunol.1403034
- Reilly JM, Dharmalingam B, Marsh SJ, Thompson V, Goebel A, Brown DA (2016) Effects of serum immunoglobulins from patients with complex regional pain syndrome (CRPS) on depolarisation-induced calcium transients in isolated dorsal root ganglion (DRG) neurons. *Exp Neurol* 277:96-102. doi:10.1016/j.expneurol.2015.12.009
- Reville K, Crean JK, Vivers S, Dransfield I, Godson C (2006) Lipoxin A4 redistributes myosin IIA and Cdc42 in macrophages: implications for phagocytosis of apoptotic leukocytes. *J Immunol* 176 (3):1878-1888. doi:10.4049/jimmunol.176.3.1878
- Rigaud M, Gemes G, Barabas ME, Chernoff DI, Abram SE, Stucky CL, Hogan QH (2008) Species and strain differences in rodent sciatic nerve anatomy: implications for studies of neuropathic pain. *Pain* 136 (1-2):188-201. doi:10.1016/j.pain.2008.01.016
- Roque AC, Silva CS, Taipa MA (2007) Affinity-based methodologies and ligands for antibody purification: advances and perspectives. *J Chromatogr A* 1160 (1-2):44-55. doi:10.1016/j.chroma.2007.05.109
- Rose NR, Bona C (1993) Defining criteria for autoimmune diseases (Witebsky's postulates revisited). *Immunol Today* 14 (9):426-430. doi:10.1016/0167-5699(93)90244-f
- Rosenbaum T, Simon SA (2007) *Frontiers in Neuroscience TRPV1 Receptors and Signal Transduction*. In: Liedtke WB, Heller S (eds) *TRP Ion Channel Function in Sensory Transduction and Cellular Signaling Cascades*. CRC Press/Taylor & Francis

- Copyright © 2007, Taylor & Francis Group, LLC., Boca Raton (FL),
Rowley MJ, Whittingham SF (2015) The Role of Pathogenic Autoantibodies
in Autoimmunity. *Antibodies* 4 (4):314-353
- Sandroni P, Benrud-Larson LM, McClelland RL, Low PA (2003) Complex
regional pain syndrome type I: incidence and prevalence in Olmsted
county, a population-based study. *Pain* 103 (1-2):199-207.
doi:10.1016/s0304-3959(03)00065-4
- Sawano S, Komiya Y, Ichitsubo R, Ohkawa Y, Nakamura M, Tatsumi R,
Ikeuchi Y, Mizunoya W (2016) A One-Step Immunostaining Method to
Visualize Rodent Muscle Fiber Type within a Single Specimen. *PLoS
One* 11 (11):e0166080. doi:10.1371/journal.pone.0166080
- Schäfers M, Geis C, Svensson CI, Luo ZD, Sommer C (2003) Selective
increase of tumour necrosis factor-alpha in injured and spared
myelinated primary afferents after chronic constrictive injury of rat
sciatic nerve. *Eur J Neurosci* 17 (4):791-804. doi:10.1046/j.1460-
9568.2003.02504.x
- Schäffer M, Beiter T, Becker HD, Hunt TK (1998) Neuropeptides: mediators
of inflammation and tissue repair? *Arch Surg* 133 (10):1107-1116.
doi:10.1001/archsurg.133.10.1107
- Schaible HG, Ebersberger A, Natura G (2011) Update on peripheral
mechanisms of pain: beyond prostaglandins and cytokines. *Arthritis
Res Ther* 13 (2):210. doi:10.1186/ar3305
- Schaible HG, Schmidt RF (1983) Responses of fine medial articular nerve
afferents to passive movements of knee joints. *J Neurophysiol* 49
(5):1118-1126. doi:10.1152/jn.1983.49.5.1118
- Schepelmann K, Messlinger K, Schmidt RF (1993) The effects of phorbol
ester on slowly conducting afferents of the cat's knee joint. *Exp Brain
Res* 92 (3):391-398. doi:10.1007/bf00229027
- Schmid AB, Coppieters MW, Ruitenber MJ, McLachlan EM (2013) Local
and remote immune-mediated inflammation after mild peripheral nerve
compression in rats. *J Neuropathol Exp Neurol* 72 (7):662-680.
doi:10.1097/NEN.0b013e318298de5b
- Scholz-Odermatt SM, Luthi F, Wertli MM, Brunner F (2019) Direct Health
Care Cost and Work Incapacity Related to Complex Regional Pain
Syndrome in Switzerland: A Retrospective Analysis from 2008 to
2015. *Pain Med* 20 (8):1559-1569. doi:10.1093/pm/pnz030
- Sebastin SJ (2011) Complex regional pain syndrome. *Indian J Plast Surg* 44
(2):298-307. doi:10.4103/0970-0358.85351
- Sensi S, Goebel A (2022) Human Auto-IgG Purification from High Volume
Serum Sample by Protein G Affinity Purification. *Bio Protoc* 12 (23).
doi:10.21769/BioProtoc.4562
- Serhan CN, Savill J (2005) Resolution of inflammation: the beginning
programs the end. *Nat Immunol* 6 (12):1191-1197. doi:10.1038/ni1276
- Sherer Y, Levy Y, Shoenfeld Y (2002) IVIG in autoimmunity and cancer--
efficacy versus safety. *Expert Opin Drug Saf* 1 (2):153-158.
doi:10.1517/14740338.1.2.153

- Sherwood ER, Toliver-Kinsky T (2004) Mechanisms of the inflammatory response. *Best Pract Res Clin Anaesthesiol* 18 (3):385-405. doi:10.1016/j.bpa.2003.12.002
- Shi C, Qiu S, Riester SM, Das V, Zhu B, Wallace AA, van Wijnen AJ, Mwale F, Iatridis JC, Sakai D, Votta-Velis G, Yuan W, Im HJ (2018) Animal models for studying the etiology and treatment of low back pain. *J Orthop Res* 36 (5):1305-1312. doi:10.1002/jor.23741
- Skaribas IM, Peccora C, Skaribas E (2019) Single S1 Dorsal Root Ganglia Stimulation for Intractable Complex Regional Pain Syndrome Foot Pain After Lumbar Spine Surgery: A Case Series. *Neuromodulation* 22 (1):101-107. doi:10.1111/ner.12780
- Sommer C, Kress M (2004) Recent findings on how proinflammatory cytokines cause pain: peripheral mechanisms in inflammatory and neuropathic hyperalgesia. *Neurosci Lett* 361 (1-3):184-187. doi:10.1016/j.neulet.2003.12.007
- Song YC, Sun GH, Lee TP, Huang JC, Yu CL, Chen CH, Tang SJ, Sun KH (2008) Arginines in the CDR of anti-dsDNA autoantibodies facilitate cell internalization via electrostatic interactions. *Eur J Immunol* 38 (11):3178-3190. doi:10.1002/eji.200838678
- Stanly TA, Fritzsche M, Banerji S, García E, Bernardino de la Serna J, Jackson DG, Eggeling C (2016) Critical importance of appropriate fixation conditions for faithful imaging of receptor microclusters. *Biol Open* 5 (9):1343-1350. doi:10.1242/bio.019943
- Stanton-Hicks M, Jänig W, Hassenbusch S, Haddox JD, Boas R, Wilson P (1995) Reflex sympathetic dystrophy: changing concepts and taxonomy. *Pain* 63 (1):127-133. doi:10.1016/0304-3959(95)00110-e
- Stanton-Hicks MD, Burton AW, Bruehl SP, Carr DB, Harden RN, Hassenbusch SJ, Lubenow TR, Oakley JC, Racz GB, Raj PP, Rauck RL, Rezaei AR (2002) An updated interdisciplinary clinical pathway for CRPS: report of an expert panel. *Pain Pract* 2 (1):1-16. doi:10.1046/j.1533-2500.2002.02009.x
- Steinbrocker O, Friedman HH, Lapin L (1954) The shoulder-hand syndrome (reflex neurovascular dystrophy of the upper extremity). *Postgrad Med* 16 (1):46-57. doi:10.1080/00325481.1954.11712276
- Stramer BM, Mori R, Martin P (2007) The inflammation-fibrosis link? A Jekyll and Hyde role for blood cells during wound repair. *J Invest Dermatol* 127 (5):1009-1017. doi:10.1038/sj.jid.5700811
- Sudeck P (1901) Über die akute (reflektorische) Knochenatrophie nach Entzündungen und Verletzungen in den Extremitäten und ihre klinischen Erscheinungen. *Fortschr Röntgenstr* 5:227-293
- Suurmond J, Diamond B (2015) Autoantibodies in systemic autoimmune diseases: specificity and pathogenicity. *J Clin Invest* 125 (6):2194-2202. doi:10.1172/jci78084
- Tajerian M, Hung V, Khan H, Lahey LJ, Sun Y, Birklein F, Krämer HH, Robinson WH, Kingery WS, Clark JD (2017) Identification of KRT16 as a target of an autoantibody response in complex regional pain syndrome. *Exp Neurol* 287 (Pt 1):14-20. doi:10.1016/j.expneurol.2016.10.011

- Taylor SS, Noor N, Urits I, Paladini A, Sadhu MS, Gibb C, Carlson T, Myrcik D, Varrassi G, Viswanath O (2021) Complex Regional Pain Syndrome: A Comprehensive Review. *Pain Ther* 10 (2):875-892. doi:10.1007/s40122-021-00279-4
- Tékus V, Hajna Z, Borbély É, Markovics A, Bagoly T, Szolcsányi J, Thompson V, Kemény Á, Helyes Z, Goebel A (2014) A CRPS-IgG-transfer-trauma model reproducing inflammatory and positive sensory signs associated with complex regional pain syndrome. *Pain* 155 (2):299-308. doi:10.1016/j.pain.2013.10.011
- THOMAS HL, FRS E (1813) WOUND IN THE RADIAL NERVE.
- Totsch SK, Sorge RE (2017) Immune System Involvement in Specific Pain Conditions. *Mol Pain* 13:1744806917724559. doi:10.1177/1744806917724559
- Toyka KV, Brachman DB, Pestronk A, Kao I (1975) Myasthenia gravis: passive transfer from man to mouse. *Science* 190 (4212):397-399. doi:10.1126/science.1179220
- Uçeyler N, Schäfers M, Sommer C (2009) Mode of action of cytokines on nociceptive neurons. *Exp Brain Res* 196 (1):67-78. doi:10.1007/s00221-009-1755-z
- Van Buyten JP, Smet I, Liem L, Russo M, Huygen F (2015) Stimulation of dorsal root ganglia for the management of complex regional pain syndrome: a prospective case series. *Pain Pract* 15 (3):208-216. doi:10.1111/papr.12170
- Varga A, Bölcskei K, Szöke E, Almási R, Czéh G, Szolcsányi J, Pethő G (2006) Relative roles of protein kinase A and protein kinase C in modulation of transient receptor potential vanilloid type 1 receptor responsiveness in rat sensory neurons in vitro and peripheral nociceptors in vivo. *Neuroscience* 140 (2):645-657. doi:10.1016/j.neuroscience.2006.02.035
- Veldman PH, Reynen HM, Arntz IE, Goris RJ (1993) Signs and symptoms of reflex sympathetic dystrophy: prospective study of 829 patients. *Lancet* 342 (8878):1012-1016. doi:10.1016/0140-6736(93)92877-v
- Verri WA, Jr., Cunha TM, Parada CA, Poole S, Cunha FQ, Ferreira SH (2006) Hypernociceptive role of cytokines and chemokines: targets for analgesic drug development? *Pharmacol Ther* 112 (1):116-138. doi:10.1016/j.pharmthera.2006.04.001
- Walcher J, Ojeda-Alonso J, Haseleu J, Oosthuizen MK, Rowe AH, Bennett NC, Lewin GR (2018) Specialized mechanoreceptor systems in rodent glabrous skin. *J Physiol* 596 (20):4995-5016. doi:10.1113/jp276608
- Wall PD, Gutnick M (1974) Properties of afferent nerve impulses originating from a neuroma. *Nature* 248 (5451):740-743. doi:10.1038/248740a0
- Wang H, Ehnert C, Brenner GJ, Woolf CJ (2006) Bradykinin and peripheral sensitization. *Biol Chem* 387 (1):11-14. doi:10.1515/bc.2006.003
- Wardemann H, Yurasov S, Schaefer A, Young JW, Meffre E, Nussenzweig MC (2003) Predominant autoantibody production by early human B cell precursors. *Science* 301 (5638):1374-1377. doi:10.1126/science.1086907

- Wasner G, Schattschneider J, Binder A, Baron R (2003) Complex regional pain syndrome--diagnostic, mechanisms, CNS involvement and therapy. *Spinal Cord* 41 (2):61-75. doi:10.1038/sj.sc.3101404
- Wasner G, Schattschneider J, Heckmann K, Maier C, Baron R (2001) Vascular abnormalities in reflex sympathetic dystrophy (CRPS I): mechanisms and diagnostic value. *Brain* 124 (Pt 3):587-599. doi:10.1093/brain/124.3.587
- Wigerblad G, Bas DB, Fernandes-Cerqueira C, Krishnamurthy A, Nandakumar KS, Rogoz K, Kato J, Sandor K, Su J, Jimenez-Andrade JM, Finn A, Bersellini Farinotti A, Amara K, Lundberg K, Holmdahl R, Jakobsson PJ, Malmström V, Catrina AI, Klareskog L, Svensson CI (2016) Autoantibodies to citrullinated proteins induce joint pain independent of inflammation via a chemokine-dependent mechanism. *Ann Rheum Dis* 75 (4):730-738. doi:10.1136/annrheumdis-2015-208094
- Willis WD, Westlund KN (1997) Neuroanatomy of the pain system and of the pathways that modulate pain. *J Clin Neurophysiol* 14 (1):2-31. doi:10.1097/00004691-199701000-00002
- Wilson J, Serpell M (2007) Complex regional pain syndrome. *Continuing Education in Anaesthesia Critical Care & Pain* 7 (2):51-54. doi:10.1093/bjaceaccp/mkm001
- Woolf C, Wiesenfeld-Hallin Z (1986) Substance P and calcitonin gene-related peptide synergistically modulate the gain of the nociceptive flexor withdrawal reflex in the rat. *Neurosci Lett* 66 (2):226-230. doi:10.1016/0304-3940(86)90195-3
- Woolf CJ, Ma Q (2007) Nociceptors--noxious stimulus detectors. *Neuron* 55 (3):353-364. doi:10.1016/j.neuron.2007.07.016
- Woolf CJ, Salter MW (2000) Neuronal plasticity: increasing the gain in pain. *Science* 288 (5472):1765-1769. doi:10.1126/science.288.5472.1765
- Wu B, Goluszko E, Christadoss P (2001) Experimental autoimmune myasthenia gravis in the mouse. *Curr Protoc Immunol Chapter 15:Unit 15.18*. doi:10.1002/0471142735.im1508s21
- Wu HY, Tang XQ, Mao XF, Wang YX (2017) Autocrine Interleukin-10 Mediates Glucagon-Like Peptide-1 Receptor-Induced Spinal Microglial β -Endorphin Expression. *J Neurosci* 37 (48):11701-11714. doi:10.1523/jneurosci.1799-17.2017
- Xu M, Bennett DLH, Querol LA, Wu LJ, Irani SR, Watson JC, Pittock SJ, Klein CJ (2020) Pain and the immune system: emerging concepts of IgG-mediated autoimmune pain and immunotherapies. *J Neurol Neurosurg Psychiatry* 91 (2):177-188. doi:10.1136/jnnp-2018-318556
- Yabuki S, Kikuchi S (1996) Positions of dorsal root ganglia in the cervical spine. An anatomic and clinical study. *Spine (Phila Pa 1976)* 21 (13):1513-1517. doi:10.1097/00007632-199607010-00004
- Yanik BM, Dauch JR, Cheng HT (2020) Interleukin-10 Reduces Neurogenic Inflammation and Pain Behavior in a Mouse Model of Type 2 Diabetes. *J Pain Res* 13:3499-3512. doi:10.2147/jpr.S264136
- Yoshimi K, Woo M, Son Y, Baudry M, Thompson RF (2002) IgG-immunostaining in the intact rabbit brain: variable but significant

- staining of hippocampal and cerebellar neurons with anti-IgG. *Brain Res* 956 (1):53-66. doi:10.1016/s0006-8993(02)03479-0
- Yu Z, Lennon VA (1999) Mechanism of intravenous immune globulin therapy in antibody-mediated autoimmune diseases. *N Engl J Med* 340 (3):227-228. doi:10.1056/nejm199901213400311
- Zhou Y, Hong Y, Huang H (2016) Triptolide Attenuates Inflammatory Response in Membranous Glomerulo-Nephritis Rat via Downregulation of NF- κ B Signaling Pathway. *Kidney Blood Press Res* 41 (6):901-910. doi:10.1159/000452591
- Zimmermann K, Hein A, Hager U, Kaczmarek JS, Turnquist BP, Clapham DE, Reeh PW (2009) Phenotyping sensory nerve endings in vitro in the mouse. *Nat Protoc* 4 (2):174-196. doi:10.1038/nprot.2008.223
- Zuercher AW, Spirig R, Baz Morelli A, Käsermann F (2016) IVIG in autoimmune disease - Potential next generation biologics. *Autoimmun Rev* 15 (8):781-785. doi:10.1016/j.autrev.2016.03.018